Effects of Congenital Visual Deprivation on the Structural and Functional Organisation of the Human Brain

Dissertation

Zum Erlangen des Doktorgrades

der Naturwissenschaften

(Dr. rer. nat.)

An der Universität Hamburg,

Fakultät für Psychologie und Bewegungswissenschaft,

Institut für Psychologie

Vorgelegt von

Madita Linke

Hamburg, 2023

Tag der Disputation: 05.12.2023

Promotionsprüfungsausschuss:

Vorsitzende: Prof. Dr. Barbara Hänel-Faulhaber

1. Dissertationsgutachterin: Prof. Dr. Brigitte Röder

2. Dissertationsgutachter: Prof. Dr. Rainer Goebel

1. Disputationsgutachter: PD Dr. Patrick Bruns

2. Disputationsgutachter: Prof. Dr. Frank Schüttauf

... we all begin with the natural equipment to live a thousand kinds of life but end in the end having lived only one.

Clifford Geertz, 1973

Abstract

Individuals treated for bilateral congenital cataracts offer a unique opportunity to investigate the impact of early visual experience on human brain development. Previous research has demonstrated that even a brief period of early visual deprivation leads to significant changes in the structural and functional organisation of the visual brain, highlighting the crucial role of experience in typical brain development. However, certain aspects of visual processing have been observed to develop independently of experience, suggesting a complex interplay of experience-dependent and experience-independent mechanisms involved in brain development. This dissertation aimed to further explore the extent of experience-dependent and experience-independent development and, in the context of two magnetic resonance imaging studies, investigated the effects of early visual deprivation on the structural organisation of the early visual cortex and the functional organisation of categorical processing.

Study 1 (Chapter 2) analysed ultra-high field MRI structural data with a submillimetre resolution, revealing profound and enduring structural changes following early visual deprivation. Furthermore, the results indicated potentially differentiated effects of early visual deprivation on various measurements of brain structure, highlighting the complex and heterogeneous developmental trajectories involved in brain development. Study 2 (Chapter 3) investigated the effects of early visual deprivation on functional categorical processing specifically focusing on distributed categorical representations and category-selective responses within distinct regions within the ventral temporal cortex. The results provide valuable insights indicating that the general organisation of categorical processing persists after early visual deprivation in form of distinguishable categorical patterns and category-selective responses in selective regions. Nevertheless, early visual experience appears to be essential for the fine-tuning and maintenance of categorical processing, as all categories exhibited impairments characterised by less distinctive categorical patterns and reduced category-selective responses.

Overall, the findings of this dissertation underscore that altered structural and functional organisation of the human brain resulting from early visual deprivation may not be fully reversible, even with many years of visual experience after sight restoration. The dissertation's comprehensive investigation reveals the multifaceted nature of brain development, highlighting the intricate interplay between experience-dependent and experience-independent mechanisms. These insights significantly contribute to our understanding of brain plasticity and emphasize the critical role of early experiences in ensuring typical brain development.

Contents

Abbreviations

3T	3 Tesla (magnetic field strength)
7T	7 Tesla (magnetic field strength)
avg-faces	face-selective region within the ventral temporal cortex
BOLD	blood oxygenation level dependency
CC individuals	congenital cataract (sight-recovery) individuals
EBA	extrastriate body area
EEG	electroencephalogram
ERP	event-related potential
FBA	fusiform body area
FFA	fusiform face area
fMRI	functional magnetic resonance imaging
fNIRS	functional near-infrared spectroscopy
GM	grey matter
IOG-faces	face-selective inferior occipital gyrus
IOS-characters	letter-selective inferior occipital sulcus
ITG-bodies	body-selective inferior temporal gyrus
LOC	lateral object complex
LOS-bodies	body-selective lateral occipital sulcus
MEG	magnetoencephalography
mFus-faces	face-selective mid-lateral fusiform gyrus
MRI	magnetic resonance imaging
MTG-bodies	body-selective middle temporal gyrus
MVPA	multivariate pattern analysis
OFA	occipital face area
OPA	occipital place area
OTS-bodies	body-selective occipital-temporal sulcus
pFus-faces	face-selective posterior lateral fusiform gyrus
pOTS-characters	letter-selective posterior occipital-temporal sulcus
PPA	parahippocampal place area
ROI	regions-of-interest
SC individuals	normally sighted control individuals
SSEP	steady-state evoked potentials
STS	superior temporal sulcus
TOS	transvers occipital gyrus
V1, V2, V3, V4	early visual regions
VI individuals	visually impaired individuals
VTC	ventral temporal cortex
VWFA	visual word form area
WM	white matter

Chapter I

General Introduction

Vision plays a fundamental role in our daily lives, shaping our perception of the world and facilitating our interactions with it. The ability to see not only provides us with crucial information about our surroundings but also influences our cognitive processes, emotional experiences, and overall well-being. Through vision, we navigate our environment, recognize faces, appreciate the beauty of nature, and indulge in the intricacies of art. In order to ensure the acquisition and maintenance of these vital visual abilities, the intricate mechanisms of the brain undergo a multitude of complex changes and adaptations throughout the lifespan of the individual.

Neuroplasticity

Our nervous system possesses a remarkable capacity to change, remodel, and reorganise itself to adapt to new situations. This characteristic ability facilitates learning, growth, and development to ensure our survival. The capacity of the nervous system to adapt is referred to as *neuroplasticity*, which is a broad and catch-all term for the diverse ways in which the nervous system reorganises itself in response to various stimuli (Bavelier & Neville, 2002). Neuroplasticity research aims to elucidate the mechanisms underlying these adaptations, by connecting changes on the molecular level to behavioural outcomes and relating these to different factors such as genetics, the environment, and experience. The knowledge gained from this can be used to foster desirable changes by suppressing unfavourable and encouraging beneficial outcomes in the form of brain activity or behaviour. For instance, a deeper understanding of neuroplastic changes can be leveraged to optimise the recovery and rehabilitation of individuals who experienced visual impairments and blindness, thereby offering potential advancements in enhancing visual perception and functionality.

While the use of the term *plasticity* was first attributed to William James in 1890, the general concept of plasticity has existed for almost 250 years (Costandi, 2016). However, from a simple correspondence concerning how mental exercise could lead to brain growth, to linking changes in neural connections to behavioural changes (Ramon y Cajal, 1928), the idea of a constantly changing brain faced considerable resistance for a relatively long period before it became accepted in the field. Initially, the persistent belief was that while the immature brain is malleable, like clay being left out in the open, it hardens over time leaving the mature brain as a fixed structure incapable of change and recovery. The theory of a constantly changing brain was only revived in the late 1940s and while the term *neural plasticity* is attributed to Jerzy Konorski (1948) it was first popularised by Donald Hebb in 1949. Since then, evidence for continued neuroplasticity across the lifespan has accumulated (Berlucchi & Buchtel, 2009) and, today, it is the generally accepted understanding that the nervous system remains

adaptable throughout life with neuroplasticity as its intrinsic property and the obligatory consequence of each sensory input, action, and association (Pascual-Leone et al., 2005).

Neuroplasticity manifests in various forms at every level of the nervous system, ranging from changes in the form of molecular activity or the structure and function of individual nerve cells to distinct cell populations, widespread neuronal networks, and brain-wide systems and behaviour whereby all levels are unquestionably connected. Although they are highly interrelated, neuroplastic changes can broadly be classified into two main types, namely *structural* and *functional plasticity*. Structural plasticity involves the formation or elimination of cells, synapses, and nerve fibre branches leading to the shaping of neural pathways and brain regions (May, 2011). In contrast, while functional plasticity can be described and classified based on various aspects and levels (Grafman, 2000; Innocenti, 2022) it generally encompasses changes in some physiological aspects of nerve cell function, such as the frequency of nervous impulses, the degree of synchronicity among a population of cells, or the response pattern concerning certain types of stimuli.

Different aspects of plasticity occur across different timeframes (Butz et al., 2009; Castaldi et al., 2020), as modifications of synapses can occur over a time range of milliseconds, synapses and dendrite branches can be created or destroyed within hours, and new cells can emerge or undergo apoptosis over several days. Other forms of neuroplastic changes occur over longer periods. For example, the structural maturation of the brain (Gilmore et al., 2018), the prolonged development of processing complex visual stimuli such as faces (Germine et al., 2011), or the recovery after brain injuries (Pascual-Leone et al., 2005) have been observed over a timeframe spanning several months or even years. In this context, some aspects of plasticity occur continuously throughout life, whereas others are only observed at specific periods of life. Especially the developing brain exhibits the most profound capacity for changes. Developmental plasticity is characterised as a remarkable sensitivity to a variety of experiences, namely the complex interplay between an individual's sensory systems and their environment. Such experiences include, among others, sensory and motor experiences, diet, or social aspects such as parent-child and peer relationships or socio-economic status (Kolb, 2018). For many of these experiences, *sensitive periods* have been identified which are defined as phases in development during which the impact of experience is particularly strong. Significantly, sensory input during a sensitive period results in the development of certain capabilities or behaviour, which would not be acquired if the appropriate stimuli were absent during that period. Consequently, typical experiences during sensitive periods ensure typical brain development and the importance of such typical experiences become especially evident when investigating the severe and long-lasting impacts of adverse and atypical experiences on the developing brain. More specifically, both structural and functional brain organisation were found to be impaired after exposure to poverty and adversity in

childhood (McLaughlin et al., 2019; Noble & Giebler, 2020). In this context, the recent COVID-19 pandemic provided an extreme and yet unique setting for investigating the effects of altered experiences, giving a striking example of the effects of atypical visual experience as observed in altered face processing in infants who experienced reduced social contacts due to emergency lockdowns and the mandatory implementation of the use of face mask coverings in public spaces (Yates et al., 2023).

The investigation of sensitive periods has greatly profited by animal studies, whereby the first systematic research concerning sensitive periods was published in 1935 by Konrad Lorenz in the form of behavioural experiments on filial imprinting in birds. Lorenz observed that within a comparably short and well-defined period after hedging, chicks would imprint on almost every moving visual object, which became their substitute mother from that moment onwards. In the early 1960s, Wiesel and Hubel (1963) first systematically investigated sensitive periods at the neural level. Originally termed *critical periods* by Wiesel and Hubel, the terms *sensitive period*, *critical period*, or occasionally *window of opportunity* are still used in various scientific fields, with fundamentally similar albeit slightly different meanings (Voss, 2013). Similar to sensitive periods, critical periods also describe increased susceptibility of the system to a certain type of sensory input during that period. However, while the term sensitive period more commonly refers to the optimal period for the application of a stimulus – before and after which the same stimuli have less influence – the term critical period usually refers to a stricter and more impactful association between timing, experience, and learning (Illingworth & Lister, 1964; Pascalis et al., 2020). As mentioned, the core idea of both terms is the same, namely that having a certain experience at one point in development has a profoundly different impact on future behaviour than having the same experience at any other point in development. For the purpose of this dissertation, the differentiation between critical and sensitive periods is negligible and the term *sensitive periods* will be used throughout.

Sensory Deprivation Studies to Determine Experience-Dependent and Experience-Independent Developmental Trajectories

Sensitive periods have been observed in various brain functions and behaviours across different species. While these periods are typically manifested in behaviour, they are primarily a characteristic of neural circuits (Knudsen, 2004). To investigate the effects of experience on neuronal development, researchers frequently manipulate sensory input, such as through visual (Levelt & Hübener, 2012) or auditory deprivation (Kral et al., 2019). Visual deprivation is particularly interesting due to methodological advantages, such as the accessibility of the eyes for experimental manipulation and the well-known visual pathway in various species. Moreover, the time at which a young individual's eyes first open serves as a selective starting point for visual development (Smith & Trachtenberg, 2007). Furthermore, beyond the purely methodological advantages, there is also a more philosophical interest in studying vision due to its dominant role as a sense in human society and culture and this interest in understanding visual processing is reflected in a range of research fields, such as neuroscience, developmental psychology, and clinical research to name only a few. The role of experience in shaping the development of the brain has been a subject of extensive research in both animal and human studies, whereby animal studies have proven particularly valuable in this regard, as they allow for the systematic manipulation of visual experience and the measurement of its effects on neural circuits. Researchers have used a variety of techniques to induce visual deprivation in animals, including dark-rearing, eyelid sutures, and denucleation. These techniques provide a means of comparing the effects of different onset and/or duration of blindness on neural development. By this comparative approach, researchers have gained a deeper understanding of the mechanisms underlying experience-dependent as well as experience-independent development in the brain.

The earliest studies by Hubel and Wiesel (1962) already characterised the development of the primary visual cortex as an initial *innate* period of development during which genetic mechanisms are the driving force in developing the basic neural organisation (Espinosa & Stryker, 2012; O'Leary et al., 2007). This period of experience-independent development is followed by a sensitive period exhibiting exceptional experience-dependent plasticity. Classical studies in the visual system of cats, non-human primates, and mice have demonstrated that even a relatively brief period of visual deprivation during a sensitive period can already lead to severe and long-lasting visual impairments (Dräger, 1975; Hubel et al., 1977; Hubel & Wiesel, 1970). These findings highlighted the importance of early visual experience for typical visual development. The investigation of sensitive periods in non-human animals commonly employs a variety of mostly invasive methods to decode the neural basis of sensitive periods. For example, anatomical tracing experiments, transcranial optical imaging, or chronic

implantation of recording electrodes were traditionally used to repeatedly sample brain regions before, during, and after manipulation of visual experiences whereas more modern approaches profit from advances in biochemistry and genetics that yield valuable insights concerning the molecular and cellular level of plastic changes. Accordingly, studies in transgenic mice and pharmacological approaches have helped to identify key aspects and molecular mechanisms involved in the timescale of sensitive periods (Levelt & Hübener, 2012). More specifically, changes in the balance of excitatory and inhibitory signals in neural circuits, along with specific alterations in the levels of neuromodulators, such as gamma-aminobutyric acid (GABA), the main inhibitory neurotransmitter, have emerged as significant regulators of sensitive period timing and cortical plasticity (for a review, see Takesian & Hensch, 2013).

Visual Deprivation in Humans

While studies in non-human animals provide valuable and essential insights into the mechanisms of neurodevelopment, given the complex cognitive functions and architecture of the human brain, it is difficult to draw direct conclusions across species. It is therefore crucial to investigate experience-dependent development directly in humans. However, the investigation of the experience-dependence of visual development in humans faces several ethical restrictions and is thus limited to cases of naturally occurring blindness, in the form of congenital blindness for example due to anophthalmia or congenital cataracts, or acquired blindness due to accidents, lesions, or developmental cataracts. Research in permanently blind individuals allows for the investigation of the adaptation to an *atypical* environment, i.e. how the human brain adapts in the absence of typical visual experiences. By comparing different onsets of blindness, conclusions can be drawn concerning sensitive periods of atypical development. However, in order to investigate the experience-dependence of *typical* visual development, studies conducted on individuals with a transient phase of congenitally visual deprivation are especially valuable and thus the preferred approach. Individuals with a history of dense bilateral congenital cataracts (CC individuals) who regained their sight later in life by surgical removal of the clouded lenses allow for an investigation into the role of early visual experience on visual brain development. By comparing CC individuals to normally sighted controls (SC individuals), conclusions can be drawn concerning which aspects of structural and functional brain organisation can be recovered after early visual deprivation, thereby unmasking sensitive periods for typical visual development. More precisely, if CC individuals show impairments in specific aspects, despite many years of visual experience, it can be concluded that early visual experience is essential for their development which in turn alludes to a sensitive period for the given aspect. In contrast, if no

differences in function, structure, or behaviour are observed, it can be concluded that early visual experience might not be essential and can subsequently be caught up at a later stage.

In contrast to animal studies, human research relies on behavioural and non-invasive neuroscientific methods to investigate the effects of early visual deprivation on visual brain functions and structure. However, although behavioural assessments indicate if a function is impaired or not, conclusions concerning the neuronal basis of this assessment are not possible. More specifically, impaired behaviour as possibly indicated by higher reaction times or error rates may have been preceded by neuronal adaptations whereas, on the other hand, the absence of behavioural changes does not necessarily prove the absence of altered neural processing as some form of neuronal compensation might result in indistinguishable behaviours. The identification of the mechanisms that may underlie modifications in brain development and behaviour is an important challenge and various neuroscientific methods, such as electroencephalogram (EEG) and magnetic resonance imaging (MRI), provide essential insights into the neural mechanisms of brain development. For instance, EEG is used to record the spontaneous electrical activity of the brain and allows researchers to track event-related potentials (ERPs) and assess different processing stages (steady-state evoked potentials, SSEP) or functional connectivity in the form of resting-state EEG, which subsequently allows for conclusions about the timing and basic functional organisation to be drawn.

The use of MRI has transformed the field of neuroscience. MRI scanners use strong magnetic fields to generate images of the brain and thus provide information about the structural, functional, and, more recently, neurochemical brain organisation. Structural MRI assesses brain structure by utilising distinct characteristics of different tissue types, such as grey matter (GM) and white matter (WM). Due to their tissue composition, GM and WM respond differently to magnetic impulses within an MRI sequence, resulting in different contrasts in the image. Functional MRI (fMRI) measures brain activity by taking advantage of changes in blood oxygenation levels, whereby the blood oxygenation level dependent (BOLD) contrast compares the relative amount of oxygenated and deoxygenated haemoglobin in relation to neural activity. Respective MRI sequences pick up on resulting differences in signal strength, which visually creates images that display active brain regions as brighter than inactive regions. The BOLD signal forms the basis for various analysis approaches that yield information concerning selectivity, representation, or synchronicity across different brain regions while methodological advances in MRI such as the use of ultra-high field imaging have led to the increased temporal and spatial resolution of images and hence more detailed imaging. These advancements are increasingly deployed to investigate mesoscopic functional organisations such as cortical laminae and columns (De Martino et al., 2018; Dumoulin et al., 2018) and to re-evaluate structural assessments (Kupers et al., 2022; Zaretskaya et al., 2018). Furthermore, adaptions in acquisition and data analysis opened the

possibility of testing young children and even infants. These studies provide essential insights into structural and functional brain development (Gilmore et al., 2018; Kosakowski et al., 2022) and form the basis for an enhanced understanding of how the different components of structural and functional development relate to one another (Geng et al., 2017; Gilmore et al., 2018).

Given the continuously expanding scope of sight restoration approaches such as retinal prosthetic devices (Beyeler et al., 2017), stem cell transplantation (Cuevas et al., 2019), and genetic therapies (Mowad et al., 2020), a well-founded understanding of the extent of neuroplastic changes following early visual deprivation is increasingly relevant.

Leveraging Transient Blindness to Investigate Sensitive Periods for the Typical Development of the Visual Cortex

Research on CC individuals has revealed that early visual deprivation can exert a profound influence on visual development, whereby specific aspects of visual processing are affected to a greater extent than others. Nevertheless, certain aspects of visual perception can remain relatively preserved, offering valuable insights into the sensitive periods for the typical development of the visual system.

Visual Perceptual Functions After Sight Restoration

Basic visual functions, such as visual acuity and contrast sensitivity, were reported to improve rapidly after sight restoration (Ellemberg et al., 1999) even after long periods of visual deprivation (Gandhi et al., 2014; Kalia et al., 2014). While the typical effects of spatial vision were reported to emerge shortly after sight restoration (Andres et al., 2017; Gandhi et al., 2015), despite many years of visual experience, visual acuity, contrast sensitivity, and stereovision never fully recover (Ellemberg et al., 1999; Maurer et al., 2007; Tytla et al., 1993). In contrast, some visual perceptual functions seem to recover completely after a transient phase of congenital blindness and, more specifically, CC individuals have been reported to be able to detect various objects based on low-level visual cues such as colour, shape, and size in an odd-ball design (McKyton et al., 2015), in addition to more complex objects such as faces. Behaviourally, CC individuals demonstrated recovered face detection capabilities, including the recognition of Mooney faces (Mondloch et al., 2003, 2013), in addition to face identification based on the shape of internal features or external contours (Le Grand et al., 2001). Furthermore, colour discrimination in general was observed to recover after both short-term (Maurer et al., 1989) and long-term visual deprivation (McKyton et al., 2015; Pitchaimuthu et al., 2019).

However, despite such gains, CC individuals were also reported to suffer from mid- and higher-level object processing impairments. For instance, shape recognition based on mid-level cues such as occlusion or depth information was reported as being impaired in such individuals (McKyton et al., 2015). Furthermore, especially visual binding processes seem to rely on early visual experience as involved in the perception of visual illusions (Putzar, Hötting, et al., 2007) or the integration of different colour facets into three-dimensional figures (Ostrovsky et al., 2009). Similarly, binding processes in the context of holistic face processing seem impaired in CC individuals (Le Grand et al., 2001) in addition to the ability to identify faces in more challenging circumstances when the head orientation and/or lighting conditions were changed (Geldart et al., 2002; Putzar, Hötting, et al., 2010).

The Visual Brain after Sight Restoration

The study of temporary early visual deprivation has not only revealed various behavioural changes but also structural and functional changes in the visual brain. This has provided crucial insights into the brain's remarkable plasticity and adaptability, and the intricate interactions between sensory experience and brain development. Such investigations have uncovered the variations in the effects of early visual deprivation and understanding these nuances has advanced our comprehension of the human brain's resilience and its response to environmental input.

Structural brain organisation is regarded as the foundation of functional development and the evidence increasingly describes a remarkably close link between structural brain organisation and various perceptual and cognitive functions. For example, structural brain organisation was reported to predict cognitive abilities such as intelligence, language, and creativity (Lebel & Beaulieu, 2011; W. Li et al., 2015; Shaw et al., 2006) and could potentially determine inter-individual differences in human behaviour and cognition (Kanai & Rees, 2011). Moreover, atypical or deficient structural development has been linked to various neurodevelopmental and psychological disorders, such as depression (Szymkowicz et al., 2016), attention deficit hyperactivity disorder (Shaw et al., 2007, 2012), autism (Courchesne et al., 2007; Hazlett et al., 2012), and schizophrenia (Rapoport et al., 2012; Rimol et al., 2012). As a result of the complexity and interplay involved, elucidating the key factors that drive structural neurodevelopment is thus essential to ensure typical brain development.

Various measurements can be considered to describe the structural organisation of the brain whereby the focus can be placed on the shape and volume of subcortical structures, the tracing of white matter tracks, or the cortex, in the form of folding and curvature, the resulting area of the cortical surface, and the depth of the cortex. The most commonly investigated cortical measurements include cortical thickness and cortical volume (Winkler et al., 2010). Cortical thickness describes the distance between

the GM-WM boundary and the boundary between GM and cerebrospinal fluid. Cortical volume, on the other hand, is not a direct structural measurement but rather the product of cortical thickness and surface area, with the surface area being the area of a specific region on the surface. While all three measurements, i.e. cortical thickness, cortical surface area, and cortical volume, exhibit individual developmental trajectories (Wierenga et al., 2014), especially the first two are genetically distinct from each other (Panizzon et al., 2009; Winkler et al., 2010). As a result, an increasing number of studies focus on cortical thickness and cortical surface area as distinct indices of structural neurodevelopment (Winkler et al., 2010, 2018). While both measurements are largely under genetic control (C. H. Chen et al., 2013; Fjell et al., 2015), experience and environmental factors have been proposed to also influence the development as various studies found negative effects on cortical thickness and surface area subsequent to exposure to adverse childhood events or a low social economic status (McLaughlin et al., 2019; Noble & Giebler, 2020; Sanders et al., 2022). The effects of experience on structural brain development were also investigated in the context of visual deprivation and the findings indicate that, as a result of congenital visual deprivation, both cortical thickness and surface area are impaired in a variety of species (Andelin et al., 2019; Jiang et al., 2009; Qiaojun Li et al., 2017; Park et al., 2009). The evidence thereby suggests that it is especially early visual experience, or the absence thereof, that drives the changes outlined above (Andelin et al., 2019; Qiaojun Li et al., 2017).

Extensive research has focused on structural changes in both non-deprived and visual cortices following permanent congenital blindness, addressing how the brain adapts to a permanent absence of visual input. Studies have also focused on structural changes in the brains of CC individuals, with a particular emphasis on the recovery of brain structure following the restoration of visual input. This research investigates how the brain adapts to the reintroduction of visual stimuli after a period of deprivation, as opposed to the permanent absence of visual input in cases of congenital blindness. Similar to studies in congenitally (and permanently) blind individuals, evidence in CC individuals indicates that a long-lasting altered structural organisation results in response to such atypical experience. In this context, impaired cortical thickness and surface area were found in the visual cortex of CC individuals, especially the early visual cortex (Guerreiro, Erfort, et al., 2015; Hölig et al., 2022), and possibly beyond the visual cortex (Feng et al., 2021). The fact that these structural aspects did not recover even after many years of restored visual experience suggests that there may be a sensitive period(s) for structural development. While numerous studies have examined the structural changes that occur in the brain following congenital visual deprivation, a gap remains in our understanding of the fine-scale structural alterations that may occur. To address this gap in knowledge, further investigation using structural MRI is needed to examine potential changes in cortical thickness, surface area, and other structural features. Since a recent study using submillimetre structural MRI reported

potentially conflicting findings in congenitally blind individuals (Kupers et al., 2022), additional research, for example involving CC individuals, could provide a more comprehensive understanding of the structural changes that occur following visual deprivation, which could have important implications for our understanding of brain plasticity and development.

Compared to behavioural findings, which only provide limited insights into whether a given function is impaired, investigating the neural processing underlying a function allows for more qualitative assessments. Specifically, when a behavioural function appears impaired, neural findings can shed light on how differences in behaviour are related to differences in neural processing. However, an absence of behavioural differences does not necessarily indicate an unaffected neural processing as compensatory mechanisms may be at play in such a case. As a result, there is growing interest in investigating the effects of early visual deprivation on the functional neural level to answer these types of questions.

Various aspects of functional neural processing from low-level to mid and high-level visual processing have been investigated in CC individuals. So far, the evidence from CC research indicates a remarkably differentiated effect of early visual deprivation on striate visual processing and extrastriate processing and, accordingly, key aspects of early visual processing were reported in CC individuals (Brockhaus et al., 2022; Pitchaimuthu et al., 2021; Sourav et al., 2018). Similar to normally sighted individuals, CC individuals exhibited a polarity inversion of the C1 ERP component (Sourav et al., 2018), in addition to structured polar angle and eccentricity maps and cortical magnification factor within their early visual cortices (Brockhaus et al., 2022). CC individuals also exhibited fundamental frequency responses in steady-state visual evoked potentials which are associated with striate visual processing (Pitchaimuthu et al., 2021). In contrast to the evidence concerning relatively unimpaired striate processing, the findings indicate more profound impairments in extrastriate processing. More specifically, the study that investigated the C1 effect in CC individuals indicated that the P1 ERP component, which is associated with extrastriate processing, was significantly attenuated in this group (Sourav et al., 2018). The P1 component has also been reported to be altered in CC individuals for more complex stimuli (Bottari et al., 2016; Röder et al., 2013), which is why it has even been proposed to be utilised as a viable biological marker for diagnosing individuals suffering from congenital cataracts (Sourav et al., 2020). Furthermore, in CC individuals, frequencies in the visual steady-state evoked potentials associated with extrastriate processing stages have been reported to be altered (Pitchaimuthu et al., 2021).

Overall, the research suggests that early visual deprivation has a greater impact on later visual processing stages than on early ones, which implies that the development of striate processing may rely less on early visual experience than the development of extrastriate processing. Notably, the experience-independent development of striate visual processing is consistent with studies conducted with congenitally blind individuals (Bock et al., 2015; Striem-Amit et al., 2015). The observation concerning the incremental effects of early visual deprivation along the visual processing hierarchy was recently generalised in the form of a proposition (Röder & Kekunnaya, 2021). Based on findings in visually deprived monkeys, it was proposed that in the context of visual development, experience-dependence increases following up the visual processing hierarchy (Hyvärinen, Carlson, et al., 1981; Hyvärinen, Hyvärinen, et al., 1981). Accordingly, early visual processing is less dependent on visual experiences and therefore more likely to recover from early visual deprivation than higher visual processing stages. This proposal has been applied to findings in humans, more specifically CC individuals, and has found confirmation in the form of the previously described differentiated effects on striate and extrastriate processing in CC individuals.

The fact that basic visual organisation has also been reported in congenitally blind individuals (Bock et al., 2015; Striem-Amit et al., 2015) suggests a high maturational bias at birth. Higher-level visual processing, however, follows a prolonged developmental trajectory and was thus proposed to depend more strongly on experiences, thereby ultimately resulting in more profound effects of visual deprivation. While the preceding hypothesis is already supported by the differentiation between striate vs extrastriate processing, it seems plausible that the differentiation can be pursued even further to high-level visual processing. In contrast to low-level visual processing, higher-level visual processing is not based on elementary features such as luminance, contrast, and orientation (Goebel et al., 2012; Sereno et al., 1995) but rather describes the recognition and categorisation of more complex visual stimuli. In this context, research involving CC individuals was particularly beneficial for studying two aspects of higher-level visual processing, namely motion and face processing (Röder & Kekunnaya, 2021), and the evidence gathered from such studies provided critical insights into the experience-dependent nature of development in these areas.

Studies in CC individuals showed remarkably differentiated effects of early visual deprivation on the processing of general motion, i.e. the perception of a coherent mass moving in one direction, and the processing of biological motion, i.e. the perception of a moving body based on an implied motion by point light figures. While motion sensitivity emerges shortly after sight-recovery (Ostrovsky et al., 2009), even after many years of visual experience, CC individuals exhibited a higher threshold for detecting global motion (Bottari et al., 2018; Hadad et al., 2012), which seemingly is not related to reduced visual acuity (Rajendran et al., 2020) and hence the impaired processing of global motion

might be related to reduced activation within the motion-selective region hMT (Guerreiro et al., 2022). Furthermore, studies have shown that the modulation of the N1 ERP in response to the visual motion coherence level was absent in CC individuals, as evidenced by similar amplitudes in response to visual stimuli with different motion coherence levels (Bottari et al., 2018; Segalowitz et al., 2017) which suggests an impaired ability to differentiate between various types of motion. In sharp contrast to these findings, CC individuals exhibit unimpaired detection (Bottari et al., 2015) and identification of biological motion (Rajendran et al., 2020), which is supported by largely unimpaired neural responses (Bottari et al., 2015). The evidence gathered from CC individuals indicates a substantial difference in experience-dependence for the developmental trajectories of global and biological motion. This differentiation in development might also provide important insights into the ongoing discussion concerning the neural mechanisms involved in the processing of biological and global motion. Accordingly, numerous publications discuss the potential overlap of the motion-selective region hMT and body-selective extrastriate body area (EBA) (Ferri et al., 2013; Spiridon et al., 2006; Weiner & Grill-Spector, 2011). Consequently, potential functionally distinct parcellations might especially be involved in the incorporated processing of body-related motion processing, i.e. biological motion and thus be distinct from general motion processing – a differentiation that might be supported by individual developmental trajectories as indicated by CC research discussed previously.

The human brain is equipped with highly specialised systems that are dedicated to processing complex and ecologically significant visual categories such as faces, objects, body parts, places, characters, and numbers. This functional specialisation plays a crucial role in visual categorisation and recognition, resulting in highly efficient visual processing. Among these categories, faces are particularly important for providing social information as they enable us to distinguish one individual from another, understand their emotions, and identify potential mates. As a result, face perception has been identified as an ecologically and evolutionarily significant phenomenon in a variety of species (Weiner & Grill-Spector, 2015). Given its significance, face processing has been extensively studied in the field of neuroscience and hence it is unsurprising that face processing is also intensively examined in CC individuals as it provides crucial insights into the extent of experience-dependent development of the face processing system. As already elaborated earlier, extensive research investigated face processing in CC individuals on a behavioural level (for example Mondloch et al., 2003). The evidence derived from such studies suggests that while simple tasks such as face detection recover after early visual deprivation, more complex aspects of face processing, such as face recognition under difficult circumstances, face identity processing, or holistic face processing, were reported to be impaired in CC individuals (Geldart et al., 2002; Le Grand et al., 2001; Mondloch et al., 2003; Putzar, Hötting, et al.,

2010). However, compared to the rather extensive behavioural evidence, comparably little is known about the effects of early visual deprivation on the neuronal mechanisms of face processing. While some evidence focused on individual aspects of face processing, such as lip-reading (Putzar, Goerendt, et al., 2010), other studies focused on the general, categorical processing of faces (Grady et al., 2014; Mondloch et al., 2013; Röder et al., 2013). Research on categorical face processing indicated that CC individuals exhibit reduced functional specialisation in the neural face processing system (Grady et al., 2014; Röder et al., 2013). In 2013, Röder and colleagues investigated the N170 ERP component, which is associated with face processing (Eimer, 2011; Gao et al., 2019). While normally sighted individuals exhibited the expected increase in the amplitude of the N170 in response to faces, CC individuals exhibited the same amplitude for faces, objects, and scrambled versions of both categories (Röder et al., 2013). Preliminary fMRI evidence indicated that CC individuals activated the same network of face-sensitive regions as normally sighted individuals, but exhibited reduced activation for faces (Grady et al., 2014). Additionally, a lack of similar impairments for the processing of places (Grady et al., 2014) might suggest that these impairments are specific to the recognition of faces that early visual deprivation uniquely affects face processing. Both studies cited here strongly emphasise the importance of early visual experience for the typical development of face-specific processing and indicate that early visual deprivation leads to long-lasting impairments in face processing. This evidence is in line with more recent findings derived from non-human primates (Arcaro et al., 2017), thereby indicating that there is a sensitive period for face-selective development.

While the studies cited in this section provide intriguing initial evidence concerning impaired categorical face processing in CC individuals, the research has not yet assessed important key aspects of categorical processing. Within the human visual cortex, the ventral temporal cortex (VTC) was shown to play a central role in the highly specialised processing of categorical visual stimuli (Grill-Spector & Weiner, 2014). MRI research indicated that within the VTC, visual categories are represented in two complementary manners, namely as distinct clusters of category-selective activation, and as distributed patterns of activation across the entire VTC (Grill-Spector & Weiner, 2014). These two organisation principles have also been referred to in the context of univariate and multivariate analysis approaches, respectively. The classical univariate analysis identifies distinct modules based on their functional selectivity, i.e. they display higher responses to a specific category of stimuli than others. A variety of such distinct functional regions was identified within the entire human visual cortex of which many are located within the VTC. In normally sighted individuals, regions such as the fusiform face area (FFA), the occipital face area (OFA), and the superior temporal sulcus (STS) were implicated in face-selective processing (Kanwisher et al., 1997; Pitcher et al., 2011) whereas the fusiform body area (FBA) and the EBA was associated with body-selective processing (Downing et al., 2001; Peelen & Downing,

2005). Furthermore, object-selective processing was located within the lateral object complex (LOC; Kourtzi & Kanwisher, 2000; Malach et al., 1995), while the parahippocampal place area (PPA) and the transverse occipital sulcus (TOS) are implicated in place- and scene-selective processing (Aguirre et al., 1998; Epstein & Kanwisher, 1998; Grill-Spector, 2003).

In contrast to the classical univariate analysis, which identifies distinct modules by their functional selectivity, multivariate analyses, such as the multivariate pattern analysis (MVPA), propose that categorical organisation is characterised as a distributed system rather than merely being the sum of distinct functionally specific areas (Haxby et al., 2001; Op De Beeck et al., 2008). Evidence for a large-scale map distinguishing between inanimate and animate visual categories has been reported (Kriegeskorte, Mur, Ruff, et al., 2008), with higher responses to animate stimuli in the lateral VTC and to inanimate stimuli in the medial VTC (Proklova et al., 2016). The differentiation between medial and lateral VTC was further underlined by reported differences in cytoarchitectonic properties (Gomez et al., 2017; Weiner et al., 2014, 2017) and connectivity (Osher et al., 2016; Saygin et al., 2012, 2016) and was claimed to be independent of methodological characteristics such as spatial resolution (Margalit et al., 2020). More importantly, sparsely distributed activation patterns across the VTC have also been reported for individual categories such as faces and objects (Haxby et al., 2001; Ishai et al., 1999), bodies (Weiner & Grill-Spector, 2010), and scenes (Cox & Savoy, 2003).

It is important to note that the multivariate view does not contradict the existence of category-selective regions. More specifically, Haxby et al. (2001) indicated that the classification of visual categories is successful even when excluding these selective regions, which emphasises the amount of categorical information present in the entire VTC. Interestingly, the same specific category-selective regions contained enough information on other, non-preferred visual categories to ensure correct classification (Haxby et al., 2001) and hence it was suggested that category-selective regions respond rather preferentially than category-exclusively (Ishai et al., 1999). Given the individual insights that both analysis approaches convey, the integration of both methods yields more detailed results. For example, a variety of categorical regions were reported to be involved in the classification of visual categories (Kravitz et al., 2011; Walther et al., 2009) and multiple regions, which had previously been considered as one distinct region, were subsequently divided into multiple clusters based on functional subdomains (Çukur et al., 2016; Weiner & Grill-Spector, 2010). More generally, it was suggested that although category-selective regions serve to distinguish between preferred and non-preferred categories (Kriegeskorte et al., 2007; Spiridon & Kanwisher, 2002), the differentiation between non-preferred categories (Spiridon & Kanwisher, 2002) or individual stimuli of one category (Eger et al., 2008; Kriegeskorte et al., 2007) involves a broader processing system.

Previous studies in CC individuals provided valuable insights into the impaired face-selective processing following early visual deprivation. However, these studies do not fully capture the multifaceted organisation of categorical processing, and their findings are limited in terms of generalisability to other visual categories beyond faces. By employing advanced neuroimaging analyses, the research can provide a more comprehensive understanding of the neural mechanisms underlying visual processing in CC individuals and further elucidate the long-term effects of early visual deprivation on the brain. For example, an MVPA analysis could provide a more nuanced understanding of how early visual deprivation affects the neural representation of different visual categories such as faces, bodies, objects, and scenes. Similarly, a region-of-interest (ROI) analysis could allow for a more detailed investigation of univariate category-selectivity in distinct regions of the brain.

Sensitive periods in humans

Research in CC individuals provides a unique opportunity to investigate sensitive periods in humans and thereby improves our understanding of the experience-driven development of the visual brain. More specifically, such research addresses the question of whether early visual experience is essential for the development of various aspects of visual processing or if these aspects can recover after early visual deprivation. If impairments are observed in CC individuals, despite decades of visual experience, it can be concluded that this aspect of visual development is linked to a sensitive period. In reference to typical developmental trajectories, two types of sensitive periods for visually-driven development have been observed. Accordingly, the effects of early visual deprivation can be direct and immediate, i.e. if a given function cannot develop due to the absence of visual input. For example, in typically sighted infants and children, visual acuity and global motion develop rapidly during the first few weeks after birth (Maurer et al., 2005) and early visual deprivation during this period is considered to prevent the construction of the neural basis of this visual function. However, in addition to immediate effects, the available evidence also indicates that early visual deprivation affects later developing visual functions such as face processing. These delayed effects have been termed *sleeper effects* and it is assumed that early visual experience is essential for the establishment or preservation of neural substrates that form the basis for the later developing function.

Based on the evidence derived from studies in transgenic mice and pharmacological approaches, animal research showed sensitive periods to be directly linked to the synergy of excitatory and inhibitory neural cells, and in this context, specifically linking the onset of sensitive periods has been linked to the maturation of inhibitory innervation (Levelt & Hübener, 2012). An increasing number of studies in humans, both after short-term visual deprivation in an experimental setting (Castaldi et al.,

2020) and subsequent to sight restoration (Raczy et al., 2022; Sourav et al., 2018), are in line with the observation that plasticity might be mediated by changes in the balance between excitatory and inhibitory circuits of the visual cortex. In CC individuals, a growing body of evidence implicates an imbalance between the excitatory and inhibitory systems and, more specifically, reduced alpha oscillatory activation has been reported in both children (W. Chen et al., 2021) and adults (Bottari et al., 2016) who experienced early visual deprivation. Significantly, alpha oscillation was previously identified as a neural marker for the inhibition of task-irrelevant neural processing (Jensen et al., 2012) and a reduced alpha oscillation in CC individuals might therefore suggest an altered excitatory-inhibitory balance, which is in line with more recent fMRI evidence concerning altered resting-state functional connectivity (Raczy et al., 2022). Impaired inhibition was also proposed to contribute to other visual impairments in CC individuals. For example, CC individuals presented an altered C1 effect (Sourav et al., 2018) and a reduced face-selective activation that may be attributed to a failed inhibitory response to other categories (Grady et al., 2014; Röder et al., 2013).

Other cases of temporary visual deprivation have been examined to further elucidate the effects of visual deprivation. Studies investigating individuals who experienced developmental cataracts or single case studies of individuals suffering from early-onset blindness who experienced long-term visual deprivation due to accidents, address the question of what happens to established visual functions after temporary visual deprivation. In addition to the sensitive periods related to visually-driven development, further evidence suggests that there are also sensitive periods for damage and recovery. Furthermore, as indicated by investigations concerning adult plasticity, the capacity for neuroplastic changes is preserved to a great extent across the lifespan, and well beyond the timepoints characterised as sensitive periods. Numerous studies aimed to establish the extent of residual plasticity, for example, using short-term (monocular) occlusion in normally sighted individuals (for a review see Castaldi et al., 2020) or by mapping changes in the visual organisation after ophthalmologic or neurologic diseases (for a review see Dumoulin & Knapen, 2018).

Summary and Outlook of this Dissertation

The neurodevelopment of the visual processing system is influenced by various factors such as genetics, the environment, and experience. Several studies, both in non-human animals and humans, have indicated that some aspects of visual processing develop without visual experience (Striem-Amit et al., 2015; van den Hurk et al., 2017) and are therefore considered to develop experience-independently. In contrast, numerous aspects of visual processing were shown to follow a prolonged developmental trajectory (Casey et al., 2005; Grill-Spector et al., 2008), which is considered an indication of experience-dependent development, whereby especially early visual experience is considered crucial for typical development and has been characterised by sensitive periods (Röder & Kekunnaya, 2021). Atypical visual experience during sensitive periods, such as early visual deprivation, was reported to result in a variety of long-lasting impairments in behaviour, and structural and functional brain organisation (Röder & Kekunnaya, 2021). The aim of this dissertation was to further investigate sensitive periods in visual development and thereby disentangle experience-dependent and experience-independent developmental trajectories for visual development. To this end, a group of unique individuals who experienced a transient phase of congenital visual deprivation due to dense bilateral cataracts (CC individuals) were investigated. In the context of two individual studies, the research presented in this dissertation aimed to investigate the impact of early visual deprivation on the structural and functional organisation of the visual brain through the analysis of MRI data.

The goal of Study 1 (Chapter 2) was to itemise and merge previous reports on structural differences in CC individuals, whereby previous studies reported impaired cortical thickness and surface area following early visual deprivation. The study presented here used advanced ultra-high field structural MRI data to compare cortical thickness and surface area on a submillimetre resolution in CC individuals and normally sighted controls. To address previous methodological differences and provide a basis for integrating the relevant research findings, the two different analysis approaches previously used for the comparison between structural measurements were incorporated, namely a vertex-wise analysis and a ROI analysis approach. Based on previous results (Feng et al., 2021; Guerreiro, Erfort, et al., 2015; Hölig et al., 2022), it was hypothesised that CC individuals would exhibit increased cortical thickness and decreased surface area within the early visual cortex in comparison to normally sighted controls indicated by both analysis approaches.

Study 2 (Chapter 3) investigated the effects of early visual deprivation on visual categorical processing of ecological categories such as faces, bodies, objects, and scenes. As previously described, categorical processing within the VTC is organised in two complementary manners: firstly, distributed as a pattern of activation across the ventral temporal cortex and secondly, in distinct clusters of category-selective

activation. Prolonged developmental trajectories for categorical selectivity, especially for faces, have suggested an experience-dependent development that is reliant on accumulated experience with age, whereby the importance of experience is also emphasised by findings long-lasting face-selective impairments in CC individuals. However, accumulating evidence indicates that the development of categorical processing does not solely depend on experience (Kosakowski et al., 2022; van den Hurk et al., 2017). To further identify experience-independent and experience-dependent developmental trajectories of categorical processing, Study 2 investigated the effects of early visual deprivation on the categorical processing of faces, bodies, objects, and scenes and specifically addressed the question if distributed representation and category-selectivity are affected differently. Based on studies in congenitally blind individuals, it was suggested that basic categorical organisation in the form of distributed representations develops independently of experience (van den Hurk et al., 2017) and hence it was anticipated that CC individuals would present the same large-scale categorical organisation as normally sighted individuals. In accordance with findings concerning face-selective impairments (Grady et al., 2014; Röder et al., 2013), it was further hypothesised that CC individuals exhibit distinct yet reduced category-selective responses for all tested categories.

This dissertation incorporated various methodological approaches to expand and refine the existing knowledge concerning CC individuals, thereby aiming to enhance our understanding of the extent to which visual brain development depends on visual experience, and further explore the potential for recovery when typical visual experience is reintroduced later in life. By investigating the interplay between early visual deprivation, brain development, and potential recovery in CC individuals, this research provides valuable insights into the intricate and dynamic process of neuroplasticity and contributes to the existing understanding of how the brain develops.

Chapter II

The Effects of Early Visual Deprivation on the Structural Organisation of the Human Brain

1. Introduction

Extended visual deprivation from birth has been shown to result in long lasting impairments in visual and multisensory processing (Lewis & Maurer, 2005, 2009; Röder & Kekunnaya, 2021, 2022). These findings have been interpreted as evidence of sensitive periods in brain development. Sensitive periods are thereby defined as epochs in life during which the brain is highly susceptible and the impact of sensory experience is particularly strong (Knudsen, 2004; Levelt & Hübener, 2012). In humans, visual sensitive periods have been studied in individuals who were born blind due to dense bilateral cataract and who regained sight later in life due to cataract removal surgery, hence referred to as CC individuals (Röder & Kekunnaya, 2021).

The main body of research on CC individuals focused on behavioural changes (Guerreiro et al., 2016b; Putzar, Hötting, et al., 2007; Sourav et al., 2019) as well as changes in functional processing across various sensory modalities, including visual processing (Grady et al., 2014; Röder et al., 2013; Sourav et al., 2018) and other senses (Bottari et al., 2018; Collignon et al., 2015; Dormal et al., 2015; Guerreiro, Putzar, et al., 2015; Putzar, Goerendt, et al., 2007). Accumulating evidence emphasises the importance of early visual experience for structural development as well (Brockhaus et al., 2022; Feng et al., 2021; Guerreiro, Erfort, et al., 2015; Hölig et al., 2022). Similar to studies in blind individuals (reviewed in Paré et al., 2023), these studies reported increased cortical thickness (Guerreiro, Erfort, et al., 2015; Hölig et al., 2022) as well as reduced surface area (Brockhaus et al., 2022; Hölig et al., 2022) in CC individuals compared to normally sighted control (SC) individuals. Therefore, it could be concluded that not only the permanent absence of vision affects brain structure (Anurova et al., 2015; Park et al., 2009). Particularly early visual experience seems important for the typical development of brain structure, indicating a sensitive period for structural development (Röder & Kekunnaya, 2022). Furthermore, newest evidence links these structural alterations to functional changes in CC individuals, such as altered resting-state connectivity (Feng et al., 2021) and retinotopic organisation (Brockhaus et al., 2022).

Especially in light of such a close interplay of structural and functional development, the importance of early visual experience on structural brain development, might relate closely to the rapid pace of postnatal structural changes within the first two years after birth. More specifically, at the age of only two years the infant brain exhibits on average 97% of adults' cortical thickness values (Lyall et al., 2015). In fact, spatial distribution of cortical thickness is already largely present at birth (G. Li et al., 2015). Moreover, within the first two years after birth, surfaces area increases 115% on average and reaches on average 69% of the adult values. Nevertheless, both cortical thickness and surface area have been reported to exhibit individual developmental trajectories and regional growth patterns of both structural measurements differed substantially (Lyall et al., 2015; Wierenga et al., 2014).

Accordingly, increasing evidence indicates that different genetic (C. H. Chen et al., 2013; Fjell et al., 2015; Panizzon et al., 2009), environmental (Raznahan et al., 2012; Sanders et al., 2022) and experience-dependent processes (Shaw et al., 2008; Sowell et al., 2004) likely drive the development of cortical thickness and surface area. Although development of brain structure has been generally linked to functional development (Gomez et al., 2017; Natu et al., 2019; Sowell et al., 2004), it was suggested that particularly the development of cortical thickness is functionally driven (C. H. Chen et al., 2011; Gogtay et al., 2004; Krongold et al., 2017; Valk et al., 2020; Westlye et al., 2010). A difference in experience-dependence might also introduce the idea that cortical thickness and surface are affected differently by early visual deprivation.

Recent advances in ultra-high field imaging, such as 7T MRI, have enabled submillimetre measurements. The advanced imaging resolution has been used to address mesoscopic functional organisation, including cortical laminae and columns (De Martino et al., 2018; Dumoulin et al., 2018) both for early visual processing (de Hollander et al., 2021) as well as for higher-level functional processing (Margalit et al., 2020). More recently, submillimetre MRI was also used to re-evaluate evidence for structural reorganisation in congenitally blind individuals (Kupers et al., 2022).

In contrast to findings in blind individuals, the reported findings in CC individuals are more selective and less consistent. For example, both increased as well as reduced cortical thickness has been reported in the visual cortex and impairments seem to manifest differently across hemispheres (Feng et al., 2021; Guerreiro, Erfort, et al., 2015; Hölig et al., 2022). Additionally, reports differ in their reported correlation of cortical thickness and visual acuity (Feng et al., 2021; Hölig et al., 2022). Results for surface area are more scarce or highly specific in terms of regions (Brockhaus et al., 2022; Hölig et al., 2022). As similar as these studies are in their conclusion that early visual deprivation does affect brain structure, they are, nevertheless, difficult to compare given the different methodological approaches they deployed. Prior studies have evaluated structural findings in CC individuals based on 3T and 1.5T structural MRI data (Feng et al., 2021; Guerreiro, Erfort, et al., 2015; Hölig et al., 2022) and applied resampling techniques to improve resolution (Guerreiro, Erfort, et al., 2015; Hölig et al., 2022). Furthermore, group differences were either computed at the vertex level (Guerreiro, Erfort, et al., 2015) or based on regions-of-interest (ROI) (Feng et al., 2021; Hölig et al., 2022). It remains therefore unanswered if there are indeed differentiated effect of early visual deprivation and how they manifest when methodological differences are set aside.

To address these methodological gaps in knowledge, submillimetre resolution structural MRI data was acquired in a group of CC individuals, who experienced early visual deprivation for a minimum of 6 months. The data of the CC individuals was compared to normally sighted controls (SC individuals) to assess the effects of early visual deprivation. In order to rule out that possible group differences, were founded in residual visual impairments as commonly observed in CC individuals, an additional third group was tested. This group consisted of visually impaired controls (VI individuals) who had pattern vision at birth yet had other congenital or acquired visual impairments. Furthermore, the two common analysis approaches for structural analyses, a vertex-wise as well as a ROI analysis were incorporated to compare cortical and surface area as two independent structural measurements of brain organisation.

Based on previous studies (Guerreiro, Erfort, et al., 2015; Hölig et al., 2022), it was predicted to find increased cortical thickness the early visual cortex of CC individuals compared to SC individuals indicated both in the vertex-wise as well as the ROI analysis. No group differences in cortical thickness were expected for the comparison of VI individuals to SC individuals. Additionally, based on previous studies (Brockhaus et al., 2022; Hölig et al., 2022), it was hypothesised that CC individuals, yet not VI individuals, would exhibit reduced surface area in comparison to SC individuals, indicated by both the vertex-wise as well as the ROI analysis.

2. Methods

Participants

The study at hand was part of a larger project consisting of two MRI sessions, one in 3T and one in 7T MRI and one behavioural session to determine visual and auditory acuity. For the study at hand only structural 7T data was analysed.

To assess the effect of a temporary congenital visual deprivation, we recruited individuals with a history of complete, dense and bilateral congenital cataract (CC) which was removed after the sixth month. Eight CC individuals (age range 32 – 48 years, *M*age = 42 years, SD_{age} = 6; 5 female) participated in the present study. The CC individuals underwent the cataract-removal surgery at an average age of 20.6 months (range 6 and 48 months). At testing, average visual acuity in the better eye measured with the Freiburg Visual Acuity & Contrast Test (FrACT) was 0.65 logMAR (SD_{acuity} = 0.37 logMAR, range: 0.16 – 1.27 logMAR). For this measurement, participants wore their typical visual aids (i.e., glasses or contact lenses). For scanning, special glasses were ordered according to each individual's prescription. ***Table 1*** contains detailed information of individuals' visual characteristics. All CC individuals were recruited in Germany based on previous study contacts or via a collaboration with the eye clinic of the UKE Hamburg, Germany. To distinguish between the effects of early visual deprivation and residual visual impairment, as commonly observed in CC individuals, we recruited an additional group of visually impaired (VI) individuals who had pattern vision from birth in at least one eye. We tested four VI individuals (age range 19 to 32 years, M_{age} = 23.5, SD_{age} = 5.0; all female; one left handed). Detailed description of their visual characteristics can be found in ***Table 1***. All VI individuals have been recruited in Hamburg, Germany, via e-mail list of the University of Hamburg for handicapped students as well as sport and social groups for blind and visually impaired individuals. A group of 18 sighted controls (SC) was recruited (age range 21 to 56 years, M_{age} = 36.1, SD_{age} = 9.8; 11 female). Eight of these 18 individuals were matched (mSC_{CC}) in age and gender to the CC participants (age range 31 - 56 years, *M*age = 42.0 years, SD_{age} = 6.9; 5 female). Average visual acuity of these mSC_{CC} participants was -0.15 logMAR (*SD*Acuity = 0.16 logMAR, range: -0.30 – 0.22 logMAR). We also matched seven SC individuals in gender and age to the VI individuals (mSC_{VI}: age range 21 to 36 years, *M*age = 26.6, SD_{age} = 4.9; all female; one left handed). SC individuals were mainly recruited in Maastricht, the Netherlands by advertisement flyer across the university campus and sport centres in the city of Maastricht. Due to difficulties in finding appropriate age matches for the CC individuals, two SC individuals were recruited in Germany based on previous study contacts.

Two additional datasets had been acquired but excluded from analysis. One SC individual had two structural scans due to technical reasons, of which only the qualitatively better scan was included and another SC individual had to be excluded due to extensive motion. All participants, regardless of

group, had normal hearing, normal tactile function, without history of neurological or psychological disorders, and eligible for MRI scanning (e.g., no metallic implants, intrauterine devices, non-removable jewellery, history of claustrophobia, heart or circulatory problems). The study was approved by the local ethics committee for the Faculty of Psychology and Human Movement Science, University Hamburg, in 2018. Each participant gave written informed consent for participating in this study and received reimbursement for travel costs and some monetary compensation for their participation.

Table 1.

Participant Characteristics and Clinical Information of Congenital Cataract (CC) and Visual Impaired (VI) Individuals.

ID	Age at testing (years)	Sex	handedness	Age at surgery (month)	Visual acuity in the better eye (logMAR)	Self-reported visual impairments
CC1	34	male	right	12	0.63	Aphakia
CC2	45	male	right	24	0.16	Aphakia, impaired stereopsis
CC3	48	female	right	48	0.58	Aphakia, impaired stereopsis and visual field
CC4	45	female	right	9	0.68	Pseudoaphakia, nystagmus, treated glaucoma, impaired visual field and stereopsis
CC5	32	female	right	24	0.18	Aphakia
CC6	46	female	right	24	1.27	Aphakia, microphthalmia, nystagmus, impaired visual field and stereopsis
CC7	46	female	right	18	1.16	Aphakia, monocular enucleation, nystagmus, impaired visual field and stereopsis
CC8	40	male	right	6	0.56	Aphakia, nystagmus, impaired visual field and stereopsis; right eye: holey iris and underdeveloped pupil, left eye: narrowed pupil and shifted vision
VI1	22	female	right		-0.06	macular inflammation
VI2	32	female	right		0.74	monocular congenital cataract
VI3	21	female	right		0.97	binocular aniridia
VI4	19	female	left		0.91	squint, astigmatism, visual field loss, suspicion of cone dystrophy and macular degeneration

Data acquisition and preprocessing

Submillimetre structural images were acquired on a 7T Siemens Magnetom equipped with a 32-channel head coil, applying an MP2RAGE sequence (240 slices, voxel size: 0.7 mm^3, TR: 5000 ms, TE: 2.47 ms, acquisition matrix: 320 x 320, FoV: 224 x 224, flip angle 1: 5°, flip angle 2: 3°). Due to strong intensity inhomogeneities in the magnetic field of 7T imaging, the original structural images were intensity bias-corrected using the unified segmentation algorithm (Ashburner & Friston, 2005) implemented in SPM 12 (Friston et al., 2007). For the bias-correction, custom parameters were applied (full-width-half-maximum/FWHM = 18 mm, sampling distance = 2 mm) following official recommendations for submillimetre processing in FreeSurfer (Zaretskaya et al., 2018). The resulting

corrected images were further processed using the neuroimaging package FreeSurfer, version 7.1.1 (http://surfer.nmr.mgh.harvard.edu/) and its default automated reconstruction procedure "recon-all" with the additional "-hires" flag for better high resolution surface reconstruction. The procedure has been described in detail for example in Fischl & Dale (2000). In short, the automated processing pipeline includes removal of non-brain tissue (Ségonne et al., 2004), Talairach transformation and volumetric segmentation of subcortical white and grey matter structures (Fischl et al., 2002, 2004), intensity normalization (Sled et al., 1998), tessellation of white and grey matter boundaries and topology correction (Fischl et al., 2001; Ségonne et al., 2007). Furthermore, surface inflation and registration of a spherical atlas based on individual cortical folding pattern to match cortical geometry (Fischl, Sereno, & Dale, 1999; Fischl, Sereno, Tootell, et al., 1999) have been performed. Before quantitative analyses could be performed, surface reconstructions were visually inspected and manual corrections were made where needed. Corrections followed standard procedures as documented on the FreeSurfer website (https://surfer.nmr.mgh.harvard.edu/fswiki/FsTutorial/TroubleshootingData) and included mainly the removal of remaining skull or dura and occasionally filling in undetected white matter voxels.

The resulting surface-based maps included vertex-wise data on cortical thickness and surface area. Cortical thickness was thereby calculated at each vertex as the closest distance from the grey matter-white matter boundary to the grey matter-cerebrospinal fluid (CSF) boundary (Fischl & Dale, 2000). White matter surface area was calculated vertex-wise as the average area of adjacent triangles of each vertex. For the group analyses, the individual cortical thickness and surface area maps were resampled to the FreeSurfer group template *fsaverage* resulting in a single group file per measurement and hemisphere. Group maps were subsequently smoothed with a 10 mm FWHM Gaussian kernel within the early visual cortex.

Statistical analysis

For further statistical analyses, the cortex was parcelled using the multi-modal brain atlas by Glasser et al. (2016) and a mask was used to restrict the analysis to the early visual cortex consisting of the bilateral regions V1, V2, V3 and V4. Within the early visual cortex two different analysis approaches were chosen to run group comparisons: First, a vertex-wise analysis was performed as implemented in FreeSurfer based on the smoothed early visual cortex group maps. Second, an external ROI analysis was calculated based on extracted structural measurements. Both analyses will be explained in more detail below.

Vertex-Wise Analyses

To investigate the effects of early visual deprivation on brain structure, cortical thickness and surface area were compared between the CC group and age- and sex-matched SC individuals (mSC_{CC}) – hence referred to as matchedCC-model, by fitting linear mixed models at each vertex using FreeSurfer. To exclude the possibility that group differences were driven by residual impairments rather than early visual deprivation, both structural measurements were also compared between the VI group and seven SC individuals matched in age and sex (mSC_{VI}), hence referred to as matchedVI-model. Due to the small sample sizes, we decided to additionally compared the CC group to all tested SC individuals (n = 18) in a model that included all three groups and age as variable of no interest, hence referred to as allSC-model. Previous research indicated that cortical surface area is highly influenced by one person's head size, respectively overall brain volume (Buckner et al., 2004). Therefore, according to general recommendations, we included estimated total intracranial volume (eTIV) as normalised covariate in all analyses of surface area. To reduce the probability of type I errors, all resulting t-value maps were entered in cluster-wise correction for multiple comparisons as implemented in FreeSurfer (Greve & Fischl, 2018). Permutation simulations were run with 1000 iterations to estimate the distribution of the maximum cluster size under the null hypothesis with a vertex-wise threshold $p < .01$ (two-sided). Clusters with a cluster-wise probability of $p < .05$ were regarded as significant.

As indicated by Hölig et al. (2022), age might have a differentiated effect on the structural measurements in CC individuals compared to SC individuals. For the allSC-model, we therefore calculated correlations between each structural measurement and age per group by fitting general linear mixed models at each vertex separately for cortical thickness and surface area. The model included group as factor and age as normalised covariate. Model slopes were compared in order to test if correlations of age and cortical thickness or surface area differed between groups. Cluster-wise correction for multiple comparisons was performed as already described with a vertex-wise threshold of $p < .01$ (two-sided) and a cluster-wise threshold of $p < .05$. For surface area, we again controlled for head size by including eTIV as normalised covariate. If group differences were indicated, group specific correlations were calculated additionally to allow for a qualitative assessment of the observed group difference. Additionally, we calculated exploratory correlations between each structural measurement, i.e. cortical thickness and surface area, with visual acuity by fitting general linear models separately for each structural measurement at each vertex of the early visual cortex.

ROI analyses

Individual mean cortical thickness and surface area values for each parcellation of the HCP atlas by Glasser et al. (2016), were obtained using FreeSurfer's aparcstats2table command, separately for cortical thickness and surface area. This resulted in one file per measurement and hemisphere, containing average values per region and subject. Further analyses were conducted in R Statistical Software (v4.2.0; R Core Team, 2022) and the data of early visual regions, i.e. bilateral V1 to V4, were selected. To ensure comparability with the vertex-wise analysis, we again focused the group comparisons on the three previously described subject model, i.e. matchedCC-model (CC vs. mSC_{CC}), matchedVI-model (VI vs. mSC_{VI}), and allSC-model (CC vs. allSC).

Linear mixed models were fitted using the *lme4* package version 1.1-29 (Bates et al., 2015). For cortical thickness, the model included group (2 levels: CC vs. mSC_{CC}, VI vs. mSC_{VI} or CC vs. allSC, respectively), hemisphere (2 levels: left, right), their interaction as fixed factors and participant as a random factor. The model specification for both matched models was as follows: cortical thickness (in mm) ~ group*hemisphere + (1|participant). For the allSC-model, we examined a possible effect of age by additionally including normalised *age* as fixed effect as well as the *group*age* interaction. The model specification was accordingly: cortical thickness ~ group*hemisphere + group*age + (1|participant). The models for comparing surface area resembled the cortical thickness models, except that they also controlled for head size. All surface area models therefore additionally included normalised *eTIV* as fixed effect as well as the interaction between *group* and *eTIV*. The model specification for the matched-models was as follows: surface area (in mm^2) ~ group*hemisphere + group*eTIV + (1|participant). The model specification for the allSC-model was: surface area ~ group*hemisphere + group*eTIV + group*age + (1|participant). All models that included age and/or eTIV have also been tested including all possible interaction effects as opposed to the specifically defined interaction terms. However, the comparisons of model-fit did not indicated significant differences, which is why the less complex models, as described above, have been selected. Degrees of freedom, *F*-test values and *p*-values were estimated with the Kenward-Roger method (*lmerTest* package, Kuznetsova et al., 2017). For each of the models, η_p^2 was estimated as effect size measurement using the package *effectsize* (Ben-Shachar et al., 2020). Pairwise comparisons of estimated marginal means were calculated using the package *emmeans* (Lenth, 2022). For the CC group, we again calculated exploratory correlations of cortical thickness and surface area, respectively, with visual acuity, separately for each region. Pearson's correlation coefficients and *p*-values were estimated using the package *psych* (William Revelle, 2023).

3. Results

Vertex-wise Analysis of Cortical Thickness

Our analysis did not show significant differences between CC individuals and normally sighted individuals, neither for the matchedCC-model, nor the allSC-model. However, on an uncorrected level, multiple clusters indicated higher cortical thickness in CC individuals compared to allSC individuals in the bilateral V1 (**Figure 1**; left hemisphere: cluster 1 - cluster size = 244 mm^2, number of vertices = 299, cluster 2 - cluster size = 67 mm^2, number of vertices = 135, cluster 3 - cluster size = 27 mm^2, number of vertices = 32 mm; right hemisphere: cluster size = 93 mm^2, number of vertices = 102; vertex-wise threshold of $p < .01$, uncorrected for multiple comparison). None of the clusters remained significant after correction for multiple comparisons ($p > .05$). The comparison of VI individuals to matched sighted controls (mSC_{VI}) did not indicate significant group differences. There were no clusters indicated on the vertex-wise-threshold of $p < .01$ for either of the matched models. Exploratory whole-brain cortical thickness group maps for all three subject models can be found in the supplementary figure S1.

Figure 1

Group Difference in Cortical Thickness Between CC Individuals and All Tested SC Individuals (allSC)

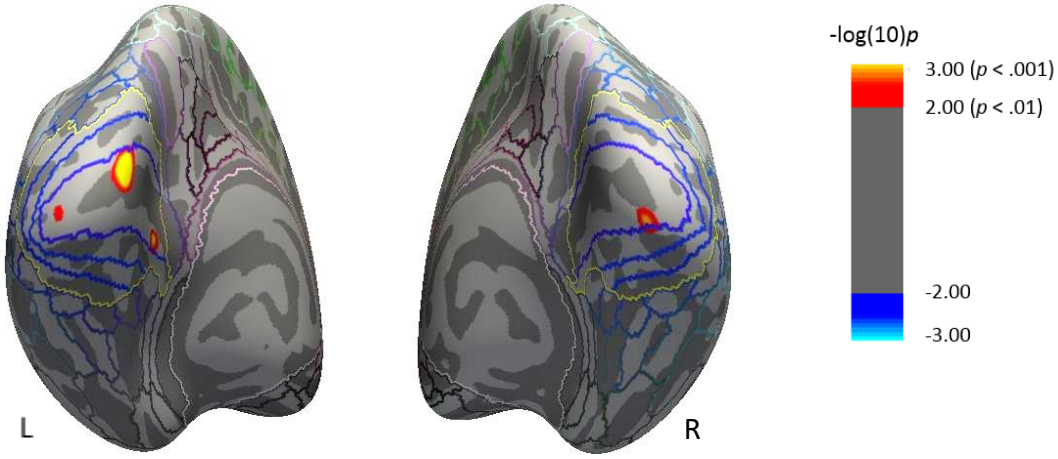

Note. Thresholded statistical significance maps (vertex-wise $p < 0.01$, two-sided, scale bar for both maps at the right side) displaying differences in cortical thickness between CC individuals and allSC individuals ($n = 18$). Maps are superimposed on the inflated surface (dark grey: sulci, light grey: gyri) of the FreeSurfer standard brain. Coloured lines indicate parcellations of the HCP-MMP1.0 atlas (Glasser et al. 2016); the yellow line highlights the early visual cortex. Clusters with higher cortical thickness in the CC group are marked in red and clusters with lower cortical thickness in blue. L = Left hemisphere, R = Right hemisphere.

Exploratory Correlation Analyses

When testing for group differences in the correlation of cortical thickness with age in the allSC-model, three clusters emerged in the left hemisphere (**Figure 2**, A): two clusters in left V1, of which one remained marginally significant after correction for multiple comparison (cluster 1: cluster size = 358 mm^2, number of vertices = 445, $p = .063$; cluster 2: cluster size = 60 mm^2, number of vertices = 100, $p > .05$), and one additional cluster in left V4 (cluster size = 21 mm^2, number of vertices = 31, $p > .05$). The right hemisphere did not indicate a significant group*age interaction.

Correlating cortical thickness with age separately for each group revealed negative correlations in the majority of vertices of left and right early visual cortex in CC individuals (**Figure 2**, B). Accordingly, CC individuals exhibited overall a decrease of cortical thickness with increased age. In SC individuals, on the contrary, correlations of cortical thickness and age were less consistent. More specifically, less vertices showed a correlation of cortical thickness and age, and correlations were not in general not as strong as observed for CC individuals. Additionally, both positive and negative correlations were indicated in the early visual cortex of SC individuals (**Figure 2**, C), indicating that while some vertices exhibited a decrease of cortical thickness with increased age others exhibited an increase.

In the CC group, the exploratory correlation analysis indicated that cortical thickness was negatively correlated with visual acuity in the majority of vertices both in the left and the right early visual cortex (**Figure 3**), which suggests the thicker the visual cortex in CC individuals, the lower their visual acuity.

Figure 2

Thresholded Results of the Correlation Analysis of Cortical Thickness and Age

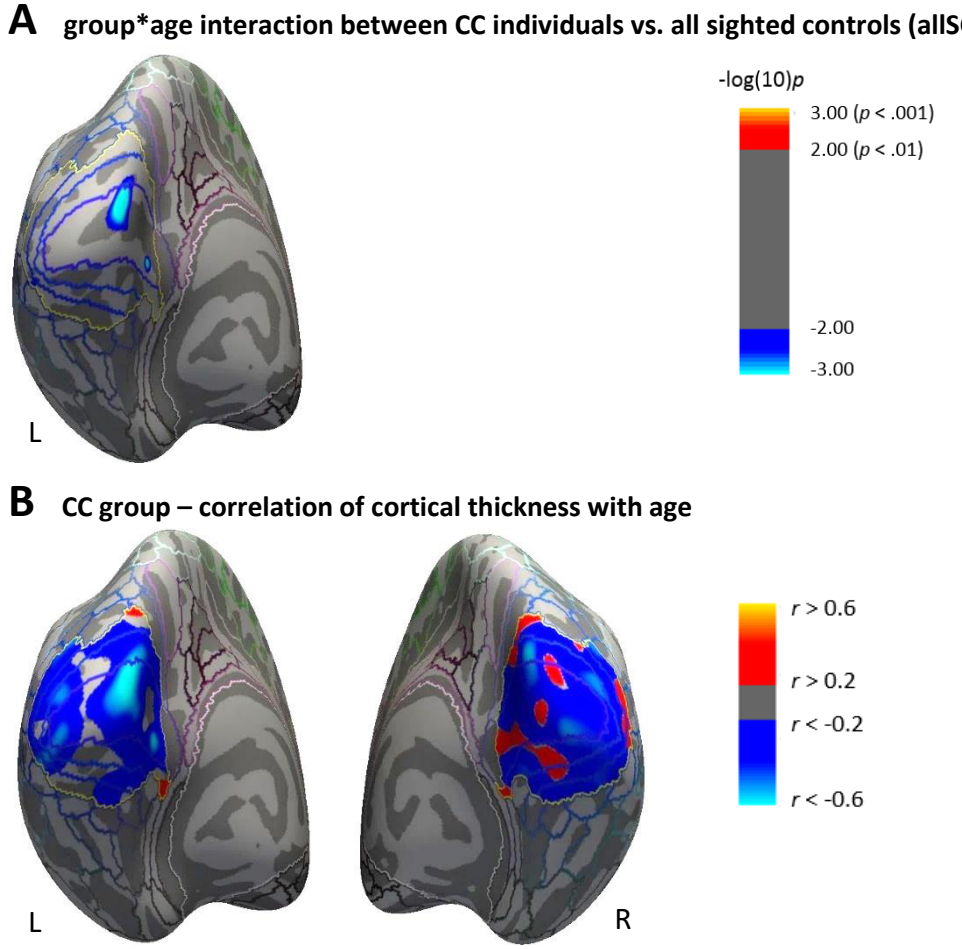

Note. **A.** Thresholded statistical significance maps (vertex-wise p < 0.01, two-sided, scale bar at the upper right side) for the group comparison of CC individuals vs. normally sighted controls (allSC; *n* = 18) of the correlation between cortical thickness and age. Clusters in blue indicate stronger age decline in cortical thickness in the CC group compared to the respective SC group. **B.** and **C.** Maps of correlation coefficients (scale bar for all maps at middle right side) for (**B**) the CC group and (**C**) normally sighted controls (allSC; *n* = 18). Correlation coefficients between -0.2 and 0.2 are not shown, correlation coefficients > 0.6 are shown in yellow, correlations coefficients < -0.6 in cyan. All maps are superimposed on the inflated surface (dark grey: sulci, light grey: gyri) of the FreeSurfer standard brain. Coloured lines indicate parcellations of the HCP-MMP1.0 atlas (Glasser et al. 2016); the yellow line highlights the early visual cortex. L = Left hemisphere, R = Right hemisphere

Figure 3

Results of the Correlation Analysis of Cortical Thickness and Visual Acuity in CC Individuals

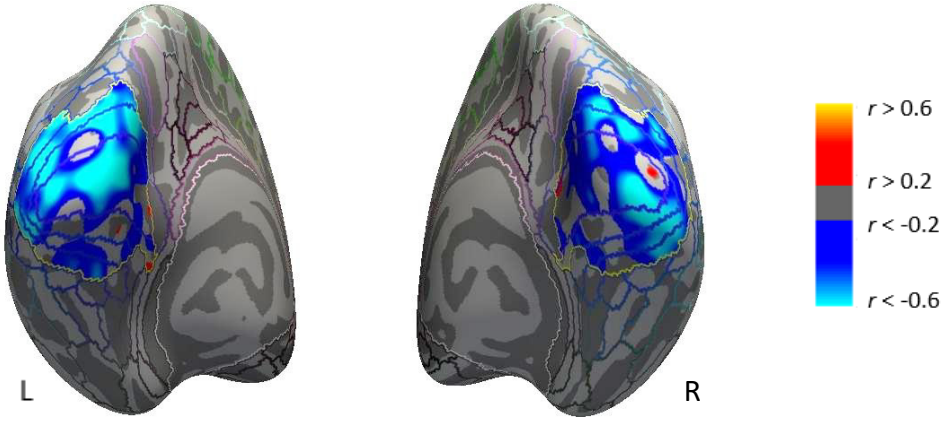

Note. Maps of correlation coefficients between cortical thickness and visual acuity for the CC group (n = 8). Scale bar at right side. Correlation coefficients between -0.2 and 0.2 are not shown, correlation coefficients > 0.6 are shown in yellow, correlations coefficients < -0.6 in cyan. All maps are superimposed on the inflated surface (dark grey: sulci, light grey: gyri) of the FreeSurfer standard brain. Coloured lines indicate parcellations of the HCP-MMP1.0 atlas (Glasser et al. 2016); the yellow line highlights the early visual cortex. L = Left hemisphere, R = Right hemisphere

Vertex-wise Analysis of Surface Area

When comparing surface area between CC individuals to SC individuals, neither the matchedCC-model (CC vs. mSC_{CC}), nor the allSC-model (CC vs. allSC) indicated significant group differences. There were no clusters indicated on the uncorrected vertex-wise-threshold of $p < .01$. On an uncorrected level, there was a cluster indicating lower surface area in VI individuals compared to matched sighted controls (mSC_{VI}) in the right V3 (

Figure *4*, cluster size = 73 mm^2, number of vertices = 88, vertex-wise threshold of $p < .01$, uncorrected for multiple comparison). The cluster, however, did not remained significant after multiple comparisons correction.

Exploratory whole-brain group maps comparing surface area for each of the three subject models can be found in the supplementary figure S2.

Figure 4

Group Difference in Surface Area Between VI Individuals and Matched Sighted Controls (mSC_{VI})

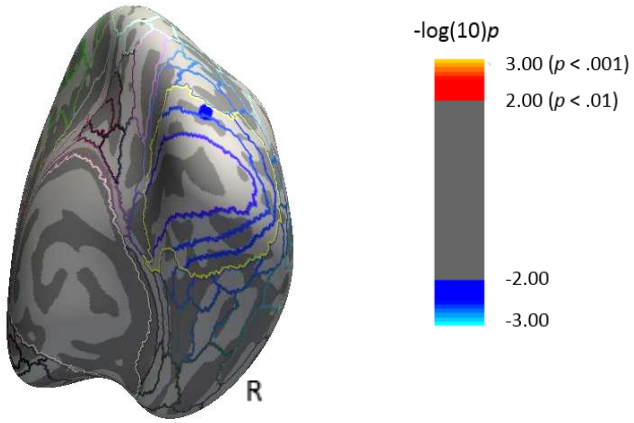

Note. Thresholded statistical significance maps (vertex-wise $p < 0.01$, two-sided, scale bar at the right side) displaying differences in surface area between VI individuals and matched SC individuals (mSC_{VI}) in the right hemisphere. Maps are superimposed on the inflated surface (dark grey: sulci, light grey: gyri) of the FreeSurfer standard brain. Coloured lines indicate parcellations of the HCP-MMP1.0 atlas (Glasser et al. 2016); the yellow line highlights the early visual cortex. Clusters with lower surface area in the VI group are marked in blue. R = Right hemisphere.

Exploratory Correlation Analyses

The exploratory age-analysis indicated no differentiated effects of age on surface area in the allSC-model ($p > .05$). In the CC group, the exploratory correlation analysis revealed clusters of both positive and negative correlation of surface area and visual acuity (**Figure *5***). More specifically, there was a bilateral cluster in the superior part of the early visual cortex in which surface area was negatively correlated with visual acuity, i.e. the greater the surface area in CC individuals, the lower their visual acuity. Additionally, the right hemisphere indicated a cluster of positive correlation in the inferior part of the early visual cortex, such that the smaller the visual cortical surface area in CC individuals, the lower their visual acuity.

Figure 5

Results of the Correlation Analysis of Surface Area and Visual Acuity in CC Individuals

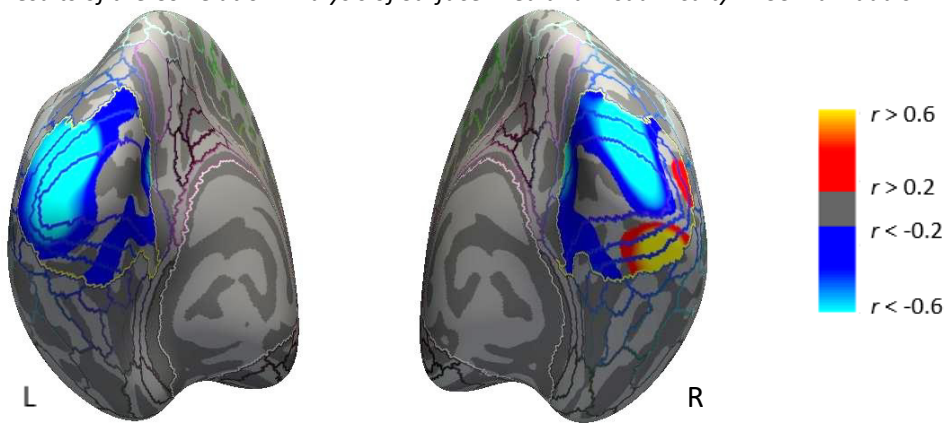

Note. Maps of correlation coefficients between surface area and visual acuity for the CC group ($n = 8$). Scale bar at right side. Correlation coefficients between -0.2 and 0.2 are not shown, correlation coefficients > 0.6 are shown in yellow, correlations coefficients < -0.6 in cyan. All maps are superimposed on the inflated surface (dark grey: sulci, light grey: gyri) of the FreeSurfer standard brain. Coloured lines indicate parcellations of the HCP-MMP1.0 atlas (Glasser et al. 2016); the yellow line highlights the early visual cortex. L = Left hemisphere, R = Right hemisphere

ROI Analysis of Cortical Thickness

For each of the regions of the early visual cortex, cortical thickness was compared for each subject model, i.e. matchedCC-model (CC vs. mSC_{CC}), matchedVI-model (VI vs. mSC_{VI}), and allSC-model (CC vs. allSC). **Figure 6** displays average individual cortical thickness values and group mean values per ROI and hemisphere.

Figure 6

Averaged Individual and Group Mean Cortical Thickness Values per ROI and Hemisphere

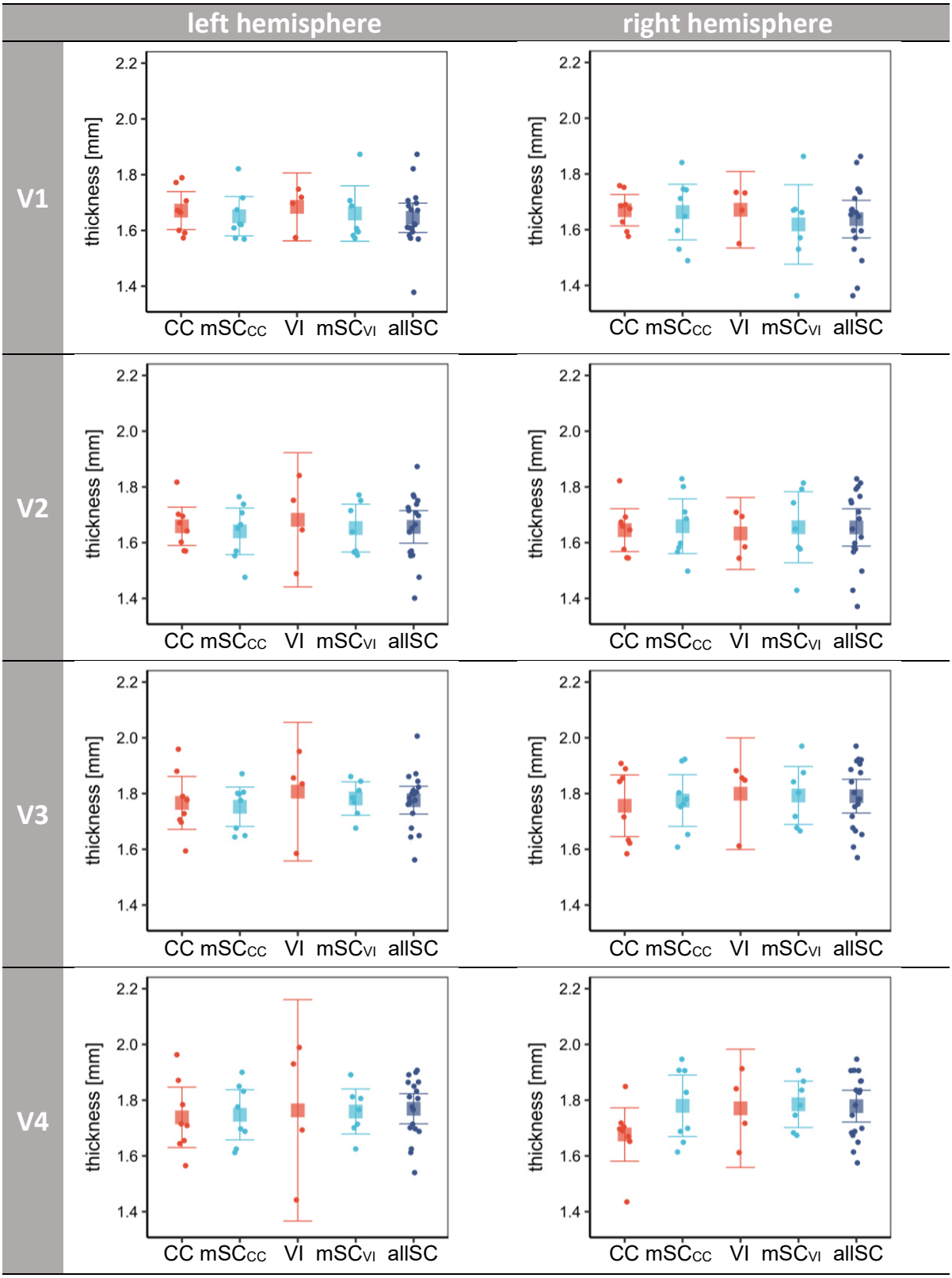

Note. Graphs display average individual (single dots) and group mean (squares) cortical thickness values per ROI and hemisphere. Regions V1, V2, V3 and V4 are depicted from top row to bottom row. The left hemisphere of each ROI is displayed on the left side, the right hemisphere on the right side. Error bars indicate the 95% confidence interval. CC = congenital cataract-reversal individuals (n = 8), mSC_{CC} = sighted controls matched in age and sex to the CC group (n = 8), VI = visually impaired individuals (n = 4), mSC_{VI} = sighted controls matched in age and sex to the VI group (n = 7), allSC = all sighted controls (n = 18).

There were no significant effects when comparing CC individuals to matched sighted controls (mSC_{CC}). The allSC-model, neither exhibited significant group differences for cortical thickness, yet there was a significant interaction of group and age in V4 ($F(1,22) = 4.58$, $p = .044$, $\eta_p^2 = 0.172$). Post-hoc correlation analysis revealed a decrease of cortical thickness with age in CC individuals while SC individuals exhibited a slight increase of cortical thickness with age in SC individuals (**Figure *7***). The comparison of VI individuals and matched sighted controls (mSC_{VI}) did not indicate significant group differences.

Figure 7

Group Specific Correlation of Cortical Thickness and Age in V4.

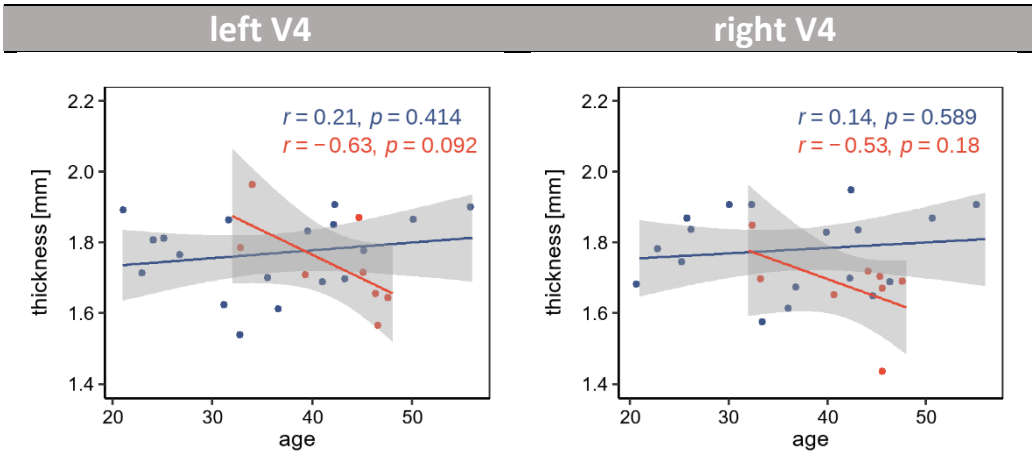

Note. Graphs display average cortical thickness values (single dots) of CC individuals (red) and allSC individuals (blue) separately for the left V4 (left side) and the right V4 (right side). Regression lines and values are displayed in the respective group colour with respective 95% confidence interval (grey band).

Exploratory correlation analysis

The exploratory correlation analysis of cortical thickness and visual acuity indicated negative correlations for each of the region, such that the thicker the early visual cortex in CC individuals the lower their visual acuity (**Table 2**). The correlations of the right V3 and right V4 were significant and the correlations in the left V1 and the left V3 were marginally significant.

Table 2

Region-Specific Correlations of Cortical Thickness and Visual Acuity.

	V1		V2		V3		V4	
	left	right	left	right	left	right	left	right
Pearson's *r*	-0.69	-0.58	-0.62	-0.60	-0.69	**-0.82**	-0.61	**-0.79**
p-value	.057	.129	.104	.113	.060	**.012**	.105	**.020**

Note. Pearson correlation coefficient *r and p-values for each of the eight regions of the early visual cortex. Significant correlations are marked in bold.*

ROI Analysis of Surface Area

Following the ROI-analysis approach, surface area was compared for each subject model, i.e. matchedCC-model (CC vs. mSC_{CC}), matchedVI-model (VI vs. mSC_{VI}), and allSC-model (CC vs. allSC), separately for each of the atlas-defined ROI within the early visual cortex. **Figure 8** displays average individual as well as group mean surface area values per ROI and hemisphere.

Figure 8

Averaged Individual and Group Mean Surface Area Values per ROI and Hemisphere

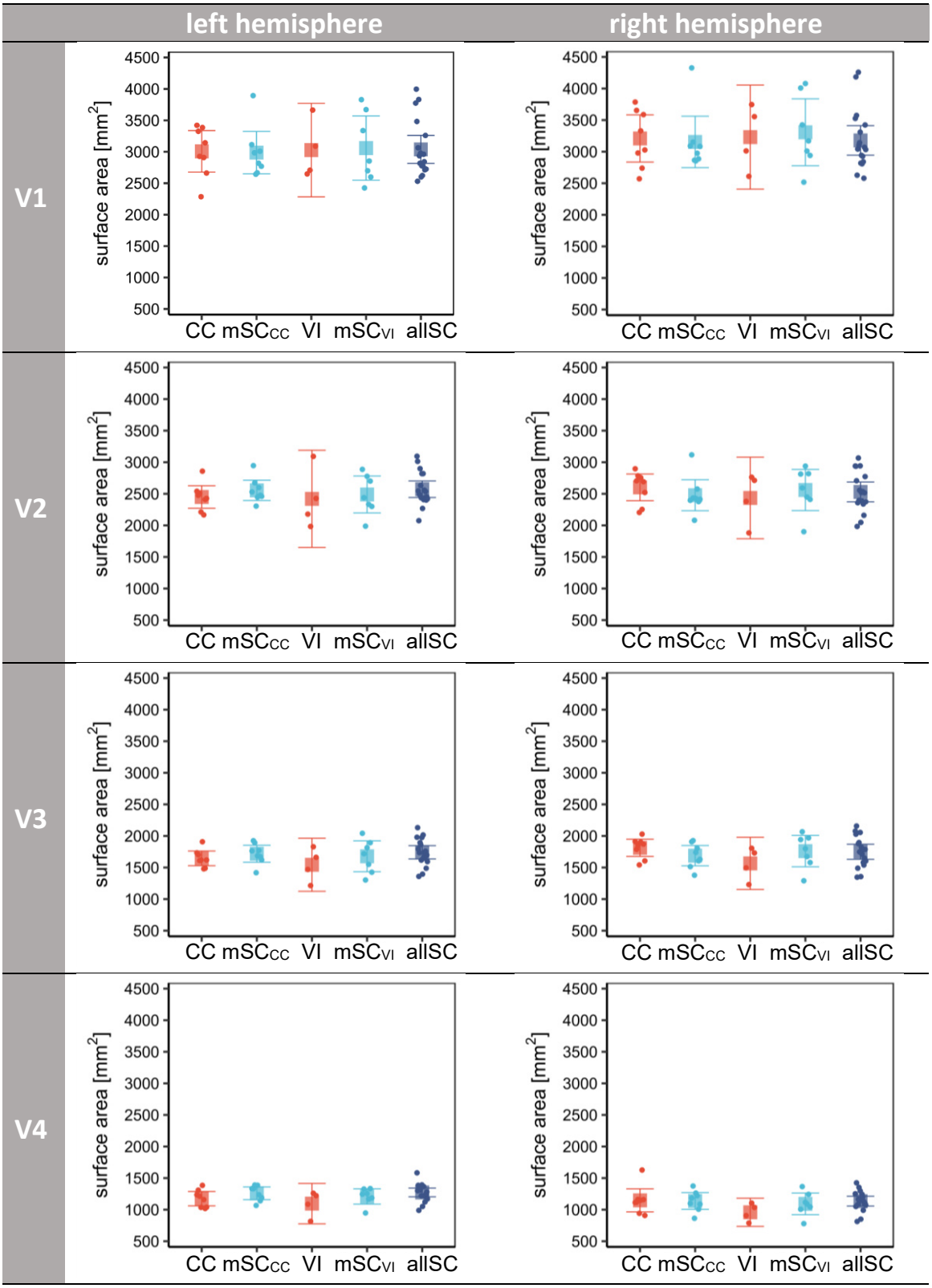

Note. Graphs display average individual (single dots, scaled by head size) and group mean (squares) surface area values per ROI and hemisphere. Regions V1, V2, V3 and V4 are depicted from top row to bottom row. The left hemisphere of each ROI is displayed on the left side, the right hemisphere on the right side. Error bars indicate the 95% confidence interval. CC = congenital cataract-reversal individuals (n = 8), mSC_{CC} = sighted controls matched in age and sex to the CC group (n = 8), VI = visually impaired individuals (n = 4), mSC_{VI} = sighted controls matched in age and sex to the VI group (n = 7), allSC = all sighted controls (n = 18).

CC individuals exhibited group specific differences in surface area mediated by hemisphere when being compared to matched SC individuals. These significant group*hemisphere interactions have been found in V2 (F(1,14) = 10.01, p = .007, η_p^2 = .417) and V3 (F(1,14) = 5.35, p = .037, η_p^2 = .276). Post-hoc comparisons revealed that in both regions CC individuals showed significantly lower surface area in the left than in the right hemisphere (left V2 < right V2, t(14) = - 2.91, p = .011; left V3 < right V3, t(14) = -2.68, p = .018). SC individuals were more likely to show the opposite, i.e. smaller surface area in the right than the left hemisphere, yet the difference did not reach significance (p > .05). Additionally, when comparing groups directly per hemisphere, the matchedCC-model indicated marginally higher surface area in the right V3 of CC individuals compared to mSC_{CC} individuals (t(21) = 1.72, p = .0997). VI individuals did not exhibit group differences in surface area.

Additionally, both matched models exhibited main effects of hemisphere. The matchedCC-model indicated that across all subjects the left V1 (M = 2996, SD = 452) was smaller than the right V1 (M = 3178, SD = 496; F(1,14) = 12.54, p = .003, η_p^2 = .472). This difference in left and right V1 was also observed for the matchedVI-model (F(1,9) = 15.33, p = .004, η_p^2 = .630). Again, surface area in the left V1 (M = 3029 mm^2; SD = 414) was smaller than the right V1 (M = 3258 mm^2; SD = 433). Additionally, for the matchedVI-model there was a main effect of hemisphere in V4 (F(1,9) = 26.26, p < .001, η_p^2 = .745) with surface area being smaller in the right V4 (M = 1044 mm^2; SD = 207) than the left V4 (M = 1165 mm^2; SD = 171).

Similar to the matchedCC-model, the allSC-model confirmed the interaction between group and hemisphere in V2 (F(1,24) = 6.54, p = .017, η_p^2 = .214) and V3 (F(1,24) = 4.62, p = .042, η_p^2 = .162). The allSC-model additionally showed a marginally significant group*hemisphere interaction in V4 (F(1,24) = 3.09, p = .092, η_p^2 = .114). More specifically, within V2 and V3 CC individuals showed significantly smaller surface area in the left than in the right hemisphere (left V2 < right V2, t(24) = -2.33, p = .029; left V3 < right V3, t(24) = -2.63, p = .015). SC individuals were more likely to show the opposite, i.e. reduced surface area in the right rather than the left hemisphere, yet the differences did not reach significance (p > .05). In V4 on the contrary, SC individuals showed significantly higher surface area in the right hemisphere than in the left (t(24) = 3.95, p < .001), while the difference in CC individuals did not reach significance (p > .05). Additionally, the allSC-model indicated differences between hemisphere in V1, V3 and V4 (significant main effect of hemisphere; V1: F(1,24) = 15.61, p < .001, η_p^2 = .394; V3: F(1,24) = 4.98, p = .035, η_p^2 = .172; V4: F(1,24) = 6.88, p = .015, η_p^2 = .223). Given that V3 and V4 were already further analysed in context of the group*hemisphere interaction, here, we only report that across all subjects, the surface area in the left V1 (M = 3015 mm^2; SD = 423) was smaller than the right V1 (M = 3173 mm^2; SD = 456).

There were no indications for group*age interactions. There were, however, a significant main effect of age in V2 ($F(1,20) = 5.39$, $p = .031$, $\eta_p^2 = .212$) as well as a marginally significant effect of age in V1 ($F(1,20) = 3.79$, $p = .066$, $\eta_p^2 = .159$) indicating that surface area declined with age. **Figure *9*** shows surface area in CC and allSC individuals as a function of age in V1 and V2.

Figure 9

Correlation of surface area and age in V1 and V2.

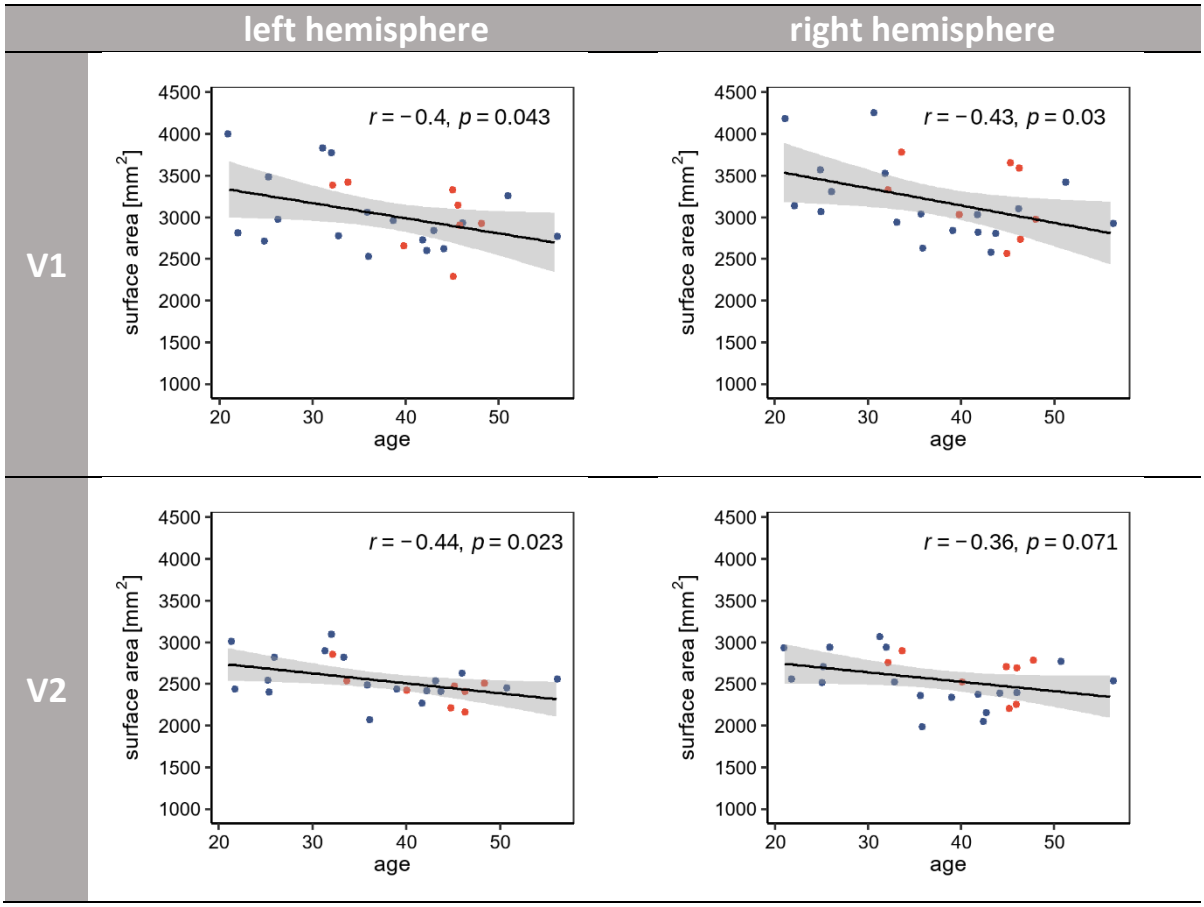

Note. Graphs display average surface area values (single dots) of CC individuals (red) and allSC individuals (red) per ROI. V1 values are plotted in the upper row, V2 values in the bottom row. The left column displays the left hemisphere of each region and the right column the right hemisphere. Regression lines and values are displayed with the respective 95% confidence interval (grey band).

Exploratory Correlation Analysis

The exploratory correlation analysis of surface area and visual acuity indicated negative correlations in the majority of regions, except for the right V3 and right V4 (**Table *3***). Accordingly, the bilateral V1, the bilateral V2 as well as the left V3 and the left V4 indicated that the greater the surface area of CC individuals, the lower their visual acuity. Conversely, the right V3 and V4 indicated a that the smaller the visual surface area in CC individuals, the lower their visual acuity. However, none of these correlations was significant.

Table 3

Region-Specific Correlations of Surface Area and Visual Acuity.

	V1		V2		V3		V4	
	left	right	left	right	left	right	left	right
Pearson's *r*	-0.29	-0.30	-0.61	-0.47	-0.59	0.18	-0.54	0.46
p-value	.488	.464	.111	.237	.125	.671	.170	.249

Note. Pearson correlation coefficient *r* and estimated *p*-values for each of the eight regions of the early visual cortex.

4. Discussion

The main goal of the present study was to investigate the effects of early visual deprivation on shaping the structural organisation of the early visual cortex and explore the potential capacity for recovery from these changes if sight is restored later in life. To this end, submillimetre structural MRI data was acquired in a group of adults who experienced a transient period of congenital visual deprivation due to dense bilateral cataract which was surgically removed later in life (CC individuals). To assess structural differences in the brain, cortical thickness and surface area of these CC individuals were compared to normally sighted controls (SC individuals) as well as individuals, who had pattern vision at birth, yet had other congenital or acquired visual impairments (VI individuals). In light of methodological differences of previous studies, an additional goal of this study was to unify previous analysis approaches. To this end, we performed a vertex-wise analysis as well as a region-of-interest (ROI) analysis for comparing cortical thickness and surface area, respectively, between groups. Based on previous studies, we expected to find increased cortical thickness and reduced surface area in the early visual cortex of CC individuals compared to SC and VI individuals.

In contrast to our hypothesis, we did not find significant group differences for cortical thickness. However, both analyses indicated higher cortical thickness in the left early visual cortex of CC individuals compared to SC individuals on a descriptive level. In partial agreement with our second hypothesis regarding surface area, the results revealed a significant group difference which was mediated by hemisphere. Specifically, CC individuals exhibited significantly reduced surface area in the left hemisphere compared to the right hemisphere. In contrast, the SC individuals tended to exhibit the opposite pattern, with greater surface area in the left hemisphere. Further, the expected lower surface area in CC individuals compared to the SC group was observed descriptively in the left hemisphere. However, unexpectedly, the CC group exhibited greater surface area than the SC group in the right hemisphere.

In conclusion, the results presented here offer valuable evidence supporting the significance of early visual experience in shaping the structural development of the visual brain. Furthermore, the results suggest the possibility of distinct effects resulting from early visual deprivation on different structural measurements, such as cortical thickness and surface area. This, in turn, opens up new avenues for further investigation and exploration in this area research especially in connection with ultra-high field MRI.

Cortical thickness

Multiple studies prior to this study at hand reported long-lasting effects of early visual deprivation on brain structure despite many years of visual experience. The majority of studies focused the investigation of cortical thickness in CC individuals on the visual cortex (Guerreiro, Erfort, et al., 2015; Hölig et al., 2022) while a single study reported changes on the whole-brain level (Feng et al., 2021). All three studies consistently reported increased cortical thickness in the early visual cortex of CC individuals compared to SC individuals (Feng et al., 2021; Guerreiro, Erfort, et al., 2015; Hölig et al., 2022). In the results presented here, likewise, higher cortical thickness in CC individuals compared to SC individuals was indicated within the left V1. However, this group difference only emerged on an uncorrected level and only when comparing CC individuals to the group of all tested sighted controls. Based on the location of these clusters, this observation resembled the reports by Hölig et al. (2022) and Feng et al. (2021). Further, in connection to the observed clusters, one might consider descriptively higher cortical thickness values in the left V1 in CC individuals compared to SC individuals in the ROI analysis resembling reports by Guerreiro et al. (2015).

The absence of significant group differences, in contrast to previous studies, necessitates careful consideration of several factors. Multiple variables could potentially contribute to the disparity in study outcomes. First and foremost, with a group of 21 CC individuals, Hölig et al. (2022) tested almost three time as many CC individuals as the study at hand. Due to the analytical approach of the vertex-wise analysis which estimates group differences at each vertex, the statistical power of this approach is limited and requires an elaborate number of subjects to yield significant results when being corrected for multiple comparisons. Even despite limiting the analysis to the early visual cortex, a sample as small as ours might have been simply underpowered in order to yield significant results. Yet it is worth noting that even the uncorrected clusters were relatively small, which suggests that the observed effects of group difference were subtle. Further, that the group differences in cortical thickness only emerged when including a larger number of subjects for the analysis might also support the notion that the lack of statistical power, stemming from the small sample size, may have influenced the results, rather than the absence of an actual effect. The observation of limited group differences due to small sample size might be supported by the resembling small clusters reported by Feng et al. (2021) who tested eleven CC individuals. Likely limited by a reduced cluster size, Feng et al. did not apply a correction for multiple comparisons for reporting group differences. A cluster-wise correction for multiple comparisons as implemented in FreeSurfer is based on cluster size and small clusters have a lesser chance of surviving corrections. Especially when applied on the whole-brain level, the correction could most likely have let to reduced results if not even the absence of significant group difference. This would explain the use of a more liberal approach to correct for false

positives, i.e. a reduced uncorrected threshold and a cluster-size minimum. Overall, limited group difference in cortical thickness for CC individuals compared to SC individuals might be influenced by limited statistical power due to a small sample.

Even more surprising was the absence of significant group differences for cortical thickness in the ROI analysis. Utilising a ROI analysis approach has the potential to enhance statistical power by averaging vertex values within each region for each subject. This method is particularly advantageous in studies with small sample sizes, as it allows for more effective testing. For example, Guerreiro et al. (2015) reported significantly increased cortical thickness in a group of only six CC individuals using this approach. However, it is important to consider that when dealing with small effects, the averaging of data within a region may lead to the loss of specific effects. In light of the vertex-wise results, it can be inferred that this may have been the scenario for the data reported in this study, despite the slightly larger sample size and without a correction for multiple comparisons.

An alternative explanation for the disparity in study outcomes could potentially stem from differences in region definition. Specifically, Guerreiro et al. (2015) employed a solely structural atlas to define regions within the visual cortex, whereas the analyses conducted here relied on the multimodal atlas by Glasser et al. (2016), which may yield distinct region definitions. It is worth considering the possibility that variations in the sizes of the calcarine sulcus and the V1, respectively, could influence data averaging within that area, thereby potentially impacting any observed group differences.

When comparing MRI study results, particularly in the context of structural MRI analyses, it is important to consider the spatial resolution of the MRI data. Evidence indicates that different magnetic field strengths have a substantial impact on the estimation of structural measurements, such as cortical thickness (Han et al., 2006). Previous studies have relied on lower magnetic field strengths, such as 1.5T (Hölig et al., 2022) and 3T (Feng et al., 2021; Guerreiro, Erfort, et al., 2015), whereas 7T MRI offers the potential for higher signal-to-noise ratio, contrast-to-noise ratio, and increased spatial resolution in the submillimetre range. Consequently, acquisitions at submillimetre resolution, combined with advanced processing techniques (Zaretskaya et al., 2018), have the potential to provide more precise tissue contrasts. Accurate tissue contrast is crucial for defining grey and white matter in the brain, which is essential for obtaining reliable surface reconstruction and, ultimately, accurate estimates of cortical thickness and surface area. Recently, the application of 7T MRI has provided an opportunity to re-evaluate structural findings in congenital blind individuals (Kupers et al., 2022). Amongst other structural measures, cortical thickness was compared between congenitally blind and normally sighted individuals. Interestingly, in contrast to previous reports (recently reviewed by Paré et al., 2023), Kupers et al. found that group differences in cortical thickness were only observed in specific areas of the visual cortex, without reaching statistical significance after

correction for multiple comparisons. Notably, these differences were not evident in the regions surrounding the calcarine sulcus, which locates V1 as the primary visual cortex.

It might be considered that the study by Kupers et al. may share similar limitations regarding statistical power with a sample size of 12 congenially blind individuals, as previously discussed for the current study. However, it is important to note that the study successfully replicated other previously reported structural changes following congenital blindness, such as volumetric alterations in grey matter volume and subcortical structures (Kupers et al., 2022). Thus, together with the results reported here, this finding might indicate on overall reduced effect of early visual deprivation on cortical thickness.

It has been proposed that the myelin content in the brain can influence the perceived boundary between grey matter and white matter (Natu et al., 2019). Specifically, Natu et al. reported that a lower myelin content in children most likely reduces the contrast which results in an inward shift of the boundary, leading to higher measurements of cortical thickness. White matter atrophy within the early visual cortex of congenitally blind individuals has been reported in previous studies (Modi et al., 2012; Shimony et al., 2006), and this finding has been further supported by the recent 7T MRI report (Kupers et al., 2022). It seems possible that previous structural analyses of cortical thickness conducted with lower MRI resolutions may have been influenced by the difference in tissue contrast, potentially leading to an overestimation of cortical thickness. However, the submillimeter resolution provided by 7T scanning has allowed for more accurate assessment, revealing diminished group differences in cortical thickness.

In sum, the evidence potentially indicates the possibility of differentiated effects of early visual deprivation on specific structural measurements. Given the distinct developmental trajectories of cortical thickness and surface area (Wierenga et al., 2014), it appears that their development may depend differently on visual experience. Accordingly, cortical thickness might be less affected by early visual deprivation than surface area.

The use of 7T MRI is still comparably new and therefore, evidence on effects of magnetic field strength, particularly on structural measurements, is still sparse. While the comparisons of structural measures have been focused on multi-site comparisons (Jovicich et al., 2006) or on the comparison of 1.5T data to 3T data (Han et al., 2006), particularly in terms of clinical application such as diagnostics, 7T imaging has proven its advantages (Balchandani & Naidich, 2015; De Ciantis et al., 2016; Van Der Kolk et al., 2013). Despite advanced image quality, 7T imaging also brings potential challenges, both in the acquisition of data as well as the analysis, that require adequate consideration to exploit its full potential. For example, imaging acquisition at ultra-high field needs to consider

increased power deposition in human tissue, and hindered maintenance of a homogeneous radiofrequency field impedes image quality. While radiofrequency inhomogeneities are primarily addressed prior to image acquisition by shimming the magnetic field, further corrections are performed during data preprocessing. Given the relatively new approach of submillimetre MRI, further methodological considerations might be needed for future standardised analyses, such as data preprocessing, bigger samples to claim strong effects or alternative approaches for estimating significance (Feng et al., 2021).

Surface Area

Along with changes in cortical thickness, reduced surface area in the early visual cortex, specifically the primary visual cortex (V1) is considered a well-established neuroanatomical consequence of early blindness, indicated by MRI results and validated by histological reports in a variety of species (Andelin et al., 2019). Similarly to the reports in permanently blind humans, reduced surface area has been reported in the early visual cortex of CC individuals (Brockhaus et al., 2022; Hölig et al., 2022) confirming that it is particularly early visual deprivation rather than late occurring visual deprivation that affects surface area (Andelin et al., 2019).

The findings presented in this study only partially align with previous results. Specifically, group differences in surface area were observed in the regions V2 and V3, suggesting that the effects of early visual deprivation may extend beyond V1, consistent with the reported finding by Hölig et al. (2022). Further, the group difference within V2 and V3 were specific to the hemispheres. Specifically, CC individuals exhibited the expected reduced surface area in comparison to SC individuals in the left hemisphere, albeit only at a descriptive level. Conversely, the right hemisphere showed the opposite trend. However, hemispheric differences within the groups were the primary contributing factor of the reported group differences. Accordingly, CC individuals displayed significantly reduced surface area in the left hemisphere compared to the right hemisphere, while SC individuals tended to exhibit the opposite pattern.

Based on previous reports (Andelin et al., 2019; Park et al., 2009), there are indication that the right early visual cortex, particularly V1/calcarine sulcus, descriptively exhibits greater surface area compared to the left early visual cortex. However, this pattern was consistent across all tested groups, including individuals with congenital blindness, early blindness, late blindness, and normally sighted individuals. Accordingly, the here observed difference in hemispheres should not have been specific to CC individuals. Furthermore, genetic investigations support a bilaterally symmetric pattern in surface area development (C. H. Chen et al., 2011, 2012), suggesting an overall limited difference

between hemispheres. Further, although neither Hölig et al. (2022) nor Brockhaus et al. (2022) directly compared surface area between hemispheres, reduced surface area in CC individuals compared to SC individuals has been reported similarly in both the left and right early visual cortex (Hölig et al., 2022). Consequently, thus far, there seem to be no indications of distinct effects of early visual deprivation that are specifically limited to one hemisphere, emphasizing the need for caution when interpreting the observed hemispheric differences in the study at hand. Considering the small sample size on which this study is based, it is important to acknowledge that individual data points may have influenced the results.

It is worth noting that the absence of group differences within the V1 region in this study specifically contradicts the findings reported by Brockhaus et al. (2022), as their analysis primarily relied on the same structural data from both CC and SC individuals. In an attempt to address this discrepancy, a preliminary analysis was conducted to explore potential factors, including differences in the matching of SC individuals, variations in V1 definition (attributable to the use of a different atlas), and the applied statistical tests. However, despite taking these factors into consideration, the disparity in study outcomes remained. Further detailed analyses may help elaborate on whether the observed differences could have arisen from variations in the software used for estimating the structural measurements.

Exploratory correlation analyses

The present study revealed notable differences in the development of cortical thickness, in contrast to surface area, with age between CC individuals and SC individuals. Specifically, the results indicated a more pronounced age-related decline in cortical thickness among CC individuals compared to SC individuals. Cortical thinning is commonly observed in typically sighted individuals from early childhood to adulthood (Amlien et al., 2016; Walhovd et al., 2016). Thus, the observed variations in age-related changes, particularly the stronger cortical thinning, may potentially signify the restoration of neural circuits compensating for the period of visual deprivation after sight is regained. In congenitally blind children, changes in cortical thickness have not been observed until the age of 13 years (Inuggi et al., 2020), yet cortical thickness in the visual cortex of congenitally blind adults might increase (Kupers & Ptito, 2014). The contrasting direction of age-related changes observed in permanently blind individuals compared to sighted and CC individuals may imply a process of visual experience-induced changes that continue until adulthood.

However, it is important to consider certain factors regarding the interpretation of these findings. Firstly, the effect of age was assessed only when comparing the CC group to the allSC group in the

respective subject model. The allSC group had a wider age range than the CC group, which could explain the reported interaction of group and age. This statistical limitation may be attributed to differences in age distribution between the two groups. Additionally, it should be emphasized that the study's sample size of CC individuals was small, and their age range was limited, with the majority aged between 40 and 48 years and only two individuals between 32 and 34 years. These factors might have impacted the accuracy of the correlation between cortical thickness and age. Nonetheless, this study, along with previous findings by Hölig et al. (2022), suggests that age may exert diverse effects on the structural organisation of the brain following a transient period of early visual deprivation. Further research should delve deeper into investigating whether neural circuits can truly resume their typical developmental trajectories, especially considering the distinct developmental trajectories of cortical thickness and surface area.

Further exploratory analyses within the CC group revealed a negative correlation between cortical thickness and visual acuity, indicating that individuals with thicker early visual cortex tend to have lower visual acuity. While previously, contradicting evidence has been reported on this relationship (Feng et al., 2021; Hölig et al., 2022) this finding underscores the potential behavioural significance of structural brain changes following early visual deprivation. Conversely, increased cortical thickness in peripherally responsive visual areas of individuals with macular degeneration has been associated with compensatory gain of function leading to spared peripheral vision, while central vision loss was associated with cortical thinning (Burge et al., 2016). This seemingly contradicting findings potentially imply the existence of various mechanisms that could potentially connect behavioral and structural changes. In contrast to Hölig et al. (2022), the results from the current study suggested a negative correlation between surface area and visual acuity in most of the early visual cortex of CC individuals, indicating that individuals with greater surface area tend to have lower visual acuity. However, an additional cluster in the right hemisphere suggested the opposite trend. It is important to note that these correlations between surface area and visual acuity did not reach significance.

In general, it is important to exercise caution when interpreting correlational findings that are based on a limited sample size, as potentially deviating individual data points within the sample can significantly impact the observed results.

The Integration of Analysis Approaches

Previous studies investigating structural differences following transient early visual deprivation have employed either a vertex-wise approach to estimate group differences (Feng et al., 2021; Hölig et al., 2022) or calculations based on average values for defined regions-of-interest (Brockhaus et al., 2022; Guerreiro, Erfort, et al., 2015). In contrast, the present study incorporated both a vertex-wise analysis and a ROI analysis to investigate the effects of early visual deprivation. Incorporating both approaches allows to directly compare the results and gain valuable insights into the specific methodological demands and advantages of each analysis method. This comparison not only enhances our understanding of the current study but also provides essential guidance for future studies in the field. Regarding cortical thickness, it seems plausible that the clusters indicating group differences were too small to survive multiple comparisons. The limited size of these clusters might also explain the lack of differences observed in the ROI-based analysis. For example, even the three clusters within the left V1 might not have been sufficient to demonstrate a group difference across the entire region of the left V1. In contrast, for surface area, the ROI-based analysis yielded results where the vertex-wise analysis indicated none. It is possible that group differences in surface area might have been more widespread, involving a greater number of vertices, yet subtler in terms of the magnitude of differences. Consequently, individual clusters might not have emerged, but the overall region could still indicate a group difference. In conclusion, considering the limitations of small sample sizes, both analysis approaches offer distinct advantages that contribute to a more comprehensive understanding of the data. Since comparative research in this area is still limited, future studies should explore the integration of these analysis methods. This is particularly relevant in light of the emerging use of ultra-high field MRI, where alternative approaches may be necessary to accurately estimate statistical significance.

Limitations

It is important to acknowledge that the sample size of the CC group consisting of eight individuals was relatively small, which is attributed to the rarity of individuals who experienced bilateral dense congenital cataracts for a minimum of 6 months. This limited sample size may have influenced the effect size of potential group differences, particularly in the vertex-wise analysis, as discussed earlier. Additionally, the inclusion of a third group with visual impairments aimed to distinguish between the effects of early visual deprivation and those associated with visual impairments. However, the sample size of this group was also limited, consisting of only four individuals, which restricts the scope of interpretation for the results. Moreover, it is important to

consider the heterogeneity of visual impairments within this group, as individuals had varying degrees of visual impairments. Despite these limitations, the study at hand provides valuable insights into the potential of submillimetre structural data and the methodological characteristics of two commonly used analysis approaches. These findings offer valuable guidance for future research, particularly in relation to the potential effects of early visual deprivation beyond the visual cortex as previously reported (Feng et al., 2021).

Conclusion

In conclusion, this study represents an important step in understanding the effects of early visual deprivation within the early visual cortex, indicating that impaired structural brain development due to visual deprivation from birth may not be fully reversible. The investigation of cortical thickness and surface area using both vertex-wise and ROI analysis approaches provides valuable insights into the comprehensive effects of early visual deprivation. The analysis of submillimetre structural data holds promise for future structural MRI analyses, suggesting potentially differentiated effects of early visual deprivation on different aspects of brain structure. However, further research is necessary to gain a comprehensive understanding of these effects and to refine the use of different analysis methods.

Chapter III

The Effects of Early Visual Deprivation on the Processing of Visual Categories

1. Introduction

The VTC in adult humans exhibits a highly specialised organisation for processing complex visual stimuli, including faces, bodies, objects, and scenes. These visual stimuli are represented in two complementary manners across the VTC. Firstly, distributed patterns of activation throughout the entire VTC encode information about the categorical membership of the visual stimuli (Haxby et al., 2001; Kriegeskorte, Mur, & Bandettini, 2008). Secondly, certain regions within the VTC respond more strongly to specific categories of stimuli than others, such as face-selective regions located along the fusiform gyrus (Kanwisher et al., 1997).

Both distinct regions as well as distributed patterns of category specific activation have been found remarkably consistent across subjects (Grill-Spector & Weiner, 2014; Kanwisher, 2010), which raises the question of how this multifaceted categorical organisation develops. Besides various anatomical factors that are considered to determine where selective regions emerge (for a review see Op de Beeck, Pillet, & Ritchie, 2019), the question of whether or not visual experience is necessary for the development still receives a lot of debate. To investigate this question, researchers have primarily focused on the development of distinct categorical regions, i.e. when do these regions emerge and are age-related changes in size or selectivity observable. fMRI research investigated the development of selective regions within the visual cortex that are involved in the processing of faces (Gathers et al., 2004; Golarai et al., 2007, 2010; Passarotti et al., 2003, 2007; Scherf et al., 2007), places and objects (Golarai et al., 2007; Scherf et al., 2007) as well as bodies (Peelen et al., 2009) and indicated late developmental changes in category-selectivity in children between the age of 4 and 11 (Cantlon et al., 2006, 2011; Golarai et al., 2007). These changes have been discussed to reflect experience-dependent developmental mechanisms given that it takes the first decade of life for these changes to occur (Golarai et al., 2015).

Particularly face-selective cortices follow a prolonged developmental trajectory and continue to develop into late adolescence (Aylward et al., 2005; Golarai et al., 2007). More specifically, face-selective regions such as FFA, OFA and the STS have been reported to take between 8 to 10 years of age to solidly form (Gathers et al., 2004; Scherf et al., 2007, 2011). A variety of neural mechanisms has been proposed to accompany this development, such as age-related changes in spatial extent of face-selective activation, both increase (Golarai et al., 2007, 2010; Pelphrey et al., 2009; Scherf et al., 2011) as well as decrease (Passarotti et al., 2003), and/or changes in response characteristics of face-selective neurons (Cantlon et al., 2011; Golarai et al., 2010), yet consensus has not been reached. These neurophysiological changes might contribute to the marked behavioural changes in categorical processing seen in late childhood. More specifically, the maturation of expert face processing mechanisms occurs around the age of 10 years, indicated by an absence of the face inversion effect

in children younger than nine years of age, and improves linearly with age (Hills & Lewis, 2018; Schwarzer, 2000). The face inversion effect has been described to result from progressive tuning of face-selective regions: while all tested age groups, i.e. children, adolescents and adults, showed similar response profiles to upright faces, only children at the age of 8 to 11 years showed higher response to inverted than upright faces - a response that decreased with age (Passarotti et al., 2007). However, face processing continues to mature even beyond the first decade of life. For example, face-recognition memory reaches adult-level around 16 years (Carey et al., 1980; Chance et al., 1982), while face-learning abilities improve even until the age of 30 years (Germine et al., 2011).

The importance of early visual exposure to faces for the formation or maintenance of the face-processing system is also emphasised by findings in visually deprived non-human animal studies. Face-deprived monkeys were able to recognise and discriminate faces within a month of face-exposure (Sugita, 2008), yet they had not developed face-selective domains, while other categorical regions, as well as retinotopic organisation, developed normally (Arcaro et al., 2017).

Although improvements in behavioural performance have been reported in late childhood as well for place-selective processing (Day, 1975; Mackworth & Bruner, 1970; Munsinger & Gummerman, 1967; Vurpillot, 1968), body-selective processing (Bank et al., 2015; Seitz, 2002; Weigelt et al., 2014) and object-selective processing (for a review see Nishimura, Scherf, & Behrmann, 2009), there is only limited evidence for neurophysiological changes in the respective category-selective regions. The emergence of these regions has been reported for middle to late childhood (Golarai et al., 2007; Peelen et al., 2009; Scherf et al., 2007). However, evidence for further age-related changes on a neurophysiological level are either inconsistent, for example in the case of place-selectivity (Chai et al., 2010; Golarai et al., 2007; Meissner et al., 2019), or not indicated at all, as in the cases of body-selectivity (Peelen et al., 2009; Pelphrey et al., 2009) or object-selectivity (Golarai et al., 2010; Scherf et al., 2007).

Despite the multitude of evidence emphasising the importance of visual experience for the developmental of categorical processing, its role is questioned considering the accumulating evidence for early maturation in infants. Specifically for faces, some studies indicated face-selective behaviour shortly after birth. More specifically, face-preferential looking is already present within the first minutes and days after birth (Goren et al., 1975; Johnson et al., 1991), which is supported by findings of adult-like face-specific cortical routs (Buiatti et al., 2019) and specialised face-processing already present at early infancy (Kouider et al., 2013). In general, neurodevelopmental research using non-invasive methods such as EEG, magnetoencephalography (MEG), and functional near-infrared

spectroscopy (fNIRS) have reported high-level responses in infants not just to faces (de Haan & Nelson, 1999; de Heering & Rossion, 2015), but also to scenes (Powell et al., 2018), and bodies (Lisboa et al., 2020; Meltzoff et al., 2018). Importantly, it has been discussed that the lack of fMRI evidence for high-level responses in infants, compared to the increasing number of behavioural studies and other electrophysiological measures, are rather a result of methodological limitation in MRI than absence of proof (McKone et al., 2012). More recently, methodological adaptations allowed to test awake infants between two and nine months of age. Similar to adults, tested infants already showed spatial organisation which differentiated between faces and places (Deen et al., 2017) and even showed category-selectivity for faces, places and bodies (Kosakowski et al., 2021). Visual experience at such a young age is comparably limited and yet adult-like processing has been reported. These findings might suggest that other, experience-independent mechanisms are involved in the development of category-selectivity.

Visual experience as the sole driving force for the development of category-selectivity might seem at odds even more so with the observation of category-selectivity being preserved in congenitally blind individuals. In congenitally blind individuals, visual areas have been observed to be activated during auditory processing, including language processing (Bedny et al., 2011; Röder et al., 2002), voice recognition (Hölig et al., 2014) and sound localization (Collignon et al., 2011; Gougoux et al., 2005). This phenomenon is referred to as cross-modal plasticity, in which visual areas are integrated into the processing of preserved modalities. Moreover, a multitude of studies reported that cross-modal organisation follows the category-selective organisation in congenitally blind individuals and can be found for the auditory modality (van den Hurk et al., 2017), as well as for the tactile modality (Ratan Murty et al., 2020). Cross-modal category-selective responses have been demonstrated in small, clustered regions within the VTC, such as face regions (Fairhall et al., 2017; Hölig et al., 2014; Ratan Murty et al., 2020), the visual word form area (VWFA; Reich, Szwed, Cohen, & Amedi, 2011; Striem-Amit, Cohen, Dehaene, & Amedi, 2012), body parts (Kitada et al., 2014; Striem-Amit & Amedi, 2014), numbers (Abboud et al., 2015), scenes and large non-manipulative objects (He et al., 2013; Wolbers et al., 2011), as well as tools and common objects (Amedi et al., 2007; Peelen et al., 2013, 2014). Additionally, multiple studies reported that sighted and blind individuals share similarities for large-scale distributed representations within the VTC (Mahon et al., 2009; Pietrini et al., 2004; van den Hurk et al., 2017). More specifically, Van den Hurk et al. were able to show that visual categorical responses in sighted individuals were able to predict auditory categorical responses in blind individuals and vice versa, which leads to the conclusion that both groups show the same underlying functional organisation, although respondent to different modalities.

Taking these reported results together might indicate that multiple mechanisms are involved in the development of specialised categorical processing. The evidence in congenitally blind individuals indicates that large-scale categorical organisation develops without visual experience. As mentioned before, the multivariate approach also includes selective regions, which would account for cross-modal categorical selectivity in distinct regions. Moreover, the experience-independent development of large-scale categorical organisation would most likely also facilitate the development in sighted individuals, which could align with early functional maturation in infants. However, visual experience and especially early visual experience seems to be essential for the maintenance and fine-tuning of univariate selectivity as indicated by the developmental studies in normally sighted individuals.

To further disentangle the effects of early visual experience and its role in the development of categorical processing, this study investigated a group of individuals, who experienced a transient period of congenital visual deprivation due to dense bilateral cataracts (CC individuals). In CC individuals, visual functions have been studied both on a basic level, such as visual acuity and peripheral vision (Lewis & Maurer, 2005), as well as on a more complex level, such as perception of illusory contour and faces (Putzar, Hötting, et al., 2007, 2010). Although face processing in CC individuals has been investigated extensively on a behavioural level (Gandhi et al., 2017; Le Grand et al., 2001; Mondloch et al., 2013; Putzar, Hötting, et al., 2010; Robbins et al., 2010), less evidence exists on the neurophysiological level of face processing. Two studies investigated the underlying neural mechanisms of categorical face processing and demonstrated face-specific impairments in CC individuals (Grady et al., 2014; Röder et al., 2013). Analysing ERPs, Röder et al. (2013) investigated the N170 component, which is a known face-sensitive neural marker (Eimer, 2011) and is discussed to originate in middle and posterior fusiform gyri (Gao et al., 2019). In normally sighted individuals, the N170 component is enhanced when being presented with faces compared to other categories. Röder et al. presented images of faces, houses and scrambled versions of both to CC individuals, individuals with developmental cataract and normally sighted individuals. Only CC individuals did not show the face-specific enhancement, but rather showed similar responses to all presented categories (Röder et al., 2013). In an fMRI study, Grady et al. (2014) reported that CC individuals showed face-specific activation in the same regions as normally sighted individuals, yet the response for faces was weaker than in sighted controls. Further, only CC individuals showed object-selective activation in face regions (Grady et al., 2014). Taking these two results together, one can conclude that CC individuals exhibit an ill-specialised face processing system, in which face-selective responses are reduced and processed rather similar to other categories.

The studies by Röder et al. (2013) and Grady et al. (2014) both suggest that CC individuals have impaired face-selective processing due to early visual deprivation. These findings highlight the importance of investigating the effects of early visual deprivation on the processing of other categories, such as bodies, objects, and scenes. Moreover, a combination of multivariate and univariate analysis techniques, such as MVPA and ROI analysis, can provide a more comprehensive understanding of the effects of early visual deprivation on visual processing and potentially shed light on new insights into the neural mechanisms involved in visual perception. To this end, we acquired functional MRI data of a group of individuals, who had experienced congenital visual deprivation due to bilateral dense cataract for a minimum of 6 months and compared them to a group of normally-sighted control (SC) individuals and a group of individuals, who experienced other (congenital or acquired) visual impairments, but had pattern vision at birth (VI individuals). All participants were presented with short video clips of faces, body parts, objects and scenes, which allowed us to test a variety of categorical responses. To investigate the effects of early visual deprivation on the processing of these visual categories, an MVPA analysis was used to provide a more nuanced understanding of the specific patterns of brain activity associated with different categories of visual stimuli, while a univariate ROI analysis was used to provide information about the activation levels of specific brain regions in response to different visual stimuli. The study at hand aims to extend previous findings not just in terms of multiple additional categories being tested, but especially because both univariate as well as multivariate analyses have been conducted.

2. Hypotheses

Multivariate analysis

1) We hypothesised that all visual categories can be classified above empirical chance level within all individuals of the three tested groups (both in within-subject classification as well as in within-group classification).

2) We expected successful classification between the SC group and the CC group.

Univariate analysis within VTC

3a) For bilateral face-selective regions mFus-faces, pFus-faces and IOG-faces, as well as for the combined region avg-faces, we expected higher responses for faces compared to the remaining stimulus categories (bodies, objects, scenes) for all three groups (CC individuals, visually impaired and normally sighted controls).

3b) However, we expected to find a reduced face-selective response in CC individuals compared to normally sighted and visually impaired controls.

4a) For bilateral body-selective region OTS-bodies, we expected a higher response for bodies compared to the remaining stimulus categories (i.e. faces, objects, scenes) in all three groups.

4b) However, we expected to find a reduced body-selective response within the OTS-bodies of CC individuals compared to normally-sighted and visually impaired controls.

5a) For the bilateral place-selective region CoS-places, we expected a higher response for places compared to the remaining stimulus categories (i.e. faces, objects, bodies) in all three tested groups.

5b) However, we expected to find a reduced place-selective response in CC individuals compared to normally sighted and visually impaired controls.

Extended findings on categorical regions

6a) For the remaining body-selective regions, which are the bilateral regions MTG-bodies, LOS-bodies and ITG-bodies, we expected a higher response for bodies compared to the remaining stimulus categories (i.e. faces, objects, scenes) in all three tested groups.

6b) However, we expected to find a reduced body-selective response in CC individuals compared to normally sighted and visually impaired controls.

7a) For place-selective right-lateralised TOS-places, we expected a higher response for places compared to the remaining stimulus categories (i.e. faces, objects, bodies) in all three tested groups.

7b) However, we expected to find a reduced place-selective response in CC individuals compared to normally sighted and visually impaired controls.

Exploratory analysis

8) We were interested to investigate and compare the categorical response profile for the remaining ROI as provided by the functional visual atlas (Rosenke et al., 2020). This included early visual regions (bilateral regions v1d, v2d, v3d, v1v, v2v, v3v) as well as regions that have other categorical preferences than tested within our paradigm, more specifically the bilateral motion-selective hMT as well as the left-lateralised character-selective regions pOTS-characters and IOS-characters.

3. Methods

Participants

The study at hand was part of a larger project consisting of two MRI sessions, one in 3T and one in 7T MRI and one behavioural session to determine visual and auditory acuity.

Detailed description on the recruitment of participants as well as inclusion and exclusion criteria can be found in the first study of this dissertation project (Chapter 2). Shortly, three groups were tested: First, a group of eight individuals who experienced complete, dense and bilateral congenital cataract (CC) for a minimum of sixth months (age range 32 – 48 years, M_{age} = 42 years, SD_{age} = 6; 5 female). The CC individuals underwent cataract-removal surgery at an average age of 20.6 months (range 6 and 48 months). The CC group was identical to the group reported for the first study of the dissertation project. **Table *4*** contains detailed information of individuals' visual characteristics. Second, a group consisting of thirteen sighted controls was recruited (allSC: M_{age} = 35.9 years, SD_{age} = 9.2 years, range 21 - 56 years, 8 female). Eight of these thirteen SC individuals were approximately matched in age and gender to the CC participants (mSC_{CC}: age range 31 - 56 years, M_{age} = 40.9 years, SD_{age} = 7.5; 5 female). Average visual acuity of these mSC participants was -0.06 logMAR (SD_{acuity} = 0.23 logMAR, range: -0.30 – 0.33 logMAR). Third, an group of visually impaired (VI) individuals was recruited who had pattern vision from birth in at least one eye. We tested three VI individuals (age range 21 – 32 years, M_{age} = 25, SD = 6.1, all female). Two individuals had congenital, yet incomplete visual impairments and one had an acquired visual impairment. Detailed description of their visual characteristics can be found in **Table *4***. All VI individuals have been recruited in Hamburg, Germany, via e-mail list of the University of Hamburg for handicapped students as well as sport and social groups for blind and visually impaired individuals. It is noteworthy, that all subjects, i.e. CC, VI and SC individuals, who participated in this study also participated in the first study (Chapter 2). However, due to technical and organisational reasons not all individuals of the VI and the SC group participated in the 3T scanning session, which was basis for the analyses at hand.

Table 4

Participant Characteristics and Clinical Information of Congenital Cataract (CC) and Visual Impaired (VI) Participants.

ID	Age at testing (years)	Sex	handedness	Age at surgery (month)	Visual acuity in the better eye (logMAR)	Self-reported visual impairments
CC1	34	male	right	12	0.63	Aphakia
CC2	45	male	right	24	0.16	Aphakia, impaired stereopsis
CC3	48	female	right	48	0.58	Aphakia, impaired stereopsis and visual field
CC4	45	female	right	9	0.68	Pseudoaphakia, nystagmus, treated glaucoma, impaired visual field and stereopsis
CC5	32	female	right	24	0.18	Aphakia
CC6	46	female	right	24	1.27	Aphakia, microphthalmia, nystagmus, impaired visual field and stereopsis
CC7	46	female	right	18	1.16	Aphakia, monocular enucleation, nystagmus, impaired visual field and stereopsis
CC8	40	male	right	6	0.56	Aphakia, nystagmus, impaired visual field and stereopsis; right eye: holey iris and underdeveloped pupil, left eye: narrowed pupil and shifted vision
VI1	22	female	right		-0.06	macular inflammation
VI2	32	female	right		0.74	monocular congenital cataract
VI3	21	female	right		0.97	binocular aniridia

The study was approved by the local ethics committee for the Faculty of Psychology and Human Movement Science, University Hamburg, in 2018. Each participant gave written informed consent for participating in this study and received reimbursement for travel costs and some monetary compensation for their participation.

Experimental Design

The experimental paradigm has been described in detail by van den Hurk et al. (2017). Briefly, participants were presented with stimuli of four different categories matched for the auditory and visual modality, with four runs per modality. Stimuli belonged to the categories of either Body, Face, Object or Scene. However, for the study at hand, only the visual modality is of interest. Each visual run consisted of four overall-blocks in which each category, i.e. Face, Body, Object, Scene, was presented once. Each category-block consisted of eight stimuli with a 200 ms interstimulus interval, followed by a 200 ms inter-block interval. The overall-blocks (consisting of all four category-blocks) were separated by a 12 s fixation-only period showing a white fixation cross on black background. In contrast to the original paradigm, two of the four overall-blocks per run were presented in colour, while the remaining two blocks were presented in black and white. The presentation order of category-blocks was counterbalanced within and between runs to account for possible order effects.

Due to technical problems, one of the normally sighted subjects was presented with a deviating presentation order, which resulted in three blocks of coloured stimuli and only one block of greyscale

stimuli. We decided to exclude this participant for the MVPA analysis due to the imbalance in category, yet keep it for the univariate analysis given that the content of categorical information is the same as for all the other subjects.

Task and Stimuli

The task and stimuli were those described in van den Hurk (2017). Briefly, visual stimuli consisted of 16 short (~1,800 ms) video clips per category (i.e. face, body, object, scene). In the face category, we presented clips like laughing or whistling. In the body category, the video clips portrayed actions like hand-clapping or footsteps. In the object category, for example, we showed clips of a car or a ball. Stimuli of the scene category showed for example a train station or waves on a beach. To assure visibility despite visual impairments of CC and VI participants, we doubled the size of the visual stimuli which resulted in an onscreen stimulus size of 28*17 cm. Participants performed a one-back task judging the categorical similarity of each stimulus to the previous stimulus on a scale from 1 (highly similar) to 4 (highly dissimilar) via button press of the dominant hand. To assess whether participants perceived the categorical differences, custom-written MATLAB code was used to analyse if participants perceived the transitioning stimuli from one category to the next category less similarly than stimuli within one category-block. More specifically, we tested if the average response of within-category trials was significantly lower than the average response in between-category trials. Based on the procedure from van den Hurk et al. (2017) we aimed to exclude subjects who responded in less than five between-category trials. However, our analysis revealed that comparably few subjects met this criterium. More specifically, only two out of eight CC individuals (25%), eight out of 13 SC individuals (61.5%) and one out of three VI individuals (33%) would have been eligible for the behavioural analysis. To allow for meaningful assessment of data we therefore included subjects who responded at least once, which resulted in only one CC individual and three SC individuals being excluded. In the case of multiple button presses, only the first response was analysed.

Data acquisition

Functional and anatomical MRI images were acquired on a 3 Tesla Siemens Magnetom Prisma Fit scanner (Erlangen, Germany) equipped with a 32-channel head coil. For functional scans, we acquired 180 - 217 single-shot echoplanar (EP) images (iPAT factor 2, type GRAPPA, acquisition matrix = 100*100, FoV = 200*200, voxel resolution = $2mm^3$, 64 slices, no inter-slice gab, TR = 2000ms, TE = 30ms, multiband factor = 2, flip angle = 77°, activated pre-scan normalisation). Before each functional

scan, which had the phase encoding direction posterior to anterior (P-A), a distortion correction run acquired five EP images with equal acquisition parameters, but opposite phase encoding direction (i.e. anterior to posterior, A-P). In addition to functional images, 3D high-resolution T1 images were acquired using a MPRAGE sequence (iPAT factor 2, type GRAPPA, 192 slices, acquisition matrix 256*256, FoV 256*256, voxel resolution $1mm^3$, no interslice gap, TR = 2300ms, TE = 2.98ms, flip angle = 9°, active pre-scan normalisation & (inline) distortion correction). Each run lasted approximately 9 minutes. Stimuli were presented using a custom-written MATLAB R2014a code (The MathWorks, Inc., Natick, Massachusetts, United States) and Psychtoolbox-3 (Brainard, 1997). In a separate behavioural session, we assessed visual acuity, contrast perception and Vernier acuity using the computer-based program FrACT (Bach, 2007) as well as colour perception using the Farnsworth Panel D-15 Test (Linksz, 1966).

Data preprocessing

Functional and structural data were preprocessed and analysed using BrainVoyager 20 (Goebel et al., 2006). Functional preprocessing consisted of slice scan-time correction (sinc interpolation), head motion correction (trilinear/sinc interpolation), and temporal high-pass filtering removing linear trends and low-frequencies below four cycles per run. Subsequently, we corrected each functional run for geometric distortions using the BrainVoyager COPE plugin. The COPE plugin estimates and corrects deformations due to non-zero off-resonance fields by using a pair of images, which are acquired in opposite phase-encoding directions. In our case, this refers to each pair of distortion correction run and the directly ensuing functional run. Individual anatomical images were initially corrected for inhomogeneities and segmented from the surrounding head tissue. The data were then transformed to standard Talairach space and automatically segmented at the grey matter-white matter boundary. To assure good segmentation results, we visually inspected each hemisphere and manually corrected the automatically created boundary if necessary. The cortex-based alignment approach implemented in BrainVoyager was used to align each subjects' curvature information to the dynamic group average of all tested subjects (*N* = 24). This resulted in an average surface reconstruction separately for the left and right hemisphere. Similar to van den Hurk et al. (2017), we manually defined the VTC on our group average surfaces for the left and right hemisphere individually by tracing well known anatomical boundaries: occipito-temporal sulcus, posterior transverse collateral sulcus, parahippocampal gyrus, and the anterior tip of the MFS (Grill-Spector & Weiner, 2014). After preprocessing, functional data were co-registered to the respective subjects' anatomical image, normalised to Talairach space and 4D volume time course files were created. For univariate analyses, 4 mm FWHM spatial smoothing was applied, while no spatial smoothing was applied for the

MVPA (Vetter et al., 2020). A two-gamma hemodynamic response function was fitted for each categorical predictor, i.e. Body, Scene, Face, Object, and z-transformed 3D motion parameters of each functional run were added as confounds.

Statistical analysis

MVPA analysis

An MVPA was used to discriminate patterns of activation for the categories Body, Face, Object and Scene, separately for colour and black and white (hence listed as "_bw") stimuli in each participant. For the analysis, we used custom-written Matlab code in combination with the NeuroElf v1.0 toolbox (NeuroElf.net). Voxel's time courses were modelled with a two gamma hemodynamic response function including categorical predictors for each of the eight categories (i.e. Face, Body, Object, Scene, Face_bw, Body_bw, Object_bw, Scene_bw) and z-transformed motion parameters. We used the resulting beta maps as trial estimations, in which each trial was labelled according to its corresponding category. The volumetric estimations were sampled to the reconstructed surfaces in depth along the vertex normals (-1mm to 3mm) using trilinear interpolation. Using the vertex alignment information from the cortex based alignment procedure, we aligned each subject's reconstructed surface to the group aligned space and applied the previously defined VTC mask. For classification, we selected vertices along the VTC mask. Beta values were normalized by z-scoring the training and testing datasets and fed into a linear support vector machine classification algorithm (LIBSVM toolbox (Chang & Lin, 2011)). The classification was performed on category pairs which were assembled separately by colour, resulting in six category pairs in colour and six pairs in black and white.

Three different classification results were of interest: within-subject classification, within-group classification and between-group classification. The concrete analysis steps will be explained more specifically per analysis. For within-subject classification, we used a leave-one-run-out cross-validation. More specifically, for each of the twelve category pairs, we trained the classifier on three runs of one subject and tested the classifier on the remaining run of that same subject. This cross-validation procedure was repeated three times so that for each subject and category pair, each run was once used as the test dataset. The resulting four classification accuracies per subject and category pair were further averaged across runs, leaving the final classification accuracy per subject and category pair. This procedure was repeated for each of the twelve category pairs and each subject. To evaluate classification performance, we performed a permutation procedure estimating the distribution parameters under the null hypothesis. For each of the four cross-validation runs, we

shuffled category labels 1000 times within each run of the training dataset and tested the classifier on the test dataset. The accuracies were then averaged across runs resulting in 1000 permutation accuracies under the null hypothesis per subject and category pair. To evaluate significance on an individual subject level, we ranked the final classification accuracy against the ranked permutation accuracies. Additionally, to evaluate classification performance on the group level, we computed the average prediction accuracy across subjects per category pair and tested it against the average permutation accuracies using a non-parametric Wilcoxon sign rank test. P-values were corrected for multiple comparisons using an FDR correction while maintaining a false discovery rate of $q = 0.05$. To furthermore compare the classification between groups directly, we averaged accuracies across all twelve category pairs per group and tested the mean difference between groups against a distribution of means, which were computed by shuffling group labels 10,000 times.

In addition to within-subject classification, between-subject classification was analysed. The procedure was similar to the within-subject classification, except that we trained and tested the classifier for each category pair on two different subjects. More specifically, we trained the classifier on the data of subject 1 and tested on the data of the remaining subjects 2-23. The two subjects belonged to either the same group, hence referred to as within-group classification, or different groups, hence referred to a between-group classification. For statistical evaluation on the individual subject level, we again performed the permutation procedure with 1000 shuffles of category labels for each test subject and subsequently tested our true classification accuracies against the averaged permutation accuracies using a non-parametric Wilcoxon sign rank test. The prediction accuracies and permutation accuracies were averaged and assigned to the training subject. To evaluate significance on the group level, we averaged the classification accuracies and permutation accuracies per category pair across training subjects. Using a non-parametric Wilcoxon sign rank test, we tested the averaged classification accuracies against the averaged permutation accuracies. All p-values were corrected for multiple comparisons with an FDR correction with $q = 0.05$.

Univariate analysis

Because we were also interested in how early visual deprivation affects categorical processing in literature-based regions, a surface-based regions of interest (ROI) analysis was performed. Voxel-based time course files were sampled to the respective individual reconstructed vertex-based surfaces. For this transformation, data was integrated in depths along the vertex normals from −1.0 mm to 3.0 mm using trilinear interpolation. Because in this study we were only interested in the categorical processing, (and not on the processing of colour) we decided to collapse categories across colour conditions. This resulted in four conditions, which were 'Body', 'Scene', 'Face', 'Object'. We computed surface-based general linear models using BrainVoyager based on the group-aligned surface information, smoothed surface time course files and motion-corrected design matrices. The latter, as previously mentioned, contained only the categorical conditions (i.e. Face, Body, Object, Scene). Because we were specifically interested in group differences within literature-based categorical regions and to increase statistical power given our small sample size (Poldrack, 2007) we used a region of interest (ROI) analysis. ROI were defined using the probabilistic functional atlas of the occipital-temporal cortex by Rosenke et al. (2020). This atlas consists of 33 regions in total, 17 regions for the left hemisphere and 16 regions for the right hemisphere, including early visual areas as well as a variety of higher-level visual regions. In the following, each region will be described briefly. For more information see Rosenke et al. (2020).

We primarily focussed the analysis on regions that are associated with the four tested categories. Of those, face-selective regions were of specific interest, given that until now effects of early visual deprivation have only been reported in the face-processing system (Grady et al., 2014). The atlas defines three bilateral face regions – in the mid-lateral fusiform gyrus (mFus-faces) and posterior lateral fusiform gyrus (pFus-faces), corresponding to the fusiform face area (Kanwisher et al., 1997), as well as in the inferior occipital gyrus (IOG-faces). Although not directly associated as such by Rosenke et al., the IOG-faces most likely reflects the OFA (Gauthier et al., 2000). The differentiation into three face-selective regions has been emphasised lately as contrary to earlier believes, the middle and posterior face-selective regions show differentiations both on the cytoarchitectural as well as the functional level (Weiner et al., 2014; Weiner & Grill-Spector, 2010; Zhen et al., 2015). We needed to consider possible differences among face-selective regions, as they might influence the conclusions of whether there are group differences or not. Yet because of our small sample size, dividing into small regions also brings the disadvantage of less statistical power. We therefore decided to also investigate the average of all three regions, which was labelled avg-faces. As body-selective regions, Rosenke et al. defined a bilateral region in the occipital-temporal sulcus, the OTS-bodies region, which corresponds to the FBA (Peelen & Downing, 2005; Schwarzlose et al., 2005), as

well as three additional bilateral regions in the lateral occipital cortex. These three regions, the middle temporal gyrus (MTG-bodies), the lateral occipital sulcus (LOS-bodies), and the inferior temporal gyrus (ITG-bodies) are together referred to as the EBA (Downing et al., 2001), a region, that again only recently has been identified as a complex of multiple subparts (Ferri et al., 2013; Weiner & Grill-Spector, 2011). The atlas entails furthermore a bilateral place-selective region within the collateral sulcus (CoS-places) corresponding to the PPA (Epstein & Kanwisher, 1998) and additionally a right-lateralised place-selective region in the transverse occipital sulcus (TOS; Hasson, 2003; also referred to as occipital place area (OPA). Unfortunately, the functional atlas does not entail regions for object processing, although object-selectivity has been tested. The reason for not including object-selective regions in the functional atlas according to the authors was a strong variability among the tested subjects, which did not allow for reliable definition (Rosenke et al., 2020). Additionally, the atlas contains two left-lateralised character-selective regions, namely the posterior occipital-temporal sulcus (pOTS-characters) and the inferior occipital sulcus (IOS-characters), the mid-level bilateral hMT, which is associated with the processing of motion (Tootell et al., 1995) and early visual regions, consisting of V1, V2 and V3, both in a dorsal and a ventral location.

Given its important role for categorical processing, we focused our analysis firstly on the VTC. We selected a sub-set of atlas regions that overlapped with our previously defined VTC mask. Five regions were selected accordingly, namely the mFus-faces, pFus-faces, IOG-faces, OTS-bodies and CoS-places. For the previously mentioned bilateral avg-faces, all three individual face regions were combined respectively for the left and right hemisphere. For each ROI, beta values were extracted for all subjects (N = 24) according to our experimental design. Our main interest was the direct comparison of CC individuals and SC individuals. Therefore, we calculated a model based on the CC individuals and a subset of eight SC individuals matched in age and sex, hence referred to as the matched-model (N = 16).

ROI analyses were performed using the statistical software R (R Core Team, 2016). For each of the ROI, a linear mixed model was fitted using the *lme4* package (Bates et al., 2015), specifying group and category as factors, a random intercept for each subject and the extracted beta values as the dependent variable. We used the *lmerTest* package (Kuznetsova et al., 2017) for obtaining *F*-test values including *p*-values with the Kenward-Roger method for estimating denominator degrees of freedom. All ANOVA outputs were collected and corrected for multiple comparisons using FDR correction while maintaining a false discovery rate of q = 0.05. If the results indicated significant or marginal significant effects, we further performed pairwise comparisons of estimated marginal means using the package *emmeans* (Lenth, 2022). For category main effects, we tested each category response averaged across groups against each of the remaining categories, resulting in six pairwise

comparisons. For a group main effect, we tested the overall group mean against the other groups. In the case of a group*category interaction, we split the data first by group to compare categories separately for each group and second by category to compare groups directly for each of the four categories. All post-hoc results were collected and an FDR correction was applied maintaining q = 0.05.

Because our sample size of eight individuals was quite small and the advantage of linear mixed models in dealing with unequal sample sizes (G. Chen et al., 2013), we wanted to investigate if possible effects would depend on the sample size and if increasing the size of our sighted control sample would give stronger results. In a second approach, we hence re-run the analysis described above based on data of all tested subjects. Accordingly, the sample consisted of 13 SC individuals, eight CC individuals and three VI individuals. We hence referred to this model as the all-subjects-model (*N* = 24).

As described above, the functional atlas contains a variety of other regions. Given the little evidence for categorical processing in the rare sample of CC individuals, we decided to make use of all ROI within the functional atlas provided by Rosenke et al. (2020). Our third point of focus included therefore the remaining ROI provided by the atlas beyond the border of VTC. Those regions were split into regions that are associated with tested categories such as places and bodies, and other regions, such as the character regions, the motion-selective hMT as well as all six early visual regions.

To summarise our ROI analyses, the study had three main goals: 1) category-selective responses within the VTC were directly compared between the CC group and eight matched SC individuals. 2) we investigated whether comparing the CC group of eight individuals to all tested SC individuals and three VI individuals would influence the results. 3) we tested possible category effects in all ROI based on the functional atlas by Rosenke et al., which expanded the regions to categorical regions outside the VTC, as well as untested categorical and early visual regions.

4. Results

Behavioural Analysis Results

The average dissimilarity of the CC group in between-category trials was 2.52 (*SD* = 1.06) and in within-category trials 2.66 (*SD* = 0.45). The SC group perceived between-category trials (*M* = 2.92, *SD* = 1.06) slightly more dissimilar than within-category trials (*M* = 2.65, *SD* = 0.53). Yet neither of the two groups exhibited the expected category differences (CC individuals: $t(6) = -0.32$, $p > .05$; SC individuals: $t(10) = 0.967$, $p > .05$). The VI group perceived the between-category trials (*M* = 3.71, *SD* = 0.33) as more dissimilar than within-category trials (*M* = 2.63, *SD* = 0.16). Due to the small sample size, no statistic evaluation has been performed.

MVPA Results

We divided the MVPA into three analyses of interest. First, we assessed within-subject classification, where training and testing the classifier was based on one subjects' data. Second, we performed within-group classification, in which we focused on all subjects of each group. Third, we run the between-group classification focussing on participants of different groups, meaning training the classifier on a subject of one group and testing on the subjects of another group.

Within-subject classification

Figure *10* displays the within-subject classification results averaged for each group. Classifications for all twelve category-pairs were significantly better than empirical chance level as calculated by the permutation tests for SC and CC group. Due to the small sample size of three individuals, the results of the VI group are only displayed for demonstration purposes. To investigated if groups differed regarding their classification results a permutation test was performed. Comparing classification results directly between groups, showed significant lower overall classification accuracies in the CC group (mean accuracy M = 88.67%, SD = 6.95) compared to the SC12 group (M = 95.31%, SD = 3.83, p = .006). The VI group (M = 95.58%, SD = 5.06) showed on average similar accuracy values to the SC group.

Figure 10

Within-Subject Classification Results for Normally Sighted Individuals, CC Individuals and VI Individuals

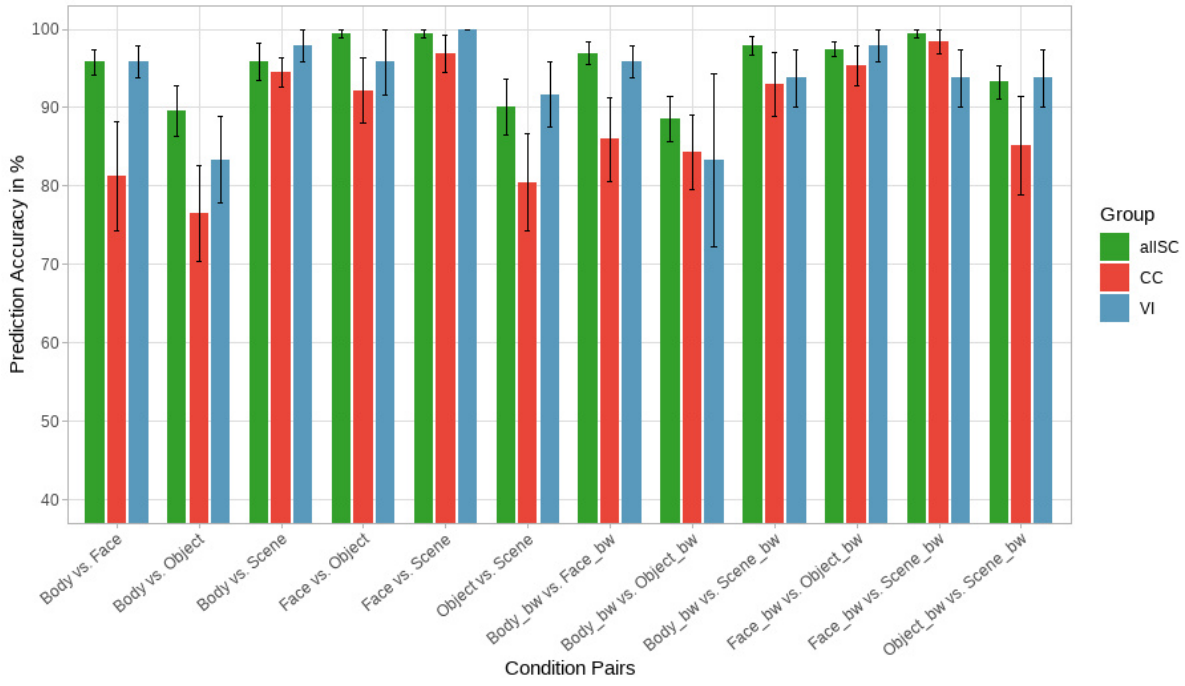

Note. Average classification results for each of the twelve category-pairs separately for normally sighted individuals (allSC; *n* = 12; displayed in green), CC individuals (CC; *n* = 8; displayed in red) and VI individuals (VI; *n* = 3; displayed in blue). Error bars represent standard errors.

Within-group classification

The within-group classification results are shown in **Figure *11***. In the SC group all category-pairs have been correctly classified. In the CC group category-pairs have been correctly classified, only 'Body vs. Scene' did not survive the correction for multiple comparisons (p = .055). The results for the VI group are again presented only for illustration purposes. Again, we compared classification results across groups and found significantly lower accuracy for the CC group (M = 71.61%, SD = 10.69) compared to the SC group (M = 80.76%, SD = 8.89, p = .019). The VI group exhibited on average accuracy values between the other two groups (M = 74.13%, SD = 12.88).

Figure 11

Within-Group Classification Results for Normally Sighted Individuals, CC Individuals and VI Individuals

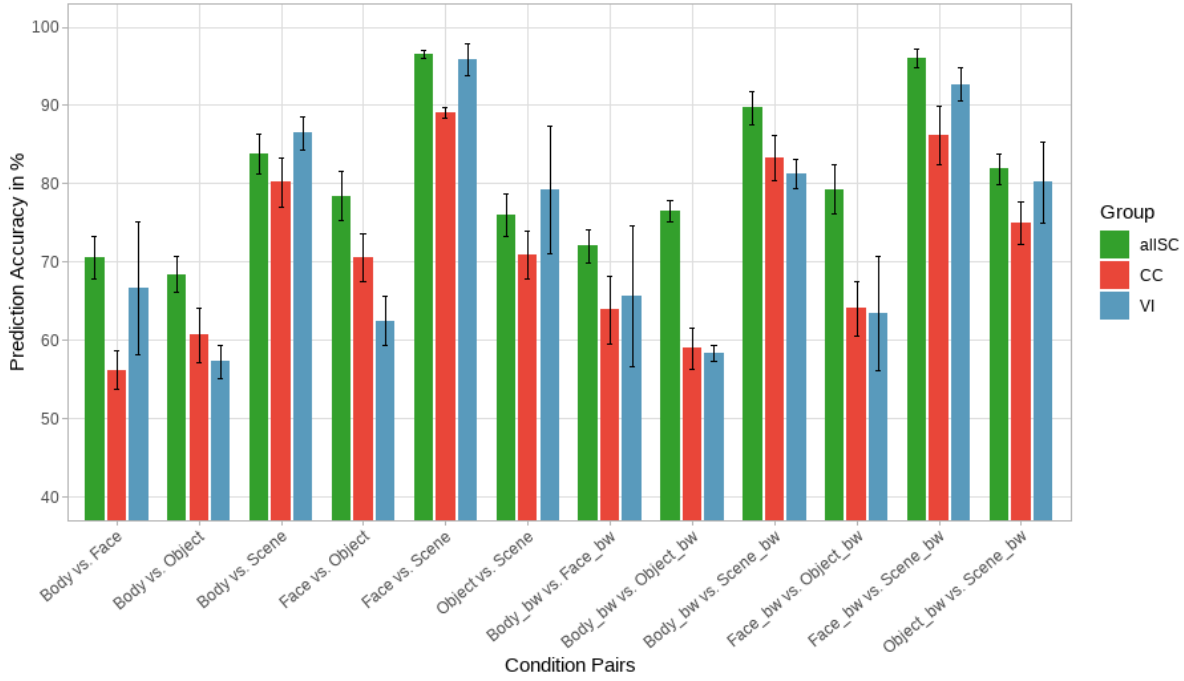

Note. Average classification results for each of the twelve category-pairs separately for normally sighted individuals (allSC; n = 12; displayed in green), CC individuals (CC; n = 8; displayed in red) and VI individuals (VI; n = 3; displayed in blue). Error bars represent standard errors.

Between group classification

We were also interested if categories could be successfully classified across groups. Again, given the small sample size of our VI group, the between-group analysis was performed only for the SC and CC groups. All category-pairs have been correctly predicted when training the classifier on the CC data and tested on the SC data (*M* = 78.72%, *SD* = 2.75) as well as when reversing the prediction direction, i.e. training on the SC data and testing on the CC data (*M* = 70.15%, *SD* = 2.44). Comparing the classification results of both prediction directions indicated no significant difference (*p* = .954). **Figure *12*** displays the average prediction accuracies for both classification directions.

Figure 12

Between Group Classification Results for Both Classification Directions

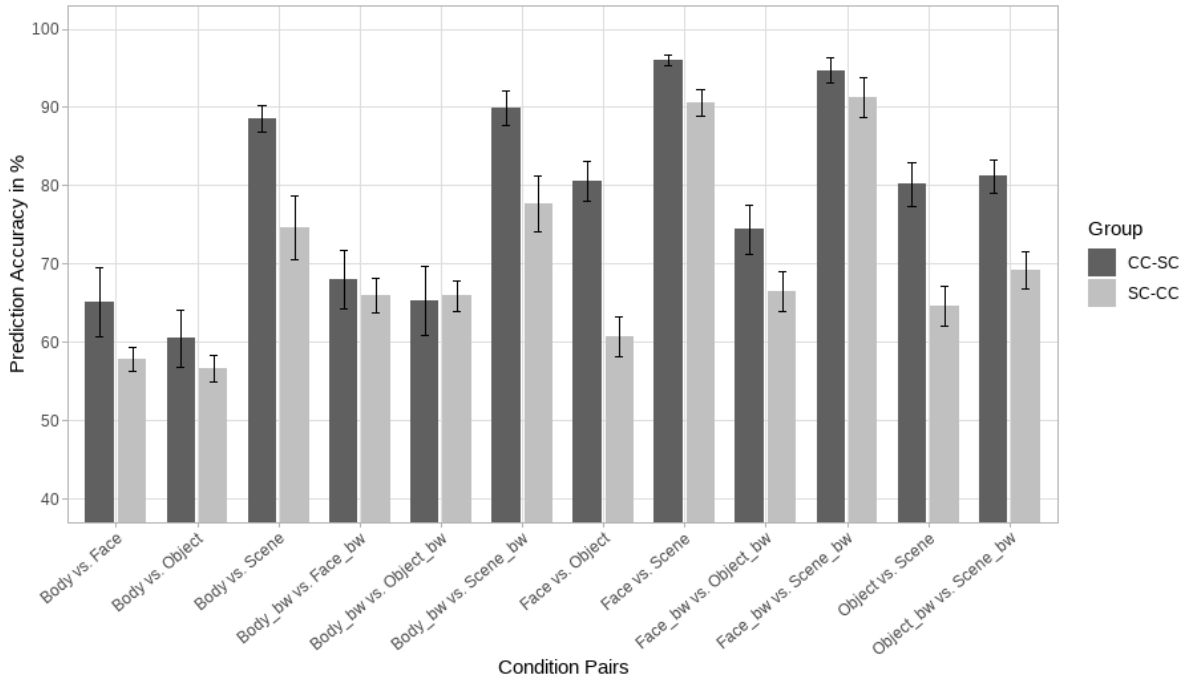

Note. Average classification results for each of the twelve category-pairs separately for CC-to-SC generalisation (dark grey) and SC-to-CC-generalisation (light grey). Error bars represent standard errors.

ROI Analysis Results Within the VTC

Because we are interested in directly comparing both subject models separately per region, we decided to list both models directly per ROI rather than reporting models separately. For readability, only the category-specific post-hoc comparisons are reported in the text, while the remaining results are listed in the Appendix B. For each ROI, tables list the average beta values per category and group and entail the mSC group, i.e. matched SC individuals, as well as the allSC group, based on the data of all tested SC individuals. For the respective graphs, rather than displaying results of the same subject twice, we decided to display the mSC individuals in light green while only the five additional SC individuals in the allSC group are displayed in dark green. All reported p values were corrected for multiple comparisons.

mFus-faces

mFus-faces_lh (matched-model). For the left mFus-faces, there was a significant main of category ($F(3,42) = 5.08$, $p = .013$, $\eta_p^2 = .266$). There was no effect of group ($F(1,14) = 2.89$, $p = .222$, $\eta_p^2 = .171$), nor a significant interaction between group and category ($F(3,42) = 1.99$, $p = .227$, $\eta_p^2 = .124$). Overall, the category Object elicited the highest response ($M = 0.96$, $SD = 0.47$) followed by Face ($M = 0.90$, $SD = 0.39$), Body ($M = 0.71$, $SD = 0.42$) and Scene ($M = 0.64$, $SD = 0.54$). The group-specific average category responses are displayed in Table 5 and in Figure 13. All post-hoc results can be found in supplementary table S1. Here, we only report the face-specific comparisons, given that they are the preferential category for the mFus-faces regions. Post-hoc pairwise comparisons revealed significant differences for 'Face vs. Scene' ($t(42) = 2.75$, $p = .015$) and a marginal difference for 'Body vs. Face' ($t(42) = -2.01$, $p = .074$).

mFus-faces_lh (all-subjects-model). Based on the data of all subjects, we found a significant effect of category ($F(3,63) = 11.68$, $p < .001$, $\eta_p^2 = .357$). There was no effect of group ($F(2,21) = 1.05$, $p = .553$, $\eta_p^2 = .091$). In contrast to the matched-model, there was a marginally significant interaction between group and category ($F(6,63) = 2.69$, $p = .054$, $\eta_p^2 = .204$).

For post-hoc comparison, we first split the data from the left hemisphere by group and compared categorical response profiles within each group. The group-specific average category responses are displayed in Table 5 and in Figure 13. SC and VI individuals exhibited the highest response to the category Face, followed by Object, Body and Scene. CC individuals on the contrary showed the highest response to the category Object, followed by Faces, Body and Scene. All post-hoc results can be found in supplementary table S14. Here, we only report the face-specific comparisons, given that they are

the preferential category. For the SC group, the comparisons 'Body vs. Face' (t(63) = -3.97, p = .001) and 'Face vs. Scene' (t(63) = 4.86, p < .001) became significant. For the VI group, only the comparison 'Face vs. Scene' became significant (t(63) = 4.31, p < .001), while 'Body vs. Face' was marginally significant (t(63) = -2.15, p = .071). For the CC group, categories did not differ significantly from each other. Secondly, we split the mFus-faces_lh data by category to compare groups directly. We found marginal differences between SC group and CC group for the category Body (t(42) = -2.04, p = .092) and the category Scene t(42) = -2.12, p = .078), as well as a marginal difference between CC group and VI group for the category Scene (t(42) = 2.18, p = .071). All further post-hoc results can be found in supplementary table S15.

mFus-faces_rh (matched-model). We found a significant effect of category (F(3,42) = 24.43, p < .001, η_p^2 = . 636). Neither was there a group effect (F(1,14) = 1.58, p = .326, η_p^2 = . 101) nor an interaction between the two (F(3,42) = 1.11, p = .428, η_p^2 = . 073). Overall, the category Face elicited the highest response (M = 1.19, SD = 0.45), followed by Object (M = 0.79, SD = 0.41), Body (M = 0.77, SD = 0.34) and Scene (M = 0.36, SD = 0.46). The group-specific average category responses are displayed in Table 6 and in Figure 14. All face-specific comparisons became significant (p < .001) and can be found in supplementary table S2 with the remaining category comparisons.

mFus-faces_rh (all-subjects-model). Similarly to the matched model, we only found a significant effect of category (F(3,63) = 27.85, p < .001, η_p^2 = .570). There was neither an effect of group (F(2,21) = 0.16, p = .878, η_p^2 = .015), nor an interaction between group and category (F(6,63) = 0.75, p = .734, η_p^2 = .067). Highest response was found for the category Face (M = 1.26, SD = 0.46), followed by Body (M = 0.83, SD = 0.37), Object (M = 0.82, SD = 0.42) and Scene (M = 0.40, SD = 0.48). All face-specific comparisons became significant ('Body vs. Face': t(63) = -4.57, p < .001; 'Face vs. Object': t(63) = 4.62, p < .001; 'Face vs. Scene' t(63) = 9.14, p < .001). The remaining post-hoc results can be found in supplementary table S16.

Categorical responses within the bilateral mFus-faces

Table 5

Individual and Group Average Categorical Responses within the mFus-faces_lh

	Body		Face		Object		Scene	
group	*M*	*SD*	*M*	*SD*	*M*	*SD*	*M*	*SD*
allSC	0.56	0.34	0.99	0.45	0.93	0.43	0.46	0.52
mSC	0.47	0.34	0.85	0.37	0.84	0.51	0.41	0.58
CC	0.95	0.37	0.95	0.43	1.07	0.42	0.87	0.41
VI	0.73	0.41	1.22	0.55	0.83	0.27	0.24	0.26

Figure 13

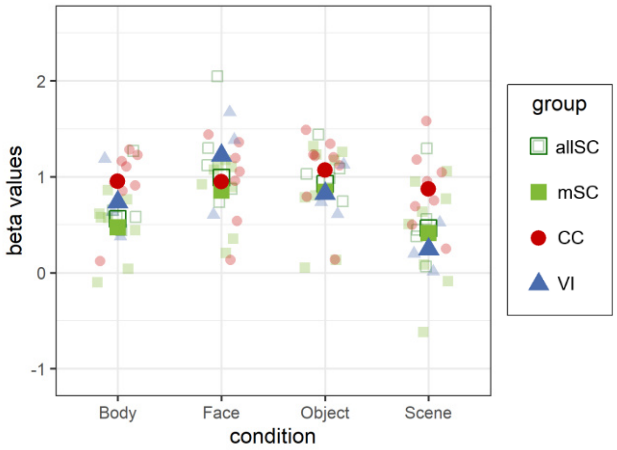

Table 6

Individual and Group Average Categorical Responses within the mFus-faces_rh

	Body		Face		Object		Scene	
group	*M*	*SD*	*M*	*SD*	*M*	*SD*	*M*	*SD*
allSC	0.81	0.35	1.32	0.49	0.77	0.48	0.34	0.60
mSC	0.65	0.27	1.18	0.55	0.65	0.49	0.20	0.57
CC	0.88	0.37	1.19	0.37	0.94	0.26	0.52	0.27
VI	0.74	0.56	1.18	0.68	0.71	0.58	0.34	0.41

Figure 14

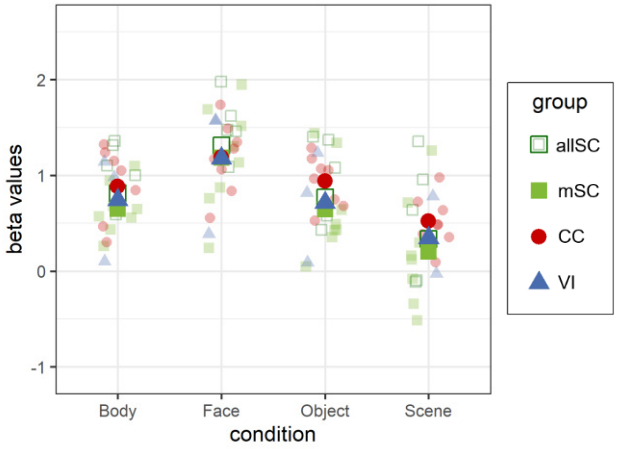

Note. Categorical responses within the bilateral mFus-faces, with values for the left mFus-faces on the upper panel and values for the right mFus-faces on the lower panel. The tables (left side) display each group's average response and standard deviation to each category. The graphs (right side) display average individual (smaller symbols, faded colours) and group mean (larger symbols, bright colours) categorical responses. CC: congenital cataract individuals (*n* = 8; displayed in red); mSC: matched sighted individuals (*n* = 8; displayed in light green); allSC: all tested sighted individuals (*n* = 13; the additional 5 SC individuals are displayed in dark green; VI: visually impaired individuals (*n* = 3).

pFus-faces

pFus-faces_lh (matched-model). There was a significant effect of category ($F(3,42) = 6.92$, $p = .002$, $\eta_p^2 = .331$). There was neither an effect for group ($F(1,14) = 2.50$, $p = .227$, $\eta_p^2 = .152$), nor an interaction between group and category ($F(3,42) = 1.66$, $p = .299$, $\eta_p^2 = .106$). The highest response was evoked by the category Object ($M = 1.28$, $SD = 0.39$), followed by Face ($M = 1.17$, $SD = 0.41$), Scene ($M = 1.02$, $SD = 0.47$) and Body ($M = 0.96$, $SD = 0.37$). The group-specific average category responses are displayed in Table 7 and in Figure 15. Post-hoc tests revealed significant differences for 'Body vs. Face' ($t(42) = -2.65$, $p = .018$) and a marginal difference for 'Face vs. Scene' ($t(42) = 1.94$, $p = .083$). The remaining post-hoc results can be found in supplementary table S3.

pFus-faces_lh (all-subjects-model). Similarly to the matched-model, we found a significant effect of category ($F(3,63) = 9.27$, $p < .001$, $\eta_p^2 = .306$). There was no effect of group ($F(2,21) = .65$, $p = .665$, $\eta_p^2 = .058$), nor an interaction between group and category ($F(6,63) = 1.48$, $p = .354$, $\eta_p^2 = .123$). The highest response in the left hemisphere was found for the category Object ($M = 1.33$, $SD = 0.37$), followed Face ($M = 1.21$, $SD = 0.42$), Scene ($M = 1.00$, $SD = 0.46$) and Body ($M = 0.98$, $SD = 0.34$). The group-specific average category responses are displayed in Table 7 and in Figure 15. The face-specific post-hoc comparisons 'Body vs. Face' ($t(63) = -2.66$, $p = .023$) and 'Face vs. Scene' ($t(63) = -3.14$, $p = .007$) became significant. The remaining post-hoc results can be found in supplementary table S17.

pFus-faces_rh (matched-model). There was a significant effect of category ($F(3,42) = 11.19$, $p < .001$, $\eta_p^2 = .444$) for the pFus-faces_rh. There was no effect of group ($F(1,14) = 1.73$, $p = .315$, $\eta_p^2 = .110$) nor an interaction between group and category ($F(3,42) = 0.81$, $p = .524$, $\eta_p^2 = .055$). The highest response was found for the category Object ($M = 1.25$, $SD = 0.35$), followed by Face ($M = 1.17$, $SD = 0.36$), Scene ($M = 0.93$, $SD = 0.40$) and Body ($M = 0.92$, $SD = 0.28$). The group-specific average category responses are displayed in Table 8 and in Figure 16. Post-hoc pairwise comparisons revealed two of the three face-specific comparisons to be significant, which were 'Body vs. Face' ($t(42) = -3.44$, $p = .003$) and 'Face vs. Scene' ($t(42) = 3.36$, $p = .003$). Additional post-hoc results are listed in supplementary table S4.

pFus-faces_rh (all-subjects-model). We found a significant effect of category ($F(3,63) = 12.56$, $p < .001$, $\eta_p^2 = .374$). Neither the effect of group ($F(2,21) = 0.34$, $p = .788$, $\eta_p^2 = .031$) nor the interaction between the two ($F(6,63) = 0.92$, $p = .665$, $\eta_p^2 = .080$) became significant. The highest response was shown for the category Object ($M = 1.29$, $SD = 0.33$), followed by Face ($M = 1.22$, $SD = 0.37$), Body ($M = 0.95$, $SD = 0.26$) and Scene ($M = 0.92$, $SD = 0.39$). The group-specific average category responses are displayed in Table 8 and in Figure 16. Similar to the left pFus-faces, face-specific comparisons 'Body

vs. Face' ($t(63) = -3.07$, $p = .009$) and 'Face vs. Scene' ($t(63) = 4.06$, $p < .001$) became significant. The remaining post-hoc results can be found in supplementary table S18.

Categorical responses within the bilateral pFus-faces

Table 7

Individual and Group Average Categorical Responses within the pFus-faces_lh

	Body		Face		Object		Scene	
group	*M*	*SD*	*M*	*SD*	*M*	*SD*	*M*	*SD*
allSC	0.88	0.34	1.23	0.34	1.32	0.41	0.93	0.53
mSC	0.77	0.35	1.13	0.35	1.15	0.40	0.82	0.55
CC	1.15	0.30	1.21	0.49	1.41	0.36	1.21	0.30
VI	0.97	0.35	1.18	0.70	1.21	0.29	0.74	0.30

Figure 15

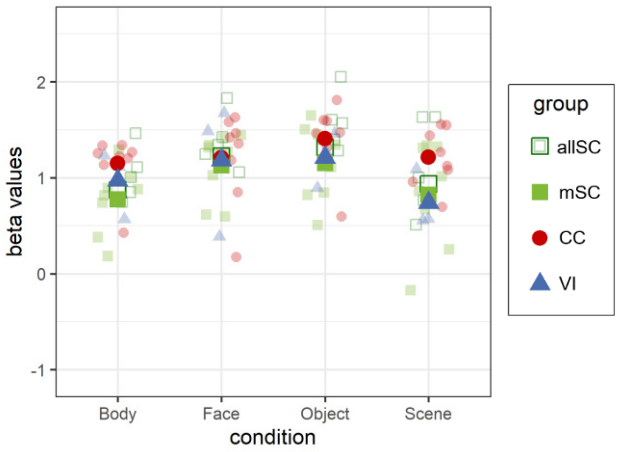

Table 8

Individual and Group Average Categorical Responses within the pFus-faces_rh

	Body		Face		Object		Scene	
group	*M*	*SD*	*M*	*SD*	*M*	*SD*	*M*	*SD*
allSC	0.89	0.26	1.25	0.35	1.25	0.38	0.87	0.47
mSC	0.81	0.27	1.14	0.38	1.13	0.39	0.81	0.51
CC	1.04	0.25	1.20	0.37	1.38	0.26	1.05	0.23
VI	1.01	0.25	1.13	0.55	1.22	0.28	0.81	0.29

Figure 16

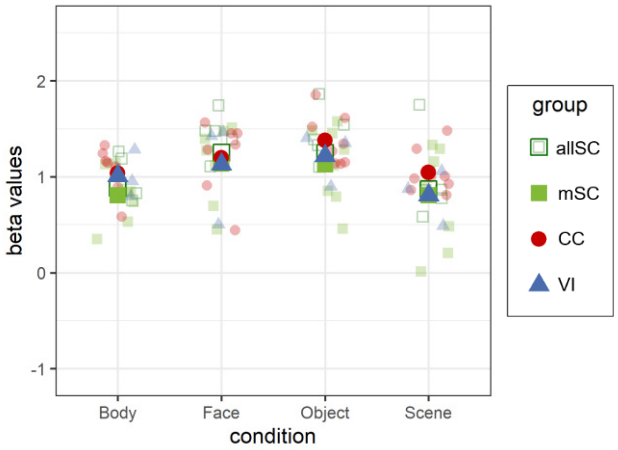

Note. Categorical responses within the bilateral pFus-faces, with values for the left pFus-faces on the upper panel and values for the right pFus-faces on the lower panel. The tables (left side) display each group's average response and standard deviation to each category. The graphs (right side) display average individual (smaller symbols, faded colours) and group mean (larger symbols, bright colours) categorical responses. CC: congenital cataract individuals ($n = 8$; displayed in red); mSC: matched sighted individuals ($n = 8$; displayed in light green); allSC: all tested sighted individuals ($n = 13$; the additional 5 SC individuals are displayed in dark green; VI: visually impaired individuals ($n = 3$).

IOG-faces

IOG-faces_lh (matched-model). For the left IOG-faces, there was a significant effect of category ($F(3,42) = 20.44$, $p < .001$, $\eta_p^2 = .593$). No effect of group found ($F(1,14) = 2.93$, $p = .222$, $\eta_p^2 = .173$). The interaction between group and category was marginally significant, however, did not survive FDR correction ($F(3,42) = 2.83$, $p = .125$, $\eta_p^2 = .168$). In the left IOG-faces, the category Face elicited the highest response ($M = 1.17$, $SD = 0.47$), followed by Object ($M = 1.16$, $SD = 0.37$), Body ($M = 0.83$, $SD = 0.38$) and Scene ($M = 0.73$, $SD = 0.38$). The group-specific average category responses are displayed in Table 9 and in Figure 17. Two of the three face-specific comparisons became significant, which were 'Body vs. Face' ($t(42) = -4.76$, $p < .001$) and 'Face vs. Scene' ($t(42) = 6.27$, $p < .001$). Additional post-hoc results are listed in supplementary table S5.

IOG-faces_lh (all-subjects-model). For the IOG-faces_lh there was a significant effect of category ($F(3,63) = 24.54$, $p < .001$, $\eta_p^2 = .539$). There was no effect of group ($F(2,21) = 0.31$, $p = .788$, $\eta_p^2 = .029$). In contrast to the matched-model, there was a marginally significant interaction between group and category ($F(6,63) = 2.47$, $p = .077$, $\eta_p^2 = .190$).

For post hoc testing, we first split the data from the left hemisphere by group to compare the responses to the categories within each group. The group-specific average category responses are displayed in Table 9 and in Figure 17. Both for SC individuals and for VI individuals the category Face elicited the highest response, followed by Object, Body and Scene. In CC individuals, the category Objects elicited the highest response, followed by Face, Body and Scene. In the SC group, post-hoc comparisons revealed the face-specific comparisons 'Body vs. Face' ($t(63) = -6.52$, $p < .001$) and 'Face vs. Scene' ($t(63) = 7.51$, $p < .001$) to be significant. For the VI group, only one face-specific comparison became significant, which was 'Face vs. Scene' ($t(63) = 4.38$, $p < .001$). Similarly in the CC group 'Face vs. Scene' was the only significant face-specific comparison ($t(63) = 2.41$, $p = .041$). All remaining post-hoc comparisons can be found in in supplementary table S19. We additionally split the IOG-faces_lh data by category to compare groups directly. Pairwise comparison did not indicate group differences (supplementary table S20).

IOG-faces_rh (matched-model). For the right IOG-faces, there was a significant effect of category ($F(3,42) = 22.40$, $p < .001$, $\eta_p^2 = .615$). There was no effect of group ($F(1,14) = 1.14$, $p = .381$, $\eta_p^2 = .075$), nor was there a interaction between the two ($F(3,42) = 1.29$, $p = .377$, $\eta_p^2 = .085$). Overall, the category Face evoked the highest response ($M = 1.30$, $SD = 0.45$), followed by Object ($M = 1.07$, $SD = 0.31$), Body ($M = 0.79$, $SD = 0.41$) and Scene ($M = 0.70$, $SD = 0.36$). The group-specific average category responses are displayed in Table 10 and in Figure 18. All face-specific comparisons became significant ('Body vs. Face' ($t(42) = -6.21$, $p < .001$), 'Face vs. Object' ($t(42) = 2.75$, $p = .015$) and 'Face vs. Scene' ($t(42) = 7.34$, $p < .001$). The remaining post-hoc results can be found in supplementary table S6.

IOG-faces_rh (all-subjects-model). Similarly to the matched model, only the effect of category became significant ($F(3,63) = 28.16$, $p < .001$, $\eta_p^2 = .573$). There was no effect of group ($F(2,21) = 0.05$, $p = .949$, $\eta_p^2 = .005$), nor was there an interaction between group and category ($F(6,63) = 1.01$, $p = .612$, $\eta_p^2 = .088$). Across groups, the highest response was found for the category Face ($M = 1.38$, $SD = 0.41$), followed by Object ($M = 1.14$, $SD = 0.30$), Body ($M = 0.85$, $SD = 0.39$) and Scene ($M = 0.72$, $SD = 0.35$). The category Face differed significantly from all other categories ('Body vs. Face': $t(63) = -6.27$, $p < .001$; 'Face vs. Object': $t(63) = 2.96$, $p = .012$; 'Face vs. Scene' $t(63) = 8.56$, $p < .001$). The group-specific average category responses are displayed in Table 9 and in Figure 17. All post-hoc comparisons can be found in supplementary table S21.

Categorical responses within the bilateral IOG-faces

Table 9

Individual and Group Average Categorical Responses within the IOG-faces_lh

	Body		Face		Object		Scene	
group	*M*	*SD*	*M*	*SD*	*M*	*SD*	*M*	*SD*
allSC	0.78	0.34	1.31	0.39	1.21	0.41	0.70	0.45
mSC	0.64	0.23	1.14	0.38	1.02	0.36	0.51	0.34
CC	1.03	0.42	1.20	0.57	1.29	0.36	0.95	0.29
VI	0.98	0.36	1.27	0.46	1.13	0.20	0.53	0.19

Figure 17

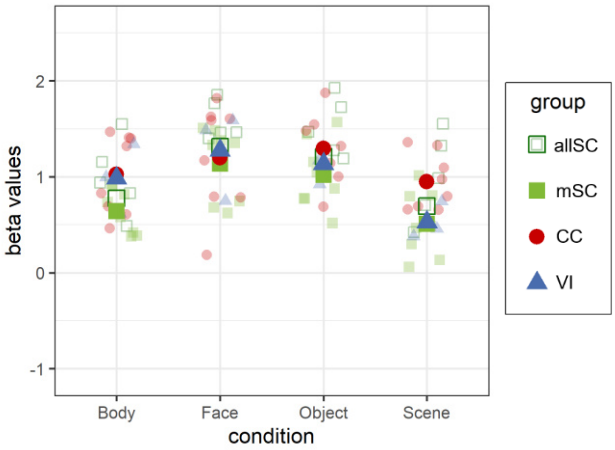

Table 10

Individual and Group Average Categorical Responses within the IOG-faces_rh

	Body		Face		Object		Scene	
group	*M*	*SD*	*M*	*SD*	*M*	*SD*	*M*	*SD*
allSC	0.77	0.35	1.41	0.34	1.14	0.34	0.70	0.40
mSC	0.63	0.24	1.30	0.38	0.98	0.29	0.59	0.39
CC	0.95	0.49	1.30	0.53	1.16	0.32	0.80	0.30
VI	0.92	0.26	1.43	0.46	1.13	0.11	0.58	0.33

Figure 18

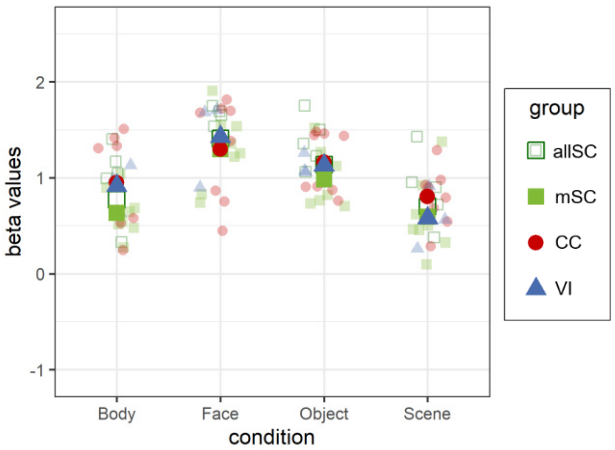

Note. Categorical responses within the bilateral IOG-faces, with values for the left IOG-faces on the upper panel and values for the right IOG-faces on the lower panel. The tables (left side) display each group's average response and standard deviation to each category. The graphs (right side) display average individual (smaller symbols, faded colours) and group mean (larger symbols, bright colours) categorical responses. CC: congenital cataract individuals (*n* = 8; displayed in red); mSC: matched sighted individuals (*n* = 8; displayed in light green); allSC: all tested sighted individuals (*n* = 13; the additional 5 SC individuals are displayed in dark green; VI: visually impaired individuals (*n* = 3).

avg-faces

avg-faces_lh (matched-model). There was a significant effect of category for the left avg-faces ($F(3,42) = 11.06$, $p < .001$, $\eta_p^2 = .441$). There was a marginal effect of group, which did not survive the FDR correction for multiple comparisons ($F(1,14) = 3.26$, $p = .167$, $\eta_p^2 = .189$). Similarly, there was a marginal interaction between group and category, which did not survive the FDR correction ($F(3,42) = 2.59$, $p = .147$, $\eta_p^2 = .156$). The highest response was evoked by the category Object ($M = 1.13$, $SD = 0.39$), followed by Face ($M = 1.08$, $SD = 0.40$), Body ($M = 0.84$, $SD = 0.36$) and Scene ($M = 0.80$, $SD = 0.42$). The group-specific average category responses are displayed in Table 11 and in Figure 19. Post-hoc pairwise comparisons revealed two of the three face-specific comparisons to be significant, which were 'Body vs. Face' ($t(42) = -3.38$, $p = .003$) and 'Face vs. Scene' ($t(42) = 3.94$, $p = .001$). All post-hoc results can be found in supplementary table S7.

avg-faces_lh (all subjects model). Similarly to the matched subjects model, results indicated a significant category effect ($F(3,63) = 18.20$, $p < .001$, $\eta_p^2 = .464$). There was no effect of group ($F(2,21) = 0.71$, $p = 0.582$, $\eta_p^2 = 0.064$). However, we found a significant group*category interaction for the left hemisphere ($F(6,63) = 2.89$, $p = .034$, $\eta_p^2 = .216$).

To investigate the group*category interaction further we first split the data by group to compute pairwise comparisons of category for each group separately. Post-hoc analyses revealed different response profiles per group. The group-specific average category responses are displayed in Table 11 and in Figure 19. In the SC group, responses were highest for the category Face, followed by Object, Body and Scene. Two face-specific comparisons indicated significant differences for 'Body vs. Face' ($t(63) = -5.50$, $p < .001$) and 'Face vs. Scene' ($t(63) = 6.00$, $p < .001$). The VI group showed a similar response profile with the highest response to the category Face, followed by Object, Body and Scene. The comparison 'Face vs. Scene' ($t(63) = 4.35$, $p < .001$) was the only face-specific comparison to become significant. Additionally, the comparison 'Body vs. Face' was marginally significant ($t(63) = -1.98$, $p = .099$). However, for the CC group the category Object elicited the highest response, followed by Face, Body and Scene. No face-specific comparison became significant. The remaining post-hoc results can be found in the supplementary table S22. Secondly, we split the data of avg-faces_lh by category to compare groups directly with each other. After correction for multiple comparisons only the comparison of 'CC vs. VI' for the category Scene was marginal significant ($t(34) = 2.01$, $p = .099$). All remaining post-hoc results are listed in supplementary table S23.

avg-faces_rh (matched-model). There was a significant effect of category ($F(3,42) = 25.65$, $p < .001$, $\eta_p^2 = .647$).There was no effect of group ($F(1,14) = 2.09$, $p = 0.255$, $\eta_p^2 = 0.130$), nor an interaction between the two ($F(3,42) = 1.46$, $p = .307$, $\eta_p^2 = .095$). In the right avg-faces, the category Face elicited the highest response ($M = 1.22$, $SD = 0.38$), followed by Object ($M = 1.04$, $SD = 0.30$), Body ($M = 0.83$, $SD = 0.30$) and Scene ($M = 0.66$, $SD = 0.31$). The group-specific average category responses are displayed in Table 12 and in Figure 20. All face-specific comparisons became significant ('Body vs. Face' ($t(42) = -5.76$, $p < .001$), 'Face vs. Object' ($t(42) = 2.61$, $p = .020$) and 'Face vs. Scene' ($t(42) = 8.19$, $p < .001$)). The remaining post-hoc results can be found in supplementary table S8.

avg-faces_rh (all subjects model). Similarly to the matched subjects model, results indicated a category effect in the right hemisphere ($F(3,63) = 35.55$, $p < .001$, $\eta_p^2 = .629$). There was no effect of group ($F(2,21) = 0.20$, $p = .823$, $\eta_p^2 = .018$), nor an interaction between the two ($F(6,63) = 1.22$, $p = .420$, $\eta_p^2 = .104$). The highest response was evoked by the category Face ($M = 1.28$, $SD = 0.38$), followed by Object ($M = 1.08$, $SD = 0.3$), Body ($M = 0.88$, $SD = 0.29$), Scene ($M = 0.68$, $SD = 0.32$). The category Face differed significantly from each of the remaining categories ('Body vs. Face' ($t(63) = -6.19$, $p < .001$); 'Face vs. Object' ($t(63) = 3.10$, $p = .007$) and 'Face vs. Scene' ($t(63) = 9.84$, $p < .001$)). Additional post-hoc results are listed in supplementary table S24.

Categorical responses within the bilateral avg-faces

Table 11

Individual and Group Average Categorical Responses within the avg-faces_lh

	Body		Face		Object		Scene	
group	*M*	*SD*	*M*	*SD*	*M*	*SD*	*M*	*SD*
allSC	0.74	0.30	1.18	0.37	1.15	0.39	0.70	0.46
mSC	0.63	0.28	1.04	0.34	1.01	0.41	0.58	0.46
CC	1.04	0.32	1.12	0.48	1.26	0.35	1.01	0.26
VI	0.90	0.37	1.23	0.57	1.06	0.17	0.50	0.16

Figure 19

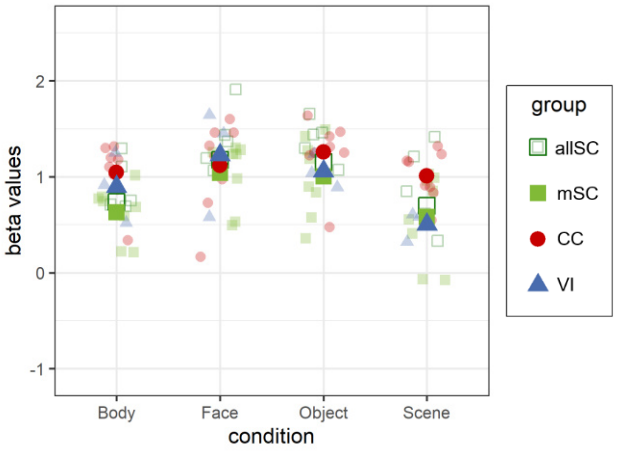

Table 12

Individual and Group Average Categorical Responses within the avg-faces_rh

	Body		Face		Object		Scene	
group	*M*	*SD*	*M*	*SD*	*M*	*SD*	*M*	*SD*
allSC	0.82	0.27	1.33	0.37	1.05	0.34	0.64	0.38
mSC	0.70	0.19	1.21	0.41	0.92	0.32	0.54	0.37
CC	0.96	0.34	1.23	0.38	1.16	0.24	0.79	0.20
VI	0.89	0.33	1.25	0.56	1.02	0.31	0.58	0.30

Figure 20

Note. Categorical responses within the bilateral avg-faces, with values for the left avg-faces on the upper panel and values for the right avg-faces on the lower panel. The tables (left side) display each group's average response and standard deviation to each category. The graphs (right side) display average individual (smaller symbols, faded colours) and group mean (larger symbols, bright colours) categorical responses. CC: congenital cataract individuals (*n* = 8; displayed in red); mSC: matched sighted individuals (*n* = 8; displayed in light green); allSC: all tested sighted individuals (*n* = 13; the additional 5 SC individuals are displayed in dark green; VI: visually impaired individuals (*n* = 3).

OTS-bodies

OTS-bodies_lh (matched-model). For the left hemisphere, there was a significant main effect category ($F(3,42) = 10.05$, $p < .001$, $\eta_p^2 = .418$). There was however, no main effect of group ($F(1,14) = 1.51$, $p = .326$, $\eta_p^2 = .098$), nor was there an interaction between the two ($F(3,42) = 1.03$, $p = .449$, $\eta_p^2 = .068$). The highest response was evoked by the category Object ($M = 1.07$, $SD = 0.49$), followed by the category Face ($M = 0.90$, $SD = 0.49$), Body ($M = 0.86$, $SD = 0.47$) and Scene ($M = 0.58$, $SD = 0.41$). The group-specific average category responses are displayed in Table 13 and in Figure 21. All post-hoc results can be found in supplementary table S9. Here, we only report the body-specific comparisons, given that they are the preferential category for the OTS-bodies regions. Pairwise comparisons indicated significant differences for 'Body vs. Object' ($t(42) = -2.31$, $p = .040$) and 'Body vs. Scene' ($t(42) = 3.10$, $p = .006$).

OTS-bodies_lh (all-subjects-model). Similarly to the matched-model, we found a significant effect of category ($F(3,63) = 11.14$, $p < .001$, $\eta_p^2 = .347$). There was no effect of group ($F(2,21) = 0.68$, $p = .665$, $\eta_p^2 = .061$), nor an interaction between group and category ($F(6,63) = 1.18$, $p = .516$, $\eta_p^2 = .101$). The category Object elicited the highest response ($M = 1.06$, $SD = 0.45$), followed by Face ($M = 0.97$, $SD = 0.44$), Body ($M = 0.87$, $SD = 0.40$) and Scene ($M = 0.53$, $SD = 0.44$). The group-specific average category responses are displayed in Table 13 and in Figure 21. The only body-specific comparison that indicated a significant difference was 'Body vs. Scene' ($t(63) = 3.88$, $p = .001$). Additional post-hoc results are listed in supplementary table S25.

OTS-bodies_rh (matched-model). For the right hemisphere, we found a significant main effect of category ($F(3,42) = 15.08$, $p < .001$, $\eta_p^2 = .519$), but no significant main effect of group ($F(1,14) = 0.46$, $p = .524$, $\eta_p^2 = .032$). Interestingly, we found a significant group*category interaction ($F(3,42) = 4.82$, $p = .016$, $\eta_p^2 = .256$). The highest response within the OTS-bodies_rh was evoked by the category Face ($M = 0.90$, $SD = 0.39$), followed by Object ($M = 0.78$, $SD = 0.38$), Body ($M = 0.72$, $SD = 0.26$) and Scene ($M = 0.39$, $SD = 0.41$).

Because of the category*group interaction in the right hemisphere, we split the data for further post-hoc analyses. Firstly, we split the data by group to examine the response profiles of each group separately. The categorical responses differed between the SC group and the CC group. All group specific average category responses can be found in Table 14 and in Figure 22. For the SC group, the category Face elicited the highest response, followed by Body, Object and Scene. Post-hoc analysis, revealed the comparisons 'Body vs. Face' ($t(42) = -2.28$, $p = .042$) and 'Body vs. Scene' ($t(42) = 4.51$, $p < .001$) to be significant. For the CC group, the highest response was evoked by the category

Object, followed by Face, Body and Scene. There was only one marginally significant body-specific comparison, which was 'Body vs. Object' ($t(42) = -1.99$, $p = .076$). Additional post-hoc results are listed in supplementary table S10. Secondly, we split the data by category to compare groups directly per category. However, no group comparison indicated differences between the SC group and the CC group (supplementary table S11).

OTS-bodies_rh (all-subjects-model). Similar to the matched model, we found significant category effect for the right OTS-bodies ($F(3,63) = 27.48$, $p < .001$, $\eta_p^2 = .567$) as well as a significant group*category interaction ($F(6,63) = 4.07$, $p = .004$, $\eta_p^2 = .279$). There was no effect of group ($F(2,21) = 0.42$, $p = .764$, $\eta_p^2 = .038$).

For the group*category interaction in the right hemisphere, we first split the data by group. The group-specific average category responses are displayed in Table 14 and in Figure 22. The SC group and the VI group exhibited a similar response pattern with the highest response to the Face category, followed by Body, Object and Scene. Both groups showed significant differences for 'Body vs. Face' (SC: $t(63) = -2.84$, $p = .015$; VI: $t(63) = -2.75$, $p = .019$) and 'Body vs. Scene' (SC: $t(63) = 6.25$, $p < .001$; VI: $t(63) = 2.70$, $p = .022$). For the CC group, the response profile showed the highest response to the category Object, followed by Face, Body and Scene. The comparison 'Body vs. Object' reached only marginal significance ($t(63) = -2.18$, $p = .068$). Further post-hoc results are listed in supplementary table S26. We additionally split the data by category and compared each group per category with each other. However, there were no significant group differences (supplementary table S27).

Categorical responses within the bilateral OTS-bodies

Table 13 **Figure 21**

Individual and Group Average Categorical Responses within the OTS-bodies_lh

	Body		Face		Object		Scene	
group	*M*	*SD*	*M*	*SD*	*M*	*SD*	*M*	*SD*
allSC	0.78	0.44	1.02	0.48	1.03	0.51	0.43	0.48
mSC	0.69	0.50	0.87	0.53	0.94	0.56	0.42	0.42
CC	1.03	0.40	0.93	0.47	1.20	0.41	0.75	0.34
VI	0.83	0.12	0.84	0.30	0.85	0.14	0.39	0.31

Table 14 **Figure 22**

Individual and Group Average Categorical Responses within the OTS-bodies_rh

	Body		Face		Object		Scene	
group	*M*	*SD*	*M*	*SD*	*M*	*SD*	*M*	*SD*
allSC	0.75	0.30	0.98	0.45	0.66	0.41	0.24	0.42
mSC	0.73	0.31	0.99	0.48	0.64	0.48	0.22	0.48
CC	0.70	0.23	0.81	0.29	0.93	0.18	0.55	0.27
VI	0.58	0.28	1.04	0.48	0.56	0.20	0.12	0.08

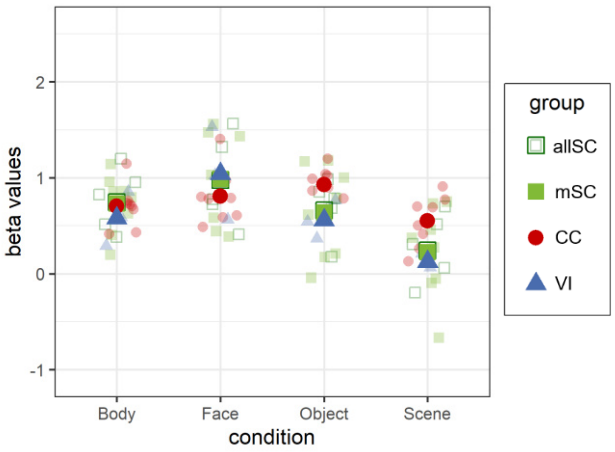

Note. Categorical responses within the bilateral OTS-bodies, with values for the left OTS-bodies on the upper panel and values for the right OTS-bodies on the lower panel. The tables (left side) display each group's average response and standard deviation to each category. The graphs (right side) display average individual (smaller symbols, faded colours) and group mean (larger symbols, bright colours) categorical responses. CC: congenital cataract individuals (*n* = 8; displayed in red); mSC: matched sighted individuals (*n* = 8; displayed in light green); allSC: all tested sighted individuals (*n* = 13; the additional 5 SC individuals are displayed in dark green; VI: visually impaired individuals (*n* = 3).

CoS-places

CoS-places_lh (matched model). For the CoS-places_lh, there was a significant main effect of category ($F(3,42) = 94.24$, $p < .001$, $\eta_p^2 = .871$). There was a marginal effect of group, which did not survive FDR correction ($F(1,14) = 3.47$, $p = .193$, $\eta_p^2 = .199$). There was no interaction of group by category ($F(3,42) = 0.94$, $p = .477$, $\eta_p^2 = .063$). In the left CoS-places, the category Scene elicited the highest response ($M = 1.38$, $SD = 0.41$), followed by Object ($M = 0.81$, $SD = 0.31$), Body ($M = 0.34$, $SD = 0.29$) and Face ($M = 0.00$, $SD = 0.29$). The group-specific average category responses are displayed in Table 15 and in Figure 23. All pairwise comparisons became significant (supplementary table S12).

CoS-places_lh (all-subjects-model). There was a significant effect of category ($F(3,63) = 157.79$, $p < .001$, $\eta_p^2 = .883$). There was no effect of group ($F(2,21) = 2.44$, $p = .209$, $\eta_p^2 = .188$). Additionally, there was a marginally significant interaction between group and category which did not survive the FDR correction for multiple comparisons ($F(6,63) = 2.14$, $p = .131$, $\eta_p^2 = .169$). The left hemisphere, showed highest response to the category Scene ($M = 1.41$, $SD = 0.48$), followed by Object ($M = 0.75$, $SD = 0.37$), Body ($M = 0.39$, $SD = 0.35$) and Face ($M = 0.06$, $SD = 0.32$). The group-specific average category responses are displayed in Table 15 and in Figure 23. All pairwise comparisons became significant (supplementary table S28).

CoS-places_rh (matched model). For the CoS-places_rh, we found a significant main effect of category ($F(3,42) = 187.37$, $p < .001$, $\eta_p^2 = .930$). There was no main effect of group ($F(1,14) = 2.54$, $p = .227$, $\eta_p^2 = .153$), nor an interaction between the two ($F(3,42) = 0.14$, $p = .938$, $\eta_p^2 = .010$). In the right CoS-places the highest response was found for Scene ($M = 1.38$, $SD = 0.41$), followed by Object ($M = 0.81$, $SD = 0.31$), Body ($M = 0.34$, $SD = 0.29$) and Face ($M = 0.00$, $SD = 0.29$). The group-specific average category responses are displayed in Table 16 and in Figure 24. All categories differed significantly from each other (supplementary table S13).

CoS-places_rh (all-subjects-model). Similarly to the matched model, we only found a significant effect of category ($F(3,63) = 267.72$, $p < .001$, $\eta_p^2 = .927$). There was no effect of group ($F(2,21) = 1.18$, $p = .516$, $\eta_p^2 = .101$), nor an interaction between group and category ($F(6,63) = 1.85$, $p = .209$, $\eta_p^2 = .150$). The right hemisphere showed the same order of categorical response with the highest response to Scene ($M = 1.47$, $SD = 0.42$), followed by Object ($M = 0.82$, $SD = 0.31$), Body ($M = 0.32$, $SD = 0.29$) and Face ($M = -0.03$, $SD = 0.30$). The group-specific average category responses are displayed in Table 16 and in Figure 24. All categories differed significantly from each other (supplementary table S29).

Categorical responses within the bilateral CoS-places

Table 15

Individual and Group Average Categorical Responses within the CoS-places_lh

	Body		Face		Object		Scene	
group	*M*	*SD*	*M*	*SD*	*M*	*SD*	*M*	*SD*
allSC	0.21	0.33	-0.08	0.29	0.65	0.38	1.31	0.46
mSC	0.24	0.35	-0.07	0.27	0.67	0.41	1.23	0.49
CC	0.62	0.23	0.30	0.16	0.83	0.31	1.46	0.50
VI	0.57	0.31	0.02	0.44	1.00	0.41	1.72	0.54

Figure 23

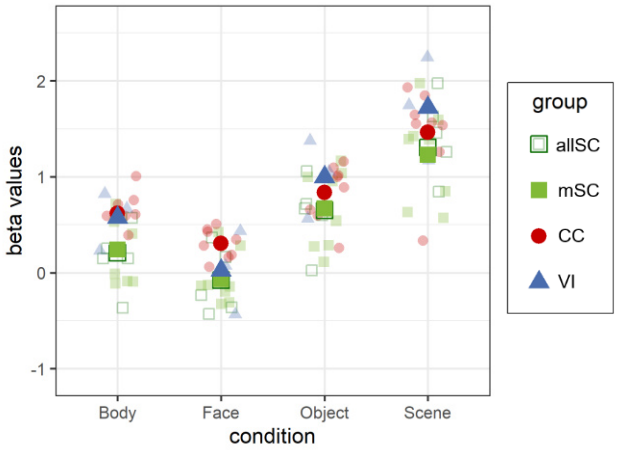

Table 16

Individual and Group Average Categorical Responses within the CoS-places_rh

	Body		Face		Object		Scene	
group	*M*	*SD*	*M*	*SD*	*M*	*SD*	*M*	*SD*
allSC	0.19	0.23	-0.09	0.29	0.73	0.30	1.41	0.47
mSC	0.20	0.25	-0.10	0.29	0.70	0.34	1.27	0.49
CC	0.48	0.28	0.10	0.28	0.92	0.26	1.49	0.31
VI	0.43	0.36	-0.14	0.37	1.00	0.42	1.69	0.52

Figure 24

Note. Categorical responses within the bilateral CoS-places, with values for the left CoS-places on the upper panel and values for the right CoS-places on the lower panel. The tables (left side) display each group's average response and standard deviation to each category. The graphs (right side) display average individual (smaller symbols, faded colours) and group mean (larger symbols, bright colours) categorical responses. CC: congenital cataract individuals (n = 8; displayed in red); mSC: matched sighted individuals (n = 8; displayed in light green); allSC: all tested sighted individuals (n = 13; the additional 5 SC individuals are displayed in dark green; VI: visually impaired individuals (n = 3).

Additional ROI Analysis Results

We additionally included the remaining regions provided by the functional atlas by Rosenke et al. (2020). All results described in the text are based on the all-subjects-model. For each region, we display average beta values with standard deviation. Additionally, we calculated separate averages for the matched SC individuals, which are listed as mSC. All post-hoc comparisons are attached as supplementary material. For readability, we only describe post-hoc comparisons that include the respective preferential category, all other comparisons are included in the respective post-hoc table.

MTG-bodies

Both left and right MTG-bodies showed a significant category effect (LH: $F(3,63) = 48.22$, $p < .001$, $\eta_p^2 = .697$; RH: $F(3,63) = 28.61$, $p < .001$, $\eta_p^2 = .577$). No further effects became significant ($p > 0.05$).

MTG-bodies_lh. The category Body ($M = 0.71$, $SD = 0.51$) elicited the highest response, followed by Face ($M = 0.65$, $SD = 0.51$), Object ($M = 0.22$, $SD = 0.40$), and Scene ($M = -0.24$, $SD = 0.33$). The group-specific average category responses are displayed in Table 17 and in Figure 25. Post-hoc tests revealed significant differences for 'Body vs. Object' ($t(63) = 5.71$, $p < .001$) and 'Body vs. Scene' ($t(63) = 10.57$, $p < .001$). Additional post-hoc results for the MTG-bodies_lh can be found in supplementary table S30.

MTG-bodies_rh. In the right MTG-bodies, the category Face elicited the highest response (M = 0.57, SD = 0.50), followed by Body (M = 0.33, SD = 0.36), Object (M = 0.03, SD = 0.29), and Scene (M = -0.34, SD = 0.31). The group-specific average category responses are displayed in Table 18 and in Figure 26. Body-specific post-hoc comparisons for 'Body vs. Object' ($t(63) = 3.11$, $p = .006$) and 'Body vs. Scene' ($t(63) = 6.64$, $p < .001$) became significant. The comparison 'Body vs. Face' was only marginal significant after FDR correction ($t(63) = -2.03$, $p = .076$). The remaining post-hoc results can be found in supplementary table S31.

Categorical responses within the bilateral MTG-bodies

Table 17

Figure 25

Individual and Group Average Categorical Responses within the MTG-bodies_lh

	Body		Face		Object		Scene	
group	*M*	*SD*	*M*	*SD*	*M*	*SD*	*M*	*SD*
allSC	0.56	0.53	0.56	0.57	0.16	0.42	-0.32	0.39
mSC	0.41	0.45	0.35	0.43	0.05	0.27	-0.32	0.30
CC	0.94	0.47	0.75	0.46	0.31	0.38	-0.14	0.25
VI	0.80	0.42	0.78	0.41	0.25	0.40	-0.17	0.24

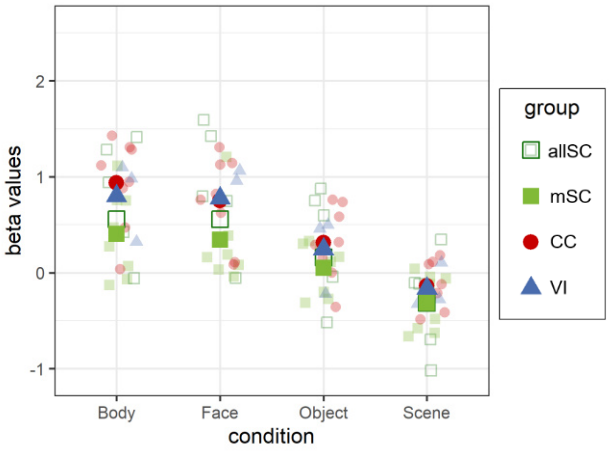

Table 18

Figure 26

Individual and Group Average Categorical Responses within the MTG-bodies_rh

	Body		Face		Object		Scene	
group	*M*	*SD*	*M*	*SD*	*M*	*SD*	*M*	*SD*
allSC	0.33	0.36	0.65	0.54	0.01	0.28	-0.39	0.32
mSC	0.18	0.35	0.55	0.50	-0.05	0.28	-0.37	0.36
CC	0.38	0.44	0.57	0.52	0.10	0.34	-0.24	0.34
VI	0.19	0.13	0.26	0.09	-0.09	0.19	-0.35	0.07

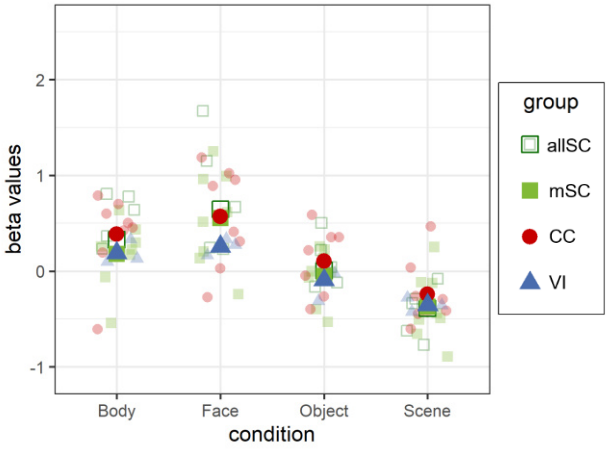

Note. Categorical responses within the bilateral MTG-bodies, with values for the left MTG-bodies on the upper panel and values for the right MTG-bodies on the lower panel. The tables (left side) display each group's average response and standard deviation to each category. The graphs (right side) display average individual (smaller symbols, faded colours) and group mean (larger symbols, bright colours) categorical responses. CC: congenital cataract individuals (*n* = 8; displayed in red); mSC: matched sighted individuals (*n* = 8; displayed in light green); allSC: all tested sighted individuals (*n* = 13; the additional 5 SC individuals are displayed in dark green; VI: visually impaired individuals (*n* = 3).

LOS-bodies

Both in left as well as in the right LOS-bodies we found a significant category effect (LH: $F(3,63) = 28.61$, $p < .001$, $\eta_p^2 = .433$; RH: $F(3,63) = 11.90$, $p < .001$, $\eta_p^2 = .362$). The left LOS-bodies additionally showed a marginal effect of group, which did not survive the FDR correction ($F(2,21) = 2.92$, $p = .164$, $\eta_p^2 = .218$). No further effects became significant ($p > 0.05$).

LOS-bodies_lh. In the left LOS-bodies the category Body elicited the highest response ($M = 1.08$, $SD = 0.68$), followed by Object ($M = 0.51$, $SD = 0.40$), and equally respondent Face ($M = 0.50$, $SD = 0.54$) and Scene ($M = 0.50$, $SD = 0.44$). The group-specific average category responses are displayed in Table 19 and in Figure 27. Post-hoc comparison results can be found in supplementary table S32. All body-selective comparisons became significant ($p < .001$).

LOS-bodies_rh. In the right LOS-bodies the category Body elicited the highest response ($M = 1.27$, $SD = 0.35$), followed by Face ($M = 0.96$, $SD = 0.45$), Object ($M = 0.86$, $SD = 0.33$), and Scene ($M = 0.64$, $SD = 0.45$). The group-specific average category responses are displayed in Table 20 and in Figure 28. Similarly to the LOS-bodies_lh, all body-selective comparisons for the LOS-bodies_rh were significant ($p < .01$). The post-hoc results are listed in supplementary table S33.

Categorical responses within the bilateral LOS-bodies

Table 19

Individual and Group Average Categorical Responses within the LOS-bodies_lh

	Body		Face		Object		Scene	
group	*M*	*SD*	*M*	*SD*	*M*	*SD*	*M*	*SD*
allSC	0.92	0.78	0.38	0.64	0.37	0.32	0.32	0.35
mSC	0.90	0.82	0.42	0.60	0.31	0.31	0.26	0.35
CC	1.35	0.40	0.77	0.21	0.78	0.40	0.88	0.35
VI	1.04	0.81	0.30	0.59	0.40	0.48	0.32	0.43

Figure 27

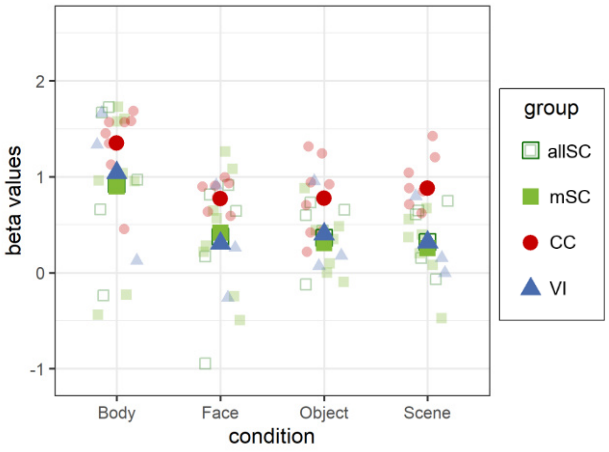

Table 20

Individual and Group Average Categorical Responses within the LOS-bodies_rh

	Body		Face		Object		Scene	
group	*M*	*SD*	*M*	*SD*	*M*	*SD*	*M*	*SD*
allSC	1.30	0.45	1.02	0.49	0.81	0.35	0.50	0.41
mSC	1.14	0.41	0.96	0.55	0.74	0.29	0.39	0.31
CC	1.22	0.23	0.98	0.47	1.00	0.32	0.93	0.47
VI	1.26	0.14	0.71	0.07	0.71	0.10	0.48	0.32

Figure 28

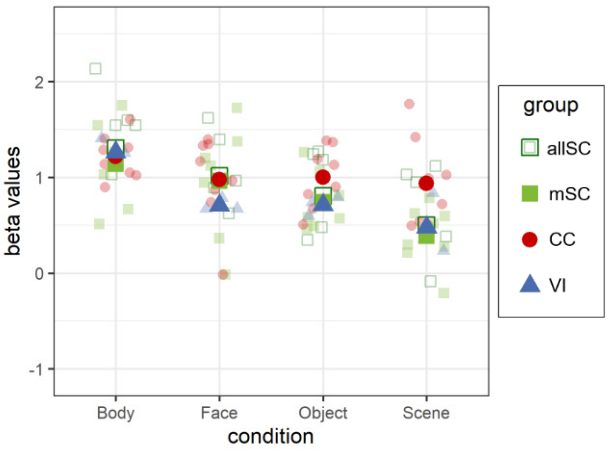

Note. Categorical responses within the bilateral LOS-bodies, with values for the left LOS-bodies on the upper panel and values for the right LOS-bodies on the lower panel. The tables (left side) display each group's average response and standard deviation to each category. The graphs (right side) display average individual (smaller symbols, faded colours) and group mean (larger symbols, bright colours) categorical responses. CC: congenital cataract individuals (*n* = 8; displayed in red); mSC: matched sighted individuals (*n* = 8; displayed in light green); allSC: all tested sighted individuals (*n* = 13; the additional 5 SC individuals are displayed in dark green; VI: visually impaired individuals (*n* = 3).

ITG-bodies

We found a significant category effect for the left (F(3,63) = 50.51, p < .001, η_p^2 = .706) and right ITG-bodies (F(3,63) = 54.22, p < .001, η_p^2 = .721). Additionally, the right ITG-bodies showed a marginal effect of group, which did not survive FDR correction (F(2,21) = 2.96, p =.163, η_p^2 =.220). No further effects became significant (p > 0.05).

ITG-bodies_lh. In the left hemisphere the category Body elicited the highest response (M = 1.49, SD = 0.46), followed by Face (M = 1.04, SD = 0.38), Object (M = 0.83, SD = 0.41) and Scene (M = 0.29, SD = 0.41). The group-specific average category responses are displayed in Table 21 and in Figure 29. All body-selective comparisons for the ITG-bodies_lh became significant (p < .001) and are listed in detail with the remaining results in supplementary table S34.

ITG-bodies_rh. The right hemisphere exhibited the same order of categorical response with the highest response to the category Body (M = 1.25, SD = 0.34), followed by Face (M = 1.11, SD = 0.40), Object (M = 0.81, SD = 0.33) and Scene (M = 0.26, SD = 0.34). The group-specific average category responses are displayed in Table 22 and in Figure 30. The body-selective comparisons 'Body vs. Object' (t(63) = 5.41, p < .001) and 'Body vs. Scene' (t(63) = 11.93, p < .001) became significant, while the comparison 'Body vs. Face' remained marginally significant after FDR correction (t(63) = 2.12, p = .063). All remaining post-hoc results are listed in supplementary table S35.

Categorical responses within the bilateral ITG-bodies

Table 21

Individual and Group Average Categorical Responses within the ITG-bodies_lh

	Body		Face		Object		Scene	
group	*M*	*SD*	*M*	*SD*	*M*	*SD*	*M*	*SD*
allSC	1.44	0.52	1.00	0.41	0.73	0.42	0.16	0.36
mSC	1.29	0.55	0.90	0.45	0.59	0.43	0.12	0.36
CC	1.60	0.39	1.19	0.32	1.03	0.44	0.54	0.42
VI	1.37	0.42	0.83	0.31	0.74	0.09	0.23	0.34

Figure 29

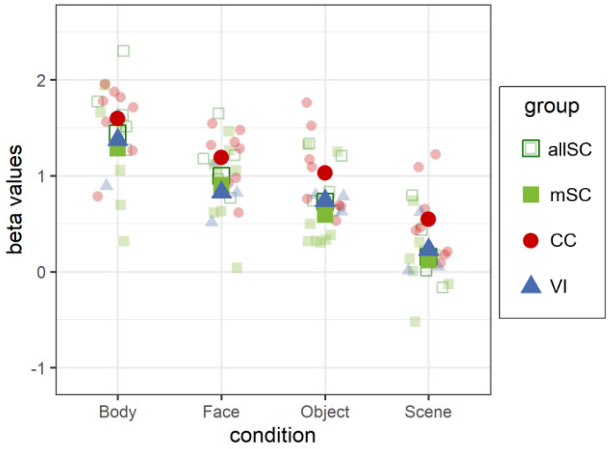

Table 22

Individual and Group Average Categorical Responses within the ITG-bodies_rh

	Body		Face		Object		Scene	
group	*M*	*SD*	*M*	*SD*	*M*	*SD*	*M*	*SD*
allSC	1.23	0.33	1.09	0.40	0.77	0.33	0.18	0.30
mSC	1.06	0.28	0.98	0.37	0.72	0.36	0.18	0.33
CC	1.39	0.32	1.30	0.35	0.96	0.36	0.44	0.41
VI	0.98	0.32	0.70	0.34	0.57	0.13	0.12	0.10

Figure 30

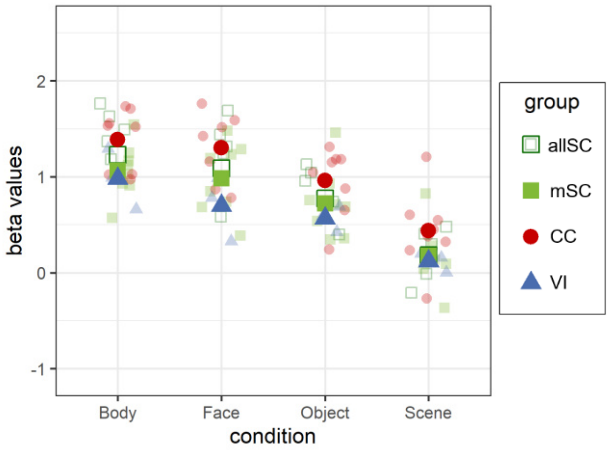

Note. Categorical responses within the bilateral ITG-bodies, with values for the left ITG-bodies on the upper panel and values for the right ITG-bodies on the lower panel. The tables (left side) display each group's average response and standard deviation to each category. The graphs (right side) display average individual (smaller symbols, faded colours) and group mean (larger symbols, bright colours) categorical responses. CC: congenital cataract individuals (*n* = 8; displayed in red); mSC: matched sighted individuals (*n* = 8; displayed in light green); allSC: all tested sighted individuals (*n* = 13; the additional 5 SC individuals are displayed in dark green; VI: visually impaired individuals (*n* = 3).

TOS-places_rh

There was a significant effect of category for the TOS-places_rh ($F(3,63) = 37.59$, $p < .001$, $\eta_p^2 = .642$) with highest response for the category Scene ($M = 1.20$, $SD = 0.40$), followed by Object ($M = 1.00$, $SD = 0.34$), Body ($M = 0.81$, $SD = 0.34$) and Face ($M = 0.57$, $SD = 0.45$). No further effects became significant ($p > 0.05$). The group-specific average category responses are displayed in Table 23 and in Figure 31. Post-hoc comparisons revealed significant differences between all scene-specific comparisons ($p < .01$). All post-hoc results are listed in supplementary table S38.

Table 23

Individual and Group Average Categorical Responses within the TOS-places_rh

	Body		Face		Object		Scene	
group	*M*	*SD*	*M*	*SD*	*M*	*SD*	*M*	*SD*
allSC	0.78	0.39	0.53	0.47	0.97	0.38	1.15	0.45
mSC	0.79	0.37	0.59	0.47	0.95	0.40	1.03	0.44
CC	0.93	0.18	0.79	0.32	1.14	0.16	1.33	0.23
VI	0.65	0.45	0.14	0.41	0.74	0.44	1.04	0.55

Figure 31

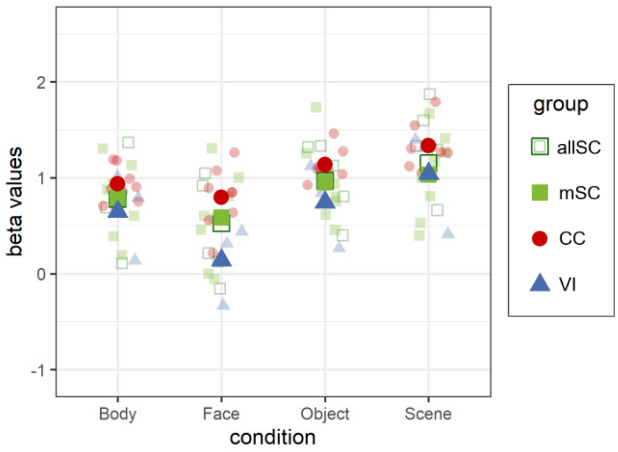

Note. Categorical responses within the right TOS-places. The table (left side) displays each group's average response and standard deviation to each category. The graph (right side) displays average individual (smaller symbols, faded colours) and group mean (larger symbols, bright colours) categorical responses. CC: congenital cataract individuals ($n = 8$; displayed in red); mSC: matched sighted individuals ($n = 8$; displayed in light green); allSC: all tested sighted individuals ($n = 13$; the additional 5 SC individuals are displayed in dark green; VI: visually impaired individuals ($n = 3$).

Exploratory Analysis

Given that the following regions had no direct association with the tested categories, no directed hypothesis have been phrased in regards to their category preferences. Post-hoc comparisons of categories main effects will only be listed in the respective post-hoc tables in the appendix, yet not listed in the results section.

pOTS-characters_lh

We found significant category effect for pOTS-characters_lh ($F(3,63) = 14.05$, $p < .001$, $\eta_p^2 = .401$). No further effects became significant ($p > 0.05$). The category Object elicited the highest response (M = 1.12, SD = 0.42), followed by Body (M = 0.93, SD = 0.40), Face (M = 0.93, SD = 0.44), and Scene (M = 0.54, SD = 0.42). The group-specific average category responses are displayed in Table 24 and in Figure 32. Post-hoc results can be found in supplementary table S36.

Table 24

Individual and Group Average Categorical Responses within the pOTS-characters_lh

	Body		Face		Object		Scene	
group	*M*	*SD*	*M*	*SD*	*M*	*SD*	*M*	*SD*
allSC	0.87	0.45	0.99	0.45	1.06	0.48	0.42	0.42
mSC	0.77	0.44	0.83	0.43	0.93	0.56	0.42	0.44
CC	1.06	0.35	0.91	0.46	1.25	0.42	0.75	0.42
VI	0.88	0.26	0.66	0.35	1.04	0.03	0.53	0.17

Figure 32

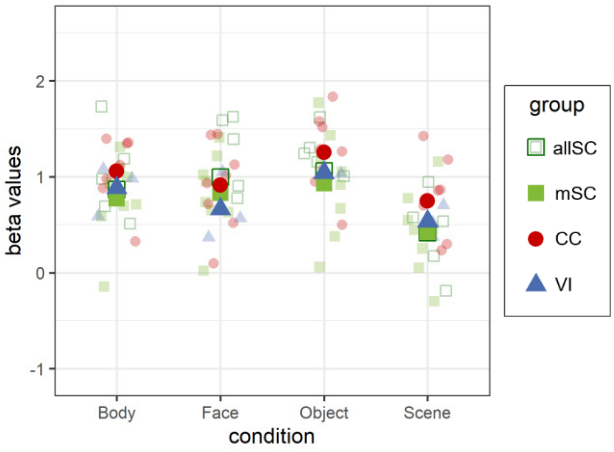

Note. Categorical responses within the left pOTS-characters. The table (left side) displays each group's average response and standard deviation to each category. The graph (right side) displays average individual (smaller symbols, faded colours) and group mean (larger symbols, bright colours) categorical responses. CC: congenital cataract individuals (n = 8; displayed in red); mSC: matched sighted individuals (n = 8; displayed in light green); allSC: all tested sighted individuals (n = 13; the additional 5 SC individuals are displayed in dark green; VI: visually impaired individuals (n = 3).

IOS-characters_lh

Analysis revealed a significant category effect for the IOS-characters_lh ($F(3,63) = 9.71$, $p < .001$, $\eta_p^2 = .316$). No further effects became significant ($p > 0.05$). Similar to the pOTS-characters_lh, we found the highest response for the category Object ($M = 1.30$, $SD = 0.33$), followed by Face ($M = 1.24$, $SD = 0.38$), Body ($M = 1.01$, $SD = 0.38$) and Scene ($M = 0.98$, $SD = 0.37$). The group-specific average category responses are displayed in Table 25 and in Figure 33. Post-hoc results can be found in supplementary table S37.

Table 25

Individual and Group Average Categorical Responses within the IOS-characters_lh

	Body		Face		Object		Scene	
group	*M*	*SD*	*M*	*SD*	*M*	*SD*	*M*	*SD*
allSC	0.96	0.39	1.24	0.32	1.32	0.39	1.01	0.44
mSC	0.85	0.40	1.11	0.32	1.11	0.30	0.82	0.29
CC	1.10	0.35	1.25	0.46	1.32	0.29	1.01	0.28
VI	0.95	0.51	1.19	0.54	1.17	0.18	0.81	0.28

Figure 33

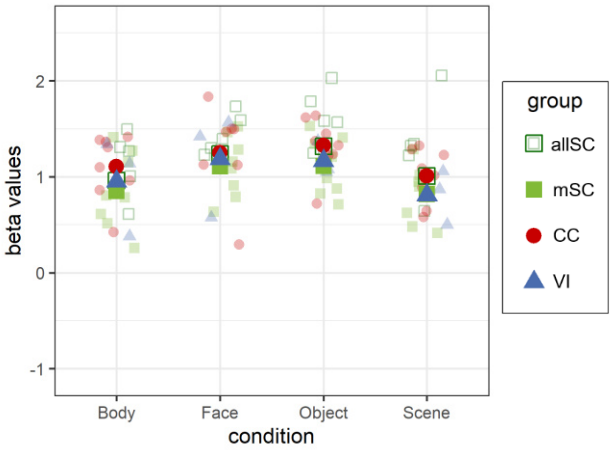

Note. Categorical responses within the left IOS-characters. The table (left side) displays each group's average response and standard deviation to each category. The graph (right side) displays average individual (smaller symbols, faded colours) and group mean (larger symbols, bright colours) categorical responses. CC: congenital cataract individuals ($n = 8$; displayed in red); mSC: matched sighted individuals ($n = 8$; displayed in light green); allSC: all tested sighted individuals ($n = 13$; the additional 5 SC individuals are displayed in dark green; VI: visually impaired individuals ($n = 3$).

hMT

We found significant category effects both for the left hMT ($F(3,63) = 57.70$, $p < .001$, $\eta_p^2 = .733$) as well as the right hMT ($F(3,63) = 112.39$, $p < .001$, $\eta_p^2 = .843$). No further effects became significant ($p > 0.05$).

hMT_lh. In the left hemisphere the highest response was elicited by the category Body (*M* = 1.19, *SD* = 0.68), followed by Face (*M* = 0.72, *SD* = 0.56), Object (*M* = 0.36, *SD* = 0.45) and Scene (*M* = -0.005, *SD* = 0.38). The group-specific average category responses are displayed in Table 26 and in Figure 34. Post-hoc results can be found in supplementary table S39.

hMT_rh. The right hemisphere followed the same order of categorical response, which were highest response to the category Body (M = 1.21, SD = 0.32), followed by Face (M = 1.00, SD = 0.36), Object (M = 0.43, SD = 0.30) and Scene (M = -0.06, SD = 0.30). The group-specific average category responses are displayed in Table 27 and in Figure 35. Post-hoc results can be found in supplementary table S40.

Categorical responses within the bilateral hMT

Table 26

Figure 34

Individual and Group Average Categorical Responses within the hMT_lh

	Body		Face		Object		Scene	
group	*M*	*SD*	*M*	*SD*	*M*	*SD*	*M*	*SD*
allSC	1.04	0.82	0.59	0.66	0.20	0.45	-0.15	0.37
mSC	0.96	0.85	0.64	0.62	0.21	0.50	-0.17	0.39
CC	1.49	0.38	0.98	0.24	0.65	0.34	0.30	0.22
VI	1.03	0.53	0.54	0.54	0.29	0.45	-0.19	0.39

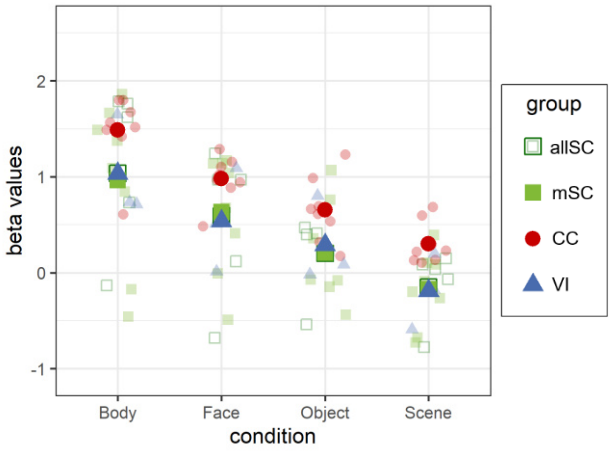

Table 27

Figure 35

Individual and Group Average Categorical Responses within the hMT_rh

	Body		Face		Object		Scene	
group	*M*	*SD*	*M*	*SD*	*M*	*SD*	*M*	*SD*
allSC	1.22	0.36	1.00	0.31	0.37	0.22	-0.15	0.23
mSC	1.02	0.31	0.91	0.30	0.33	0.26	-0.16	0.29
CC	1.23	0.31	1.07	0.45	0.56	0.43	0.10	0.39
VI	1.09	0.23	0.82	0.34	0.31	0.14	-0.11	0.14

Note. Categorical responses within the bilateral hMT, with values for the left hMT on the upper panel and values for the right hMT on the lower panel. The tables (left side) display each group's average response and standard deviation to each category. The graphs (right side) display average individual (smaller symbols, faded colours) and group mean (larger symbols, bright colours) categorical responses. CC: congenital cataract individuals (*n* = 8; displayed in red); mSC: matched sighted individuals (*n* = 8; displayed in light green); allSC: all tested sighted individuals (*n* = 13; the additional 5 SC individuals are displayed in dark green; VI: visually impaired individuals (*n* = 3).

V1 – dorsal

For both left ($F(3,63) = 12.38$, $p < .001$, $\eta_p^2 = .371$) and right v1d ($F(3,63) = 25.89$, $p < .001$, $\eta_p^2 = .552$) we found a significant category effect, as well as a marginal group effect for v1d_rh ($F(2,21) = 4.67$, $p = .058$). Further, before FDR correction, we found a marginal group effect for the left v1d as well as indications for group*category interactions in both hemisphere, which did not survive FDR correction ($p > .05$).

V1d_lh. For the left hemisphere, we found the highest response for the category Scene (*M* = 1.43, *SD* = 0.46), followed by Object (*M* = 1.16, *SD* = 0.36), Face (*M* = 1.11, *SD* = 0.37) and Body (*M* = 1.04, *SD* = 0.36). The group-specific average category responses are displayed in Table 28 and in Figure 36. Post-hoc results can be found in supplementary table S41.

V1d_rh. In regards to the category effect of v1d_rh, we found highest responses for the category Scene (M = 1.61, SD = 0.51), followed by Object (M = 1.21, SD = 0.40), Body (M = 1.01, SD = 0.35) and Face (M = 0.93, SD = 0.37). The group-specific average category responses are displayed in Table 29 and in Figure 37. Post-hoc results can be found in the supplementary tables S42 and S43. In regards to the marginal group effect, CC individuals showed the highest overall response (M = 1.41, SD = 0.28), followed by SC individuals (M = 1.14, SD = 0.52) and VI individuals (M = 0.78, SD = 0.47). Only the comparison between CC group and VI group became significant (t(21) = 2.96, p = .035).

Categorical responses within the bilateral dorsal V1

Table 28

Individual and Group Average Categorical Responses within the v1d_lh

	Body		Face		Object		Scene	
group	*M*	*SD*	*M*	*SD*	*M*	*SD*	*M*	*SD*
allSC	0.95	0.32	1.11	0.32	1.12	0.38	1.50	0.51
mSC	0.84	0.31	0.98	0.27	0.97	0.36	1.34	0.47
CC	1.30	0.28	1.23	0.38	1.35	0.23	1.47	0.33
VI	0.70	0.37	0.75	0.40	0.87	0.41	0.99	0.39

Figure 36

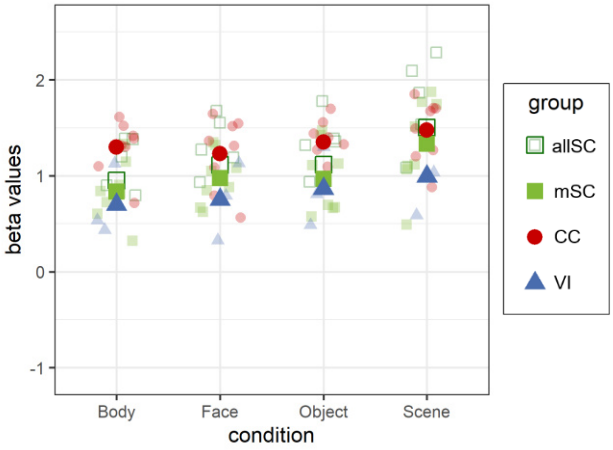

Table 29

Individual and Group Average Categorical Responses within the v1d_rh

	Body		Face		Object		Scene	
group	*M*	*SD*	*M*	*SD*	*M*	*SD*	*M*	*SD*
allSC	0.91	0.34	0.83	0.31	1.17	0.38	1.68	0.55
mSC	0.86	0.39	0.79	0.35	1.03	0.34	1.50	0.54
CC	1.31	0.15	1.21	0.28	1.43	0.18	1.71	0.25
VI	0.66	0.21	0.61	0.43	0.81	0.65	1.03	0.62

Figure 37

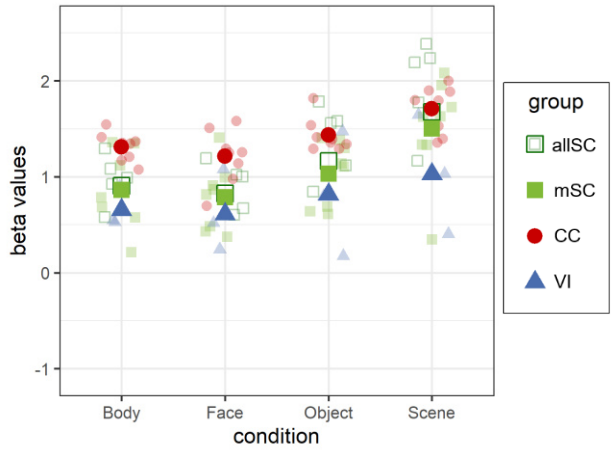

Note. Categorical responses within the bilateral dorsal V1, with values for the left v1d on the upper panel and values for the right v1d on the lower panel. The tables (left side) display each group's average response and standard deviation to each category. The graphs (right side) display average individual (smaller symbols, faded colours) and group mean (larger symbols, bright colours) categorical responses. CC: congenital cataract individuals (*n* = 8; displayed in red); mSC: matched sighted individuals (*n* = 8; displayed in light green); allSC: all tested sighted individuals (*n* = 13; the additional 5 SC individuals are displayed in dark green; VI: visually impaired individuals (*n* = 3).

V1 – ventral

For both left and right v1v, we found a significant category effect (LH: $F(3,63) = 33.25$, $p < .001$, $\eta_p^2 = .613$) RH: $F(3,63) = 45.15$, $p < .001$, $\eta_p^2 = .683$). However, for the left hemisphere we additionally found a group*category interaction ($F(6,63) = 3.65$, $p = .010$, $\eta_p^2 = .258$). The right v1v additionally exhibited a marginal group effect, which did not survive FDR correction ($F(2,21) = 3.63$, $p = .107$, $\eta_p^2 = .257$). No further effects became significant ($p > 0.05$).

V1v_lh. To investigate the group-category interaction further, we split the data of the v1v_lh by group. The group-specific average category responses are displayed in Table 30 and in Figure 38. For SC and VI individuals, the category Scene elicited the highest response, followed by Object, Face and Body. For CC individuals, the category Scene also elicited the highest response but followed then by Object, Body and Face. Post-hoc-analyses revealed for SC individuals significant differences between all categories except for 'Face vs. Object'. Both for VI and CC individuals only the three comparisons with the highest category 'Scene' became significant, i.e. 'Body vs. Scene', 'Scene vs. Face', 'Scene vs. Object'. Post-hoc results can be found in supplementary table S44. When splitting the data by category, three group comparisons became marginally significant. More specifically, for the category Body, CC individuals showed a higher response than SC and VI individuals. Additionally, CC individuals showed higher responses than VI individuals in the category 'Object'. Post-hoc results can be found in supplementary table S45.

V1v_rh. In the right v1v, the highest response was found for the category Scene ($M = 1.58$, $SD = 0.61$), followed by Object ($M = 1.03$, $SD = 0.50$), Body ($M = 0.95$, $SD = 0.44$) and Face ($M = 0.82$, $SD = 0.49$). The group-specific average category responses are displayed in Table 31 and in Figure 39. Post-hoc-comparison can be found in the supplementary table S46.

Categorical responses within the bilateral ventral V1

Table 30

Individual and Group Average Categorical Responses within the v1v_lh

	Body		Face		Object		Scene	
group	*M*	*SD*	*M*	*SD*	*M*	*SD*	*M*	*SD*
allSC	0.92	0.30	1.11	0.31	1.17	0.32	1.71	0.47
mSC	0.85	0.29	1.00	0.29	1.06	0.29	1.59	0.45
CC	1.31	0.30	1.25	0.40	1.35	0.22	1.61	0.36
VI	0.73	0.56	0.80	0.87	0.81	0.66	1.23	0.66

Figure 38

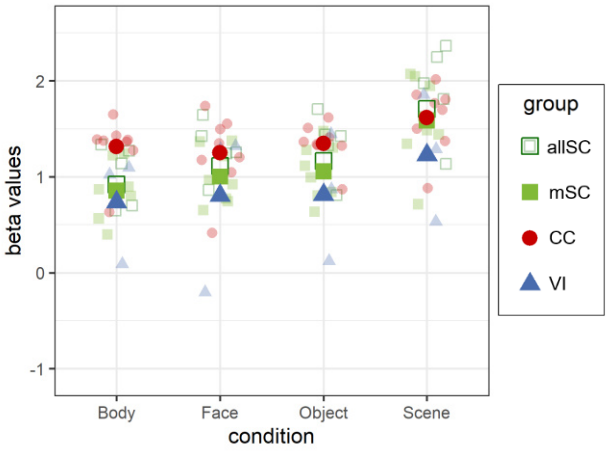

Table 31

Individual and Group Average Categorical Responses within the v1v_rh

	Body		Face		Object		Scene	
group	*M*	*SD*	*M*	*SD*	*M*	*SD*	*M*	*SD*
allSC	0.87	0.43	0.74	0.44	1.01	0.48	1.63	0.61
mSC	0.80	0.45	0.69	0.42	0.88	0.44	1.41	0.59
CC	1.25	0.12	1.13	0.21	1.29	0.13	1.75	0.27
VI	0.54	0.65	0.35	0.82	0.48	0.84	0.90	0.95

Figure 39

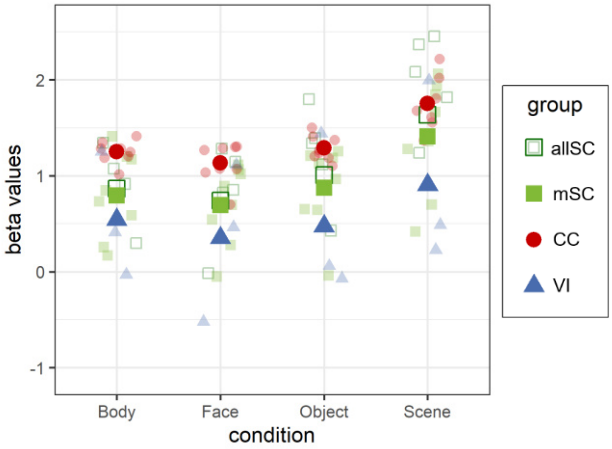

Note. Categorical responses within the bilateral ventral V1, with values for the left v1v on the upper panel and values for the right v1v on the lower panel. The tables (left side) display each group's average response and standard deviation to each category. The graphs (right side) display average individual (smaller symbols, faded colours) and group mean (larger symbols, bright colours) categorical responses. CC: congenital cataract individuals (*n* = 8; displayed in red); mSC: matched sighted individuals (*n* = 8; displayed in light green); allSC: all tested sighted individuals (*n* = 13; the additional 5 SC individuals are displayed in dark green; VI: visually impaired individuals (*n* = 3).

V2 – dorsal

There was a significant category effect both for the v2d_lh ($F(3,63) = 5.47$, $p = .006$, $\eta_p^2 = .207$) as well for the v2d_rh ($F(3,63) = 15.86$, $p < .001$, $\eta_p^2 = .430$). No further effects became significant ($p > 0.05$).

V2d_lh. For the left v2d, the category Scene (*M* = 1.34, *SD* = 0.42) elicited the highest response, followed by Body (*M* = 1.21, *SD* = 0.34), Object (*M* = 1.18, *SD* = 0.35) and Face (*M* = 1.12, *SD* = 0.35). The group-specific average category responses are displayed in Table 32 and in Figure 40. Post-hoc-comparison can be found in the supplementary table S47.

V2d_rh. For the right v2d, the category Scene elicited the highest response (M = 1.40, SD = 0.43), followed by Object (M = 1.24, SD = 0.37), Body (M = 1.02, SD = 0.31) and Face (M = 1.02, SD = 0.37). The group-specific average category responses are displayed in Table 33 and in Figure 41. Post-hoc-comparison can be found in the supplementary table S48.

Categorical responses within the bilateral dorsal V2

Table 32

Individual and Group Average Categorical Responses within the v2d_lh

	Body		Face		Object		Scene	
group	*M*	*SD*	*M*	*SD*	*M*	*SD*	*M*	*SD*
allSC	1.15	0.30	1.14	0.30	1.14	0.38	1.38	0.50
mSC	1.02	0.25	1.01	0.28	1.00	0.39	1.20	0.40
CC	1.40	0.34	1.22	0.38	1.36	0.24	1.39	0.30
VI	0.96	0.29	0.71	0.27	0.90	0.27	1.07	0.22

Figure 40

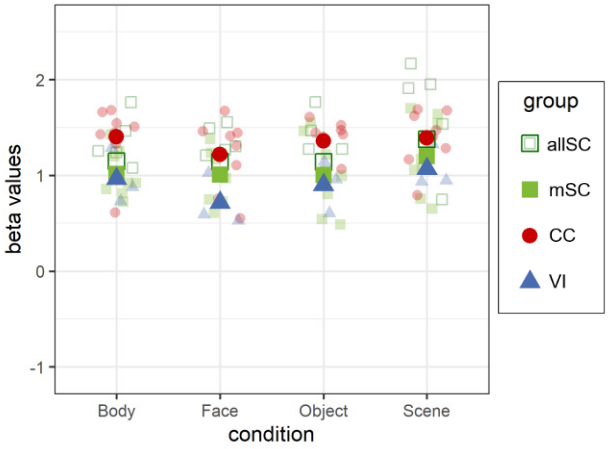

Table 33

Individual and Group Average Categorical Responses within the v2d_rh

	Body		Face		Object		Scene	
group	*M*	*SD*	*M*	*SD*	*M*	*SD*	*M*	*SD*
allSC	0.92	0.29	0.96	0.36	1.17	0.46	1.35	0.55
mSC	0.82	0.30	0.79	0.36	0.95	0.43	1.09	0.47
CC	1.26	0.21	1.23	0.29	1.39	0.18	1.52	0.25
VI	0.83	0.29	0.76	0.46	1.08	0.20	1.29	0.08

Figure 41

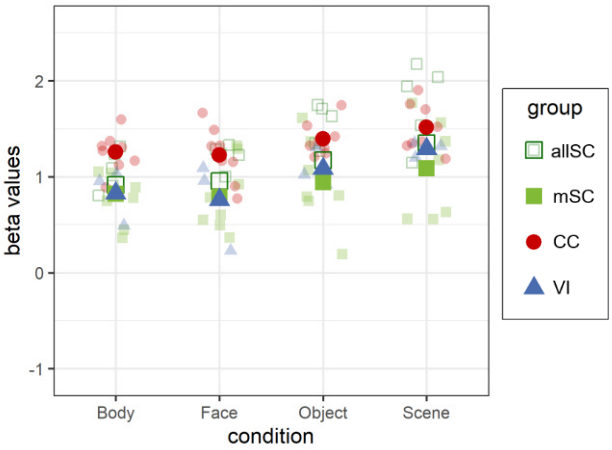

Note. Categorical responses within the bilateral dorsal V2, with values for the left v2d on the upper panel and values for the right v2d on the lower panel. The tables (left side) display each group's average response and standard deviation to each category. The graphs (right side) display average individual (smaller symbols, faded colours) and group mean (larger symbols, bright colours) categorical responses. CC: congenital cataract individuals (n = 8; displayed in red); mSC: matched sighted individuals (n = 8; displayed in light green); allSC: all tested sighted individuals (n = 13; the additional 5 SC individuals are displayed in dark green; VI: visually impaired individuals (n = 3).

V2 – ventral

Both in the left as well as in the right v2v, we found a significant effect of category (LH: $F(3,63) = 24.59$, $p < .001$, $\eta_p^2 = .539$; RH: $F(3,63) = 61.19$, $p < .001$, $\eta_p^2 = .744$) as well as marginal group effects (LH: $F(2,21) = 4.01$, $p = .083$, $\eta_p^2 = .276$; RH: $F(2,21) = 4.59$, $p = .058$, $\eta_p^2 = .304$). No further effects became significant ($p > 0.05$).

V2v_lh. In the left v2v, the category Scene elicited the highest response ($M = 1.44$, $SD = 0.59$), followed by Object ($M = 1.05$, $SD = 0.53$), Face ($M = 0.99$, $SD = 0.54$) and Body ($M = 0.93$, $SD = 0.51$). The group-specific average category responses are displayed in Table 34 and in Figure 42. Post-hoc-comparison can be found in the supplementary tables S49 and S50. Overall, the CC group ($M = 1.38$, $SD = 0.30$) showed higher responses than the SC group ($M = 1.08$, $SD = 0.52$) and VI group ($M = 0.49$, $SD = 0.81$). Post-hoc pairwise comparisons indicated a significant difference between the CC group and the VI group ($t(21) = 2.81$, $p = .047$).

V2v_rh. In the v2v_rh Scene as well elicited the highest responses ($M = 1.55$, $SD = 0.57$), followed by Object ($M = 1.08$, $SD = 0.48$), Body ($M = 0.83$, $SD = 0.40$), and Face ($M = 0.81$, $SD = 0.47$). The group-specific average category responses are displayed in Table 35 and in Figure 43. Post-hoc-comparison can be found in the supplementary tables S51 and S52. Similarly to the v2v_lh, in v2v_rh the CC group ($M = 1.32$, $SD = 0.30$) showed overall higher response than the SC group ($M = 1.05$, $SD = 0.53$) and the VI group ($M = 0.50$, $SD = 0.78$). Pairwise comparisons indicated a significant difference between CC group and VI group ($t(21) = 3.01$, $p = .032$).

Categorical responses within the bilateral ventral V2

Table 34

Individual and Group Average Categorical Responses within the v2v_lh

	Body		Face		Object		Scene	
group	*M*	*SD*	*M*	*SD*	*M*	*SD*	*M*	*SD*
allSC	0.85	0.46	0.97	0.44	1.01	0.48	1.47	0.53
mSC	0.86	0.33	0.91	0.31	0.98	0.32	1.37	0.40
CC	1.27	0.23	1.24	0.32	1.34	0.20	1.65	0.27
VI	0.37	0.74	0.43	1.05	0.43	0.89	0.73	1.03

Figure 42

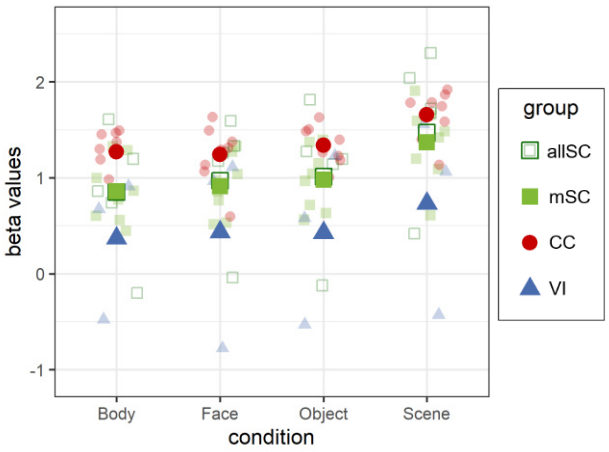

Table 35

Individual and Group Average Categorical Responses within the v2v_rh

	Body		Face		Object		Scene	
group	*M*	*SD*	*M*	*SD*	*M*	*SD*	*M*	*SD*
allSC	0.77	0.35	0.77	0.38	1.05	0.41	1.59	0.53
mSC	0.67	0.33	0.65	0.34	0.92	0.40	1.40	0.50
CC	1.10	0.10	1.11	0.19	1.34	0.12	1.73	0.23
VI	0.39	0.66	0.23	0.84	0.47	0.84	0.92	1.05

Figure 43

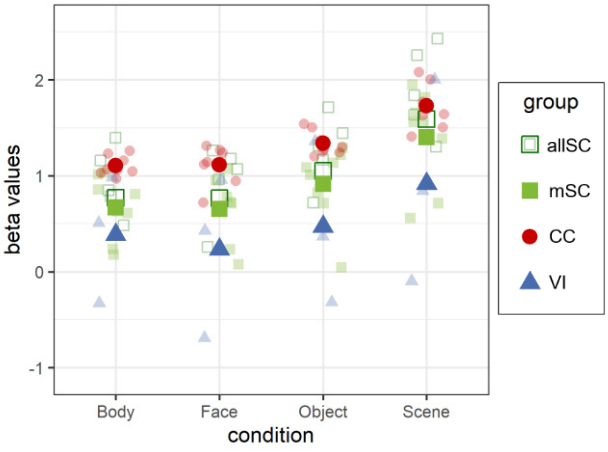

Note. Categorical responses within the bilateral ventral V2, with values for the left v2v on the upper panel and values for the right v2v on the lower panel. The tables (left side) display each group's average response and standard deviation to each category. The graphs (right side) display average individual (smaller symbols, faded colours) and group mean (larger symbols, bright colours) categorical responses. CC: congenital cataract individuals (*n* = 8; displayed in red); mSC: matched sighted individuals (*n* = 8; displayed in light green); allSC: all tested sighted individuals (*n* = 13; the additional 5 SC individuals are displayed in dark green; VI: visually impaired individuals (*n* = 3).

V3 – dorsal

We found a significant category effect both for v3d_lh ($F(3,63) = 16.14$, $p < .001$, $\eta_p^2 = .435$) as well as for the v3d_rh ($F(3,63) = 15.04$, $p < .001$, $\eta_p^2 = .417$). No further effects became significant ($p > 0.05$).

V3d_lh. In the left v3d, the category Scene elicited the highest response ($M = 1.35$, $SD = 0.36$), followed by Object ($M = 1.27$, $SD = 0.31$), Body ($M = 1.20$, $SD = 0.30$) and Face ($M = 0.99$, $SD = 0.37$). The group-specific average category responses are displayed in Table 36 and in Figure 44. Post-hoc-comparison can be found in the supplementary table S53.

V3d_rh. The right v3d followed the same categorical response with highest response to Scene ($M = 1.30$, $SD = 0.42$), followed by Object ($M = 1.18$, $SD = 0.41$), Body ($M = 1.07$, $SD = 0.34$), Face ($M = 0.89$, $SD = 0.43$). The group-specific average category responses are displayed in Table 37 and in Figure 45. Post-hoc-comparison can be found in the supplementary table S54.

Categorical responses within the bilateral dorsal V3

Table 36

Individual and Group Average Categorical Responses within the v3d_lh

	Body		Face		Object		Scene	
group	*M*	*SD*	*M*	*SD*	*M*	*SD*	*M*	*SD*
allSC	1.19	0.34	1.01	0.38	1.26	0.37	1.36	0.44
mSC	1.07	0.33	0.87	0.34	1.11	0.37	1.19	0.40
CC	1.28	0.27	1.09	0.33	1.35	0.25	1.37	0.29
VI	1.08	0.26	0.66	0.38	1.11	0.14	1.24	0.19

Figure 44

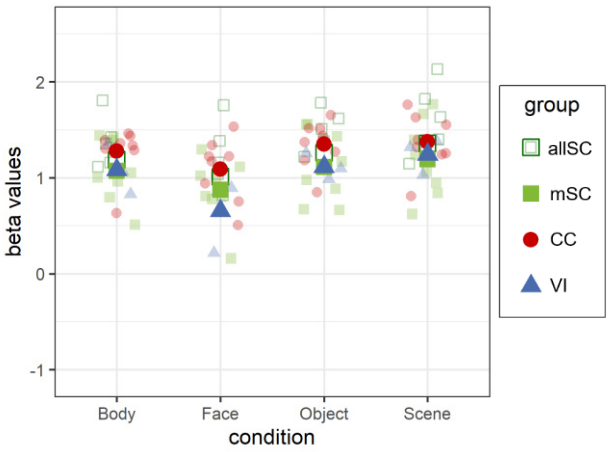

Table 37

Individual and Group Average Categorical Responses within the v3d_rh

	Body		Face		Object		Scene	
group	*M*	*SD*	*M*	*SD*	*M*	*SD*	*M*	*SD*
allSC	1.03	0.38	0.84	0.50	1.10	0.51	1.23	0.54
mSC	0.84	0.31	0.60	0.45	0.86	0.44	0.99	0.36
CC	1.19	0.25	1.04	0.28	1.34	0.18	1.44	0.19
VI	0.96	0.37	0.72	0.46	1.09	0.22	1.23	0.12

Figure 45

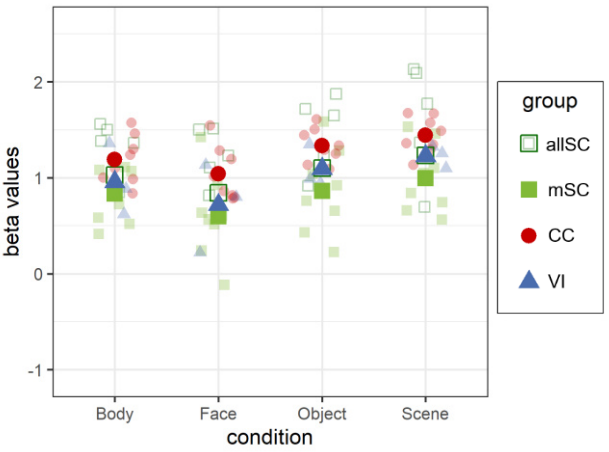

Note. Categorical responses within the bilateral dorsal V3, with values for the left v3d on the upper panel and values for the right v3d on the lower panel. The tables (left side) display each group's average response and standard deviation to each category. The graphs (right side) display average individual (smaller symbols, faded colours) and group mean (larger symbols, bright colours) categorical responses. CC: congenital cataract individuals (*n* = 8; displayed in red); mSC: matched sighted individuals (*n* = 8; displayed in light green); allSC: all tested sighted individuals (*n* = 13; the additional 5 SC individuals are displayed in dark green; VI: visually impaired individuals (*n* = 3).

V3 - ventral

We found a significant category effect both for the v3v_lh ($F(3,63) = 23.35$, $p < .001$, $\eta_p^2 = .527$) as well as for the v3v_rh ($F(3,63) = 71.47$, $p < .001$, $\eta_p^2 = .773$). No further effects became significant ($p > 0.05$).

V3v_lh. In left hemisphere, we found the highest response for the category Scene (*M* = 1.44, *SD* = 0.44), followed by Object (*M* = 1.19, *SD* = 0.44), Body (*M* = 1.06, *SD* = 0.45), Face (*M* = 1.03, *SD* = 0.51). The group-specific average category responses are displayed in Table 38 and in Figure 46. Post-hoc-comparison can be found in the supplementary table S55.

V3v_rh. In the right v3v, the highest response was found for the category Scene (M = 1.58, SD = 0.46), Object (M = 1.25, SD = 0.44), Body (M = 0.94, SD = 0.37), Face (M = 0.91, SD = 0.51). The group-specific average category responses are displayed in Table 39 and in Figure 47. Post-hoc-comparison can be found in the supplementary table S56.

Categorical responses within the bilateral ventral V3

Table 38

Individual and Group Average Categorical Responses within the v3v_lh

	Body		Face		Object		Scene	
group	*M*	*SD*	*M*	*SD*	*M*	*SD*	*M*	*SD*
allSC	1.01	0.36	1.03	0.33	1.17	0.34	1.44	0.41
mSC	0.97	0.38	0.94	0.35	1.11	0.35	1.27	0.36
CC	1.29	0.30	1.19	0.37	1.35	0.25	1.53	0.32
VI	0.69	0.90	0.63	1.21	0.81	0.98	1.19	0.85

Figure 46

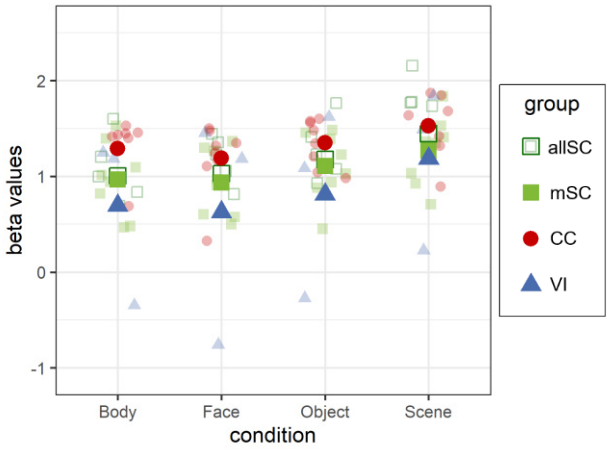

Table 39

Individual and Group Average Categorical Responses within the *v3v_rh*

	Body		Face		Object		Scene	
group	*M*	*SD*	*M*	*SD*	*M*	*SD*	*M*	*SD*
allSC	0.92	0.32	0.91	0.43	1.23	0.42	1.60	0.51
mSC	0.85	0.37	0.81	0.44	1.10	0.40	1.42	0.51
CC	1.10	0.17	1.11	0.23	1.43	0.16	1.69	0.18
VI	0.62	0.79	0.39	1.06	0.86	0.83	1.25	0.73

Figure 47

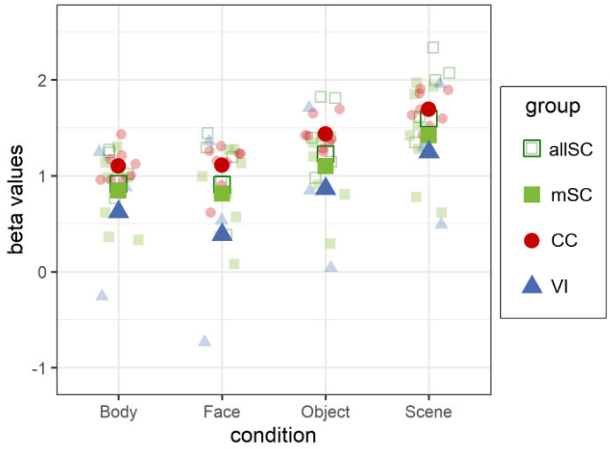

Note. Categorical responses within the bilateral ventral V3, with values for the left v3v on the upper panel and values for the right v3v on the lower panel. The tables (left side) display each group's average response and standard deviation to each category. The graphs (right side) display average individual (smaller symbols, faded colours) and group mean (larger symbols, bright colours) categorical responses. CC: congenital cataract individuals (*n* = 8; displayed in red); mSC: matched sighted individuals (*n* = 8; displayed in light green); allSC: all tested sighted individuals (*n* = 13; the additional 5 SC individuals are displayed in dark green; VI: visually impaired individuals (*n* = 3).

5. Discussion

The present study investigated the influence of transient congenital visual deprivation on visual categorical processing of four prominent visual categories, namely faces, bodies, objects, and scenes. To this end, we acquired functional MRI data of three different groups: a group of individuals with a history of congenital dense bilateral cataract (CC individuals), a group of normally sighted controls (SC individuals), and a group of visually impaired controls (VI individuals). Given the multifaceted organisation of categorical processing, we applied two different analysis approaches to investigate possible effects of early visual deprivation. First, we used the multivariate pattern analysis (MVPA) to investigate whether early visual deprivation affects the distributed neural pattern of the four tested categories within the ventral temporal cortex (VTC). Second, we used a univariate region of interest (ROI) analysis to investigate whether CC individuals exhibit different categorical response profiles in distinct category-selective regions due to their experience of early visual deprivation. In general, the results revealed that while the large-scale categorical organisation was relatively unaffected by early visual deprivation, it did affect categorical fine-tuning in form of less distinctive distributed information within the VTC as well as ill-specialised processing in category-selective regions. Thus, the study at hand did not just replicate previously reported face-selective impairments in CC individuals, but additionally described similar effects for other visual categories.

Effects of Early Visual Deprivation on Categorical Representations

As predicted, all visual categories have been classified above empirical chance level both in the CC group and the SC group. However, when comparing the average classification accuracies directly between groups, both within-subject as well as within-group classification, the SC group yielded significantly higher classification accuracies than the CC group. Furthermore, in accordance with our hypothesis, classification was successful between the SC group and the CC group with less accurate classification when training on SC data as compared to the accuracies obtained when training on the CC data. In order to differentiate between effects of congenitally visual deprivation and effects of residual visual impairments, we also included a third group consisting of three VI individuals. For the VI group, all categories have been classified with comparably high accuracy. However, due to the small sample size results cannot be discussed on a statistical level.

Overall, the MVPA results indicated that CC individuals did not just exhibit distinguishable categorical patterns, but furthermore, as suggested by the successful between-group classification, exhibited the same large-scale categorical organisation as SC individuals. Nevertheless, the reduced classification accuracies in CC individuals might suggest that the nature of discriminant information present in the

input vertices differs not just between CC individuals and SC individuals, but already among CC individuals. Given that the data of the VI group exhibited more similarities to the SC group than to the CC group might suggest that early visual deprivation rather than reduced visual acuity have led to changes in CC individuals, which most likely are characterised as inconsistent categorical patterns in CC individuals rather than consistent group differences compared to SC individuals. As the MVPA classification results do not indicate where within the VTC these group differences occur or how they are characterised, there are multiple explanations to consider. Less accurate classification in CC individuals compared to SC individuals could be the result of otherwise organised categorical patterns in CC individuals. For example, face-selective patterns in the VTC of CC individuals might have involved different vertices than in SC individuals. An alternative explanation might be that CC individuals simply exhibited a reduced extent of category information, which would also result in confounded classification results. However, given the successful between-group classification for all category pairs in both prediction directions, i.e. training on CC data and testing on SC data, and vice versa, it seems unlikely that both groups deviate in their categorical organisations.

To our knowledge, the present study was the first that used MVPA to investigate the influence of early visual deprivation on distributed categorical representations within the VTC. The results provide new evidence that despite a prolonged period of congenital visual deprivation, CC individuals exhibited categorical differentiation as well as highly similar large-scale organisation to SC individuals. As this conclusion is based on cross-sectional data, we cannot claim whether distributed categorical organisation develops independently of early visual deprivation or largely recovers of such. However, evidence in congenitally blind individuals proposes that basic neural organisation, such as retinotopic and large-scale categorical organisation, rather develops independently of visual experience (Bock et al., 2015; Striem-Amit et al., 2015; van den Hurk et al., 2017). Furthermore, based on previous research in CC individuals, it has been discussed that visual functions with a high organisational bias, therefore highly matured after birth, are less affected by early visual deprivation (Röder & Kekunnaya, 2021). The here reported results align with this conclusion as CC individuals exhibited a highly comparable large-scale categorical organisation to SC individuals. Nevertheless, the results also indicated that the lack of early visual experience leads to inconsistent categorical organisation in CC individuals despite many years of visual recovery. This finding might also explain the reported asymmetry in between-group classification direction. This asymmetry resembles those of other studies (Paquette et al., 2018; van den Hurk et al., 2017) and it has been proposed that generalisation works best from lower to higher signal-to-noise ratio (van den Hurk & Op de Beeck, 2019). This conclusion does fit the here presented data as CC individuals exhibited less accurate within-subject

classification, i.e. low signal-to-noise ratio, than SC individuals, i.e. high signal-to-noise ratio, and better between-group classification results have been obtained for classification from CC individuals to SC individuals.

Effects of Early Visual Deprivation on Category-Selectivity

It was hypothesised that all three groups would show the designated category-selectivity as indicated by the functional atlas in the respective regions. More specifically, it was hypothesised that face-selective regions would show higher responses to faces than the other categories, body-selective regions would exhibit higher responses to bodies than other categories and scene-selective regions higher responses to scenes than to any other category. However, we expected CC individuals to exhibit reduced responses to the respective preferred category than the other groups. Furthermore, we were interested in the categorical response profiles of other regions provided by the functional atlas that have not been associated with one of the tested categories.

In regards to face-selectivity, in partial agreement with both hypotheses, right hemispheric face-regions were more likely to exhibit face-selectivity equally for all three groups, while left hemispheric regions were more likely to exhibit impaired face-selectivity in CC individuals. These face-selective impairments were not just characterised by less face-selective response as expected. In fact, CC individuals exhibited higher responses to object than faces and increased responses to non-preferred categories. These findings for left-lateralised face-selective impairments manifested specifically for the all-subjects model and were stronger in the avg-face region than in the individual face-regions. In partial agreement with the hypotheses, body-selectivity was found in the majority of body-selective regions, though not within the VTC, while all scene-selective regions showed scene-selectivity as expected. In contrast to the hypotheses, there was no evidence for a reduced body-selective nor scene-selective response in CC individuals. Nevertheless, CC individuals tended to show higher non-preferential responses both in body- and scene-selective regions, respectively. Additionally, there were indications for overall higher responses in CC individuals in respective regions. For the exploratory part of the analysis, we found that all additional regions exhibited a preference for one of the tested categories, although not originally associated with it. While CC individuals showed no difference in category-preference, there were indications for overall higher responses in CC individuals as for example in the majority of early visual regions.

So far, research on categorical processing in CC individuals focussed mainly on faces. Overall, we were able to replicate findings of face-specific impairments in CC individuals as reported by Grady et al. (2014) and Röder et al. (2013). Similar to Grady et al., we demonstrated that CC individuals showed less face-selective responses than SC individuals. However, in contrast to Grady et al., we found object-selective responses within face-selective regions were not unique for CC individuals as also SC individuals exhibited high responses to objects. Yet more interestingly, it is the category preference that differed between groups. Despite the fact that the reduced response towards the preferred category in CC individuals was unique for faces, tendencies for higher non-preferential responses were also observed in body- and scene-selective regions. Moreover, CC individuals also exhibited overall higher responses than the other groups also in non-categorical regions.

In contrast to the hypotheses, not all regions exhibited category-preferences as expected. The stronger face-selective responses in right than in left lateralised face-selective regions is frequently reported in various face-selective regions (Rossion et al., 2000; Yovel et al., 2008; Zhen et al., 2015) and has been referred to as right lateralised face-selectivity. The bilateral lack of face-preference in the pFus-faces, however, asks for an alternative explanation other than the right lateralisation of face-selectivity. Rosenke et al. defined the functional atlas without including object-selective regions as it could not be reliably located due to insufficient activation patterns. However, this does not mean, that there are no object-selective vertices in the VTC as various reviews and studies (Grill-Spector & Weiner, 2014; Weiner, Natu, et al., 2018) as well as other functional atlases (Julian et al., 2012) have reported beforehand. It seems therefore very likely that the reported response in the pFus-faces reflected object-selective vertices rather than face-selective vertices. Evidence has been reported according to which posterior fusiform regions in contrast to anterior fusiform regions, did not indicate face-selective impairments in CC individuals (Grady et al., 2014). Grady et al. concluded, that this finding might be related to different levels of specialisation for face-selective processing. In this study at hand, we did not find group differences either for the pFus-faces, which would agree with the conclusion by Grady and colleagues. Nevertheless, there was overall more object- than face-selective responses both in the SC group as well as in the CC group, which weakens the argument in the first place and makes the mentioned influence by object-selective vertices more likely.

Furthermore, despite the indications of group by condition effect in the right OTS-bodies, this result seems more likely to reflect face-selective rather than body-selective impairments in CC individuals. This interpretation is mainly based on the overall face-preferences in SC and VI individuals and object-preference in CC individuals, and dissimilarities to the other tested body-selective regions. This in general reduced body-selective response in the OTS-bodies, commonly referred to as the fusiform body area (FBA), might be associated with substantial overlap of FBA and the face-selective FFA

(Schwarzlose et al., 2005), which might result in high face-selective responses in general. Moreover, in the left FBA body-selective activation is less common if not even absent at all (Taylor et al., 2007). The here reported lack of body-specific response in all groups within OTS-bodies, left as well as right hemisphere, might therefore reflect either overall minor univariate body-selectivity within the fusiform gyrus, or influence of other vertices selective to other visual categories, such as faces or objects, due to individual deviations from the functional localiser.

In general, evidence indicated that early visual experience might be essential, besides other aspects, for the development of the inhibitory neural network (Reh et al., 2020). Previous research in CC individuals has discussed that early visual deprivation might have interrupted the development of inhibitory neural mechanisms in CC individuals (for a review see Röder & Kekunnaya, 2021). More specifically, reduced neural inhibition in CC individuals has been associated with increased response in striate processing (Sourav et al., 2018), reduced posterior alpha oscillatory activity (Bottari et al., 2016) and ill-specialised face-processing (Röder et al., 2013). The here reported results provide further evidence that face-selective impairments in CC individuals might partially be associated with impaired inhibition which resulted in increased responses to non-preferred categories. Yet more importantly, these results are the first that indicate that impaired inhibition might similarly affect the processing of other visual categories, such as body- and scene-selective processing.

Methodological Considerations and Limitations

Our data suggest that while distributed representations in CC individuals were slightly affected yet equal for all categories, univariate selectivity showed elaborate but highly specific, that is mostly face-specific, impairments in CC individuals. The question arises as to what causes the discrepancy between analyses regarding individual categories, i.e., why does congenital visual deprivation lead to such differentiated levels of impaired fine-tuning for different visual categories, although MVPA identified similar impairments for all categories.

First, one has to consider that MVPA and ROI analyses were based on differently sized brain regions. While the MVPA was analysed for the entire VTC, category-selective ROI were considerably smaller and constitute only peaks of activation within the much bigger distributed activation pattern across the whole VTC (Haxby et al., 2001). Considering face-selectivity, we were able to show that the MVPA indicated impairments in CC individuals also manifested in individual face-selective regions. Even more so, our results propose the idea that less-distinct face-selective patterns are driven by less

differentiated responses towards the tested categories, i.e. reduced face-selective response coupled with increased non-preferred responses. However, this was not the case for body- and scene-selective processing. The MVPA analysis indicated impaired classification for both bodies as well as scenes, yet there were no significant indications of impaired univariate selectivity in neither body-selective nor scene-selective regions. Due to the size difference of the tested regions, i.e. VTC vs. distinct regions, it might be plausible that reported impairments in the MVPA analysis reflect group differences outside the respective regions. Using scene-selectivity as an example, MVPA might have detected less scene-selective neurons within the VTC yet outside the PPA. Thus, the MVPA detected impaired scene-selectivity for CC individuals within the VTC, yet no group differences were found in the univariate analysis because the PPA itself was unaffected. Alternatively, impaired classification as reported by the MVPA might also be linked to a reduced number of category-selective neurons within the distinct region. Yet to compensate the most likely resulting reduced category-selectivity, neurons would have needed to acquire some kind of neural compensation mechanism (Grill-Spector et al., 2008). However, we did not just report a lack of group difference, but in fact tendencies for increased responses in CC individuals. Therefore, rather than impairments in the distinct region, it seems more likely that the extent of scene-selectivity in CC individuals was reduced. In fact, developmental studies reported an age-related increase of activation volume for face-selective regions (Golarai et al., 2007, 2010; Peelen et al., 2009; Pelphrey et al., 2009; Scherf et al., 2007, 2011; but see Passarotti et al., 2003) as well as scene-selective regions (Golarai et al., 2007; Meissner et al., 2019). It seems plausible that early visual deprivation leads to an interruption of this developmental process and results in a reduced extent of category-selectivity in CC individuals. Since age-related volume increase has not been reported for object-selective (Golarai et al., 2007, 2010; Scherf et al., 2007) or body-selective regions (Peelen et al., 2009; Pelphrey et al., 2009), and findings for scenes-selective regions are in fact not as consistent as for faces-selective regions, further research is needed to confirm this consideration.

The second aspect that might explain the discrepancy in univariate and multivariate results is that MVPA and univariate analyses reflect different aspects of functional processing. MVPA identifies the underlying neural pattern in terms of their informational content, i.e. what information is represented in a vertex. The classical univariate analysis focuses on a region's function, i.e. responses towards preferred and non-preferential categories. The different aspects both analyses reflect, contribute essentially to the understanding of functional processing, but at the same time also make it difficult to draw a direct conclusion from one analysis to the other. A less precise categorical organisation, i.e. less categorical fine-tuning, might lead to less univariate selectivity as there is reduced category-specific information decoded. Yet even if a specific neuron contains relevant information that leads to the differentiation of stimuli, does not mean that this information is

necessarily used in the processing of that stimulus (Williams et al., 2007). Findings of patient and stimulation studies emphasise the causal role of category-selective regions in behavioural outcome (Pitcher et al., 2009; Schalk et al., 2017; Wada & Yamamoto, 2001). For distributed representations such as representational similarity patterns, evidence for a causal relation with behaviour is still scarce, despite repeated reports of a correlational link (Cohen et al., 2014; Groen et al., 2018). For example, intracranial electronic stimulation of the FFA appears to affect only face-specific processing, but not the perception of other, non-face objects (Parvizi et al., 2012; Schalk et al., 2017). In the absence of evidence directly linking one method with the other, one has to consider that the here reported MVPA and univariate results are merely coincidental. Accordingly, the impaired processing of faces is unique in its finding given that it's the only category exhibiting impairments in both multivariate as well as univariate analyses.

The third considerable aspect that might have influenced the here reported results lies in the methodological basis for each analysis. In contrast to the classical univariate ROI analysis, MVPA allows for much more sensitive detection of small differences between stimuli or groups (Cox & Savoy, 2003; Norman et al., 2006), as the analysis is based on a voxel-by-voxel analysis and entails therefore more data points. This has been reported in various patient studies as for example in prosopagnosia patients: While the classical univariate analysis failed to detect any group differences for face and object discriminability, MVPA revealed significantly reduced discriminability for congenitally prosopagnosia patients compared to control subjects (Rivolta et al., 2014). In terms of the here reported results, effects of early visual deprivation might be smaller in body- and scene-selective cortices than in face-selective cortices and simply not sufficient for significant univariate effects, while MVPA was sensitive enough to detect these smaller differences.

The fourth aspect in considering the result differences is based on the development of category-selective processing and might indicate why the effects of early visual deprivation manifest the strongest on face-selective cortices. Despite intriguing new evidence for early maturation of some category-selectivity (Kosakowski et al., 2021), it seems undeniable that visual experience still is essential for the emergence of other category-selective regions (Kosakowski et al., 2021), further categorical fine-tuning of univariate selectivity and representation similarity (Cohen et al., 2019; Deen et al., 2017; Golarai et al., 2007; Scherf et al., 2011) and/or maintenance of category-selectivity (Huber et al., 2015). Yet especially the development of face-selective processing, has been reported to follow a unique developmental trajectory. Firstly, face-selective regions have been reported to take longer to mature than other regions – far beyond the first decade of life (Aylward et al., 2005; Golarai et al., 2010; Peelen et al., 2009; Scherf et al., 2007). Secondly, previous research in CC individuals identified a sensitive period for the typical development of face-selective processing

(Röder & Kekunnaya, 2021). More specifically, it is assumed that early visual deprivation leads to an interruption of essential sensory input which further leads to persistent impairments in CC individuals despite many years of recovery. Both arguments indicate a unique development trajectory for face-selective processing. Accordingly, face-selectivity more than any other visual category is affected by early visual deprivation either due to the reduced extent of face-experience and/or from missing the sensitive period that guarantees the typical development.

Given that our univariate results primarily replicate face-selective impairments in CC individuals, it is tempting to conclude that the development of other visual categories is not subject to a sensitive period during which visual input is necessary for normal development. However, that conclusion would be premature and dismiss the still meaningful indications of ill-specialised processing of the remaining tested visual categories, such as bodies, objects and scenes. The here reported results simply show that visual input during early infancy is not as necessary for the processing of bodies, objects and scenes as it is for faces. Whether body- and scene-selectivity – possible object-selectivity as well – recovers to a higher degree or is simply less affected in the first place has to be left unanswered to this point.

Overall, a variety of underlying processes and developing neural mechanisms might have contributed to these differentiated results and need to be considered in their interpretation. Besides the previously mentioned increase in activation volume, developmental changes in the response characteristics have been proposed as well. Face-selective changes with age have been mainly described as an increase in the face-selective response or overall face-selectivity (Golarai et al., 2010, 2015; Grill-Spector et al., 2008; Scherf et al., 2007), but also as reduced responses towards unpreferred stimuli such as objects (Cantlon et al., 2011). Similar although less consistent findings have been reported for the development of scene-selectivity. Individual studies have reported an increased response magnitude in the right PPA, which is also positively correlated with recognition memory (Chai, 2010) or an increased bilateral scene-selectivity characterised by higher scene-selective response as well as reduced response towards non-preferred stimuli (Meissner et al., 2019). Furthermore, even if regions show similar functional changes, anatomical evidence proposes different underlying microstructural mechanisms that interplay with the functional changes (Gomez et al., 2017; Natu et al., 2019). Therefore, the maturation of category-selectivity might not just follow individual developmental trajectories but might as well be accompanied by various anatomical mechanisms. Both mentioned functional changes, that is the age-related increase in selectivity as well as the increase in activation volume have been proposed to be dependent on visual experience (Cohen et al., 2019; Golarai et al., 2015). Therefore, early visual deprivation might have led to

impaired processing in CC individuals either by a reduced extent of category-selective information within the VTC, as specifically referred to in the first argument, and/or reduced category-selectivity within distinct regions. And although respective evidence in normally sighted individuals is so far limited to face-selective and scene-selective regions, based on our results it seems likely that similar developmental changes occur in other visual categories. It might therefore be suggested that early visual deprivation leads to ill-specialised category organisation in CC individuals, which manifests not just in reduced category-selectivity but also in a reduced extent of categorical information.

There are some limitations of the present study which need discussion. To assure that participants perceived the different visual categories, we assessed participants' dissimilarity ratings of the presented stimuli during scanning. Our analysis revealed that in terms of percentage, fewer CC individuals than SC individuals would have met the original testing criterion. Nevertheless, in the adapted analysis, neither the CC group nor the SC group perceived the tested categories differently. The residual visual impairments in CC individuals might have made it more difficult for CC individuals to fulfil the task. Yet the lack in perceived category differences might not solely be related to these visual impairments given that both groups failed in perceiving the expected category differences. Most importantly, however, both fMRI analyses revealed that to a great extent both SC individuals as well as CC individuals did exhibit differentiated categorical responses. It seems therefore more likely that the findings might have revealed a misunderstanding or uncertainty of task rather than a failure in categorical processing. Still, this finding was surprising given that no such problems have occurred in the original study by van den Hurk (2017) and the task remained the same for this study.

We furthermore need to acknowledge that we tested only small groups considering eight CC individuals and three VI individuals. However, given the rarity of suitable participants, both congenital cataract individuals as well as late required visually impaired individuals, comparable sample sizes are commonly observed (Guerreiro et al., 2016a, 2016b; Guerreiro, Erfort, et al., 2015; Guerreiro, Putzar, et al., 2015). Multiple steps have been taken to account for possible difficulties. Two separate data models have been calculated enabling the direct comparison of CC and SC individuals in the matched-model as well as a comparison based on a higher number of control subjects in the all-subjects model. Linear mixed models have been calculated instead of classical ANOVA to allow for better analysis with unbalanced sample sizes (G. Chen et al., 2013). Two different analysis methods have been applied of which MVPA has been proven to be highly sensitive to even with small effects (Cox & Savoy, 2003; Norman et al., 2006). Most importantly, we were able to replicate findings of face-selective impairments in CC individuals based on slightly bigger samples (Grady et al., 2014; Röder et al., 2013), which allows for similar conclusions of other findings in this study. Nevertheless, further research is

needed to make conclusive statements regarding effects of early visual deprivation on the development of body- and scene-selectivity, given the inconsistent findings of developmental research and the absence of related studies in CC individuals.

Moreover, no independent functional localiser data had been acquired due to limited resources. Instead, an independent localiser was used for the definition of functional ROI. Due to the objective definition of ROI using the atlas, we were unable to assess information about individual differences in region location or differences in size, which might be important sources of information for possible effects of early visual deprivation on the development of category processing as described previously. Furthermore, the atlas by Rosenke et al. did not include object-selective region(s), which given our study design would have been agreeable to draw cohesive conclusions. One could argue that keeping the category of objects in the analysis despite no respective region might have influenced the conclusions. And in fact, we do see object preference, where the atlas indicates other preferences as for example in the bilateral pFus-faces. However, keeping the category of objects as the fourth category allowed us to draw specific conclusions as for example object-preference in CC individuals similar to the findings by Grady et al. (2014), which we would not have been able to detect if excluded. At the same time, using an object localiser has mentionable advantages. In absence of independent functional localiser data, functional ROI are commonly defined by dividing the data into definition and test dataset. However, given the already limited amount of data, this would most likely result in a considerable data loss. Using the independent localiser therefor allowed for a highly specific definition of ROI as well as preventing data loss. Furthermore, identical ROI for all subjects allow for objective testing and direct comparison, that is for example within typical face-selective regions (based on the data of normally sighted individuals), do CC individuals exhibit differences. Despite ROI size being a considerable source of information, group-specific differences in ROI size might also confound further analyses. Especially if CC individuals would show smaller ROI, as discussed previously, this might influence the overall activation levels and ideally would have to be controlled for. Future research might combine both approaches in order to answer some of the proposed explanations. Additionally, the atlas by Rosenke et al. also entailed regions, which we would not have been able to investigate otherwise. By using the functional atlas, we were able to investigate if CC individuals would exhibit otherwise located category-selectivity and possible effects of early visual deprivation of other visual regions.

Conclusion

The present study provides new evidence for differentiated effects of early visual deprivation on the development of categorical processing. While we found the large-scale categorical organisation to be relatively unaffected by early visual deprivation, categorical fine-tuning and particularly face-selective processing exhibited impairments. In general, previous evidence indicated lower-level visual processing to be less affected by early visual deprivation than higher-level processing or to recover to a larger extent, for example striate vs extrastriate processing reported by Sourav et al. (2018). Consequently, it has been suggested that the effects of early visual deprivation increase following the visual processing hierarchy (Röder & Kekunnaya, 2021). Based on the results reported here, a more differentiated view on the effects of early visual deprivation might be necessary. More specifically, our data suggests that it is specifically the maintenance and fine-tuning of category-selectivity rather than the neural set-up, i.e. the large-scale categorical organisation, that is affected by early visual deprivation. This is also supported by the observation that visual functions with a high organisational bias are less affected by early visual deprivation than visual functions that follow a prolonged development and are more dependent on visual experience (Röder & Kekunnaya, 2021). In fact, basic neural set-up, such as retinotopy and categorical organisation has been reported in congenitally blind individuals (Bock et al., 2015; Striem-Amit et al., 2015; van den Hurk et al., 2017) and therefore might develop without visual experience in contrast to experience-dependent development of category-selectivity in normally sighted individuals (Grill-Spector et al., 2008).

In conclusion, together with previous evidence, the here presented results convey compelling evidence for the differential development trajectories of distributed categorical representation and univariate selectivity especially in relation to their dependence on early visual experience.

Chapter IV

General discussion

The Experience-(In)dependent Development of the Human Brain

Neurodevelopment involves a highly complex and dynamic process that encompasses the growth, organisation, and maturation of the brain. Influenced by a fine interplay involving innate genetic programs, environmental factors, and experiences, this process results in the formation of neuronal circuits in early brain development. With genetics laying the foundation for structural and functional development, heightened susceptibility towards experiences enables individuals to adapt to their unique environments (Fagiolini et al., 2009; Knudsen, 2004). However, this susceptibility also conveys vulnerability as atypical experiences can impact the neuronal organisation and have enduring effects (Röder & Kekunnaya, 2021). Understanding the extent to which experience-independent and experience-dependent factors influence brain development, in addition to comprehending the interplay between structural and functional development, is essential for gaining profound insights into the complex processes that drive the remarkable development of the human brain.

In recent decades, sophisticated non-invasive brain imaging techniques have undergone progressive expansion, leading to an enhanced understanding of brain structure and function. Among these techniques, MRI has emerged as the primary modality for both clinical and research applications. MRI and its various adaptations offer valuable insights into brain tissue morphology, structural composition, spatio-temporal signals of brain activity, connectivity, and metabolic changes. Furthermore, because MRI not only permits the scanning of the brains of young children but also the repeated scanning of the same individual over time, it is particularly useful for investigating neurodevelopmental pathways. Extensive MRI research has focused on brain development by observing inter-individual differences or intra-individual time changes in brain structure or function, either by comparing different age groups or by tracking individuals in their brain development. Moreover, MRI studies on twins have elucidated the relative contributions of genetics and environment on developmental trajectories, by comparing similarities between monozygotic twins, who share approximately 100% of the same genes, and dizygotic twins, who share approximately 50% of the same genes. Neonatal twin studies highlight the highly heterogeneous and complex impact of genetic influences on early brain development, while the significance of experiences in shaping the brain increases over time (Maggioni et al., 2020). Accumulating evidence describes the spatiotemporal patterning of cortical development in the human brain following a hierarchical development from lower-order primary and unimodal cortices to higher-order transmodal association cortices (Sydnor et al., 2021). In general, the order in which the cortex matures corresponds to cognitive milestones in human development (Giedd, 2004; Gogtay et al., 2004; Sowell et al., 2003, 2004). Primary sensory and motor systems mature earliest, followed by temporal and parietal association cortices involved in basic language skills and spatial attention. The prefrontal and

lateral temporal cortices, which integrate primary sensorimotor processes and modulate basic attention and language processes, appear to mature last. This reported hierarchical development parallels post-mortem studies in non-human and human primates suggesting a protracted development of the prefrontal cortex in comparison to sensorimotor cortices (Bourgeois & Rakic, 1996; Huttenlocher, 1979).

Notably, a significant portion of the structural cortical development occurs prenatally, thereby resulting in an advanced structure of the infant's brain at birth (Knickmeyer et al., 2008; G. Li et al., 2015). Moreover, the majority of developmental changes in the structural brain occur within the first two years of life (Giedd & Rapoport, 2010; Gilmore et al., 2018; Wierenga et al., 2014). Given that experience at this age is limited, this early structural maturation implies a highly routed genetic basis (Rakic, 2009). However, genetic influences on brain development exhibit regional specificity, with posterior regions – particularly occipital and parietal areas – being more influenced by genetics compared to frontal regions, and also differ concerning various structural measures (Maggioni et al., 2020). More specifically, cortical thickness and surface area are both highly heritable, yet genetically uncorrelated (Panizzon et al., 2009; Winkler et al., 2010) and influenced by regionally distinct genetic factors (C. H. Chen et al., 2012, 2015; Rimol, Panizzon, et al., 2010; Schmitt et al., 2008). Moreover, surface area has been implicated as having a stronger genetic influence compared to cortical thickness (Jha et al., 2018; Maggioni et al., 2020), which might be related to the observation that surface area rather than cortical thickness differs across species (Fish et al., 2008). In contrast, the development of cortical thickness is considered more functionally driven given its posterior-to-anterior trajectory and the thereby high resemblance to functional maturation (C. H. Chen et al., 2011; Gogtay et al., 2004; Krongold et al., 2017; Valk et al., 2020; Westlye et al., 2010).

These observed changes in brain structure may have implications for brain function as this hierarchical pattern of development is not just observable in terms of the general functional development, but already within the visual system (Braddick & Atkinson, 2011). The visual system consists of a series of interconnected processing areas, each handling increasingly complex visual information (Goebel et al., 2012). In the development of the visual system, low-level visual processing exhibits a high degree of maturation at birth (Arcaro & Livingstone, 2017; Ellis et al., 2021) and matures earlier than higher-level visual processing (Casey et al., 2005; Gomez et al., 2018). This hierarchy is believed to reflect the way in which the brain processes visual information requiring a gradual extraction of relevant stimulus properties (DiCarlo et al., 2012; Serre et al., 2007) as also exemplified by neural networks (LeCun et al., 2015). Over time, the brain undergoes adaptive changes through learning and exposure, gradually becoming more specialized, which leads to greater

efficiency and accuracy of higher-level visual processing (Brants et al., 2016; Gauthier & Nelson, 2001; Golarai et al., 2015; Hills & Lewis, 2018).

More complex higher-level visual processing, such as visual categories, follows a more protracted development with distinct trajectories for different category-selective areas (Grill-Spector et al., 2008). In recent years, these trajectories have been extensively investigated for categories such as faces, bodies, scenes, and objects and especially the manifestation of these category-selective regions has been considered experience-dependent, given that their development spans across the first decade of life (Aylward et al., 2005; Gathers et al., 2004; Golarai et al., 2007; Passarotti et al., 2003; Pelphrey et al., 2009; Scherf et al., 2007). However, recent advances in MRI acquisition techniques have enabled researchers to test awake infants and challenge the notion of delayed onset of category-selective regions (Deen et al., 2017; Kosakowski et al., 2022). Of these, one study reported adult-like category-selective responses in infants as young as 2 months (Kosakowski et al., 2022). These findings suggest an earlier onset of categorical processing than previously thought, which potentially strengthens the influence of experience-independent mechanisms during development. In fact, a growing body of evidence suggests that genetics can also influence the categorical organisation and, in this context, Abbasi et al. reported that category-selectivity maps for faces, bodies, objects, and scenes were more similar in monozygotic than in dizygotic twins (Abbasi et al., 2020). Another study found that monozygotic twins tend to exhibit greater similarities in their response to faces and scenes compared to words (Polk et al., 2007). This evidence does not just indicate the involvement of genes in high-level visual organisation but moreover might suggest a stronger genetic influence on natural and evolutionary-relevant categories such as faces and scenes, in contrast to man-made objects.

As the evidence mounts in support of experience-independent early functional development, it has been discussed that – perhaps not surprisingly – early functional and structural development might be closely intertwined. Overall, cognitive ability in infants, children, and adults is associated with individual differences in various structural measures (Girault et al., 2020; Karama et al., 2009; Narr et al., 2007; Shaw et al., 2006). More specifically, structural differences might potentially explain inter-individual differences in behaviour (Genon et al., 2022; Kanai & Rees, 2011) and have been linked to intelligence (Colom et al., 2006; Narr et al., 2007; Shaw et al., 2006), creativity (W. Li et al., 2015; Takeuchi et al., 2010), and memory (Maguire et al., 2000). Similarly, abnormal structural development has been extensively linked to various neurodevelopmental, neurological, and psychological diseases such as schizophrenia (Haijma et al., 2013; Rapoport et al., 2012; van Erp et al., 2018), bi-polar (Hanford et al., 2016; Rimol et al., 2012; Rimol, Hartberg, et al., 2010), and depressive disorders (Qian Li et al., 2020) in addition to autism (Courchesne et al., 2007;

Khundrakpam et al., 2017; Pagnozzi et al., 2018; Zielinski et al., 2014) and attention-deficit/hyperactivity disorder (Albajara Sáenz et al., 2019).

The close link between structure and function is also specifically observable for categorical organisation, and structural characteristics have been considered to determine where category-selective regions emerge (Grill-Spector & Weiner, 2014). More specifically, within the VTC, functional regions have been consistently and predictably located (Aguirre et al., 1998; Epstein & Kanwisher, 1998; Grill-Spector et al., 1999; Kanwisher et al., 1997; Malach et al., 1995), whereby this consistent organisation is not unique to humans and numerous studies have suggested a more fundamental basis for the categorical organisation that extends beyond humans. Specifically, these studies have shown a high degree of similarity in categorical organisation between humans and other non-human primates (Rakic, 2009) and similar categorical organisation has been reported in non-human primates for the large-scale categorical organisation (Kriegeskorte, Mur, Ruff, et al., 2008) and distinct regions for faces, bodies, and scenes (Lafer-Sousa et al., 2016; Nasr et al., 2011; Natu et al., 2021; Pinsk et al., 2009; Rajimehr et al., 2011).

These similarities between species support an evolutionary and genetically driven early brain development, with a highly interconnected progression of structure and function. Based on animal studies, a broader concept emerged, in which the cortex is prenatally patterned by a combined action of various genetic mechanisms involving transcription factors, morphogens, and signalling molecules (O'Leary et al., 2007). These genetic gradients provide regional boundaries for the initial formation of cortical areas, distinguished from one another by their cyto- and chemoarchitecture, and input and output connections, that ultimately serve diverse cortical functions (Espinosa & Stryker, 2012). This genetic patterning has also been identified in humans with parcellations into regions of maximal shared genetic influence (Chen, 2013) which, to some extent, are already present at birth (Ball et al., 2020). The resulting structural characteristics that accompany the patterns further guide functional development. For instance, the categorical organisation is highly influenced by the cortical folding patterns in the VTC (Weiner et al., 2014; Weiner, Barnett, et al., 2018; Witthoft et al., 2014) and the mid-fusiform gyrus serves as an anatomical landmark involved in the predictable location of the mid-fusiform face area (Weiner et al., 2014; Weiner & Grill-Spector, 2010), and the separation of face-selective from place-selective regions (Nasr et al., 2011). Other structural characteristics have also been implicated in the development of functional organisation, such as connectivity fingerprints (Osher et al., 2016; Saygin et al., 2012, 2016) and cytoarchitectonic properties (Weiner et al., 2017). These factors not only result in a consistent location of functional representation relative to cortical folds, but also a consistent spatial relationship among functional representations, both for distinct selective regions and large-scale maps.

Despite the broad influences of genetics on visual development, experience remains crucial. In the 1960s, Hubel and Wiesel made ground-breaking discoveries by recording the neural activity of visually deprived cats and monkeys (reviewed by Daw, 2009). They found that selective receptive fields and functional architecture could develop without visual experience, indicating the involvement of innate mechanisms in determining the organisation of receptive fields and cortical columns (Hubel et al., 1976; Hubel & Wiesel, 1963). This innate phase, however, was followed by a period during which visual experience was crucial for the refined development of the striate visual cortex (Wiesel & Hubel, 1965) – a sensitive period.

The discovery of the crucial role of early visual input in striate visual cortex development sparked extensive research into the plasticity of the visual system (Daw, 2009). This research area also encompasses investigations into the extent to which cortical representation of other sensory modalities, such as auditory and somatosensory input, change in the absence of visual input (López-Bendito et al., 2022; Pavani & Röder, 2012; Rauschecker & Harris, 1983; Rauschecker & Korte, 1993). Overall, Hubel and Wiesel 's (1963) discovery of an innate phase followed by a sensitive period of visual experience has had a significant impact on the understanding of cortical development and plasticity in the visual system. Following their work, many authors have made contributions to the study of synaptic reorganisations that are associated with monocular and binocular deprivation, examining the effects of deprivation on other areas of the visual system and the development of visual properties beyond binocularity in a wide range of species.

In visually deprived humans, such as congenitally blind individuals, extensive research investigated structural and functional changes both in the ‘visual’ and in other, non-deprived cortices (Noppeney, 2007; Röder & Kekunnaya, 2022). While the investigation of permanently blind individuals usually addresses the adaptability of the brain in the complete absence of visual input, this line of research also provides valuable insights into the experience-independent aspects of visual development. Persisting organisational principles in typically visual cortices in congenitally blind individuals (Bock et al., 2015; Trampel et al., 2011; van den Hurk et al., 2017) suggest that these principles have developed independently of visual experience. However, there is still much to be learned about the interplay between genetic factors and early sensory experience in shaping typical visual development.

One promising avenue for addressing this gap in knowledge is through the study of individuals who experienced a transient period of visual deprivation due to congenital cataracts and who underwent surgery later in life to restore their vision. This unique population presents a valuable opportunity to investigate the potential for recovery of the originally deprived visual system. By examining the behavioural changes and neural organisation in CC individuals, researchers can gain insights into the plasticity of the visual system and whether it is capable of returning to its typical developmental

trajectory. Moreover, this research elucidates the interplay between experience-independent factors and experience in shaping the development of the visual brain, thereby providing a more comprehensive understanding of the mechanisms underlying visual processing. If visual structure or function is found to be impaired in CC individuals, it suggests that early visual experience is essential for the typical development of these functions and that they cannot be fully recovered even after many years of seeing. On the other hand, if visual structure or function is found to be largely unaffected in CC individuals, it suggests that they do not rely as much on early visual experience. Overall, studying CC individuals can deepen our understanding of the role of early visual experience in shaping the brain and inform suitable and targeted interventions for individuals with visual impairments.

Chapter summary – The Effects of Early Visual Deprivation on the Structural Organisation

The aim of Study 1 (Chapter 2) was to investigate the impact of a transient period of early visual deprivation on the structural organisation of the early visual cortex. Several studies indicated that congenital visual deprivation leads to long-lasting structural changes as most recently reviewed by Paré et al. (2023). Previous studies on congenitally blind individuals have indicated higher cortical thickness and reduced surface area within the visual cortex compared to sighted individuals or those experiencing late-onset blindness (Andelin et al., 2019; Anurova et al., 2015; Bridge et al., 2009; Jiang et al., 2009; Park et al., 2009; Qin et al., 2013). Similarly, research on individuals with congenital cataracts has shown an increased cortical thickness and reduced surface area (Feng et al., 2021; Guerreiro, Erfort, et al., 2015; Hölig et al., 2022), highlighting the crucial role of early visual experience in the typical development of the visual brain. Furthermore, these findings imply that impaired brain structure cannot fully recover from congenital visual deprivation.

In order to delve deeper into the consequences of early visual deprivation, the first study conducted within the framework of this dissertation (Chapter 2) examined advanced ultra-high field MRI data with submillimetre resolution in a group of eight individuals who had experienced congenital cataracts. This investigation focused on analysing cortical thickness and surface area as distinct structural measures. It was hypothesised that CC individuals would exhibit increased cortical thickness and reduced surface area within the early visual cortex in comparison to normally sighted individuals. Furthermore, the study aimed to establish a methodological foundation for the direct comparison of results using two commonly employed analysis approaches for assessing structural differences: a vertex-wise analysis and a ROI analysis.

In contrast to the results from previous studies in CC individuals, the current investigation indicated differences in cortical thickness between the CC and SC individuals, only at an exploratory level, i.e. without applying corrections for multiple comparisons. Regarding surface area, the study revealed a significant group by hemisphere interaction whereby CC individuals exhibited significantly reduced surface area in the left hemisphere compared to the right hemisphere. In contrast, the SC individuals tended to exhibit the opposite pattern, with larger surface area in the left hemisphere. Interestingly, descriptively, the expected smaller surface area in CC individuals compared to the SC group was observed in the left hemisphere. However, unexpectedly, the CC group exhibited larger surface area than the SC group in the right hemisphere.

The Experience-(In)dependence of Structural Brain Development

The development of brain structure is influenced by both experience-dependent and experience-independent factors. While genetics have been reported to play a significant role in shaping basic brain organisation, early visual experience is essential for the typical development of the structural organisation of the visual brain. Structural changes following early visual deprivation are most consistently reported in the visual cortex and visual pathway and include reduced WM and GM volume, reduced surface area, and increased cortical thickness (reviewed by Paré et al., 2023).

While the results presented here are substantially in line with previous reports on changes in surface area reported here, they indicate only limited effects of early visual deprivation on cortical thickness. Although contradicting the majority of the evidence gathered in both congenitally blind and CC individuals, it is noteworthy that another recent study using ultra-high field MRI data with submillimetre resolution has also reported only limited effects on cortical thickness (Kupers et al., 2022). The contradicting reports may be attributed to methodological differences such as the increased spatial resolution in submillimetre MRI, as discussed extensively in Chapter 2. However, it is important to note that while reports of grey matter changes due to early visual deprivation within the occipital lobe are commonly referred to as 'amongst the most consistent' findings (Paré et al., 2023), the body of evidence is not unanimous. Increased cortical thickness in congenitally blind individuals has been reported in '11 out of 14 studies' (Paré et al., 2023) in at least one occipital lobe area, whereas only in '8 out of 14 studies' within the peri-calcarine area (Kupers et al., 2022), which amounts to '8 out of 15 studies' when including the results by Kupers et al. (2022).

As previously elaborated, cortical thickness and surface area follow distinct developmental trajectories over the life span (Gilmore et al., 2018; Wierenga et al., 2014). Specifically, imaging studies have revealed an initial increase of cortical thickness which peaks around the age of 1 – 2 years and continuously declines thereafter (Amlien et al., 2016; Walhovd et al., 2016; Wang et al., 2019), whereas surface area continues to expand well into early adolescence (Amlien et al., 2016) followed by a slow decline (Wierenga et al., 2014).

The developmental changes in cortical thickness have been proposed to be associated with alterations in the synaptic architecture of grey matter, characterised by an initial period of synaptogenesis, i.e. the formation of synapses, and followed by synaptic pruning, i.e. the elimination of synapses (Huttenlocher et al., 1982). Therefore, differences in cortical thickness observed after early visual deprivation have been suggested to indicate a disruption in synaptic pruning in the absence of typical visual experience (Jiang et al., 2009; Park et al., 2009), which is supported by findings in visually deprived monkeys indicating that synaptic pruning rather than synaptogenesis

depended on visual experience (Bourgeois et al., 2000). However, more recently, cortical thinning has been linked to age-related changes in myelination and, in this context, an increase in myelination alters the contrast of the apparent boundary between grey and white matter, shifting it outward and producing thinner GM (Natu et al., 2019; Vandekar et al., 2015; Whitaker et al., 2016).

Accordingly, in the context of structural changes resulting from early visual deprivation, it could be argued that the impact of visual deprivation is potentially more pronounced on WM than cortical thickness, which would align with the diminished effects on cortical thickness indicated by the findings presented here and in the study by Kupers et al. (2022). In fact, WM atrophy has been reported in congenitally blind individuals (Paré et al., 2023) and was also replicated by recent ultra-high field MRI results (Kupers et al., 2022).

On the basis of histological and MRI results, changes in surface area have been attributed to early visual deprivation affecting the expansion in surface area that occurs early in development (Andelin et al., 2019), rather than the decline observed later in development (Wierenga et al., 2014). Again, these changes could potentially be associated with impaired WM development, as cortical surface expansion during typical development has been associated with the myelination of WM fibers (Cafiero et al., 2019).

Overall, distinct developmental trajectories of cortical thickness and surface area, are possibly characterised by different extent of experience-dependence. With cortical thickness assumed to follow a more functionally driven maturation (Krongold et al., 2017; Valk et al., 2020), it appears highly plausible to expect stronger effects of visual deprivation than on surface area, which is attributed a stronger genetic influence (Jha et al., 2018). However, the results presented here, along with the findings by Kupers et al. (2022), may be interpreted as the opposite, thereby indicating reduced effects of early visual deprivation on cortical thickness compared to surface area.

Nevertheless, the potentially limited effects of early visual deprivation on cortical thickness do not imply a generally limited effect of visual deprivation on structural brain organisation. Interestingly, developmental studies with children suggested that changes in surface area, rather than cortical thickness, are the driving factor behind the observed reduction in GM volume in occipital regions (Lyall et al., 2015; Sowell et al., 2002), which might explain findings of reduced GM volume and surface area, even despite limited changes in cortical thickness.

In summary, this Study 1 of this dissertation explored the consequences of early visual deprivation on the structural organisation of the early visual cortex. Through analyses of submillimetre structural data, enduring yet distinct effects of early visual deprivation were observed. Thus, Study 1 provides evidence for a sensitive period of structural brain development in humans and in this context,

structural organisation cannot fully recover from a transient period of early visual deprivation. These findings enhance our understanding of how early visual deprivation influences the developmental trajectory of the visual cortex and emphasise the intricate interplay between visual experience and brain structure. Further investigation by future research is needed to ascertain whether these differentiated effects are attributable to methodological factors due to the relatively new application of ultra-high field MRI or indicative of substantial underlying differences.

Chapter summary – The Effects of Early Visual Deprivation on the Categorical Organisation

In addition to long-lasting structural impairments, early visual deprivation has also been reported to affect various visual functions (Röder & Kekunnaya, 2021). Study 2 (Chapter 3) investigated the effects of early visual deprivation specifically on visual categorical processing. Accumulating evidence indicates experience-independent developmental mechanisms involved in the development of category-selective processing (Kosakowski et al., 2022; van den Hurk et al., 2017). However, previous research has shown persistent impairments in face processing in CC individuals (Le Grand et al., 2004; Mondloch et al., 2013), highlighting the importance of early visual experience for the typical development of face processing. To date, very few studies focused on the neural basis of these face-selective impairments and the results indicated that these impairments were mainly driven by reduced face-selective responses in CC individuals (Grady et al., 2014; Röder et al., 2013). However, despite these valuable initial insights, important aspects of categorical processing were not investigated yet. To examine the multifaceted organisation of categorical processing, the Study 2 combined two methods that allowed detangling the role of experience-dependent and experience-independent development, focusing on the large-scale categorical representation and category-selectivity within distinct regions. Based on evidence in congenitally blind individuals (Mahon et al., 2009; van den Hurk et al., 2017), It was hypothesised that CC individuals would exhibit the same large-scale categorical organisation as normally sighted individuals. Additionally, it was hypothesised that within category-selective regions, CC individuals would exhibit category-selective responses, which would, however, be characterised by reduced responses to the respective preferred categories, similar to findings in face-selective regions (Grady et al., 2014).

In accordance with the hypothesis, CC individuals exhibited distinguishable categorical patterns for faces, bodies, objects, and scenes, and the same large-scale categorical organisation as SC individuals. Yet, notably, CC individuals exhibited less distinctive representation of the four categories, which was not just observable in contrast to normally sighted individuals, but already among the CC individuals. Moreover, face-selective impairments were confirmed in CC individuals. Significantly, however, the results demonstrated that these impairments were not just characterized by reduced face-selective response but also by increased responses to the non-preferred categories. And while the extent of impaired category-selectivity in CC individuals was unique for faces, other visual categories such as bodies, and scenes also indicated impaired processing to some extent.

The Experience-(In)dependence of Categorical Development

Visual processing in the human brain exhibits individual and highly specific developmental trajectories. Lower-level visual processing matures earlier compared to higher-level visual processing, which undergoes longer developmental periods (Casey et al., 2005; Sydnor et al., 2021). This difference in maturation suggests that the development of functional processing is influenced by both experience-dependent and experience-independent mechanisms. It has been proposed that early-maturing functions present a high maturational bias at birth and are therefore less experience-dependent in their development, thereby rendering them more resilient to atypical visual input (Levi, 2005; Röder & Kekunnaya, 2021). Conversely, slower-developing functions depend more strongly on experience, which also makes them more vulnerable to atypical visual experience (Röder & Kekunnaya, 2021). As a consequence, various structures and functions may be sensitive to visual deprivation at different stages of development.

Particularly, categorical processing undergoes a protracted period of development and maturation (Grill-Spector et al., 2008), which would, accordingly, imply a substantial dependence on early visual experience. In fact, previous studies have demonstrated this through the significant impairment of face-selective processing in CC individuals (Grady et al., 2014; Röder et al., 2013), underscoring the significance of early visual experience for the typical development of face processing. Notably, the findings presented in Study 2 (Chapter 3) clearly establish that impaired categorical processing is not exclusive to faces. In fact, all four examined categories - faces, bodies, objects, and scenes - exhibited impaired processing.

Nevertheless, it is crucial to emphasise that CC individuals exhibited distinguishable categorical representations and demonstrated category-selective responses within the respective regions. This finding suggests that the fundamental organisation of categorical processing develops despite the transient period of early visual deprivation. This conclusion aligns with accumulating evidence that supports the involvement of experience-independent mechanisms in the development of categorical processing supported by findings of persistent categorical organisation in congenital blind individuals (van den Hurk et al., 2017), early functional maturation in infants (Deen et al., 2017; Kosakowski et al., 2022), and strong genetic influences (Abbasi et al., 2020; Polk et al., 2007).

The results presented in this dissertation provide essential insights into the extent to which categorical processing is affected by early visual deprivation. While the existing literature extensively discusses face-specific impairments (Maurer, 2017; Röder & Kekunnaya, 2021), the results derived from Study 2 clearly emphasise the severity of impairment in contrast to other categories as specifically indicated by impaired category-selectivity within respective regions. Especially in light of

these new findings contrasting different categories, raise the question of why early visual deprivation has such profound effects on face processing. Consistent with the aforementioned relationship of increased experience-dependence following a prolonged developmental, differentiated effects of early visual deprivation may be attributed to the complex and diverse developmental trajectories of visual categorical processing (Grill-Spector et al., 2008) and specifically face-selective regions exhibit a prolonged developmental period extending beyond childhood (Golarai et al., 2007, 2010; Scherf et al., 2007). In contrast, object-selective and body-selective regions have been reported to reach an adult-like spatial extent and show mature responses during early childhood (Golarai et al., 2007; Peelen et al., 2009; Pelphrey et al., 2009; Scherf et al., 2007), whereas the evidence for developmental changes in scene-selective regions is less consistent (Chai et al., 2010; Golarai et al., 2007; Meissner et al., 2019).

The unique development of face processing is even more highlighted by the specific role of genes in determining the development face perception (Duchaine et al., 2007; Grueter et al., 2007; Wilmer et al., 2010; Zhu et al., 2010) and the distinguished structural changes, such as microstructural proliferation (Gomez et al., 2017) and an increase in myelination (Natu et al., 2019), the parallel these changes. While the recent evidence in the context of early maturation of categorical processing in infants potentially challenges the claimed sleeper effect of early visual deprivation on face processing, it only extents the encompassed developmental trajectory.

To conclude, the results presented in this dissertation provide important insights into the effects of early visual deprivation on visual categorical processing. More specifically, it was shown that the general categorical set-up does develop independently of early visual experience, although early visual experience is crucial for the maintenance and fine-tuning of categorical responses.

The Effects of Early Visual Deprivation

In line with findings in congenitally blind individuals (Qin et al., 2013), the broad picture emerging from the recent decades of research in CC individuals seems to be that the impact of early visual deprivation on brain structure is particularly prominent in early visual regions, while the effects on brain function appear to increase from lower-level to higher-level visual processing (Röder & Kekunnaya, 2021). This dissertation provides evidence supporting these observations, indicating that even with years of visual experiences after sight restoration, impaired structural and functional brain development due to visual deprivation from birth is not fully reversible. Recent evidence directly linked altered early visual brain structure to changes in early visual processing (Brockhaus et al., 2022; Feng et al., 2021). Yet, these changes in altered early visual organisation may have implications beyond the initial stages, potentially affecting higher-level visual processing due to factors such as the feedforward hierarchy of visual processing (Serre et al., 2007; Ungerleider & Mishkin, 1982), non-sequential development (Maurer & Lewis, 2018), or structural changes that limit functional recovery (Hölig et al., 2022) resulting in altered functional developmental trajectories impacting high-level visual processing (Vogelsang et al., 2018). While the precise mechanisms of neuroplasticity remain elusive, it is indisputable that the development of the brain's structure and function is intricately interconnected (Sydnor et al., 2021) and a multitude of experience-dependent and experience-independent neural mechanisms are involved in the maturation of the brain (Knudsen, 2004).

Clinical and Practical Implications

Dense bilateral cataracts are a leading cause of avoidable blindness (Gogate et al., 2010). Although cataracts are easily treatable in adulthood, their presence at birth leads to considerably poorer outcomes (Allen, 2020; Bronsard et al., 2018). As a result, the immediate treatment of children born with dense bilateral cataracts is crucial because any delay in addressing the condition exposes them to visual deprivation, resulting in long-lasting impairments and hindering typical development. There is strong evidence that even brief periods of bilateral visual deprivation have extensive implications (Lewis & Maurer, 2009; Röder & Kekunnaya, 2021) and long-lasting impairments have been observed in various aspects of visual processing, including low-level functions (Ellemberg et al., 1999; Maurer et al., 2007), social perception (Geldart et al., 2002; Le Grand et al., 2004), and high-level categorical processing (Grady et al., 2014; Röder et al., 2013). The findings of this dissertation also demonstrate the profound effects of early visual deprivation on the structural and functional organisation of the visual brain.

While various studies emphasize the importance of early treatment of congenital cataracts (Gogate et al., 2010), they also suggest that even late surgery yields a (subjectively) increased quality of life for individuals affected by cataracts (Kalia et al., 2017). Research on the impact of visual deprivation, as explored in the context of this dissertation, contributes to our understanding of the experience-dependence of the visual system and helps identifying the visual abilities that should be assessed, prioritized, and targeted for counselling, assessment, and rehabilitation purposes. By focusing on the visual abilities that have a significant impact on daily function and quality of life, this knowledge can help improve interventions and support individuals in maximizing their visual potential. Recent advances in retinal gene therapy offer new ways of reversing blindness, which renews the interest in the crucial role of plasticity after sight restoration (Mowad et al., 2020). While improvements in visual function are highly dependent on age, with treatment effectiveness significantly declining with advancing age (Fronius et al., 2014), the neurodevelopmental perspective gives reason for optimism, as several studies indicate a capacity to develop visual skills beyond the traditionally recognized sensitive period (reviewed by Castaldi et al., 2020; Levi, 2005). While neuroplasticity has been considered to be preserved for higher-level functions in adulthood, such as learning and memory (Fuchs & Flügge, 2014), the adult cortex also retains some potential for visual plasticity as demonstrated by the behavioural and neural changes associated with perceptual learning (Beyeler et al., 2017; Hills & Lewis, 2018; Watanabe & Sasaki, 2015). For example, adults with amblyopia can improve their perceptual performance through extensive practice using challenging visual tasks, which potentially results in improved visual acuity (Levi, 2005). To enhance future (re)habilitation services, it is crucial to delve deeper into the neuroscientific aspects associated with visual

development and plasticity. Despite promising advancements in sight restoration techniques such as the "bionic eye" (Beyeler et al., 2017), it is important to recognize that certain limitations persist as practice alone may not be sufficient to enhance certain visual abilities, even despite a prolonged period of normal vision (Šikl et al., 2013). This either emphasizes the importance of early treatment or the need for alternative ways of enhancing adults' plasticity. While the application of manipulating biochemical constraints is currently not feasible in a rehabilitation context, there is an increasing body of evidence suggesting that such interventions can enhance the plasticity of the human visual cortex (Castaldi et al., 2020).

Methodological Characteristics

Various methodological aspects shall be considered as they have contributed significantly in the course of this dissertational project. First and foremost, this dissertation was based on the opportunity to study a unique population of individuals who experienced a transient period of congenital visual deprivation due to dense bilateral cataract. Given the rareness of such individuals, the here presented results provide essential and valuable insights into the existential role of early visual experience on the development of the brain. An accumulating number of studies apply computational modelling and deep neural networks to exploit sensitive periods and the effects of visual deprivation (Thomas & Johnson, 2006; Vogelsang et al., 2018). In contrast to these modelling approaches, our study adopted a data-driven and empirical analysis to extract valuable information directly from the collected data and thus reflecting actual neural changes following early visual deprivation.

The acquisition of data from individuals with visual impairments to incorporate them as a second control group posed additional challenges. Despite the inherent difficulties in recruitment, it was imperative to include three to four VI individuals in both studies of this dissertation, as this inclusion played a crucial role in exploring the data and provided valuable context to the findings. Considering the inherent heterogeneity of visual impairments within the VI group and the therefor resulting variations in onset and severity, it may be prudent for future studies to explore the utilization of glasses that simulate specific visual impairments. Such an approach would enable researchers to investigate the immediate effects of visual impairments on visual processing without inducing underlying neural changes. By employing these simulated glasses, researchers could assess the impact of different types of visual impairments on visual processing, thereby expanding our understanding of the specific effects and implications. This would contribute to more targeted interventions and support for individuals with visual impairments.

One of the notable characteristics made this dissertation was the unique opportunity to acquire MRI data in Maastricht, which, despite presenting some recruitment challenges, provided an exceptional chance to obtain both 3T and 7T MRI data. The utilization of 7T scanning proved particularly advantageous for capturing submillimetre structural measurements, enabling a more comprehensive analysis of structural changes following early visual deprivation, as elaborated in Study 1 (Chapter 2). Although group analyses with this comparatively new analysis approach of 7T MRI data still require additional methodological considerations (Zaretskaya et al., 2018), the use of this advanced scanning technique has provided intriguing insights into the effects of early visual deprivation on the structural organisation of the visual brain (Kupers et al., 2022; Trampel et al., 2011).

Both studies of this dissertation incorporated a comparison of analysis methods either for examining effects of transient congenital visual deprivation on the structural organisation of the early visual cortex in Study 1 (Chapter 2) or on the functional organisation of visual categorical processing in Study 2 (Chapter 3). In both studies, this incorporation of analysis approaches provided an essential gain of insights into the effects of early visual deprivation and thus the understanding of the highly complex and divers development of the structural and functional organisation of the brain.

Summary and General Conclusion

Altered sensory experience during early development has the potential to induce plastic changes in the nervous system, influencing both the structural and functional organisation of the brain. By studying individuals who experienced a transient period of congenital visual deprivation and who regained sight only later in life, this dissertation aimed to explore the mechanisms of experience-dependent development. Specifically, the investigation sought to determine whether and to what extent neural circuits originally deprived of visual input could recover and resume their typical developmental trajectory following sight restoration. Within the context of two MRI studies, this dissertation addressed the question of how early visual deprivation affects the structural (Study 1) and functional organisation (Study 2) of the visual brain by investigating a unique group of individuals who had congenital dense bilateral cataracts for a minimum of six months and comparing them to normally sighted and visually impaired controls.

Study 1 (Chapter 2) analysed ultra-high field MRI structural data with a submillimetre resolution to examine the impact of early visual deprivation and compared cortical thickness and surface area, respectively, between groups to assess structural changes. The results of the analysis revealed enduring impairments in the structural organisation of the early visual cortex. Furthermore, the study unveiled potential differentiated effects of early visual deprivation on various structural measurements, which might emphasise the complex and heterogeneous development of the human brain. These findings provide valuable insights into the consequences of early visual deprivation and contribute to our understanding of brain development.

Study 2 (Chapter 3) investigated the impact of early visual deprivation on the functional processing of four visual categories, namely faces, bodies, objects, and scenes. The findings of Study 2 clearly demonstrate impaired categorical processing across all four categories following early visual deprivation indicated by less distinctive categorical representations and reduced category-selectivity in selective regions. Notably, the results highlight that the severity of impairments is particularly pronounced for faces. However, it is important to note that CC individuals did exhibited distinguishable categorical patterns and category-specific responses, suggesting that certain aspects of categorical processing persist after a transient period of early visual deprivation. In conclusion, the study suggests that the development of large-scale categorical organisation occurs independently of early visual experience, while emphasising its crucial role for the maintenance and fine-tuning of specialized categorical processing.

The findings of this study underscore that even after many years of visual experience following sight restoration, the structural organisation of the early visual cortex remains impaired. This suggests that

the early visual structure established during critical periods of development may not be fully reversible. The consequences of visual deprivation extend beyond structural abnormalities, as impaired categorical processing of neural representations was observed across multiple distinct category-selective regions. These findings indicate that the impairments resulting from early visual deprivation extend to both the structural and functional aspects of brain development. The disrupted organisation of the early visual cortex and impaired categorical processing underscore the intricate interplay between early visual experience and the development of neural circuitry. The implication of these results is that visual deprivation from birth can have long-lasting consequences for the structural and functional development of the brain. This highlights the importance of early intervention and visual stimulation to promote optimal brain development in individuals with congenital visual deprivation.

In conclusion, this dissertation provides compelling evidence that the effects of early visual deprivation on brain structure and function are enduring and not fully reversible after sight restoration, emphasising the critical role of early visual experience in shaping the developing brain. Through comprehensive analyses of the effects of early visual deprivation, this dissertation contributes to our understanding of how altered sensory experiences during sensitive periods can shape the structural and functional development of the human brain. It highlights the importance of early intervention and rehabilitation strategies to facilitate optimal recovery and mitigate the long-term consequences of early sensory deprivation.

References

Abbasi, N., Duncan, J., & Rajimehr, R. (2020). Genetic influence is linked to cortical morphology in category-selective areas of visual cortex. *Nature Communications*, *11*(1). https://doi.org/10.1038/s41467-020-14610-8

Abboud, S., Maidenbaum, S., Dehaene, S., & Amedi, A. (2015). A number-form area in the blind. *Nature Communications*, *6*(1), 6026. https://doi.org/10.1038/ncomms7026

Aguirre, G. K., Zarahn, E., & D'Esposito, M. (1998). An area within human ventral cortex sensitive to "building" stimuli: Evidence and implications. *Neuron*, *21*(2), 373–383. https://doi.org/10.1016/S0896-6273(00)80546-2

Albajara Sáenz, A., Villemonteix, T., & Massat, I. (2019). Structural and functional neuroimaging in attention-deficit/hyperactivity disorder. *Developmental Medicine and Child Neurology*, *61*(4), 399–405. https://doi.org/10.1111/dmcn.14050

Allen, L. E. (2020). Childhood cataract. In *Paediatrics and Child Health (United Kingdom)* (Vol. 30, Issue 1, pp. 28–32). Churchill Livingstone. https://doi.org/10.1016/j.paed.2019.10.005

Amedi, A., Stern, W. M., Camprodon, J. A., Bermpohl, F., Merabet, L. B., Rotman, S., Hemond, C., Meijer, P., & Pascual-Leone, A. (2007). Shape conveyed by visual-to-auditory sensory substitution activates the lateral occipital complex. *Nature Neuroscience*, *10*(6), 687–689. https://doi.org/10.1038/nn1912

Amlien, I. K., Fjell, A. M., Tamnes, C. K., Grydeland, H., Krogsrud, S. K., Chaplin, T. A., Rosa, M. G. P., & Walhovd, K. B. (2016). Organizing principles of human cortical development - thickness and area from 4 to 30 Years: Insights from comparative primate neuroanatomy. *Cerebral Cortex*, *26*(1), 257–267. https://doi.org/10.1093/cercor/bhu214

Andelin, A. K., Olavarria, J. F., Fine, I., Taber, E. N., Schwartz, D., Kroenke, C. D., & Stevens, A. A. (2019). The effect of onset age of visual deprivation on visual cortex surface area across-species. *Cerebral Cortex*, *29*(10), 4321–4333. https://doi.org/10.1093/cercor/bhy315

Andres, E., McKyton, A., Ben-Zion, I., & Zohary, E. (2017). Size constancy following long-term visual deprivation. In *Current Biology* (Vol. 27, Issue 14, pp. R696–R697). Cell Press. https://doi.org/10.1016/j.cub.2017.05.071

Anurova, I., Renier, L. A., De Volder, A. G., Carlson, S., & Rauschecker, J. P. (2015). Relationship Between Cortical Thickness and Functional Activation in the Early Blind. *Cerebral Cortex*, *25*(8), 2035–2048. https://doi.org/10.1093/cercor/bhu009

Arcaro, M. J., & Livingstone, M. S. (2017). A hierarchical, retinotopic proto-organization of the primate visual system at birth. *ELife*, *6*. https://doi.org/10.7554/eLife.26196

Arcaro, M. J., Schade, P. F., Vincent, J. L., Ponce, C. R., & Livingstone, M. S. (2017). Seeing faces is necessary for face-domain formation. *Nature Neuroscience*, *20*(10), 1404–1412. https://doi.org/10.1038/nn.4635

Ashburner, J. T., & Friston, K. J. (2005). Unified segmentation. *NeuroImage*, *26*(3), 839–851. https://doi.org/10.1016/j.neuroimage.2005.02.018

Aylward, E. H., Park, J. E., Field, K. M., Parsons, A. C., Richards, T. L., Cramer, S. C., & Meltzoff, A. N. (2005). Brain activation during face perception: Evidence of a developmental change. *Journal of Cognitive Neuroscience*, *17*(2), 308–319. https://doi.org/10.1162/0898929053124884

Balchandani, P., & Naidich, T. P. (2015). Ultra-High-Field MR Neuroimaging. *American Journal of Neuroradiology*, *36*(7), 1204–1215. https://doi.org/10.3174/AJNR.A4180

Ball, G., Seidlitz, J., O'Muircheartaigh, J., Dimitrova, R., Fenchel, D., Makropoulos, A., Christiaens, D., Schuh, A., Passerat-Palmbach, J., Hutter, J., Cordero-Grande, L., Hughes, E., Price, A., Hajnal, J. V., Rueckert, D., Robinson, E. C., & Edwards, A. D. (2020). Cortical morphology at birth reflects spatiotemporal patterns of gene expression in the fetal human brain. *PLoS Biology*, *18*(11), e3000976. https://doi.org/10.1371/journal.pbio.3000976

Bank, S., Rhodes, G., Read, A., & Jeffery, L. (2015). Face and body recognition show similar improvement during childhood. *Journal of Experimental Child Psychology*, *137*, 1–11. https://doi.org/10.1016/j.jecp.2015.02.011

Bates, D., Mächler, M., Bolker, B., & Walker, S. (2015). Fitting Linear Mixed-Effects Models Using {lme4}. *Journal of Statistical Software*, *67*(1), 1–48. https://doi.org/10.18637/jss.v067.i01

Bavelier, D., & Neville, H. J. (2002). Cross-modal plasticity: where and how? : Abstract : Nature Reviews Neuroscience. *Nature Reviews. Neuroscience*, *3*(6), 443–452. https://doi.org/10.1038/nrn848

Bedny, M., Pascual-Leone, A., Dodell-Feder, D., Fedorenko, E., & Saxe, R. R. (2011). Language processing in the occipital cortex of congenitally blind adults. *Proceedings of the National Academy of Sciences of the United States of America*, *108*(11), 4429–4434. https://doi.org/10.1073/pnas.1014818108

Ben-Shachar, M. S., Lüdecke, D., & Makowski, D. (2020). {e}ffectsize: Estimation of Effect Size Indices and Standardized Parameters. *Journal of Open Source Software*, *5*(56), 2815. https://doi.org/10.21105/joss.02815

Berlucchi, G., & Buchtel, H. A. (2009). Neuronal plasticity: Historical roots and evolution of meaning. *Experimental Brain Research*, *192*(3), 307–319. https://doi.org/10.1007/s00221-008-1611-6

Beyeler, M., Rokem, A., Boynton, G. M., & Fine, I. (2017). Learning to see again: biological constraints on cortical plasticity and the implications for sight restoration technologies. *Journal of Neural Engineering*, *14*(5), 051003. https://doi.org/10.1088/1741-2552/AA795E

Bock, A. S., Binda, P., Benson, N. C., Bridge, H., Watkins, K. E., & Fine, I. (2015). Resting-state retinotopic organization in the absence of retinal input and visual experience. *Journal of Neuroscience*, *35*(36), 12366–12382. https://doi.org/10.1523/JNEUROSCI.4715-14.2015

Bottari, D., Kekunnaya, R., Hense, M., Troje, N. F., Sourav, S., & Röder, B. (2018). Motion processing after sight restoration: No competition between visual recovery and auditory compensation. *NeuroImage*, *167*, 284–296. https://doi.org/10.1016/j.neuroimage.2017.11.050

Bottari, D., Troje, N. F., Ley, P., Hense, M., Kekunnaya, R., & Röder, B. (2015). The neural development of the biological motion processing system does not rely on early visual input. *Cortex*, *71*, 359–367. https://doi.org/10.1016/j.cortex.2015.07.029

Bottari, D., Troje, N. F., Ley, P., Hense, M., Kekunnaya, R., & Röder, B. (2016). Sight restoration after congenital blindness does not reinstate alpha oscillatory activity in humans. *Scientific Reports*, *6*(1), 1–10. https://doi.org/10.1038/srep24683

Bourgeois, J.-P., Goldman-Rakic, P. S., & Rakic, P. (2000). Formation, elimination and stabilization of synapses in the primate cerebral cortex. *The New Cognitive Neurosciences*, *2*, 45–53.

Bourgeois, J.-P., & Rakic, P. (1996). Synaptogenesis in the occipital cortex of macaque monkey devoid of retinal input from early embryonic stages. *European Journal of Neuroscience*, *8*(5), 942–950. https://doi.org/10.1111/j.1460-9568.1996.tb01581.x

Braddick, O., & Atkinson, J. (2011). Development of human visual function. In *Vision Research* (Vol. 51, Issue 13, pp. 1588–1609). Pergamon. https://doi.org/10.1016/j.visres.2011.02.018

Brants, M., Bulthé, J., Daniels, N., Wagemans, J., & Op de Beeck, H. P. (2016). How learning might strengthen existing visual object representations in human object-selective cortex. *NeuroImage*, *127*, 74–85. https://doi.org/10.1016/j.neuroimage.2015.11.063

Bridge, H., Cowey, A., Ragge, N., & Watkins, K. (2009). Imaging studies in congenital anophthalmia reveal preservation of brain architecture in "visual" cortex. *Brain*, *132*(12), 3467–3480. https://doi.org/10.1093/brain/awp279

Brockhaus, C., Zhan, M., Linke, M., Hölig, C., Kekunnaya, R., van den Hoof, R., Goebel, R., & Röder, B. (2022). The effect of a temporary congenital blindness on the refinement of adult retinotopic organization of early visual regions [Conference presentation]. *Society for Neuroscience*. https://www.sfn.org/meetings/neuroscience-2022/

Bronsard, A., Geneau, R., Duke, R., Kandeke, L., Nsibirwa, S. G., Ulaikere, M., & Courtright, P. (2018). Cataract in children in sub-Saharan Africa: an overview. *Expert Review of Ophthalmology*, *13*(6), 343–350. https://doi.org/10.1080/17469899.2018.1555037

Buckner, R. L., Head, D., Parker, J., Fotenos, A. F., Marcus, D., Morris, J., & Snyder, A. Z. (2004). A unified approach for morphometric and functional data analysis in young, old, and demented adults using automated atlas-based head size normalization: Reliability and validation against manual measurement of total intracranial volume. *NeuroImage*, *23*(2), 724–738. https://doi.org/10.1016/j.neuroimage.2004.06.018

Buiatti, M., Di Giorgio, E., Piazza, M., Polloni, C., Menna, G., Taddei, F., Baldo, E., & Vallortigara, G. (2019). Cortical route for facelike pattern processing in human newborns. *Proceedings of the National Academy of Sciences of the United States of America*, *116*(10), 4625–4630. https://doi.org/10.1073/pnas.1812419116

Burge, W. K., Griffis, J. C., Nenert, R., Elkhetali, A., Decarlo, D. K., Ver Hoef, L. W., Ross, L. A., & Visscher, K. M. (2016). Cortical thickness in human V1 associated with central vision loss. *Scientific Reports*, *6*. https://doi.org/10.1038/srep23268

Butz, M., Wörgötter, F., & van Ooyen, A. (2009). Activity-dependent structural plasticity. *Brain Research Reviews*, *60*(2), 287–305. https://doi.org/10.1016/j.brainresrev.2008.12.023

Cafiero, R., Brauer, J., Anwander, A., & Friederici, A. D. (2019). The concurrence of cortical surface area expansion and white matter myelination in human brain development. *Cerebral Cortex*, *29*(2), 827–837. https://doi.org/10.1093/cercor/bhy277

Cantlon, J. F., Brannon, E. M., Carter, E. J., & Pelphrey, K. A. (2006). Functional imaging of numerical processing in adults and 4-y-old children. *PLoS Biology*, *4*(5), 844–854. https://doi.org/10.1371/journal.pbio.0040125

Cantlon, J. F., Pinel, P., Dehaene, S., & Pelphrey, K. A. (2011). Cortical representations of symbols, objects, and faces are pruned back during early childhood. *Cerebral Cortex*, *21*(1), 191–199. https://doi.org/10.1093/cercor/bhq078

Carey, S., Diamond, R., & Woods, B. (1980). Development of face recognition: A maturational component? *Developmental Psychology*, *16*(4), 257–269. https://doi.org/10.1037/0012-1649.16.4.257

Casey, B. J., Tottenham, N., Liston, C., & Durston, S. (2005). Imaging the developing brain: What have we learned about cognitive development? *Trends in Cognitive Sciences*, *9*(3), 104–110. https://doi.org/10.1016/j.tics.2005.01.011

Castaldi, E., Lunghi, C., & Morrone, M. C. (2020). Neuroplasticity in adult human visual cortex. *Neuroscience and Biobehavioral Reviews*, *112*, 542–552. https://doi.org/10.1016/j.neubiorev.2020.02.028

Chai, X. J., Ofen, N., Jacobs, L. F., & Gabrieli, J. D. E. (2010). Scene complexity: Influence on perception, memory, and evelopment in the medial temporal lobe. *Frontiers in Human Neuroscience*, *4*, 21. https://doi.org/10.3389/fnhum.2010.00021

Chance, J. E., Turner, A. L., & Goldstein, A. G. (1982). Development of differential recognition for own- and other-race faces. *Journal of Psychology: Interdisciplinary and Applied*, *112*(1), 29–37. https://doi.org/10.1080/00223980.1982.9923531

Chang, C.-C., & Lin, C.-J. (2011). LIBSVM: A library for support vector machines. *ACM Transactions on Intelligent Systems and Technology*, *2*(3), 27:1--27:27.

Chen, C. H., Fiecas, M., Gutiérrez, E. D., Panizzon, M. S., Eyler, L. T., Vuoksimaa, E., Thompson, W. K., Fennema-Notestine, C., Hagler, D. J., Jernigan, T. L., Neale, M. C., Franz, C. E., Lyons, M. J., Fischl, B., Tsuang, M. T., Dale, A. M., & Kremen, W. S. (2013). Genetic topography of brain morphology. *Proceedings of the National Academy of Sciences of the United States of America*, *110*(42), 17089–17094. https://doi.org/10.1073/pnas.1308091110

Chen, C. H., Gutierrez, E. D., Thompson, W., Panizzon, M. S., Jernigan, T. L., Eyler, L. T., Fennema-Notestine, C., Jak, A. J., Neale, M. C., Franz, C. E., Lyons, M. J., Grant, M. D., Fischl, B., Seidman, L. J., Tsuang, M. T., Kremen, W. S., & Dale, A. M. (2012). Hierarchical genetic organization of human cortical surface area. *Science*, *335*(6076), 1634–1636. https://doi.org/10.1126/science.1215330

Chen, C. H., Panizzon, M. S., Eyler, L. T., Jernigan, T. L., Thompson, W., Fennema-Notestine, C., Jak, A. J., Neale, M. C., Franz, C. E., Hamza, S., Lyons, M. J., Grant, M. D., Fischl, B., Seidman, L. J., Tsuang, M. T., Kremen, W. S., & Dale, A. M. (2011). Genetic Influences on Cortical Regionalization in the Human Brain. *Neuron*, *72*(4), 537–544. https://doi.org/10.1016/j.neuron.2011.08.021

Chen, C. H., Peng, Q., Schork, A. J., Lo, M. T., Fan, C. C., Wang, Y., Desikan, R. S., Bettella, F., Hagler, D. J., Westlye, L. T., Kremen, W. S., Jernigan, T. L., Le Hellard, S., Steen, V. M., Espeseth, T., Huentelman, M., Håberg, A. K., Agartz, I., Djurovic, S., … Hsiao, J. (2015). Large-scale genomics unveil polygenic architecture of human cortical surface area. *Nature Communications*, *6*(1), 1–7. https://doi.org/10.1038/ncomms8549

Chen, G., Saad, Z. S., Britton, J. C., Pine, D. S., & Cox, R. W. (2013). Linear mixed-effects modeling approach to FMRI group analysis. *NeuroImage*, *73*, 176–190. https://doi.org/10.1016/j.neuroimage.2013.01.047

Chen, W., Lan, L., Xiao, W., Li, J., Liu, J., Zhao, F., Wang, C. D., Zheng, Y., Chen, W., & Cai, Y. (2021). Reduced Functional Connectivity in Children With Congenital Cataracts Using Resting-State Electroencephalography Measurement. *Frontiers in Neuroscience*, *15*, 404. https://doi.org/10.3389/fnins.2021.657865

Cohen, M. A., Dilks, D. D., Koldewyn, K., Weigelt, S., Feather, J., Kell, A. J., Keil, B., Fischl, B., Zöllei, L., Wald, L. L., Saxe, R. R., & Kanwisher, N. (2019). Representational similarity precedes category selectivity in the developing ventral visual pathway. *NeuroImage*, *197*, 565–574. https://doi.org/10.1016/j.neuroimage.2019.05.010

Cohen, M. A., Konkle, T., Rhee, J. Y., Nakayama, K., & Alvarez, G. A. (2014). Processing multiple visual objects is limited by overlap in neural channels. *Proceedings of the National Academy of Sciences of the United States of America*, *111*(24), 8955–8960. https://doi.org/10.1073/pnas.1317860111

Collignon, O., Dormal, G., de Heering, A., Lepore, F., Lewis, T. L., & Maurer, D. (2015). Long-Lasting Crossmodal Cortical Reorganization Triggered by Brief Postnatal Visual Deprivation. *Current Biology*, *25*(18), 2379–2383. https://doi.org/10.1016/j.cub.2015.07.036

Collignon, O., Vandewalle, G., Voss, P., Albouy, G., Charbonneau, G., Lassonde, M., & Lepore, F. (2011). Functional specialization for auditory–spatial processing in the occipital cortex of congenitally blind humans. *Proceedings of the National Academy of Sciences*, *108*(11), 4435–4440.

Colom, R., Jung, R. E., & Haier, R. J. (2006). Distributed brain sites for the g-factor of intelligence. *NeuroImage*, *31*(3), 1359–1365. https://doi.org/10.1016/J.NEUROIMAGE.2006.01.006

Costandi, M. (2016). *Neuroplasticity*. The MIT Press. https://doi.org/10.7551/mitpress/10499.001.0001

Courchesne, E., Pierce, K., Schumann, C. M., Redcay, E., Buckwalter, J. A., Kennedy, D. P., & Morgan, J. (2007). Mapping early brain development in autism. In *Neuron* (Vol. 56, Issue 2, pp. 399–413). Cell Press. https://doi.org/10.1016/j.neuron.2007.10.016

Cox, D. D., & Savoy, R. L. (2003). Functional magnetic resonance imaging (fMRI) "brain reading": Detecting and classifying distributed patterns of fMRI activity in human visual cortex. *NeuroImage*, *19*(2), 261–270. https://doi.org/10.1016/S1053-8119(03)00049-1

Cuevas, E., Parmar, P., & Sowden, J. C. (2019). Restoring Vision Using Stem Cells and Transplantation. In *Advances in Experimental Medicine and Biology* (Vol. 1185, pp. 563–567). Springer. https://doi.org/10.1007/978-3-030-27378-1_92

Çukur, T., Huth, A. G., Nishimoto, S., & Gallant, J. L. (2016). Functional subdomains within scene-selective cortex: Parahippocampal place area, retrosplenial complex, and occipital place area. *Journal of Neuroscience*, *36*(40), 10257–10273. https://doi.org/10.1523/JNEUROSCI.4033-14.2016

Daw, N. W. (2009). The foundations of development and deprivation in the visual system. *Journal of Physiology*, *587*(12), 2769–2773. https://doi.org/10.1113/jphysiol.2009.170001

Day, M. C. (1975). Developmental trends in visual scanning. *Advances in Child Development and Behavior*, *10*(C), 153–193. https://doi.org/10.1016/S0065-2407(08)60010-5

De Ciantis, A., Barba, C., Tassi, L., Cosottini, M., Tosetti, M., Costagli, M., Bramerio, M., Bartolini, E., Biagi, L., Cossu, M., Pelliccia, V., Symms, M. R., & Guerrini, R. (2016). 7T MRI in focal epilepsy with unrevealing conventional field strength imaging. *Epilepsia*, *57*(3), 445–454. https://doi.org/10.1111/epi.13313

de Haan, M., & Nelson, C. A. (1999). Brain activity differentiates face and object processing in 6-month-old infants. *Developmental Psychology*, *35*(4), 1113–1121. https://doi.org/10.1037/0012-1649.35.4.1113

de Heering, A., & Rossion, B. (2015). Rapid categorization of natural face images in the infant right hemisphere. *ELife*, *4*(JUNE), 1–14. https://doi.org/10.7554/eLife.06564

de Hollander, G., van der Zwaag, W., Qian, C., Zhang, P., & Knapen, T. (2021). Ultra-high field fMRI reveals origins of feedforward and feedback activity within laminae of human ocular dominance columns. *NeuroImage*, *228*, 117683. https://doi.org/10.1016/j.neuroimage.2020.117683

De Martino, F., Yacoub, E., Kemper, V., Moerel, M., Uludag, K., De Weerd, P., Ugurbil, K., Goebel, R., & Formisano, E. (2018). The impact of ultra-high field MRI on cognitive and computational neuroimaging. *NeuroImage*, *168*, 366–382. https://doi.org/10.1016/j.neuroimage.2017.03.060

Deen, B., Richardson, H., Dilks, D. D., Takahashi, A., Keil, B., Wald, L. L., Kanwisher, N., & Saxe, R. R. (2017). Organization of high-level visual cortex in human infants. *Nature Communications*, *8*, 13995. https://doi.org/10.1038/ncomms13995

DiCarlo, J. J., Zoccolan, D., & Rust, N. C. (2012). How does the brain solve visual object recognition? In *Neuron* (Vol. 73, Issue 3, pp. 415–434). Cell Press. https://doi.org/10.1016/j.neuron.2012.01.010

Dormal, G., Lepore, F., Harissi-Dagher, M., Albouy, G., Bertone, A., Rossion, B., & Collignon, O. (2015). Tracking the evolution of crossmodal plasticity and visual functions before and after sight restoration. *Journal of Neurophysiology*, *113*(6), 1727–1742. https://doi.org/10.1152/jn.00420.2014

Downing, P. E., Jiang, Y., Shuman, M., & Kanwisher, N. (2001). A cortical area selective for visual processing of the human body. *Science*, *293*(5539), 2470–2473. https://doi.org/10.1126/science.1063414

Dräger, U. C. (1975). Receptive fields of single cells and topography in mouse visual cortex. *Journal of Comparative Neurology*, *160*(3), 269–289. https://doi.org/10.1002/CNE.901600302

Duchaine, B., Germine, L., & Nakayama, K. (2007). Family resemblance: Ten family members with prosopagnosia and within-class object agnosia. *Cognitive Neuropsychology*, *24*(4), 419–430. https://doi.org/10.1080/02643290701380491

Dumoulin, S. O., Fracasso, A., van der Zwaag, W., Siero, J. C. W., & Petridou, N. (2018). Ultra-high field MRI: Advancing systems neuroscience towards mesoscopic human brain function. *NeuroImage*, *168*, 345–357. https://doi.org/10.1016/j.neuroimage.2017.01.028

Dumoulin, S. O., & Knapen, T. (2018). How visual cortical organization is altered by ophthalmologic and neurologic disorders. *Annual Review of Vision Science*, *4*, 357–379. https://doi.org/10.1146/annurev-vision-091517-033948

Eger, E., Ashburner, J. T., Haynes, J. D., Dolan, R. J., & Rees, G. (2008). fMRI activity patterns in human LOC carry information about object exemplars within category. *Journal of Cognitive Neuroscience*, *20*(2), 356–370. https://doi.org/10.1162/jocn.2008.20019

Eimer, M. (2011). The Face-Sensitivity of the N170 Component. In *Frontiers in Human Neuroscience* (Vol. 5, p. 119). https://www.frontiersin.org/article/10.3389/fnhum.2011.00119

Ellemberg, D., Lewis, T. L., Maurer, D., Hong Lui, C., & Brent, H. P. (1999). Spatial and temporal vision in patients treated for bilateral congenital cataracts. *Vision Research*, *39*(20), 3480–3489. https://doi.org/10.1016/S0042-6989(99)00078-4

Ellis, C. T., Yates, T. S., Skalaban, L. J., Bejjanki, V. R., Arcaro, M. J., & Turk-Browne, N. B. (2021). Retinotopic organization of visual cortex in human infants. *Neuron*, *109*(16), 2616-2626.e6. https://doi.org/10.1016/j.neuron.2021.06.004

Epstein, R., & Kanwisher, N. (1998). A cortical representation the local visual environment. *Nature*, *392*(6676), 598–601. https://doi.org/10.1038/33402

Espinosa, J. S., & Stryker, M. P. (2012). Development and Plasticity of the Primary Visual Cortex. *Neuron*, *75*(2), 230–249. https://doi.org/10.1016/j.neuron.2012.06.009

Fagiolini, M., Jensen, C. L., & Champagne, F. A. (2009). Epigenetic influences on brain development and plasticity. *Current Opinion in Neurobiology*, *19*(2), 207–212. https://doi.org/10.1016/j.conb.2009.05.009

Fairhall, S. L., Porter, K. B., Bellucci, C., Mazzetti, M., Cipolli, C., & Gobbini, M. I. (2017). Plastic reorganization of neural systems for perception of others in the congenitally blind. *NeuroImage*, *158*, 126–135. https://doi.org/10.1016/j.neuroimage.2017.06.057

Feng, Y., Collignon, O., Maurer, D., Yao, K., & Gao, X. (2021). Brief Postnatal Visual Deprivation Triggers Long-Lasting Interactive Structural and Functional Reorganization of the Human

Cortex. *Frontiers in Medicine*, *8*, 752021. https://doi.org/10.3389/fmed.2021.752021

Ferri, S., Kolster, H., Jastorff, J., & Orban, G. A. (2013). The overlap of the EBA and the MT/V5 cluster. *NeuroImage*, *66*, 412–425. https://doi.org/10.1016/j.neuroimage.2012.10.060

Fischl, B., & Dale, A. M. (2000). Measuring the thickness of the human cerebral cortex from magnetic resonance images. *Proceedings of the National Academy of Sciences of the United States of America*, *97*(20), 11050–11055.

Fischl, B., Liu, A. K., & Dale, A. M. (2001). Automated manifold surgery: constructing geometrically accurate and topologically correct models of the human cerebral cortex. *{IEEE} Medical Imaging*, *20*(1), 70–80.

Fischl, B., Salat, D. H., Busa, E., Albert, M. S., Dieterich, M., Haselgrove, C., van der Kouwe, A. J. W., Killiany, R. J., Kennedy, D., Klaveness, S., Montillo, A., Makris, N., Rosen, B. R., & Dale, A. M. (2002). Whole brain segmentation: automated labeling of neuroanatomical structures in the human brain. *Neuron*, *33*(3), 341–355. https://doi.org/10.1016/S0896-6273(02)00569-X

Fischl, B., Salat, D. H., van der Kouwe, A. J. W., Makris, N., Ségonne, F., Quinn, B. T., & Dale, A. M. (2004). Sequence-independent segmentation of magnetic resonance images. *NeuroImage*, *23*(Supplement 1), S69–S84. https://doi.org/DOI: 10.1016/j.neuroimage.2004.07.016

Fischl, B., Sereno, M. I., & Dale, A. M. (1999). Cortical Surface-Based Analysis: II: Inflation, Flattening, and a Surface-Based Coordinate System. *NeuroImage*, *9*(2), 195–207. https://doi.org/10.1006/nimg.1998.0396

Fischl, B., Sereno, M. I., Tootell, R. B. H., & Dale, A. M. (1999). High-resolution intersubject averaging and a coordinate system for the cortical surface. *Human Brain Mapping*, *8*(4), 272–284. https://doi.org/10.1002/(SICI)1097-0193(1999)8:4<272::AID-HBM10>3.0.CO;2-4

Fish, J. L., Dehay, C., Kennedy, H., & Huttner, W. B. (2008). Making bigger brains - The evolution of neural-progenitor-cell division. *Journal of Cell Science*, *121*(17), 2783–2793. https://doi.org/10.1242/jcs.023465

Fjell, A. M., Grydeland, H., Krogsrud, S. K., Amlien, I. K., Rohani, D. A., Ferschmann, L., Storsve, A. B., Tamnes, C. K., Sala-Llonch, R., Due-Tønnessen, P., Bjørnerud, A., Sølsnes, A. E., Håberg, A. K., Skranes, J., Bartsch, H., Chen, C. H., Thompson, W. K., Panizzon, M. S., Kremen, W. S., … Walhovd, K. B. (2015). Development and aging of cortical thickness correspond to genetic organization patterns. *Proceedings of the National Academy of Sciences of the United States of America*, *112*(50), 15462–15467. https://doi.org/10.1073/pnas.1508831112

Friston, K. J., Ashburner, J. T., Kiebel, S. J., Nichols, T. E., & Penny, W. D. (2007). Statistical Parametric Mapping: The Analysis of Functional Brain Images. In *Statistical Parametric Mapping The Analysis of Functional Brain Images* (Vol. 8). Elsevier/Academic Press. http://books.elsevier.com/neuro/?isbn=9780123725608&srccode=89660

Fronius, M., Cirina, L., Ackermann, H., Kohnen, T., & Diehl, C. M. (2014). Efficiency of electronically monitored amblyopia treatment between 5 and 16 years of age: New insight into declining susceptibility of the visual system. *Vision Research*, *103*(1), 11–19. https://doi.org/10.1016/j.visres.2014.07.018

Fuchs, E., & Flügge, G. (2014). Adult neuroplasticity: More than 40 years of research. *Neural Plasticity*, *2014*. https://doi.org/10.1155/2014/541870

Gandhi, T. K., Ganesh, S., & Sinha, P. (2014). Improvement in spatial imagery following sight onset late in childhood. *Psychological Science*, *25*(3), 693–701. https://doi.org/10.1177/0956797613513906

Gandhi, T. K., Kalia, A., Ganesh, S., & Sinha, P. (2015). Immediate susceptibility to visual illusions after sight onset. In *Current Biology* (Vol. 25, Issue 9, pp. R358–R359). Cell Press. https://doi.org/10.1016/j.cub.2015.03.005

Gandhi, T. K., Singh, A. K., Swami, P., Ganesh, S., & Sinha, P. (2017). Emergence of categorical face perception after extended early-onset blindness. *Proceedings of the National Academy of Sciences of the United States of America*, *114*(23), 6139–6143. https://doi.org/10.1073/pnas.1616050114

Gao, C., Conte, S., Richards, J. E., Xie, W., & Hanayik, T. (2019). The neural sources of N170: Understanding timing of activation in face-selective areas. *Psychophysiology*, *56*(6), e13336. https://doi.org/10.1111/psyp.13336

Gathers, A. D., Bhatt, R. S., Corbly, C. R., Farley, A. B., & Joseph, J. E. (2004). Developmental shifts in cortical loci for face and object recognition. *NeuroReport*, *15*(10), 1549–1553. https://doi.org/10.1097/01.wnr.0000133299.84901.86

Gauthier, I., & Nelson, C. A. (2001). The development of face expertise. In *Current Opinion in Neurobiology* (Vol. 11, Issue 2, pp. 219–224). Elsevier Current Trends. https://doi.org/10.1016/S0959-4388(00)00200-2

Gauthier, I., Tarr, M. J., Moylan, J., Skudlarski, P., Gore, J. C., & Anderson, A. W. (2000). The fusiform "face area" is part of a network that processes faces at the individual level. *Journal of Cognitive Neuroscience*, *12*(3), 495–504. https://doi.org/10.1162/089892900562165

Geldart, S., Mondloch, C. J., Maurer, D., de Schonen, S., & Brent, H. P. (2002). The effect of early visual deprivation on the development of face processing. *Developmental Science*, *5*(4), 490–501. https://doi.org/10.1111/1467-7687.00242

Geng, X., Li, G., Lu, Z., Gao, W., Wang, L., Shen, D., Zhu, H., & Gilmore, J. H. (2017). Structural and maturational covariance in early childhood brain development. *Cerebral Cortex*, *27*(3), 1795–1807. https://doi.org/10.1093/cercor/bhw022

Genon, S., Eickhoff, S. B., & Kharabian, S. (2022). Linking interindividual variability in brain structure to behaviour. *Nature Reviews Neuroscience*, *23*(5), 307–318. https://doi.org/10.1038/s41583-022-00584-7

Germine, L. T., Duchaine, B., & Nakayama, K. (2011). Where cognitive development and aging meet: Face learning ability peaks after age 30. *Cognition*, *118*(2), 201–210. https://doi.org/10.1016/j.cognition.2010.11.002

Giedd, J. N. (2004). Structural Magnetic Resonance Imaging of the Adolescent Brain. *Annals of the New York Academy of Sciences*, *1021*(1), 77–85. https://doi.org/10.1196/ANNALS.1308.009

Giedd, J. N., & Rapoport, J. L. (2010). Structural MRI of Pediatric Brain Development: What Have We Learned and Where Are We Going? *Neuron*, *67*(5), 728–734. https://doi.org/10.1016/j.neuron.2010.08.040

Gilmore, J. H., Knickmeyer, R. C., & Gao, W. (2018). Imaging structural and functional brain development in early childhood. In *Nature Reviews Neuroscience* (Vol. 19, Issue 3, pp. 123–137). Nature Publishing Group. https://doi.org/10.1038/nrn.2018.1

Girault, J. B., Cornea, E., Goldman, B. D., Jha, S. C., Murphy, V. A., Li, G., Wang, L., Shen, D., Knickmeyer, R. C., Styner, M., & Gilmore, J. H. (2020). Cortical Structure and Cognition in Infants and Toddlers. *Cerebral Cortex*, *30*(2), 786–800. https://doi.org/10.1093/CERCOR/BHZ126

Goebel, R., Esposito, F., & Formisano, E. (2006). Analysis of Functional Image Analysis Contest (FIAC)

data with BrainVoyager QX: From single-subject to cortically aligned group General Linear Model analysis and self-organizing group Independent Component Analysis. *Human Brain Mapping*, *27*(5), 392–401. https://doi.org/10.1002/hbm.20249

Goebel, R., Muckli, L., & Kim, D.-S. (2012). Visual System. In *The Human Nervous System* (pp. 1301–1327). Elsevier. https://doi.org/10.1016/B978-0-12-374236-0.10037-9

Gogate, P., Khandekar, R., Shrishrimal, M., Dole, K., Taras, S., Kulkarni, S., Ranade, S., & Deshpande, M. (2010). Delayed presentation of cataracts in children: Are they worth operating upon. *Ophthalmic Epidemiology*, *17*(1), 25–33. https://doi.org/10.3109/09286580903450338

Gogtay, N., Giedd, J. N., Lusk, L., Hayashi, K. M., Greenstein, D., Vaituzis, A. C., Nugent, T. F., Herman, D. H., Clasen, L. S., Toga, A. W., Rapoport, J. L., & Thompson, P. M. (2004). Dynamic mapping of human cortical development during childhood through early adulthood. *Proceedings of the National Academy of Sciences of the United States of America*, *101*(21), 8174–8179. https://doi.org/10.1073/pnas.0402680101

Golarai, G., Ghahremani, D. G., Whitfield-Gabrieli, S., Reiss, A., Eberhardt, J. L., Gabrieli, J. D. E., & Grill-Spector, K. (2007). Differential development of high-level visual cortex correlates with category-specific recognition memory. *Nature Neuroscience*, *10*(4), 512–522. http://dx.doi.org/10.1038/nn1865

Golarai, G., Liberman, A., & Grill-Spector, K. (2015). Experience Shapes the Development of Neural Substrates of Face Processing in Human Ventral Temporal Cortex. *Cerebral Cortex*, *27*(2), bhv314. https://doi.org/10.1093/cercor/bhv314

Golarai, G., Liberman, A., Yoon, J. M. D., & Grill-Spector, K. (2010). Differential development of the ventral visual cortex extends through adolescence. *Frontiers in Human Neuroscience*, *3*(FEB), 80. https://doi.org/10.3389/neuro.09.080.2009

Gomez, J., Barnett, M. A., Natu, V. S., Mezer, A., Palomero-Gallagher, N., Weiner, K. S., Amunts, K., Zilles, K., & Grill-Spector, K. (2017). Microstructural proliferation in human cortex is coupled with the development of face processing. *Science*, *355*(6320), 68–71. https://doi.org/10.1126/science.aag0311

Gomez, J., Natu, V., Jeska, B., Barnett, M. A., & Grill-Spector, K. (2018). Development differentially sculpts receptive fields across early and high-level human visual cortex. *Nature Communications*, *9*(1). https://doi.org/10.1038/s41467-018-03166-3

Goren, C. C., Sarty, M., & Wu, P. Y. K. (1975). Visual following and pattern discrimination of face like stimuli by newborn infants. *Pediatrics*, *56*(4), 544–549.

Gougoux, F., Zatorre, R. J., Lassonde, M., Voss, P., & Lepore, F. (2005). A Functional Neuroimaging Study of Sound Localization: Visual Cortex Activity Predicts Performance in Early-Blind Individuals. *PLoS Biology*, *3*(2), e27. https://doi.org/10.1371/journal.pbio.0030027

Grady, C. L., Mondloch, C. J., Lewis, T. L., & Maurer, D. (2014). Early visual deprivation from congenital cataracts disrupts activity and functional connectivity in the face network. *Neuropsychologia*, *57*(1), 122–139. https://doi.org/10.1016/j.neuropsychologia.2014.03.005

Grafman, J. (2000). Conceptualizing functional neuroplasticity. *Journal of Communication Disorders*, *33*(4), 345–356. https://doi.org/10.1016/S0021-9924(00)00030-7

Greve, D. N., & Fischl, B. (2018). False positive rates in surface-based anatomical analysis. *NeuroImage*, *171*, 6–14. https://doi.org/10.1016/j.neuroimage.2017.12.072

Grill-Spector, K. (2003). The neural basis of object perception. In *Current Opinion in Neurobiology* (Vol. 13, Issue 2, pp. 159–166). https://doi.org/10.1016/S0959-4388(03)00040-0

Grill-Spector, K., Golarai, G., & Gabrieli, J. D. E. (2008). Developmental neuroimaging of the human ventral visual cortex. *Trends in Cognitive Sciences*, *12*(4), 152–162. https://doi.org/10.1016/j.tics.2008.01.009

Grill-Spector, K., Kushnir, T., Edelman, S., Avidan, G., Itzchak, Y., & Malach, R. (1999). Differential processing of objects under various viewing conditions in the human lateral occipital complex. *Neuron*, *24*(1), 187–203. https://doi.org/10.1016/S0896-6273(00)80832-6

Grill-Spector, K., & Weiner, K. S. (2014). The functional architecture of the ventral temporal cortex and its role in categorization. In *Nature Reviews Neuroscience* (Vol. 15, Issue 8, pp. 536–548). Nature Publishing Group. https://doi.org/10.1038/nrn3747

Groen, I. I. A., Greene, M. R., Baldassano, C., Fei-Fei, L., Beck, D. M., & Baker, C. I. (2018). Distinct contributions of functional and deep neural network features to representational similarity of scenes in human brain and behavior. *ELife*, *7*. https://doi.org/10.7554/ELIFE.32962

Grueter, M., Grueter, T., Bell, V., Horst, J., Laskowski, W., Sperling, K., Halligan, P. W., Ellis, H. D., & Kennerknecht, I. (2007). Hereditary prosopagnosia: The first case series. *Cortex*, *43*(6), 734–749. https://doi.org/10.1016/S0010-9452(08)70502-1

Guerreiro, M. J. S., Erfort, M. V., Henssler, J., Putzar, L., & Röder, B. (2015). Increased visual cortical thickness in sight-recovery individuals. *Human Brain Mapping*, *36*(12), 5265–5274. https://doi.org/10.1002/hbm.23009

Guerreiro, M. J. S., Kekunnaya, R., & Röder, B. (2022). Top-down modulation of visual cortical processing after transient congenital blindness. *Neuropsychologia*, *174*, 108338. https://doi.org/10.1016/j.neuropsychologia.2022.108338

Guerreiro, M. J. S., Putzar, L., & Röder, B. (2015). The effect of early visual deprivation on the neural bases of multisensory processing. *Brain*, *138*(6), 1499–1504. https://doi.org/10.1093/brain/awv076

Guerreiro, M. J. S., Putzar, L., & Röder, B. (2016a). The effect of early visual deprivation on the neural bases of auditory processing. *The Journal of Neuroscience*, *36*(5), 1620 LP – 1630. http://www.jneurosci.org/content/36/5/1620.abstract

Guerreiro, M. J. S., Putzar, L., & Röder, B. (2016b). Persisting cross-modal changes in sight-recovery individuals modulate visual perception. *Current Biology*, *26*(22), 3096–3100. https://doi.org/10.1016/j.cub.2016.08.069

Hadad, B. S., Maurer, D., & Lewis, T. L. (2012). Sparing of sensitivity to biological motion but not of global motion after early visual deprivation. *Developmental Science*, *15*(4), 474–481. https://doi.org/10.1111/j.1467-7687.2012.01145.x

Haijma, S. V., Van Haren, N., Cahn, W., Koolschijn, P. C. M. P., Hulshoff Pol, H. E., & Kahn, R. S. (2013). Brain volumes in schizophrenia: A meta-analysis in over 18 000 subjects. *Schizophrenia Bulletin*, *39*(5), 1129–1138. https://doi.org/10.1093/schbul/sbs118

Han, X., Jovicich, J., Salat, D. H., van der Kouwe, A., Quinn, B., Czanner, S., Busa, E., Pacheco, J., Albert, M. S., Killiany, R. J., Maguire, P., Rosas, D., Makris, N., Dale, A. M., Dickerson, B., & Fischl, B. (2006). Reliability of MRI-derived measurements of human cerebral cortical thickness: The effects of field strength, scanner upgrade and manufacturer. *NeuroImage*, *32*(1), 180–194. https://doi.org/10.1016/j.neuroimage.2006.02.051

Hanford, L. C., Nazarov, A., Hall, G. B., & Sassi, R. B. (2016). Cortical thickness in bipolar disorder: a systematic review. *Bipolar Disorders*, *18*(1), 4–18. https://doi.org/10.1111/BDI.12362

Haxby, J. V., Gobbini, M. I., Furey, M. L., Ishai, A., Schouten, J. L., & Pietrini, P. (2001). Distributed

and overlapping representations of faces and objects in ventral temporal cortex. *Science*, *293*(5539), 2425–2430. https://doi.org/10.1126/science.1063736

Hazlett, H. C., Gu, H., McKinstry, R. C., Shaw, D. W. W., Botteron, K. N., Dager, S. R., Styner, M., Vachet, C., Gerig, G., Paterson, S. J., Schultz, R. T., Estes, A. M., Evans, A. C., & Piven, J. (2012). Brain volume findings in 6-month-old infants at high familial risk for autism. *American Journal of Psychiatry*, *169*(6), 601–608. https://doi.org/10.1176/appi.ajp.2012.11091425

He, C., Peelen, M. V., Han, Z., Lin, N., Caramazza, A., & Bi, Y. (2013). Selectivity for large nonmanipulable objects in scene-selective visual cortex does not require visual experience. *NeuroImage*, *79*, 1–9. https://doi.org/10.1016/j.neuroimage.2013.04.051

Hills, P. J., & Lewis, M. B. (2018). The development of face expertise: Evidence for a qualitative change in processing. *Cognitive Development*, *48*, 1–18. https://doi.org/10.1016/j.cogdev.2018.05.003

Hölig, C., Föcker, J., Best, A., Röder, B., & Büchel, C. (2014). Crossmodal plasticity in the fusiform gyrus of late blind individuals during voice recognition. *NeuroImage*, *103*, 374–382. https://doi.org/10.1016/j.neuroimage.2014.09.050

Hölig, C., Guerreiro, M. J. S., Lingareddy, S., Kekunnaya, R., & Röder, B. (2022). Sight restoration in congenitally blind humans does not restore visual brain structure. *Cerebral Cortex*. https://doi.org/10.1093/cercor/bhac197

Hubel, D. H., & Wiesel, T. N. (1963). Receptive fields of cells in striate cortex of very young, visually inexperienced kittens. *Journal of Neurophysiology*, *26*, 994–1002. https://doi.org/10.1152/jn.1963.26.6.994

Hubel, D. H., & Wiesel, T. N. (1970). The period of susceptibility to the physiological effects of unilateral eye closure in kittens. *The Journal of Physiology*, *206*(2), 419–436. https://doi.org/10.1113/jphysiol.1970.sp009022

Hubel, D. H., Wiesel, T. N., & LeVay, S. (1977). Plasticity of ocular dominance columns in monkey striate cortex. *Philosophical Transactions of the Royal Society of London. Series B, Biological Sciences*, *278*(961), 377–409. https://doi.org/10.1098/rstb.1977.0050

Hubel, D. H., Wiesel, T. N., & LeVay, S. (1976). Functional architecture of area 17 in normal and monocularly deprived macaque monkeys. *Cold Spring Harbor Symposia on Quantitative Biology*, *40*, 581–589.

Huber, E., Webster, J. M., Brewer, A. A., MacLeod, D. I. A., Wandell, B. A., Boynton, G. M., Wade, A. R., & Fine, I. (2015). A Lack of Experience-Dependent Plasticity After More Than a Decade of Recovered Sight. *Psychological Science*, *26*(4), 393–401. https://doi.org/10.1177/0956797614563957

Huttenlocher, P. R. (1979). Synaptic density in human frontal cortex - Developmental changes and effects of aging. *Brain Research*, *163*(2), 195–205. https://doi.org/10.1016/0006-8993(79)90349-4

Huttenlocher, P. R., de Courten, C., Garey, L. J., & Van der Loos, H. (1982). Synaptogenesis in human visual cortex - evidence for synapse elimination during normal development. *Neuroscience Letters*, *33*(3), 247–252. https://doi.org/10.1016/0304-3940(82)90379-2

Hyvärinen, J., Carlson, S., & Hyvärinen, L. (1981). Early visual deprivation alters modality of neuronal responses in area 19 of monkey cortex. *Neuroscience Letters*, *26*(3), 239–243. https://doi.org/10.1016/0304-3940(81)90139-7

Hyvärinen, J., Hyvärinen, L., & Linnankoski, I. (1981). Modification of parietal association cortex and

functional blindness after binocular deprivation in young monkeys. *Experimental Brain Research*, *42*(1), 1–8. https://doi.org/10.1007/BF00235723

Illingworth, R. S., & Lister, J. (1964). The critical or sensitive period, with special reference to certain feeding problems in infants and children. *The Journal of Pediatrics*, *65*(6), 839–848. https://doi.org/10.1016/S0022-3476(64)80006-8

Innocenti, G. M. (2022). Defining neuroplasticity. In *Handbook of Clinical Neurology* (Vol. 184, pp. 3–18). Elsevier. https://doi.org/10.1016/B978-0-12-819410-2.00001-1

Inuggi, A., Pichiecchio, A., Ciacchini, B., Signorini, S., Morelli, F., & Gori, M. (2020). Multisystemic Increment of Cortical Thickness in Congenital Blind Children. *Cerebral Cortex Communications*, *1*(1), 1–11. https://doi.org/10.1093/texcom/tgaa071

Ishai, A., Ungerleider, L. G., Martin, A., Schouten, J. L., & Haxby, J. V. (1999). Distributed representation of objects in the human ventral visual pathway. *Proceedings of the National Academy of Sciences of the United States of America*, *96*(16), 9379–9384. https://doi.org/10.1073/pnas.96.16.9379

Jensen, O., Bonnefond, M., & VanRullen, R. (2012). An oscillatory mechanism for prioritizing salient unattended stimuli. *Trends in Cognitive Sciences*, *16*(4), 200–206. https://doi.org/10.1016/J.TICS.2012.03.002

Jha, S. C., Xia, K., Schmitt, J. E., Ahn, M., Girault, J. B., Murphy, V. A., Li, G., Wang, L., Shen, D., Zou, F., Zhu, H., Styner, M., Knickmeyer, R. C., & Gilmore, J. H. (2018). Genetic influences on neonatal cortical thickness and surface area. *Human Brain Mapping*, *39*(12), 4998–5013. https://doi.org/10.1002/hbm.24340

Jiang, J., Zhu, W., Shi, F., Liu, Y., Li, J., Qin, W., Li, K., Yu, C., & Jiang, T. (2009). Thick Visual Cortex in the Early Blind. *The Journal of Neuroscience*, *29*(7), 2205–2211. https://doi.org/10.1523/JNEUROSCI.5451-08.2009

Johnson, M. H., Dziurawiec, S., Ellis, H., & Morton, J. (1991). Newborns' preferential tracking of face-like stimuli and its subsequent decline. *Cognition*, *40*(1–2), 1–19. https://doi.org/10.1016/0010-0277(91)90045-6

Jovicich, J., Czanner, S., Greve, D. N., Haley, E., van der Kouwe, A., Gollub, R., Kennedy, D., Schmitt, F., Brown, G., MacFall, J., Fischl, B., & Dale, A. M. (2006). Reliability in multi-site structural MRI studies: Effects of gradient non-linearity correction on phantom and human data. *NeuroImage*, *30*(2), 436–443. https://doi.org/10.1016/j.neuroimage.2005.09.046

Julian, J. B., Fedorenko, E., Webster, J. M., & Kanwisher, N. (2012). An algorithmic method for functionally defining regions of interest in the ventral visual pathway. *NeuroImage*, *60*(4), 2357–2364. https://doi.org/10.1016/j.neuroimage.2012.02.055

Kalia, A., Gandhi, T. K., Chatterjee, G., Swami, P., Dhillon, H., Bi, S., Chauhan, N., Gupta, S. D., Sharma, P., Sood, S., Ganesh, S., Mathur, U., & Sinha, P. (2017). Assessing the impact of a program for late surgical intervention in early-blind children. *Public Health*, *146*, 15–23. https://doi.org/10.1016/j.puhe.2016.12.036

Kalia, A., Lesmes, L. A., Dorr, M., Gandhi, T. K., Chatterjee, G., Ganesh, S., Bex, P. J., & Sinha, P. (2014). Development of pattern vision following early and extended blindness. *Proceedings of the National Academy of Sciences of the United States of America*, *111*(5), 2035–2039. https://doi.org/10.1073/pnas.1311041111

Kanai, R., & Rees, G. (2011). The structural basis of inter-individual differences in human behaviour and cognition. In *Nature Reviews Neuroscience* (Vol. 12, Issue 4, pp. 231–242). Nature Publishing Group. https://doi.org/10.1038/nrn3000

Kanwisher, N. (2010). Functional specificity in the human brain: A window into the functional architecture of the mind. *Proceedings of the National Academy of Sciences*, *107*(25), 11163–11170. https://doi.org/10.1073/PNAS.1005062107

Kanwisher, N., McDermott, J., & Chun, M. M. (1997). The fusiform face area: A module in human extrastriate cortex specialized for face perception. *Journal of Neuroscience*, *17*(11), 4302–4311. https://doi.org/10.1523/jneurosci.17-11-04302.1997

Karama, S., Ad-Dab'bagh, Y., Haier, R. J., Deary, I. J., Lyttelton, O. C., Lepage, C., & Evans, A. C. (2009). Erratum to "Positive association between cognitive ability and cortical thickness in a representative US sample of healthy 6 to 18 year-olds" (DOI:10.1016/j.intell.2008.09.006). *Intelligence*, *37*(4), 432–442. https://doi.org/10.1016/j.intell.2009.03.010

Khundrakpam, B. S., Lewis, J. D., Kostopoulos, P., Carbonell, F., & Evans, A. C. (2017). Cortical thickness abnormalities in autism spectrum disorders through late childhood, adolescence, and adulthood: A large-scale mri study. *Cerebral Cortex*, *27*(3), 1721–1731. https://doi.org/10.1093/cercor/bhx038

Kitada, R., Yoshihara, K., Sasaki, A. T., Hashiguchi, M., Kochiyama, T., & Sadato, N. (2014). The brain network underlying the recognition of hand gestures in the blind: The supramodal role of the extrastriate body area. *Journal of Neuroscience*, *34*(30), 10096–10108. https://doi.org/10.1523/JNEUROSCI.0500-14.2014

Knickmeyer, R. C., Gouttard, S., Kang, C., Evans, D., Wilber, K., Smith, J. K., Hamer, R. M., Lin, W., Gerig, G., & Gilmore, J. H. (2008). A structural MRI study of human brain development from birth to 2 years. *Journal of Neuroscience*, *28*(47), 12176–12182. https://doi.org/10.1523/JNEUROSCI.3479-08.2008

Knudsen, E. I. (2004). Sensitive periods in the development of the brain and behavior. *Journal of Cognitive Neuroscience*, *16*(8), 1412–1425. https://doi.org/10.1162/0898929042304796

Kolb, B. (2018). Brain Plasticity and Experience. In *The Neurobiology of Brain and Behavioral Development* (pp. 341–389). Academic Press. https://doi.org/10.1016/B978-0-12-804036-2.00013-3

Kosakowski, H. L., Cohen, M. A., Takahashi, A., Keil, B., & Kanwisher, N. (2021). Selective Responses to Faces, Scenes, and Bodies in the Ventral Visual Pathway of Infants. *PsyArXiv*. https://doi.org/10.31234/OSF.IO/7HQCU

Kosakowski, H. L., Cohen, M. A., Takahashi, A., Keil, B., Kanwisher, N., & Saxe, R. (2022). Selective responses to faces, scenes, and bodies in the ventral visual pathway of infants. *Current Biology*, *32*(2), 265-274.e5. https://doi.org/10.1016/j.cub.2021.10.064

Kouider, S., Stahlhut, C., Gelskov, S. V., Barbosa, L. S., Dutat, M., De Gardelle, V., Christophe, A., Dehaene, S., & Dehaene-Lambertz, G. (2013). A neural marker of perceptual consciousness in infants. *Science*, *340*(6130), 376–380. https://doi.org/10.1126/science.1232509

Kourtzi, Z., & Kanwisher, N. (2000). Cortical regions involved in perceiving object shape. *Journal of Neuroscience*, *20*(9), 3310–3318. https://doi.org/10.1523/jneurosci.20-09-03310.2000

Kral, A., Dorman, M. F., & Wilson, B. S. (2019). Neuronal Development of Hearing and Language: Cochlear Implants and Critical Periods. *Annual Review of Neuroscience*, *42*, 47–65. https://doi.org/10.1146/annurev-neuro-080317-061513

Kravitz, D. J., Saleem, K. S., Baker, C. I., & Mishkin, M. (2011). A new neural framework for visuospatial processing. In *Nature Reviews Neuroscience* (Vol. 12, Issue 4, pp. 217–230). Nature Publishing Group. https://doi.org/10.1038/nrn3008

Kriegeskorte, N., Formisano, E., Sorger, B., & Goebel, R. (2007). Individual faces elicit distinct response patterns in human anterior temporal cortex. *Proceedings of the National Academy of Sciences of the United States of America*, *104*(51), 20600–20605. https://doi.org/10.1073/pnas.0705654104

Kriegeskorte, N., Mur, M., & Bandettini, P. A. (2008). Representational similarity analysis - connecting the branches of systems neuroscience. *Frontiers in Systems Neuroscience*, *2*(NOV), 4. https://doi.org/10.3389/neuro.06.004.2008

Kriegeskorte, N., Mur, M., Ruff, D. A., Kiani, R., Bodurka, J., Esteky, H., Tanaka, K., & Bandettini, P. A. (2008). Matching Categorical Object Representations in Inferior Temporal Cortex of Man and Monkey. *Neuron*, *60*(6), 1126–1141. https://doi.org/10.1016/j.neuron.2008.10.043

Krongold, M., Cooper, C., & Bray, S. (2017). Modular development of cortical gray matter across childhood and adolescence. *Cerebral Cortex*, *27*(2), 1125–1136. https://doi.org/10.1093/cercor/bhv307

Kupers, R., & Ptito, M. (2014). Compensatory plasticity and cross-modal reorganization following early visual deprivation. *Neuroscience and Biobehavioral Reviews*, *41*, 36–52. https://doi.org/10.1016/j.neubiorev.2013.08.001

Kupers, R., Zhan, M., Paré, S., Dricot, L., Vaessen, M., & de Gelder, B. (2022). Brain morphometric changes in congenitally blind subjects: a 7 Tesla MRI study. *BioRxiv*, 2022.05.18.492367. https://doi.org/10.1101/2022.05.18.492367

Kuznetsova, A., Brockhoff, P. B., & Christensen, R. H. B. (2017). {lmerTest} Package: Tests in Linear Mixed Effects Models. *Journal of Statistical Software*, *82*(13), 1–26. https://doi.org/10.18637/jss.v082.i13

Lafer-Sousa, R., Conway, B. R., & Kanwisher, N. (2016). Color-Biased Regions of the Ventral Visual Pathway Lie between Face- and Place-Selective Regions in Humans, as in Macaques. *The Journal of Neuroscience*, *36*(5), 1682 LP – 1697. http://www.jneurosci.org/content/36/5/1682.abstract

Le Grand, R., Mondloch, C. J., Maurer, D., & Brent, H. P. (2001). Early visual experience and face processing. *Nature*, *410*(6831), 890–890. https://doi.org/10.1038/35073749

Le Grand, R., Mondloch, C. J., Maurer, D., & Brent, H. P. (2004). Impairment in Holistic Face Processing Following Early Visual Deprivation. *Psychological Science*, *15*(11), 762–768. https://doi.org/10.1111/j.0956-7976.2004.00753.x

Lebel, C., & Beaulieu, C. (2011). Longitudinal development of human brain wiring continues from childhood into adulthood. *Journal of Neuroscience*, *31*(30), 10937–10947. https://doi.org/10.1523/JNEUROSCI.5302-10.2011

LeCun, Y., Bengio, Y., & Hinton, G. (2015). Deep learning. *Nature*, *521*(7553), 436–444. https://doi.org/10.1038/nature14539

Lenth, R. V. (2022). *emmeans: Estimated Marginal Means, aka Least-Squares Means*. https://cran.r-project.org/package=emmeans

Levelt, C. N., & Hübener, M. (2012). Critical-Period Plasticity in the Visual Cortex. *Annual Review of Neuroscience*, *35*(1), 309–330. https://doi.org/10.1146/annurev-neuro-061010-113813

Levi, D. M. (2005). Perceptual learning in adults with amblyopia: A reevaluation of critical periods in human vision. *Developmental Psychobiology*, *46*(3), 222–232. https://doi.org/10.1002/dev.20050

Lewis, T. L., & Maurer, D. (2005). Multiple sensitive periods in human visual development: Evidence

from visually deprived children. *Developmental Psychobiology*, *46*(3), 163–183. https://doi.org/10.1002/dev.20055

Lewis, T. L., & Maurer, D. (2009). Effects of early pattern deprivation on visual development. In *Optometry and Vision Science* (Vol. 86, Issue 6, pp. 640–646). Lippincott Williams and Wilkins. https://doi.org/10.1097/OPX.0b013e3181a7296b

Li, G., Lin, W., Gilmore, J. H., & Shen, D. (2015). Spatial patterns, longitudinal development, and hemispheric asymmetries of cortical thickness in infants from birth to 2 years of age. *Journal of Neuroscience*, *35*(24), 9150–9162. https://doi.org/10.1523/JNEUROSCI.4107-14.2015

Li, Qian, Zhao, Y., Chen, Z., Long, J., Dai, J., Huang, X., Lui, S., Radua, J., Vieta, E., Kemp, G. J., Sweeney, J. A., Li, F., & Gong, Q. (2020). Meta-analysis of cortical thickness abnormalities in medication-free patients with major depressive disorder. *Neuropsychopharmacology*, *45*(4), 703–712. https://doi.org/10.1038/s41386-019-0563-9

Li, Qiaojun, Song, M., Xu, J., Qin, W., Yu, C., & Jiang, T. (2017). Cortical thickness development of human primary visual cortex related to the age of blindness onset. *Brain Imaging and Behavior*, *11*(4), 1029–1036. https://doi.org/10.1007/s11682-016-9576-8

Li, W., Li, X., Huang, L., Kong, X.-Z., Yang, W., Wei, D., Li, J., Cheng, H., Zhang, Q., Qiu, J., & Liu, J. (2015). Brain structure links trait creativity to openness to experience. *Social Cognitive and Affective Neuroscience*, *10*(2), 191–198. https://doi.org/10.1093/scan/nsu041

Lisboa, I. C., Queirós, S., Miguel, H., Sampaio, A., Santos, J. A., & Pereira, A. F. (2020). Infants' cortical processing of biological motion configuration – A fNIRS study. *Infant Behavior and Development*, *60*, 101450. https://doi.org/10.1016/j.infbeh.2020.101450

López-Bendito, G., Aníbal-Martínez, M., & Martini, F. J. (2022). Cross-Modal Plasticity in Brains Deprived of Visual Input Before Vision. In *Annual Review of Neuroscience* (Vol. 45, pp. 471–489). https://doi.org/10.1146/annurev-neuro-111020-104222

Lyall, A. E., Shi, F., Geng, X., Woolson, S., Li, G., Wang, L., Hamer, R. M., Shen, D., & Gilmore, J. H. (2015). Dynamic development of regional cortical thickness and surface area in early childhood. *Cerebral Cortex*, *25*(8), 2204–2212. https://doi.org/10.1093/cercor/bhu027

Mackworth, N. H., & Bruner, J. S. (1970). How adults and children search and recognize pictures. *Human Development*, *13*(3), 149–177. https://doi.org/10.1159/000270887

Maggioni, E., Squarcina, L., Dusi, N., Diwadkar, V. A., & Brambilla, P. (2020). Twin MRI studies on genetic and environmental determinants of brain morphology and function in the early lifespan. *Neuroscience and Biobehavioral Reviews*, *109*, 139–149. https://doi.org/10.1016/j.neubiorev.2020.01.003

Maguire, E. A., Gadian, D. G., Johnsrude, I. S., Good, C. D., Ashburner, J. T., Frackowiak, R., & Frith, C. D. (2000). Navigation-related structural change in the hippocampi of taxi drivers. *Proceedings of the National Academy of Sciences of the United States of America*, *97*(8), 4398–4403. https://doi.org/10.1073/pnas.070039597

Mahon, B. Z., Anzellotti, S., Schwarzbach, J., Zampini, M., & Caramazza, A. (2009). Category-specific organization in the human brain does not require visual experience. *Neuron*, *63*(3), 397–405. https://doi.org/10.1016/j.neuron.2009.07.012

Malach, R., Reppas, J. B., Benson, R. R., Kwong, K. K., Jiang, H., Kennedy, W. A., Ledden, P. J., Brady, T. J., Rosen, B. R., & Tootell, R. B. H. (1995). Object-related activity revealed by functional magnetic resonance imaging in human occipital cortex. *Proceedings of the National Academy of Sciences of the United States of America*, *92*(18), 8135–8139. https://doi.org/10.1073/pnas.92.18.8135

Margalit, E., Jamison, K. W., Weiner, K. S., Vizioli, L., Zhang, R. Y., Kay, K. N., & Grill-Spector, K. (2020). Ultra-high-resolution fMRI of Human Ventral Temporal Cortex Reveals Differential Representation of Categories and Domains. *Journal of Neuroscience*, *40*(15), 3008–3024. https://doi.org/10.1523/JNEUROSCI.2106-19.2020

Maurer, D. (2017). Critical periods re-examined: Evidence from children treated for dense cataracts. *Cognitive Development*, *42*, 27–36. https://doi.org/10.1016/j.cogdev.2017.02.006

Maurer, D., & Lewis, T. L. (2018). Visual Systems. In *The Neurobiology of Brain and Behavioral Development* (pp. 213–233). Elsevier Inc. https://doi.org/10.1016/B978-0-12-804036-2.00008-X

Maurer, D., Lewis, T. L., & Brent, H. P. (1989). The effects of deprivation on human visual development: studies of children treated for cataracts. In *Psychological Development in Infancy* (pp. 139–227). Elsevier.

Maurer, D., Lewis, T. L., & Mondloch, C. J. (2005). Missing sights : consequences for visual cognitive development. *TRENDS in Cognitive Science*, *9*(3), 10–17. https://doi.org/10.1016/j.tics.2005.01.006

Maurer, D., Mondloch, C. J., & Lewis, T. L. (2007). Effects of early visual deprivation on perceptual and cognitive development. In *Progress in Brain Research* (Vol. 164, pp. 87–104). Elsevier. https://doi.org/10.1016/S0079-6123(07)64005-9

May, A. (2011). Experience-dependent structural plasticity in the adult human brain. *Trends in Cognitive Sciences*, *15*(10), 475–482. https://doi.org/10.1016/j.tics.2011.08.002

McKone, E., Crookes, K., Jeffery, L., & Dilks, D. D. (2012). A critical review of the development of face recognition: Experience is less important than previously believed. *Cognitive Neuropsychology*, *29*(1–2), 174–212. https://doi.org/10.1080/02643294.2012.660138

McKyton, A., Ben-Zion, I., Doron, R., & Zohary, E. (2015). The Limits of Shape Recognition following Late Emergence from Blindness. *Current Biology*, *25*(18), 2373–2378. https://doi.org/https://doi.org/10.1016/j.cub.2015.06.040

McLaughlin, K. A., Weissman, D., & Bitrán, D. (2019). Childhood adversity and neural development: A systematic review. *Annual Review of Developmental Psychology*, *1*(1), 277–312. https://doi.org/10.1146/annurev-devpsych-121318-084950

Meissner, T. W., Nordt, M., & Weigelt, S. (2019). Prolonged functional development of the parahippocampal place area and occipital place area. *NeuroImage*, *191*, 104–115. https://doi.org/10.1016/j.neuroimage.2019.02.025

Meltzoff, A. N., Ramírez, R. R., Saby, J. N., Larson, E., Taulu, S., & Marshall, P. J. (2018). Infant brain responses to felt and observed touch of hands and feet: an MEG study. *Developmental Science*, *21*(5), 12651. https://doi.org/10.1111/desc.12651

Modi, S., Bhattacharya, M., Singh, N., Tripathi, R. P., & Khushu, S. (2012). Effect of visual experience on structural organization of the human brain: A voxel based morphometric study using DARTEL. *European Journal of Radiology*, *81*(10), 2811–2819. https://doi.org/10.1016/j.ejrad.2011.10.022

Mondloch, C. J., Le Grand, R., & Maurer, D. (2003). Early visual experience is necessary for the development of some—but not all—aspects of face processing. In O. Pascalis & A. Slater (Eds.), *The Development of Face Processing in Infancy and Early Childhood* (pp. 99–117). https://139.57.65.11/psychology/research/infantchild/Mondloch_Chapter_2003.pdf

Mondloch, C. J., Segalowitz, S. J., Lewis, T. L., Dywan, J., Le Grand, R., & Maurer, D. (2013). The

effect of early visual deprivation on the development of face detection. *Developmental Science*, *16*(5), 728–742. https://doi.org/10.1111/desc.12065

Mowad, T. G., Willett, A. E., Mahmoudian, M., Lipin, M., Heinecke, A., Maguire, A. M., Bennett, J., & Ashtari, M. (2020). Compensatory Cross-Modal Plasticity Persists After Sight Restoration. *Frontiers in Neuroscience*, *14*. https://doi.org/10.3389/fnins.2020.00291

Munsinger, H., & Gummerman, K. (1967). Identification of form in patterns of visual noise. *Journal of Experimental Psychology*, *75*(1), 81–87. https://doi.org/10.1037/h0024890

Narr, K. L., Woods, R. P., Thompson, P. M., Szeszko, P., Robinson, D., Dimtcheva, T., Gurbani, M., Toga, A. W., & Bilder, R. M. (2007). Relationships between IQ and Regional Cortical Gray Matter Thickness in Healthy Adults. *Cerebral Cortex*, *17*(9), 2163–2171. https://doi.org/10.1093/CERCOR/BHL125

Nasr, S., Liu, N., Devaney, K. J., Yue, X., Rajimehr, R., Ungerleider, L. G., & Tootell, R. B. H. (2011). Scene-selective cortical regions in human and nonhuman primates. *Journal of Neuroscience*, *31*(39), 13771–13785. https://doi.org/10.1523/JNEUROSCI.2792-11.2011

Natu, V. S., Arcaro, M. J., Barnett, M. A., Gomez, J., Livingstone, M. S., Grill-Spector, K., & Weiner, K. S. (2021). Sulcal Depth in the Medial Ventral Temporal Cortex Predicts the Location of a Place-Selective Region in Macaques, Children, and Adults. *Cerebral Cortex*, *31*(1), 48–61. https://doi.org/10.1093/cercor/bhaa203

Natu, V. S., Gomez, J., Barnett, M. A., Jeska, B., Kirilina, E., Jaeger, C., Zhen, Z., Cox, S., Weiner, K. S., Weiskopf, N., & Grill-Spector, K. (2019). Apparent thinning of human visual cortex during childhood is associated with myelination. *Proceedings of the National Academy of Sciences of the United States of America*, *116*(41), 20750–20759. https://doi.org/10.1073/pnas.1904931116

Nishimura, M., Scherf, S., & Behrmann, M. (2009). Development of object recognition in humans. *F1000 Biology Reports*, *1*. https://doi.org/10.3410/b1-56

Noble, K. G., & Giebler, M. A. (2020). The neuroscience of socioeconomic inequality. In *Current Opinion in Behavioral Sciences* (Vol. 36, pp. 23–28). https://doi.org/10.1016/j.cobeha.2020.05.007

Noppeney, U. (2007). The effects of visual deprivation on functional and structural organization of the human brain. *Neuroscience & Biobehavioral Reviews*, *31*(8), 1169–1180. https://doi.org/10.1016/j.neubiorev.2007.04.012

Norman, K. A., Polyn, S. M., Detre, G. J., & Haxby, J. V. (2006). Beyond mind-reading: multi-voxel pattern analysis of fMRI data. In *Trends in Cognitive Sciences* (Vol. 10, Issue 9, pp. 424–430). Elsevier Current Trends. https://doi.org/10.1016/j.tics.2006.07.005

O'Leary, D. D. M., Chou, S. J., & Sahara, S. (2007). Area patterning of the mammalian cortex. In *Neuron* (Vol. 56, Issue 2, pp. 252–269). Cell Press. https://doi.org/10.1016/j.neuron.2007.10.010

Op De Beeck, H. P., Haushofer, J., & Kanwisher, N. (2008). Interpreting fMRI data: Maps, modules and dimensions. In *Nature Reviews Neuroscience* (Vol. 9, Issue 2, pp. 123–135). Nat Rev Neurosci. https://doi.org/10.1038/nrn2314

Op de Beeck, H. P., Pillet, I., & Ritchie, J. B. (2019). Factors Determining Where Category-Selective Areas Emerge in Visual Cortex. *Trends in Cognitive Sciences*, *23*(9), 784–797. https://doi.org/10.1016/j.tics.2019.06.006

Osher, D. E., Saxe, R. R., Koldewyn, K., Gabrieli, J. D. E., Kanwisher, N., & Saygin, Z. M. (2016).

Structural Connectivity Fingerprints Predict Cortical Selectivity for Multiple Visual Categories across Cortex. *Cerebral Cortex*, *26*(4), 1668–1683. https://doi.org/10.1093/cercor/bhu303

Ostrovsky, Y., Meyers, E., Ganesh, S., Mathur, U., & Sinha, P. (2009). Visual Parsing After Recovery From Blindness. *Psychological Science*, *20*(12), 1484–1491. https://doi.org/10.1111/j.1467-9280.2009.02471.x

Pagnozzi, A. M., Conti, E., Calderoni, S., Fripp, J., & Rose, S. E. (2018). A systematic review of structural MRI biomarkers in autism spectrum disorder: A machine learning perspective. *International Journal of Developmental Neuroscience*, *71*, 68–82. https://doi.org/10.1016/j.ijdevneu.2018.08.010

Panizzon, M. S., Fennema-Notestine, C., Eyler, L. T., Jernigan, T. L., Prom-Wormley, E., Neale, M., Jacobson, K., Lyons, M. J., Grant, M. D., Franz, C. E., Xian, H., Tsuang, M., Fischl, B., Seidman, L. J., Dale, A. M., & Kremen, W. S. (2009). Distinct genetic influences on cortical surface area and cortical thickness. *Cerebral Cortex*, *19*(11), 2728–2735. https://doi.org/10.1093/cercor/bhp026

Paquette, S., Takerkart, S., Saget, S., Peretz, I., & Belin, P. (2018). Cross-classification of musical and vocal emotions in the auditory cortex. *Annals of the New York Academy of Sciences*, *1423*(1), 329–337. https://doi.org/10.1111/nyas.13666

Paré, S., Bleau, M., Dricot, L., Ptito, M., & Kupers, R. (2023). Brain structural changes in blindness: a systematic review and an anatomical likelihood estimation (ALE) meta-analysis. *Neuroscience & Biobehavioral Reviews*, *150*, 105165. https://doi.org/10.1016/J.NEUBIOREV.2023.105165

Park, H. J., Lee, J. D., Kim, E. Y., Park, B., Oh, M. K., Lee, S. C., & Kim, J. J. (2009). Morphological alterations in the congenital blind based on the analysis of cortical thickness and surface area. *NeuroImage*, *47*(1), 98–106. https://doi.org/10.1016/j.neuroimage.2009.03.076

Parvizi, J., Jacques, C., Foster, B. L., Withoft, N., Rangarajan, V., Weiner, K. S., & Grill-Spector, K. (2012). Electrical stimulation of Human Fusiform face-selective regions distorts face perception. *Journal of Neuroscience*, *32*(43), 14915–14920. https://doi.org/10.1523/JNEUROSCI.2609-12.2012

Pascalis, O., Fort, M., & Quinn, P. C. (2020). Development of face processing: are there critical or sensitive periods? In *Current Opinion in Behavioral Sciences* (Vol. 36, pp. 7–12). Elsevier. https://doi.org/10.1016/j.cobeha.2020.05.005

Pascual-Leone, A., Amedi, A., Fregni, F., & Merabet, L. B. (2005). The plastic human brain cortex. In *Annual Review of Neuroscience* (Vol. 28, pp. 377–401). Annual Reviews. https://doi.org/10.1146/annurev.neuro.27.070203.144216

Passarotti, A. M., Paul, B. M., Bussiere, J. R., Buxton, R. B., Wong, E. C., & Stiles, J. (2003). The development of face and location processing: An fMRI study. *Developmental Science*, *6*(1), 100–117. https://doi.org/10.1111/1467-7687.00259

Passarotti, A. M., Smith, J., DeLano, M., & Huang, J. (2007). Developmental differences in the neural bases of the face inversion effect show progressive tuning of face-selective regions to the upright orientation. *NeuroImage*, *34*(4), 1708–1722. https://doi.org/10.1016/j.neuroimage.2006.07.045

Pavani, F., & Röder, B. (2012). Cross-modal plasticity as a consequence of sensory loss: Insights from blindness and deafness. In *Stein, B. E. (Ed.) The new handbook of multisensory processes. (2012 pp 607-626) Cambridge,* (pp. 607–626).

Peelen, M. V., Bracci, S., Lu, X., He, C., Caramazza, A., & Bi, Y. (2013). Tool selectivity in left occipitotemporal cortex develops without vision. *Journal of Cognitive Neuroscience*, *25*(8), 1225–1234. https://doi.org/10.1162/jocn_a_00411

Peelen, M. V., & Downing, P. E. (2005). Selectivity for the human body in the fusiform gyrus. *Journal of Neurophysiology*, *93*(1), 603–608. https://doi.org/10.1152/jn.00513.2004

Peelen, M. V., Glaser, B., Vuilleumier, P., & Eliez, S. (2009). Differential development of selectivity for faces and bodies in the fusiform gyrus. *Developmental Science*, *12*(6), F16–F25. https://doi.org/10.1111/j.1467-7687.2009.00916.x

Peelen, M. V., He, C., Han, Z., Caramazza, A., & Bi, Y. (2014). Nonvisual and visual object shape representations in occipitotemporal cortex: Evidence from congenitally blind and sighted adults. *Journal of Neuroscience*, *34*(1), 163–170. https://doi.org/10.1523/JNEUROSCI.1114-13.2014

Pelphrey, K. A., Lopez, J., & Morris, J. P. (2009). Developmental continuity and change in responses to social and nonsocial categories in human extrastriate visual cortex. *Frontiers in Human Neuroscience*, *3*(SEP), 25. https://doi.org/10.3389/neuro.09.025.2009

Pietrini, P., Furey, M. L., Ricciardi, E., Gobbini, M. I., Wu, W. H. C., Cohen, L., Guazzelli, M., & Haxby, J. V. (2004). Beyond sensory images: Object-based representation in the human ventral pathway. *Proceedings of the National Academy of Sciences of the United States of America*, *101*(15), 5658–5663. https://doi.org/10.1073/pnas.0400707101

Pinsk, M. A., Arcaro, M. J., Weiner, K. S., Kalkus, J. F., Inati, S. J., Gross, C. G., & Kastner, S. (2009). Neural representations of faces and body parts in macaque and human cortex: A comparative fMRI study. *Journal of Neurophysiology*, *101*(5), 2581–2600. https://doi.org/10.1152/jn.91198.2008

Pitchaimuthu, K., Dormal, G., Sourav, S., Shareef, I., Rajendran, S. S., Ossandón, J. P., Kekunnaya, R., & Röder, B. (2021). Steady state evoked potentials indicate changes in nonlinear neural mechanisms of vision in sight recovery individuals. *Cortex*, *144*, 15–28. https://doi.org/10.1016/j.cortex.2021.08.001

Pitchaimuthu, K., Sourav, S., Bottari, D., Banerjee, S., Shareef, I., Kekunnaya, R., & Röder, B. (2019). Color vision in sight recovery individuals. *Restorative Neurology and Neuroscience*, *37*(6), 583–590. https://doi.org/10.3233/RNN-190928

Pitcher, D., Charles, L., Devlin, J. T., Walsh, V., & Duchaine, B. (2009). Triple Dissociation of Faces, Bodies, and Objects in Extrastriate Cortex. *Current Biology*, *19*(4), 319–324. https://doi.org/10.1016/J.CUB.2009.01.007

Pitcher, D., Dilks, D. D., Saxe, R. R., Triantafyllou, C., & Kanwisher, N. (2011). Differential selectivity for dynamic versus static information in face-selective cortical regions. *NeuroImage*, *56*(4), 2356–2363. https://doi.org/10.1016/j.neuroimage.2011.03.067

Poldrack, R. A. (2007). Region of interest analysis for fMRI. *Social Cognitive and Affective Neuroscience*, *2*(1), 67–70. https://doi.org/10.1093/scan/nsm006

Polk, T. A., Park, J., Smith, M. R., & Park, D. C. (2007). Nature versus nurture in ventral visual cortex: A functional magnetic resonance imaging study of twins. *Journal of Neuroscience*, *27*(51), 13921–13925. https://doi.org/10.1523/JNEUROSCI.4001-07.2007

Powell, L. J., Deen, B., & Saxe, R. R. (2018). Using individual functional channels of interest to study cortical development with fNIRS. *Developmental Science*, *21*(4), 12595. https://doi.org/10.1111/desc.12595

Proklova, D., Kaiser, D., & Peelen, M. V. (2016). Disentangling representations of object shape and object category in human visual cortex: The animate-inanimate distinction. *Journal of Cognitive Neuroscience*, *28*(5), 680–692. https://doi.org/10.1162/jocn_a_00924

Putzar, L., Goerendt, I., Heed, T., Richard, G., Büchel, C., & Röder, B. (2010). The neural basis of lip-reading capabilities is altered by early visual deprivation. *Neuropsychologia*, *48*(7), 2158–2166. https://doi.org/10.1016/j.neuropsychologia.2010.04.007

Putzar, L., Goerendt, I., Lange, K., Rösler, F., & Röder, B. (2007). Early visual deprivation impairs multisensory interactions in humans. *Nature Neuroscience*, *10*(1097-6256 (Print)), 1243–1245. https://doi.org/10.1038/nn1978

Putzar, L., Hötting, K., & Röder, B. (2010). Early visual deprivation affects the development of face recognition and of audio-visual speech perception. *Restorative Neurology and Neuroscience*, *28*(2), 251–257. https://doi.org/10.3233/RNN-2010-0526

Putzar, L., Hötting, K., Rösler, F., & Röder, B. (2007). The development of visual feature binding processes after visual deprivation in early infancy. *Vision Res*, *47*(20), 2616–2626. https://doi.org/10.1016/j.visres.2007.07.002

Qin, W., Liu, Y., Jiang, T., & Yu, C. (2013). The Development of Visual Areas Depends Differently on Visual Experience. *PLoS ONE*, *8*(1), e53784. https://doi.org/10.1371/journal.pone.0053784

R Core Team. (2022). *R: A Language and Environment for Statistical Computing*. https://www.r-project.org/

Raczy, K., Hölig, C., Guerreiro, M. J. S., Lingareddy, S., Kekunnaya, R., & Röder, B. (2022). Typical resting-state activity of the brain requires visual input during an early sensitive period. *Brain Communications*, *4*(4). https://doi.org/10.1093/braincomms/fcac146

Rajendran, S. S., Bottari, D., Shareef, I., Pitchaimuthu, K., Sourav, S., Troje, N. F., Kekunnaya, R., & Röder, B. (2020). Biological action identification does not require early visual input for development. *ENeuro*, *7*(5). https://doi.org/10.1523/ENEURO.0534-19.2020

Rajimehr, R., Devaney, K. J., Bilenko, N. Y., Young, J. C., & Tootell, R. B. H. (2011). The "parahippocampal place area" responds preferentially to high spatial frequencies in humans and monkeys. *PLoS Biology*, *9*(4), e1000608. https://doi.org/10.1371/journal.pbio.1000608

Rakic, P. (2009). Evolution of the neocortex: A perspective from developmental biology. In *Nature Reviews Neuroscience* (Vol. 10, Issue 10, pp. 724–735). Nature Publishing Group. https://doi.org/10.1038/nrn2719

Ramon y Cajal, S. (1928). Degeneration and regeneration of the nervous system. In *Degeneration and regeneration of the nervous system.* Clarendon Press.

Rapoport, J. L., Giedd, J. N., & Gogtay, N. (2012). Neurodevelopmental model of schizophrenia: Update 2012. *Molecular Psychiatry*, *17*(12), 1228–1238. https://doi.org/10.1038/mp.2012.23

Ratan Murty, N. A., Teng, S., Beeler, D., Mynick, A., Oliva, A., & Kanwisher, N. (2020). Visual experience is not necessary for the development of face-selectivity in the lateral fusiform gyrus. *Proceedings of the National Academy of Sciences of the United States of America*, 2020.02.25.964890. https://doi.org/10.1073/pnas.2004607117

Rauschecker, J. P., & Harris, L. R. (1983). Auditory compensation of the effects of visual deprivation in the cat's superior colliculus. *Experimental Brain Research*, *50*(1), 69–83. https://doi.org/10.1007/BF00238233

Rauschecker, J. P., & Korte, M. (1993). Auditory compensation for early blindness in cat cerebral cortex. *Journal of Neuroscience*, *13*(10), 4538–4548. https://doi.org/10.1523/jneurosci.13-10-04538.1993

Raznahan, A., Greenstein, D., Lee, N. R., Clasen, L. S., & Giedd, J. N. (2012). Prenatal growth in humans and postnatal brain maturation into late adolescence. *Proceedings of the National*

Academy of Sciences of the United States of America, *109*(28), 11366–11371. https://doi.org/10.1073/pnas.1203350109

Reh, R. K., Dias, B. G., Nelson, C. A., Kaufer, D., Werker, J. F., Kolb, B., Levine, J. D., & Hensch, T. K. (2020). Critical period regulation across multiple timescales. In *Proceedings of the National Academy of Sciences of the United States of America* (Vol. 117, Issue 38, pp. 23242–23251). National Academy of Sciences. https://doi.org/10.1073/pnas.1820836117

Reich, L., Szwed, M., Cohen, L., & Amedi, A. (2011). A ventral visual stream reading center independent of visual experience. *Current Biology*, *21*(5), 363–368. https://doi.org/10.1016/j.cub.2011.01.040

Rimol, L. M., Hartberg, C. B., Nesvåg, R., Fennema-Notestine, C., Hagler, D. J., Pung, C. J., Jennings, R. G., Haukvik, U. K., Lange, E., Nakstad, P. H., Melle, I., Andreassen, O. A., Dale, A. M., & Agartz, I. (2010). Cortical Thickness and Subcortical Volumes in Schizophrenia and Bipolar Disorder. *Biological Psychiatry*, *68*(1), 41–50. https://doi.org/10.1016/j.biopsych.2010.03.036

Rimol, L. M., Nesvåg, R., Hagler, D. J., Bergmann, Ø., Fennema-Notestine, C., Hartberg, C. B., Haukvik, U. K., Lange, E., Pung, C. J., Server, A., Melle, I., Andreassen, O. A., Agartz, I., & Dale, A. M. (2012). Cortical volume, surface area, and thickness in schizophrenia and bipolar disorder. *Biological Psychiatry*, *71*(6), 552–560. https://doi.org/10.1016/j.biopsych.2011.11.026

Rimol, L. M., Panizzon, M. S., Fennema-Notestine, C., Eyler, L. T., Fischl, B., Franz, C. E., Hagler, D. J., Lyons, M. J., Neale, M. C., Pacheco, J., Perry, M. E., Schmitt, J. E., Grant, M. D., Seidman, L. J., Thermenos, H. W., Tsuang, M. T., Eisen, S. A., Kremen, W. S., & Dale, A. M. (2010). Cortical Thickness Is Influenced by Regionally Specific Genetic Factors. *Biological Psychiatry*, *67*(5), 493–499. https://doi.org/10.1016/j.biopsych.2009.09.032

Rivolta, D., Woolgar, A., Palermo, R., Butko, M., Schmalzl, L., & Williams, M. A. (2014). Multi-voxel pattern analysis (MVPA) reveals abnormal fMRI activity in both the “core” and “extended” face network in congenital prosopagnosia. *Frontiers in Human Neuroscience*, *8*(November), 925. https://doi.org/10.3389/fnhum.2014.00925

Robbins, R. A., Nishimura, M., Mondloch, C. J., Lewis, T. L., & Maurer, D. (2010). Deficits in sensitivity to spacing after early visual deprivation in humans: A comparison of human faces, monkey faces, and houses. *Developmental Psychobiology*, *52*(8), 775–781. https://doi.org/10.1002/dev.20473

Röder, B., & Kekunnaya, R. (2021). Visual experience dependent plasticity in humans. In *Current Opinion in Neurobiology* (Vol. 67, pp. 155–162). Elsevier Current Trends. https://doi.org/10.1016/j.conb.2020.11.011

Röder, B., & Kekunnaya, R. (2022). Effects of Early Visual Deprivation. In *Oxford Research Encyclopedia of Psychology*. Oxford University Press. https://doi.org/10.1093/acrefore/9780190236557.013.839

Röder, B., Ley, P., Shenoy, B. H., Kekunnaya, R., & Bottari, D. (2013). Sensitive periods for the functional specialization of the neural system for human face processing. *Proceedings of the National Academy of Sciences of the United States of America*, *110*(42), 16760–16765. https://doi.org/10.1073/pnas.1309963110

Röder, B., Stock, O., Bien, S., Neville, H. J., & Rösler, F. (2002). Speech processing activates visual cortex in congenitally blind humans. *European Journal of Neuroscience*, *16*(5), 930–936. https://doi.org/10.1046/j.1460-9568.2002.02147.x

Rosenke, M., van Hoof, R., van den Hurk, J., & Goebel, R. (2020). A probabilistic functional parcellation of human occipito-temporal cortex. *BioRxiv*, 2020.01.22.916239.

https://doi.org/10.1101/2020.01.22.916239

Rossion, B., Dricot, L., Devolder, A., Bodart, J. M., Crommelinck, M., De Gelder, B., & Zoontjes, R. (2000). Hemispheric asymmetries for whole-based and part-based face processing in the human fusiform gyrus. *Journal of Cognitive Neuroscience*, *12*(5), 793–802. https://doi.org/10.1162/089892900562606

Sanders, A. F. P., Baum, G. L., Harms, M. P., Kandala, S., Bookheimer, S. Y., Dapretto, M., Somerville, L. H., Thomas, K. M., Van Essen, D. C., Yacoub, E., & Barch, D. M. (2022). Developmental trajectories of cortical thickness by functional brain network: The roles of pubertal timing and socioeconomic status. *Developmental Cognitive Neuroscience*, *57*, 101145. https://doi.org/10.1016/j.dcn.2022.101145

Saygin, Z. M., Osher, D. E., Koldewyn, K., Reynolds, G., Gabrieli, J. D. E., & Saxe, R. R. (2012). Anatomical connectivity patterns predict face selectivity in the fusiform gyrus. *Nature Neuroscience*, *15*(2), 321–327. https://doi.org/10.1038/nn.3001

Saygin, Z. M., Osher, D. E., Norton, E. S., Youssoufian, D. A., Beach, S. D., Feather, J., Gaab, N., Gabrieli, J. D. E., & Kanwisher, N. (2016). Connectivity precedes function in the development of the visual word form area. *Nature Neuroscience*, *19*(9), 1250–1255. https://doi.org/10.1038/nn.4354

Schalk, G., Kapeller, C., Guger, C., Ogawa, H., Hiroshima, S., Lafer-Sousa, R., Saygin, Z. M., Kamada, K., & Kanwisher, N. (2017). Facephenes and rainbows: Causal evidence for functional and anatomical specificity of face and color processing in the human brain. *Proceedings of the National Academy of Sciences of the United States of America*, *114*(46), 12285–12290. https://doi.org/10.1073/pnas.1713447114

Scherf, K. S., Behrmann, M., Humphreys, K., & Luna, B. (2007). Visual category-selectivity for faces, places and objects emerges along different developmental trajectories. In *Developmental Science* (Vol. 10, Issue 4, pp. F15–F30). John Wiley & Sons, Ltd. https://doi.org/10.1111/j.1467-7687.2007.00595.x

Scherf, K. S., Luna, B., Avidan, G., & Behrmann, M. (2011). What precedes which: Developmental neural tuning in face-and place-related cortex. *Cerebral Cortex*, *21*(9), 1963–1980. https://doi.org/10.1093/cercor/bhq269

Schmitt, J. E., Lenroot, R., Wallace, G. L., Ordaz, S., Taylor, K. N., Kabani, N., Greenstein, D., Lerch, J., Kendler, K. S., Neale, M. C., & Giedd, J. N. (2008). Identification of genetically mediated cortical networks: A multivariate study of pediatric twins and siblings. *Cerebral Cortex*, *18*(8), 1737–1747. https://doi.org/10.1093/cercor/bhm211

Schwarzer, G. (2000). Development of face processing: The effect of face inversion. *Child Development*, *71*(2), 391–401. https://doi.org/10.1111/1467-8624.00152

Schwarzlose, R. F., Baker, C. I., & Kanwisher, N. (2005). Separate face and body selectivity on the fusiform gyrus. *Journal of Neuroscience*, *25*(47), 11055–11059. https://doi.org/10.1523/JNEUROSCI.2621-05.2005

Segalowitz, S. J., Sternin, A., Lewis, T. L., Dywan, J., & Maurer, D. (2017). Electrophysiological evidence of altered visual processing in adults who experienced visual deprivation during infancy. *Developmental Psychobiology*, *59*(3), 375–389. https://doi.org/10.1002/dev.21502

Ségonne, F., Dale, A. M., Busa, E., Glessner, M., Salat, D. H., Hahn, H. K., & Fischl, B. (2004). A hybrid approach to the skull stripping problem in MRI. *NeuroImage*, *22*(3), 1060–1075. https://doi.org/DOI: 10.1016/j.neuroimage.2004.03.032

Ségonne, F., Pacheco, J., & Fischl, B. (2007). Geometrically accurate topology-correction of cortical

surfaces using nonseparating loops. *IEEE Trans Med Imaging*, *26*, 518–529.

Seitz, K. (2002). Parts and wholes in person recognition: Developmental trends. *Journal of Experimental Child Psychology*, *82*(4), 367–381. https://doi.org/10.1016/S0022-0965(02)00106-6

Serre, T., Oliva, A., & Poggio, T. (2007). A feedforward architecture accounts for rapid categorization. *Proceedings of the National Academy of Sciences of the United States of America*, *104*(15), 6424–6429. https://doi.org/10.1073/pnas.0700622104

Shaw, P., Eckstrand, K., Sharp, W., Blumenthal, J., Lerch, J. P., Greenstein, D., Clasen, L., Evans, A., Giedd, J., & Rapoport, J. L. (2007). Attention-deficit/hyperactivity disorder is characterized by a delay in cortical maturation. *Proceedings of the National Academy of Sciences*, *104*(49), 19649–19654. https://doi.org/10.1073/pnas.0707741104

Shaw, P., Greenstein, D., Lerch, J., Clasen, L. S., Lenroot, R., Gogtay, N., Evans, A. C., Rapoport, J., & Giedd, J. N. (2006). Intellectual ability and cortical development in children and adolescents. *Nature*, *440*(7084), 676–679. https://doi.org/10.1038/nature04513

Shaw, P., Kabani, N. J., Lerch, J., Eckstrand, K., Lenroot, R., Gogtay, N., Greenstein, D., Clasen, L. S., Evans, A. C., Rapoport, J. L., Giedd, J. N., & Wise, S. P. (2008). Neurodevelopmental trajectories of the human cerebral cortex. *Journal of Neuroscience*, *28*(14), 3586–3594. https://doi.org/10.1523/JNEUROSCI.5309-07.2008

Shaw, P., Malek, M., Watson, B., Sharp, W., Evans, A. C., & Greenstein, D. (2012). Development of cortical surface area and gyrification in attention-deficit/hyperactivity disorder. *Biological Psychiatry*, *72*(3), 191–197. https://doi.org/10.1016/j.biopsych.2012.01.031

Shimony, J. S., Burton, H., Epstein, A. A., McLaren, D. G., Sun, S. W., & Snyder, A. Z. (2006). Diffusion tensor imaging reveals white matter reorganization in early blind humans. *Cerebral Cortex*, *16*(11), 1653–1661. https://doi.org/10.1093/cercor/bhj102

Šikl, R., Šimeček, M., Porubanová-Norquist, M., Bezdíček, O., Kremláček, J., Stodůlka, P., Fine, I., & Ostrovsky, Y. (2013). Vision after 53 years of blindness. *I-Perception*, *4*(8), 498–507. https://doi.org/10.1068/i0611

Sled, J. G., Zijdenbos, A. P., & Evans, A. C. (1998). A nonparametric method for automatic correction of intensity nonuniformity in MRI data. *IEEE Trans Med Imaging*, *17*, 87–97.

Smith, S. L., & Trachtenberg, J. T. (2007). Experience-dependent binocular competition in the visual cortex begins at eye opening. *Nature Neuroscience*, *10*(3), 370–375. https://doi.org/10.1038/nn1844

Sourav, S., Bottari, D., Kekunnaya, R., & Röder, B. (2018). Evidence of a retinotopic organization of early visual cortex but impaired extrastriate processing in sight recovery individuals. *Journal of Vision*, *18*(3), 22. https://doi.org/10.1167/18.3.22

Sourav, S., Bottari, D., Shareef, I., Kekunnaya, R., & Röder, B. (2020). An electrophysiological biomarker for the classification of cataract-reversal patients: A case-control study. *EClinicalMedicine*, *27*, 100559. https://doi.org/10.1016/j.eclinm.2020.100559

Sourav, S., Kekunnaya, R., Shareef, I., Banerjee, S., Bottari, D., & Röder, B. (2019). A protracted sensitive period regulates the development of cross-modal sound–shape associations in humans. *Psychological Science*, *30*(10), 1473–1482. https://doi.org/10.1177/0956797619866625

Sowell, E. R., Peterson, B. S., Thompson, P. M., Welcome, S. E., Henkenius, A. L., & Toga, A. W. (2003). Mapping cortical change across the human life span. *Nature Neuroscience 2003 6:3*,

6(3), 309–315. https://doi.org/10.1038/nn1008

Sowell, E. R., Thompson, P. M., Leonard, C. M., Welcome, S. E., Kan, E., & Toga, A. W. (2004). Longitudinal mapping of cortical thickness and brain growth in normal children. *Journal of Neuroscience*, *24*(38), 8223–8231. https://doi.org/10.1523/JNEUROSCI.1798-04.2004

Sowell, E. R., Trauner, D. A., Gamst, A., & Jernigan, T. L. (2002). Development of cortical and subcortical brain structures in childhood and adolescence: A structural MRI study. *Developmental Medicine and Child Neurology*, *44*(1), 4–16. https://doi.org/10.1111/j.1469-8749.2002.tb00253.x

Spiridon, M., Fischl, B., & Kanwisher, N. (2006). Location and spatial profile of category-specific regions in human extrastriate cortex. *Human Brain Mapping*, *27*(1), 77–89. https://doi.org/10.1002/hbm.20169

Spiridon, M., & Kanwisher, N. (2002). How distributed is visual category information in human occipito-temporal cortex? An fMRI study. *Neuron*, *35*(6), 1157–1165. https://doi.org/10.1016/S0896-6273(02)00877-2

Striem-Amit, E., & Amedi, A. (2014). Visual Cortex Extrastriate Body-Selective Area Activation in Congenitally Blind People "Seeing" by Using Sounds. *Current Biology*, *24*(6), 687–692. https://doi.org/10.1016/J.CUB.2014.02.010

Striem-Amit, E., Cohen, L., Dehaene, S., & Amedi, A. (2012). Reading with Sounds: Sensory Substitution Selectively Activates the Visual Word Form Area in the Blind. *Neuron*, *76*(3), 640–652. https://doi.org/10.1016/j.neuron.2012.08.026

Striem-Amit, E., Ovadia-Caro, S., Caramazza, A., Margulies, D. S., Villringer, A., & Amedi, A. (2015). Functional connectivity of visual cortex in the blind follows retinotopic organization principles. *Brain*, *138*(6), 1679–1695. https://doi.org/10.1093/brain/awv083

Sugita, Y. (2008). Face perception in monkeys reared with no exposure to faces. *Proceedings of the National Academy of Sciences of the United States of America*, *105*(1), 394–398. https://doi.org/10.1073/pnas.0706079105

Sydnor, V. J., Larsen, B., Bassett, D. S., Alexander-Bloch, A., Fair, D. A., Liston, C., Mackey, A. P., Milham, M. P., Pines, A., Roalf, D. R., Seidlitz, J., Xu, T., Raznahan, A., & Satterthwaite, T. D. (2021). Neurodevelopment of the association cortices: Patterns, mechanisms, and implications for psychopathology. *Neuron*, *109*(18), 2820–2846. https://doi.org/10.1016/j.neuron.2021.06.016

Szymkowicz, S. M., McLaren, M. E., Kirton, J. W., O'Shea, A., Woods, A. J., Manini, T. M., Anton, S. D., & Dotson, V. M. (2016). Depressive symptom severity is associated with increased cortical thickness in older adults. *International Journal of Geriatric Psychiatry*, *31*(4), 325–333. https://doi.org/10.1002/gps.4324

Takesian, A. E., & Hensch, T. K. (2013). Balancing plasticity/stability across brain development. In *Progress in Brain Research* (Vol. 207, pp. 3–34). Elsevier. https://doi.org/10.1016/B978-0-444-63327-9.00001-1

Takeuchi, H., Taki, Y., Sassa, Y., Hashizume, H., Sekiguchi, A., Fukushima, A., & Kawashima, R. (2010). White matter structures associated with creativity: Evidence from diffusion tensor imaging. *NeuroImage*, *51*(1), 11–18. https://doi.org/10.1016/J.NEUROIMAGE.2010.02.035

Thomas, M. S. C., & Johnson, M. H. (2006). The computational modeling of sensitive periods. *Developmental Psychobiology*, *48*(4), 337–344. https://doi.org/10.1002/dev.20134

Tootell, R. B. H., Reppas, J. B., Kwong, K. K., Malach, R., Born, R. T., Brady, T. J., Rosen, B. R., &

Belliveau, J. W. (1995). Functional analysis of human MT and related visual cortical areas using magnetic resonance imaging. *Journal of Neuroscience*, *15*(4), 3215–3230. https://doi.org/10.1523/jneurosci.15-04-03215.1995

Trampel, R., Ott, D. V. M., & Turner, R. (2011). Do the congenitally blind have a stria of gennari? first intracortical insights in vivo. *Cerebral Cortex*, *21*(9), 2075–2081. https://doi.org/10.1093/cercor/bhq282

Tytla, M. E., Lewis, T. L., Maurer, D., & Brent, H. P. (1993). Stereopsis after congenital cataract. *Investigative Ophthalmology & Visual Science*, *34*(5), 1767–1773.

Ungerleider, L. G., & Mishkin, M. (1982). Two cortical visual systems. In D. J. Ingle, M. A. Goodale, & R. J. . W. Mansfield (Eds.), *Analysis of Visual Behavior* (pp. 549–586). MIT Press, Cambridge, MA.

Valk, S. L., Xu, T., Margulies, D. S., Masouleh, S. K., Paquola, C., Goulas, A., Kochunov, P., Smallwood, J., Yeo, B. T. T., Bernhardt, B. C., & Eickhoff, S. B. (2020). Shaping brain structure: Genetic and phylogenetic axes of macroscale organization of cortical thickness. *Science Advances*, *6*(39). https://doi.org/10.1126/sciadv.abb3417

van den Hurk, J., & Op de Beeck, H. P. (2019). Generalization asymmetry in multivariate cross-classification: When representation A generalizes better to representation B than B to A. In *bioRxiv* (p. 592410). bioRxiv. https://doi.org/10.1101/592410

van den Hurk, J., Van Baelen, M., & Op de Beeck, H. P. (2017). Development of visual category selectivity in ventral visual cortex does not require visual experience. *Proceedings of the National Academy of Sciences of the United States of America*, *114*(22), E4501–E4510. https://doi.org/10.1073/pnas.1612862114

Van Der Kolk, A. G., Hendrikse, J., Zwanenburg, J. J. M., Visser, F., & Luijten, P. R. (2013). Clinical applications of 7 T MRI in the brain. *European Journal of Radiology*, *82*(5), 708–718. https://doi.org/10.1016/J.EJRAD.2011.07.007

van Erp, T. G. M., Walton, E., Hibar, D. P., Schmaal, L., Jiang, W., Glahn, D. C., Pearlson, G. D., Yao, N., Fukunaga, M., Hashimoto, R., Okada, N., Yamamori, H., Bustillo, J. R., Clark, V. P., Agartz, I., Mueller, B. A., Cahn, W., de Zwarte, S. M. C., Hulshoff Pol, H. E., … Turner, J. A. (2018). Cortical Brain Abnormalities in 4474 Individuals With Schizophrenia and 5098 Control Subjects via the Enhancing Neuro Imaging Genetics Through Meta Analysis (ENIGMA) Consortium. *Biological Psychiatry*, *84*(9), 644–654. https://doi.org/10.1016/j.biopsych.2018.04.023

Vandekar, S. N., Shinohara, R. T., Raznahan, A., Roalf, D. R., Ross, M., Deleo, N., Ruparel, K., Verma, R., Wolf, D. H., Gur, R. C., Gur, R. E., & Satterthwaite, T. D. (2015). Topologically Dissociable Patterns of Development of the Human Cerebral Cortex. *The Journal of Neuroscience*, *35*(2), 599. https://doi.org/10.1523/JNEUROSCI.3628-14.2015

Vetter, P., Bola, Ł., Reich, L., Bennett, M., Muckli, L., & Amedi, A. (2020). Decoding Natural Sounds in Early "Visual" Cortex of Congenitally Blind Individuals. *Current Biology*, *30*(15), 3039-3044.e2. https://doi.org/10.1016/J.CUB.2020.05.071

Vogelsang, L., Gilad-Gutnick, S., Ehrenberg, E., Yonas, A., Diamond, S., Held, R., & Sinha, P. (2018). Potential downside of high initial visual acuity. *Proceedings of the National Academy of Sciences of the United States of America*, *115*(44), 11333–11338. https://doi.org/10.1073/pnas.1800901115

Voss, P. (2013). Sensitive and critical periods in visual sensory deprivation. *Frontiers in Psychology*, *4*(SEP), 664. https://doi.org/10.3389/FPSYG.2013.00664/BIBTEX

Vurpillot, E. (1968). The development of scanning strategies and their relation to visual

differentiation. *Journal of Experimental Child Psychology*, *6*(4), 632–650. https://doi.org/10.1016/0022-0965(68)90108-2

Wada, Y., & Yamamoto, T. (2001). Selective impairment of facial recognition due to a haematoma restricted to the right fusiform and lateral occipital region. *Journal of Neurology, Neurosurgery & Psychiatry*, *71*(2), 254–257. https://doi.org/10.1136/JNNP.71.2.254

Walhovd, K. B., Fjell, A. M., Giedd, J. N., Dale, A. M., & Brown, T. T. (2016). Through Thick and Thin: A Need to Reconcile Contradictory Results on Trajectories in Human Cortical Development. *Cerebral Cortex*, *27*(2), 1–10. https://doi.org/10.1093/cercor/bhv301

Walther, D. B., Caddigan, E., Fei-Fei, L., & Beck, D. M. (2009). Natural scene categories revealed in distributed patterns of activity in the human brain. *Journal of Neuroscience*, *29*(34), 10573–10581. https://doi.org/10.1523/JNEUROSCI.0559-09.2009

Wang, F., Lian, C., Wu, Z., Zhang, H., Li, T., Meng, Y., Wang, L., Lin, W., Shen, D., & Li, G. (2019). Developmental topography of cortical thickness during infancy. *Proceedings of the National Academy of Sciences of the United States of America*, *116*(32), 15855–15860. https://doi.org/10.1073/pnas.1821523116

Watanabe, T., & Sasaki, Y. (2015). Perceptual learning: Toward a comprehensive theory. *Annual Review of Psychology*, *66*, 197–221. https://doi.org/10.1146/annurev-psych-010814-015214

Weigelt, S., Koldewyn, K., Dilks, D. D., Balas, B., McKone, E., & Kanwisher, N. (2014). Domain-specific development of face memory but not face perception. *Developmental Science*, *17*(1), 47–58. https://doi.org/10.1111/desc.12089

Weiner, K. S., Barnett, M. A., Lorenz, S., Caspers, J., Stigliani, A., Amunts, K., Zilles, K., Fischl, B., & Grill-Spector, K. (2017). The Cytoarchitecture of Domain-specific Regions in Human High-level Visual Cortex. *Cerebral Cortex (New York, N.Y. : 1991)*, *27*(1), 146–161. https://doi.org/10.1093/cercor/bhw361

Weiner, K. S., Barnett, M. A., Witthoft, N., Golarai, G., Stigliani, A., Kay, K. N., Gomez, J., Natu, V. S., Amunts, K., Zilles, K., & Grill-Spector, K. (2018). Defining the most probable location of the parahippocampal place area using cortex-based alignment and cross-validation. *NeuroImage*, *170*, 373–384. https://doi.org/10.1016/j.neuroimage.2017.04.040

Weiner, K. S., Golarai, G., Caspers, J., Chuapoco, M. R., Mohlberg, H., Zilles, K., Amunts, K., & Grill-Spector, K. (2014). The mid-fusiform sulcus: A landmark identifying both cytoarchitectonic and functional divisions of human ventral temporal cortex. *NeuroImage*, *84*, 453–465. https://doi.org/10.1016/j.neuroimage.2013.08.068

Weiner, K. S., & Grill-Spector, K. (2010). Sparsely-distributed organization of face and limb activations in human ventral temporal cortex. *NeuroImage*, *52*(4), 1559–1573. https://doi.org/10.1016/j.neuroimage.2010.04.262

Weiner, K. S., & Grill-Spector, K. (2011). Not one extrastriate body area: Using anatomical landmarks, hMT+, and visual field maps to parcellate limb-selective activations in human lateral occipitotemporal cortex. *NeuroImage*, *56*(4), 2183–2199. https://doi.org/10.1016/j.neuroimage.2011.03.041

Weiner, K. S., & Grill-Spector, K. (2015). The evolution of face processing networks. *Trends in Cognitive Sciences*, *19*(5), 240–241. https://doi.org/10.1016/j.tics.2015.03.010

Weiner, K. S., Natu, V. S., & Grill-Spector, K. (2018). On object selectivity and the anatomy of the human fusiform gyrus. In *NeuroImage* (Vol. 173, pp. 604–609). Academic Press. https://doi.org/10.1016/j.neuroimage.2018.02.040

Westlye, L. T., Walhovd, K. B., Dale, A. M., Bjørnerud, A., Due-Tønnessen, P., Engvig, A., Grydeland, H., Tamnes, C. K., Østby, Y., & Fjell, A. M. (2010). Differentiating maturational and aging-related changes of the cerebral cortex by use of thickness and signal intensity. *NeuroImage*, *52*(1), 172–185. https://doi.org/10.1016/j.neuroimage.2010.03.056

Whitaker, K. J., Vértes, P. E., Romero-Garciaa, R., Váša, F., Moutoussis, M., Prabhu, G., Weiskopf, N., Callaghan, M. F., Wagstyl, K., Rittman, T., Tait, R., Ooi, C., Suckling, J., Inkster, B., Fonagy, P., Dolan, R. J., Jones, P. B., Goodyer, I. M., & Bullmore, E. T. (2016). Adolescence is associated with genomically patterned consolidation of the hubs of the human brain connectome. *Proceedings of the National Academy of Sciences of the United States of America*, *113*(32), 9105–9110. https://doi.org/10.1073/pnas.1601745113

Wierenga, L. M., Langen, M., Oranje, B., & Durston, S. (2014). Unique developmental trajectories of cortical thickness and surface area. *NeuroImage*, *87*, 120–126. https://doi.org/10.1016/j.neuroimage.2013.11.010

Wiesel, T. N., & Hubel, D. H. (1965). Comparison of the effects of unilateral and bilateral eye closure on cortical unit responses in kittens. *Journal of Neurophysiology*, *28*(6), 1029–1040.

William Revelle. (2023). *psych: Procedures for Psychological, Psychometric, and Personality Research*. https://cran.r-project.org/package=psych

Williams, M. A., Dang, S., & Kanwisher, N. (2007). Only some spatial patterns of fMRI response are read out in task performance. *Nature Neuroscience*, *10*(6), 685–686. https://doi.org/10.1038/nn1900

Wilmer, J. B., Germine, L., Chabris, C. F., Chatterjee, G., Williams, M., Loken, E., Nakayama, K., & Duchaine, B. (2010). Human face recognition ability is specific and highly heritable. *Proceedings of the National Academy of Sciences of the United States of America*, *107*(11), 5238–5241. https://doi.org/10.1073/pnas.0913053107

Winkler, A. M., Greve, D. N., Bjuland, K. J., Nichols, T. E., Sabuncu, M. R., Håberg, A. K., Skranes, J., & Rimol, L. M. (2018). Joint analysis of cortical area and thickness as a replacement for the analysis of the volume of the cerebral cortex. *Cerebral Cortex*, *28*(2), 738–749. https://doi.org/10.1093/cercor/bhx308

Winkler, A. M., Kochunov, P., Blangero, J., Almasy, L., Zilles, K., Fox, P. T., Duggirala, R., & Glahn, D. C. (2010). Cortical thickness or grey matter volume? The importance of selecting the phenotype for imaging genetics studies. *NeuroImage*, *53*(3), 1135–1146. https://doi.org/10.1016/j.neuroimage.2009.12.028

Witthoft, N., Nguyen, M. L., Golarai, G., LaRocque, K. F., Liberman, A., Smith, M. E., & Grill-Spector, K. (2014). Where Is Human V4? Predicting the Location of hV4 and VO1 from Cortical Folding. *Cerebral Cortex*, *24*(9), 2401–2408. https://doi.org/10.1093/CERCOR/BHT092

Wolbers, T., Klatzky, R. L., Loomis, J. M., Wutte, M. G., & Giudice, N. A. (2011). Modality-independent coding of spatial layout in the human brain. *Current Biology*, *21*(11), 984–989. https://doi.org/10.1016/j.cub.2011.04.038

Yates, T. S., Ellis, C. T., & Turk-Browne, N. B. (2023). Face processing in the infant brain after pandemic lockdown. *Developmental Psychobiology*, *65*(1), e22346. https://doi.org/10.1002/dev.22346

Yovel, G., Tambini, A., & Brandman, T. (2008). The asymmetry of the fusiform face area is a stable individual characteristic that underlies the left-visual-field superiority for faces. *Neuropsychologia*, *46*(13), 3061–3068. https://doi.org/10.1016/j.neuropsychologia.2008.06.017

Zaretskaya, N., Fischl, B., Reuter, M., Renvall, V., & Polimeni, J. R. (2018). Advantages of cortical surface reconstruction using submillimeter 7 T MEMPRAGE. *NeuroImage*, *165*, 11–26. https://doi.org/10.1016/J.NEUROIMAGE.2017.09.060

Zhen, Z., Yang, Z., Huang, L., Kong, X.-Z., Wang, X., Dang, X., Huang, Y., Song, Y., & Liu, J. (2015). Quantifying interindividual variability and asymmetry of face-selective regions: A probabilistic functional atlas. *NeuroImage*, *113*, 13–25. https://doi.org/10.1016/j.neuroimage.2015.03.010

Zhu, Q., Song, Y., Hu, S., Li, X., Tian, M., Zhen, Z., Dong, Q., Kanwisher, N., & Liu, J. (2010). Heritability of the Specific Cognitive Ability of Face Perception. *Current Biology*, *20*(2), 137–142. https://doi.org/10.1016/j.cub.2009.11.067

Zielinski, B. A., Prigge, M. B. D., Nielsen, J. A., Froehlich, A. L., Abildskov, T. J., Anderson, J. S., Fletcher, P. T., Zygmunt, K. M., Travers, B. G., Lange, N., Alexander, A. L., Bigler, E. D., & Lainhart, J. E. (2014). Longitudinal changes in cortical thickness in autism and typical development. *Brain*, *137*(6), 1799–1812. https://doi.org/10.1093/brain/awu083

Appendix A - Structural Whole-Brain Group Difference Maps

Figure S1

Exploratory Whole-Brain Cortical Thickness Group Maps

A **CC individuals vs. matched sighted controls (mSC_{CC})**

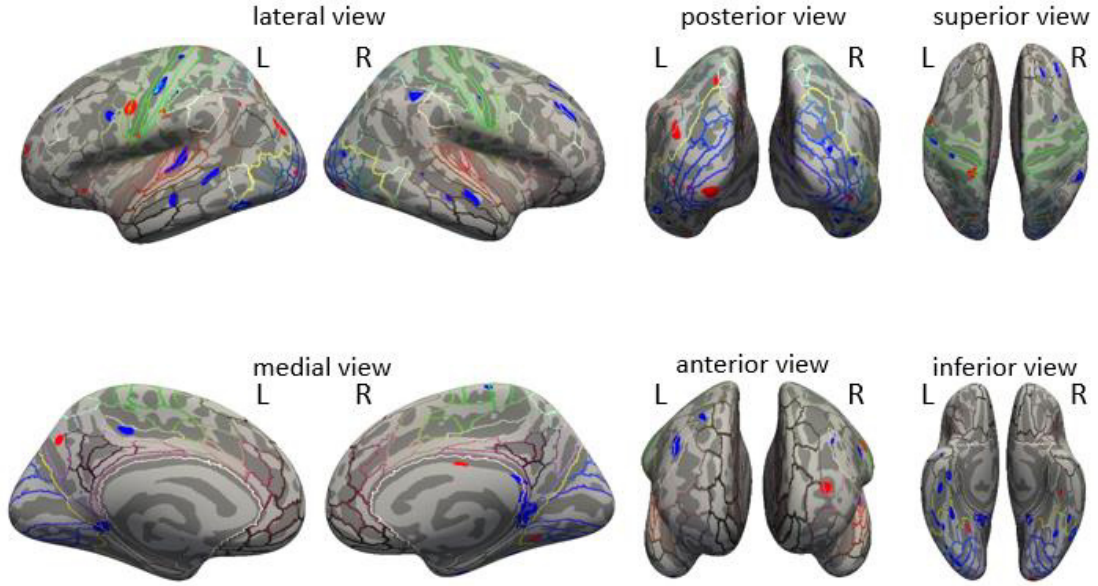

B **CC individuals vs. all sighted controls (allSC)**

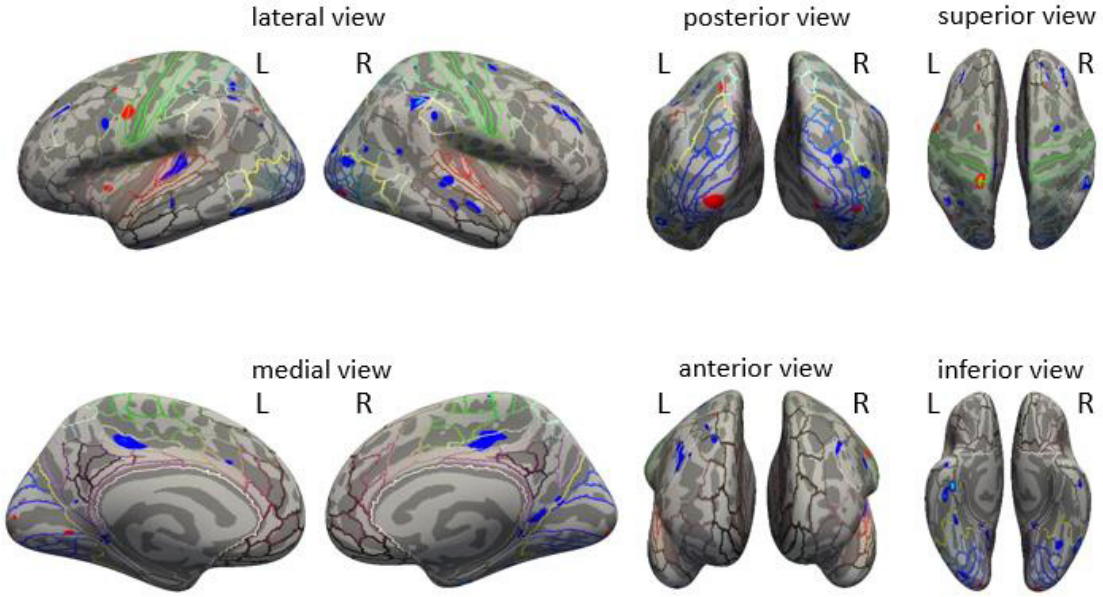

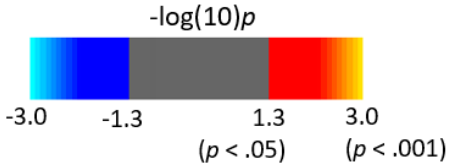

Whole-brain statistical significance maps: Cortical thickness. Thresholded statistical significance maps (vertex-wise $p < 0.05$, two-sided, scale bar for all maps at bottom) displaying cortical surface area differences (A) between CC individuals and matched sighted controls (mSC_{CC}), and (B) between CC individuals and all tested sighted controls (allSC). Clusters with larger cortical surface area in the CC group are marked in red and clusters with lower surface area in blue. All maps are superimposed on the inflated surface (dark grey: sulci, light grey: gyri) of the FreeSurfer standard brain. Coloured lines indicate parcellations of the HCP-MMP1.0 atlas (Glasser et al. 2016); the yellow line highlights the early visual cortex. L = Left hemisphere, R = Right hemisphere.

Figure S2

Exploratory Whole-Brain Surface Area Group Maps

A **CC individuals vs. matched sighted controls (mSC_{CC})**

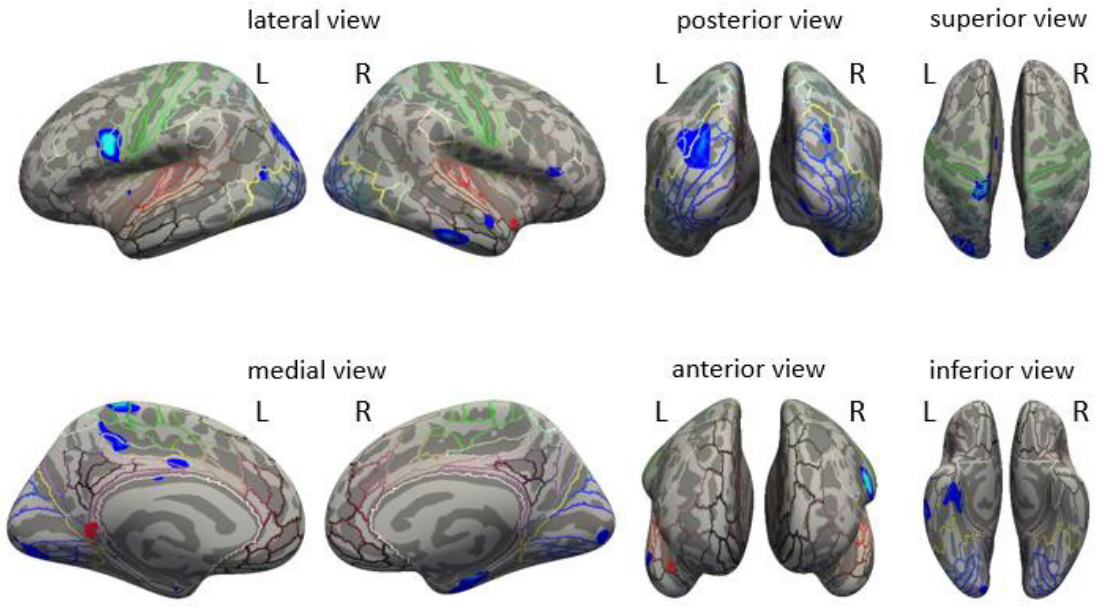

B **CC individuals vs. all sighted controls (allSC)**

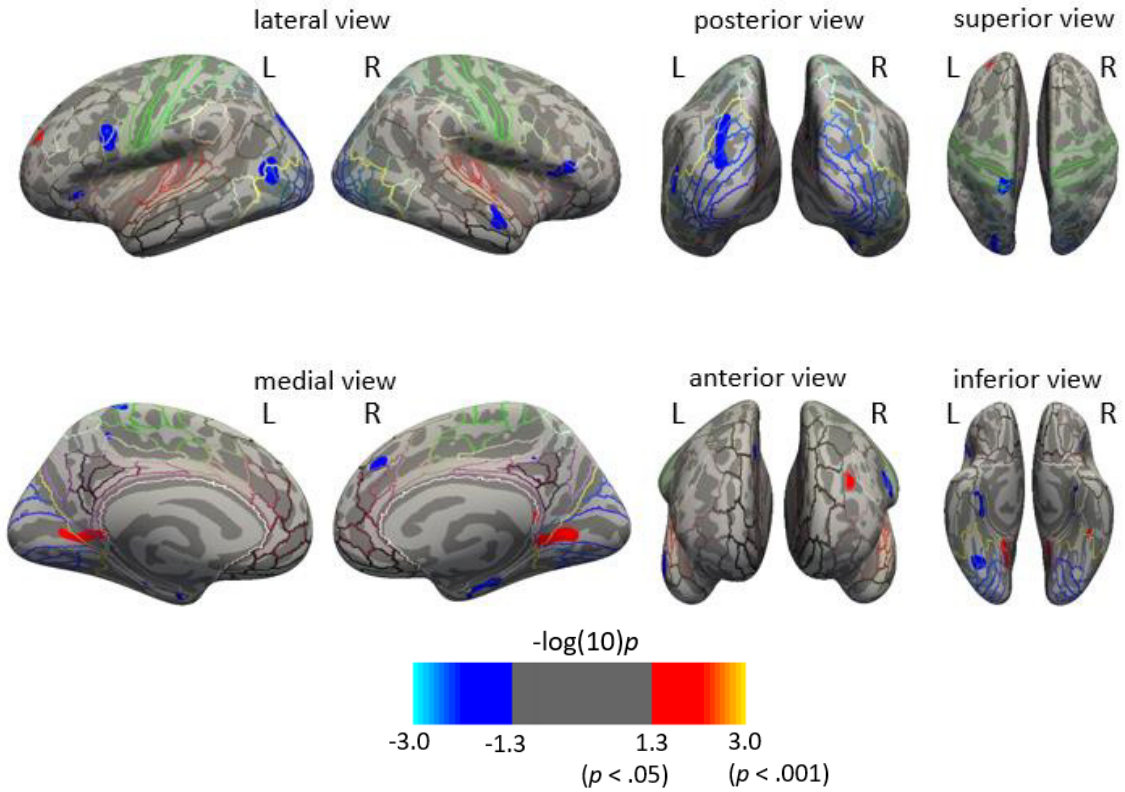

Whole-brain statistical significance maps: Surface area. Thresholded statistical significance maps (vertex-wise p < 0.05, two-sided, scale bar for all maps at the bottom) displaying cortical surface area differences (A) between CC individuals and matched sighted controls (mSC_{CC}), and (B) between CC individuals and all tested sighted controls (allSC). Clusters with larger cortical surface area in the CC group are marked in red and clusters with lower surface area in blue. All maps are superimposed on the inflated surface (dark grey: sulci, light grey: gyri) of the FreeSurfer standard brain. Coloured lines indicate parcellations of the HCP-MMP1.0 atlas (Glasser et al. 2016); the yellow line highlights the early visual cortex. L = Left hemisphere, R = Right hemisphere.

Appendix B - Post-Hoc Calculations Functional Analysis

Post-Hoc Calculations for the matched-Model Separately per Region

The tables presented here list the respective comparisons separately per category-pair or in case of a group condition interaction, a comparison of category-pair separated by group or a comparison of group separated by category-pair. The tables list the respective difference value (Estimate), the standard error (SE), the *t*-value with respective degrees of freedom (*t*(df)), as well as the uncorrected (p_{uncorr}) and corrected *p*-values (p_{corr}).

mFus-faces

Table S1

Results of Pairwise Comparisons of Conditions Within the mFus-faces_lh

contrast	Estimate	SE	*t*(42)	p_{uncorr}	p_{corr}
Body - Face	-0.19	0.09	-2.01	.051	.074
Body - Object	-0.24	0.09	-2.60	**.013**	**.020**
Body - Scene	0.07	0.09	0.74	.461	.512
Face - Object	-0.06	0.09	-0.59	.559	.602
Face - Scene	0.26	0.09	2.75	**.009**	**.015**
Object - Scene	0.31	0.09	3.34	**.002**	**.003**

Table S2

Results of Pairwise Comparisons of Conditions Within the mFus-faces_rh

contrast	Estimate	SE	*t*(42)	p_{uncorr}	p_{corr}
Body - Face	-0.42	0.01	-4.34	**< .001**	**< .001**
Body - Object	-0.03	0.01	-0.27	.786	.821
Body - Scene	0.41	0.01	4.21	**< .001**	**< .001**
Face - Object	0.39	0.01	4.07	**< .001**	**< .001**
Face - Scene	0.83	0.01	8.56	**< .001**	**< .001**
Object - Scene	0.43	0.01	4.49	**< .001**	**< .001**

pFus-faces

Table S3

Results of Pairwise Comparisons of Conditions Within the pFus-faces_lh

contrast	Estimate	SE	*t*(42)	p_{uncorr}	p_{corr}
Body - Face	-0.21	0.08	-2.65	**.011**	**.018**
Body - Object	-0.32	0.08	-4.09	**< .001**	**< .001**
Body - Scene	-0.06	0.08	-0.71	.479	.524
Face - Object	-0.11	0.08	-1.44	.157	.200
Face - Scene	0.15	0.08	1.94	.060	.083
Object - Scene	0.26	0.08	3.38	**.002**	**.003**

Table S4

Results of Pairwise Comparisons of Conditions Within the pFus-faces_rh

contrast	Estimate	SE	*t*(42)	p_{uncorr}	p_{corr}
Body - Face	-0.25	0.07	-3.44	**.001**	**.003**
Body - Object	-0.33	0.07	-4.65	**< .001**	**< .001**
Body - Scene	-0.01	0.07	-0.08	.937	.937
Face - Object	-0.09	0.07	-1.21	.233	.286
Face - Scene	0.24	0.07	3.36	**.002**	**.003**
Object - Scene	0.33	0.07	4.57	**< .001**	**< .001**

IOG-faces

Table S5

Results of Pairwise Comparisons of Conditions Within the IOG-faces_lh

contrast	Estimate	SE	*t*(42)	p_{uncorr}	p_{corr}
Body - Face	-0.34	0.07	-4.76	**< .001**	**< .001**
Body - Object	-0.32	0.07	-4.59	**< .001**	**< .001**
Body - Scene	0.11	0.07	1.51	.138	.179
Face - Object	0.01	0.07	0.17	.863	.883
Face - Scene	0.44	0.07	6.27	**< .001**	**< .001**
Object - Scene	0.43	0.07	6.10	**< .001**	**< .001**

Table S6

Results of Pairwise Comparisons of Conditions Within the IOG-faces_rh

contrast	Estimate	SE	*t*(42)	p_{uncorr}	p_{corr}
Body - Face	-0.51	0.08	-6.21	**< .001**	**< .001**
Body - Object	-0.28	0.08	-3.46	**.001**	**.003**
Body - Scene	0.09	0.08	1.13	.264	.319
Face - Object	0.22	0.08	2.75	**.009**	**.015**
Face - Scene	0.60	0.08	7.34	**< .001**	**< .001**
Object - Scene	0.37	0.08	4.59	**< .001**	**< .001**

avg-faces

Table S7

Results of Pairwise Comparisons of Conditions Within the avg-faces_lh

contrast	estimate	SE	*t*(42)	p_{uncorr}	p_{corr}
Body - Face	-0.24	0.08	-3.38	**.002**	**.003**
Body - Object	-0.30	0.08	-4.10	**< .001**	**< .001**
Body - Scene	0.04	0.08	0.56	.578	.605
Face - Object	-0.05	0.08	-0.72	.476	.509
Face - Scene	0.28	0.08	3.94	**< .001**	**.001**
Object - Scene	0.34	0.08	4.66	**< .001**	**< .001**

Table S8

Results of Pairwise Comparisons of Conditions Within the avg-faces_rh

contrast	estimate	SE	*t*(42)	p_{uncorr}	p_{corr}
Body - Face	-0.39	0.07	-5.76	**< .001**	**< .001**
Body - Object	-0.21	0.07	-3.15	**.003**	**.005**
Body - Scene	0.16	0.07	2.43	**.020**	**.030**
Face - Object	0.18	0.07	2.61	**.013**	**.020**
Face - Scene	0.55	0.07	8.19	**< .001**	**< .001**
Object - Scene	0.38	0.07	5.58	**< .001**	**< .001**

OTS-bodies

Table S9

Results of Pairwise Comparisons of Conditions Within the OTS-bodies_lh

contrast	estimate	SE	$t(42)$	p_{uncorr}	p_{corr}
Body - Face	-0.04	0.09	-0.44	.662	.703
Body - Object	-0.21	0.09	-2.31	**.026**	**.040**
Body - Scene	0.28	0.09	3.10	**.003**	**.006**
Face - Object	-0.17	0.09	-1.87	.069	.094
Face - Scene	0.32	0.09	3.54	**.001**	**.002**
Object - Scene	0.48	0.09	5.40	**< .001**	**< .001**

Table S10

Results of Pairwise Comparisons of Conditions per Group Within the OTS-bodies_rh

group	contrast	estimate	SE	*t*(42)	p_{uncorr}	p_{corr}
mSC	Body - Face	-0.26	0.11	-2.28	**.028**	**.042**
	Body - Object	0.09	0.11	0.83	.411	.464
	Body - Scene	0.51	0.11	4.51	**< .001**	**< .001**
	Face - Object	0.35	0.11	3.11	**.003**	**.006**
	Face - Scene	0.77	0.11	6.78	**< .001**	**< .001**
	Object - Scene	0.41	0.11	3.68	**.001**	**.002**
CC	Body - Face	-0.10	0.11	-0.92	.361	.415
	Body - Object	-0.22	0.11	-1.99	.053	.076
	Body - Scene	0.15	0.11	1.34	.187	.234
	Face - Object	-0.12	0.11	-1.07	.291	.345
	Face - Scene	0.26	0.11	2.26	**.029**	**.043**
	Object - Scene	0.38	0.11	3.33	**.002**	**.003**

Table S11

Results of Pairwise Comparisons of Groups per Condition Within the OTS-bodies_rh

condition	contrast	estimate	SE	*t*(27)	p_{uncorr}	p_{corr}
Body	mSC - CC	0.03	0.18	0.16	.871	.883
Face	mSC - CC	0.18	0.18	1.02	.315	.368
Object	mSC - CC	-0.29	0.18	-1.62	.116	.153
Scene	mSC - CC	-0.33	0.18	-1.84	.077	.103

CoS-places

Table S12

Results of Pairwise Comparisons of Conditions Within the CoS-places_lh

contrast	estimate	SE	*t*(42)	p_{uncorr}	p_{corr}
Body - Face	0.31	0.08	4.06	**< .001**	**< .001**
Body - Object	-0.32	0.08	-4.25	**< .001**	**< .001**
Body - Scene	-0.92	0.08	-12.00	**< .001**	**< .001**
Face - Object	-0.63	0.08	-8.31	**< .001**	**< .001**
Face - Scene	-1.23	0.08	-16.06	**< .001**	**< .001**
Object - Scene	-0.59	0.08	-7.75	**< .001**	**< .001**

Table S13

Results of Pairwise Comparisons of Conditions Within the CoS-places_rh

contrast	estimate	SE	*t*(42)	p_{uncorr}	p_{corr}
Body - Face	0.34	0.06	5.47	**< .001**	**< .001**
Body - Object	-0.47	0.06	-7.61	**< .001**	**< .001**
Body - Scene	-1.04	0.06	-16.83	**< .001**	**< .001**
Face - Object	-0.81	0.06	-13.07	**< .001**	**< .001**
Face - Scene	-1.38	0.06	-22.30	**< .001**	**< .001**
Object - Scene	-0.57	0.06	-9.23	**< .001**	**< .001**

Post-Hoc Calculations for the All-Subject-Model Separately per Region

mFus-faces

Table S14

Pairwise Comparisons of Conditions per Group Within the mFus-faces_lh

group	contrast	Estimate	SE	*t*(63)	p_{uncorr}	p_{corr}
allSC	Body - Face	-0.43	0.11	-3.97	**< .001**	**< .001**
	Body - Object	-0.36	0.11	-3.35	**.001**	**.004**
	Body - Scene	0.10	0.11	0.89	.378	.521
	Face - Object	0.07	0.11	0.62	.538	.639
	Face - Scene	0.53	0.11	4.86	**< .001**	**< .001**
	Object - Scene	0.46	0.11	4.24	**< .001**	**< .001**
CC	Body - Face	0.00	0.14	0.04	.972	.972
	Body - Object	-0.12	0.14	-0.84	.402	.536
	Body - Scene	0.08	0.14	0.59	.560	.654
	Face - Object	-0.12	0.14	-0.88	.383	.521
	Face - Scene	0.08	0.14	0.55	.583	.676
	Object - Scene	0.20	0.14	1.43	.158	.264
VI	Body - Face	-0.49	0.23	-2.15	**.035**	.071
	Body - Object	-0.09	0.23	-0.40	.688	.750
	Body - Scene	0.49	0.23	2.16	**.034**	.071
	Face - Object	0.40	0.23	1.75	.086	.159
	Face - Scene	0.98	0.23	4.31	**< .001**	**< .001**
	Object - Scene	0.58	0.23	2.57	**.013**	**.029**

Table S15

Results of Pairwise Comparisons of Groups per Condition Within the mFus-faces_lh

condition	contrast	Estimate	SE	*t*(42)	p_{uncorr}	p_{corr}
Body	allSC - CC	-0.39	0.19	-2.04	**.047**	.092
	allSC - VI	-0.17	0.27	-0.63	.530	.639
	CC - VI	0.22	0.29	0.76	.453	.566
Face	allSC - CC	0.05	0.19	0.24	.808	.840
	allSC - VI	-0.23	0.27	-0.84	.408	.539
	CC - VI	-0.27	0.29	-0.95	.346	.492
Object	allSC - CC	-0.14	0.19	-0.75	.459	.567
	allSC - VI	0.10	0.27	0.37	.713	.771
	CC - VI	0.24	0.29	0.85	.402	.536
Scene	allSC - CC	-0.41	0.19	-2.12	**.039**	.078
	allSC - VI	0.22	0.27	0.81	.422	.545
	CC - VI	0.63	0.29	2.18	**.035**	.071

Table S16

Results of Pairwise Comparisons of Conditions Within the mFus-faces_rh

contrast	Estimate	SE	$t(63)$	p_{uncorr}	p_{corr}
Body - Face	-0.41	0.09	-4.57	**< .001**	**< .001**
Body - Object	0.00	0.09	0.05	.962	.970
Body - Scene	0.41	0.09	4.57	**< .001**	**< .001**
Face - Object	0.42	0.09	4.62	**< .001**	**< .001**
Face - Scene	0.83	0.09	9.14	**< .001**	**< .001**
Object - Scene	0.41	0.09	4.52	**< .001**	**< .001**

pFus-faces

Table S17

Results of Pairwise Comparisons of Conditions Within the pFus-faces_lh

contrast	Estimate	SE	*t*(63)	p_{uncorr}	p_{corr}
Body - Face	-0.21	0.08	-2.66	**.010**	**.023**
Body - Object	-0.31	0.08	-4.03	**< .001**	**.001**
Body - Scene	0.04	0.08	0.48	.630	.705
Face - Object	-0.11	0.08	-1.37	.176	.283
Face - Scene	0.24	0.08	3.14	**.003**	**.007**
Object - Scene	0.35	0.08	4.51	**< .001**	**< .001**

Table S18

Results of Pairwise Comparisons of Conditions Within the pFus-faces_rh

contrast	Estimate	SE	*t*(63)	p_{uncorr}	p_{corr}
Body - Face	-0.22	0.07	-3.07	**.003**	**.009**
Body - Object	-0.30	0.07	-4.32	**< .001**	**< .001**
Body - Scene	0.07	0.07	0.99	.324	.470
Face - Object	-0.09	0.07	-1.25	.214	.341
Face - Scene	0.29	0.07	4.06	**< .001**	**< .001**
Object - Scene	0.37	0.07	5.31	**< .001**	**< .001**

IOG-faces

Table S19

Results of Pairwise Comparisons of Conditions per Group Within the IOG-faces_lh

group	contrast	Estimate	SE	*t*(63)	p_{uncorr}	p_{corr}
allSC	Body - Face	-0.54	0.08	-6.52	**< .001**	**< .001**
	Body - Object	-0.43	0.08	-5.30	**< .001**	**< .001**
	Body - Scene	0.08	0.08	0.98	.329	.472
	Face - Object	0.10	0.08	1.23	.224	.353
	Face - Scene	0.62	0.08	7.51	**< .001**	**< .001**
	Object - Scene	0.52	0.08	6.28	**< .001**	**< .001**
CC	Body - Face	-0.17	0.10	-1.66	.102	.182
	Body - Object	-0.27	0.10	-2.56	**.013**	**.029**
	Body - Scene	0.08	0.10	0.75	.454	.566
	Face - Object	-0.09	0.10	-0.91	.369	.518
	Face - Scene	0.25	0.10	2.41	**.019**	**.041**
	Object - Scene	0.35	0.10	3.32	**.002**	**.004**
VI	Body - Face	-0.29	0.17	-1.70	.094	.172
	Body - Object	-0.15	0.17	-0.88	.381	.521
	Body - Scene	0.46	0.17	2.67	**.010**	**.023**
	Face - Object	0.14	0.17	0.82	.415	.543
	Face - Scene	0.75	0.17	4.38	**< .001**	**< .001**
	Object - Scene	0.61	0.17	3.56	**.001**	**.002**

Table S20

Results of Pairwise Comparisons of Groups per Condition Within the IOG-faces_lh

condition	contrast	Estimate	SE	*t*(33)	p_{uncorr}	p_{corr}
Body	allSC - CC	-0.25	0.18	-1.39	.175	.283
	allSC - VI	-0.21	0.26	-0.81	.425	.545
	CC - VI	0.04	0.27	0.16	.877	.904
Face	allSC - CC	0.11	0.18	0.63	.534	.639
	allSC - VI	0.04	0.26	0.15	.884	.904
	CC - VI	-0.08	0.27	-0.28	.783	.820
Object	allSC - CC	-0.08	0.18	-0.46	.649	.715
	allSC - VI	0.08	0.26	0.30	.765	.817
	CC - VI	0.16	0.27	0.59	.559	.654
Scene	allSC - CC	-0.25	0.18	-1.40	.172	.283
	allSC - VI	0.17	0.26	0.66	.514	.628
	CC - VI	0.42	0.27	1.55	.130	.226

Table S21

Results of Pairwise Comparisons of Conditions Within the IOG-faces_rh

contrast	Estimate	SE	*t*(63)	p_{uncorr}	p_{corr}
Body - Face	-0.50	0.08	-6.27	**< .001**	**< .001**
Body - Object	-0.26	0.08	-3.31	**.002**	**.004**
Body - Scene	0.18	0.08	2.29	**.025**	.054
Face - Object	0.24	0.08	2.96	**.004**	**.012**
Face - Scene	0.68	0.08	8.56	**< .001**	**< .001**
Object - Scene	0.45	0.08	5.60	**< .001**	**< .001**

avg-faces

Table S22

Results of Pairwise Comparisons of Conditions per Group Within the avg-faces_lh

group	contrast	estimate	SE	*t*(63)	p_{uncorr}	p_{corr}
allSC	Body - Face	-0.44	0.08	-5.50	**< .001**	**< .001**
	Body - Object	-0.41	0.08	-5.19	**< .001**	**< .001**
	Body - Scene	0.04	0.08	0.49	.622	.707
	Face - Object	0.02	0.08	0.31	.756	.794
	Face - Scene	0.48	0.08	6.00	**< .001**	**< .001**
	Object - Scene	0.45	0.08	5.68	**< .001**	**< .001**
CC	Body - Face	-0.08	0.10	-0.75	.458	.574
	Body - Object	-0.21	0.10	-2.10	**.039**	.077
	Body - Scene	0.03	0.10	0.32	.748	.794
	Face - Object	-0.14	0.10	-1.36	.179	.279
	Face - Scene	0.11	0.10	1.07	.289	.418
	Object - Scene	0.25	0.10	2.43	**.018**	**.038**
VI	Body - Face	-0.33	0.17	-1.98	.052	.099
	Body - Object	-0.16	0.17	-0.96	.339	.452
	Body - Scene	0.39	0.17	2.37	**.021**	**.043**
	Face - Object	0.17	0.17	1.02	.312	.438
	Face - Scene	0.72	0.17	4.35	**< .001**	**< .001**
	Object - Scene	0.55	0.17	3.33	**.001**	**.004**

Table S23

Results of Pairwise Comparisons of Groups per Condition Within the avg-faces_lh

condition	contrast	estimate	SE	$t(34)$	p_{uncorr}	p_{corr}
Body	allSC - CC	-0.30	0.17	-1.82	.078	.133
	allSC - VI	-0.16	0.24	-0.66	.511	.632
	CC - VI	0.15	0.25	0.58	.566	.679
Face	allSC - CC	0.06	0.17	0.35	.730	.786
	allSC - VI	-0.05	0.24	-0.20	.840	.850
	CC - VI	-0.11	0.25	-0.42	.674	.745
Object	allSC - CC	-0.10	0.17	-0.62	.536	.653
	allSC - VI	0.10	0.24	0.40	.691	.754
	CC - VI	0.20	0.25	0.79	.433	.559
Scene	allSC - CC	-0.31	0.17	-1.86	.072	.128
	allSC - VI	0.20	0.24	0.82	.420	.551
	CC - VI	0.51	0.25	2.01	.053	.099

Table S24

Results of Pairwise Comparisons of Conditions Within the avg-faces_rh

contrast	estimate	SE	$t(63)$	p_{uncorr}	p_{corr}
Body - Face	-0.38	0.06	-6.19	**< .001**	**< .001**
Body - Object	-0.19	0.06	-3.09	**.003**	**.007**
Body - Scene	0.22	0.06	3.65	**.001**	**.001**
Face - Object	0.19	0.06	3.10	**.003**	**.007**
Face - Scene	0.60	0.06	9.84	**< .001**	**< .001**
Object - Scene	0.41	0.06	6.75	**< .001**	**< .001**

OTS-bodies

Table S25

Results of Pairwise Comparisons of Conditions Within the OTS-bodies_lh

contrast	estimate	SE	$t(63)$	p_{uncorr}	p_{corr}
Body - Face	-0.05	0.09	-0.51	.613	.692
Body - Object	-0.14	0.09	-1.51	.136	.233
Body - Scene	0.36	0.09	3.88	**< .001**	**.001**
Face - Object	-0.09	0.09	-1.00	.320	.470
Face - Scene	0.41	0.09	4.38	**< .001**	**< .001**
Object - Scene	0.50	0.09	5.39	**< .001**	**< .001**

Table S26

Results of Pairwise Comparisons of Conditions per Group Within the OTS-bodies_rh

group	contrast	estimate	SE	*t*(63)	p_{uncorr}	p_{corr}
allSC	Body - Face	-0.23	0.08	-2.84	**.006**	**.015**
	Body - Object	0.09	0.08	1.08	.283	.429
	Body - Scene	0.50	0.08	6.25	**< .001**	**< .001**
	Face - Object	0.32	0.08	3.92	**< .001**	**.001**
	Face - Scene	0.73	0.08	9.09	**< .001**	**< .001**
	Object - Scene	0.42	0.08	5.17	**< .001**	**< .001**
CC	Body - Face	-0.10	0.10	-1.01	.315	.470
	Body - Object	-0.22	0.10	-2.18	**.033**	.068
	Body - Scene	0.15	0.10	1.47	.146	.247
	Face - Object	-0.12	0.10	-1.17	.245	.381
	Face - Scene	0.26	0.10	2.48	**.016**	**.035**
	Object - Scene	0.38	0.10	3.66	**.001**	**.002**
VI	Body - Face	-0.46	0.17	-2.75	**.008**	**.019**
	Body - Object	0.02	0.17	0.11	.912	.926
	Body - Scene	0.45	0.17	2.70	**.009**	**.022**
	Face - Object	0.48	0.17	2.86	**.006**	**.015**
	Face - Scene	0.92	0.17	5.45	**< .001**	**< .001**
	Object - Scene	0.43	0.17	2.59	**.012**	**.028**

Table S27

Results of Pairwise Comparisons of Groups per Condition Within the OTS-bodies_rh

condition	contrast	estimate	SE	$t(37)$	p_{uncorr}	p_{corr}
Body	allSC - CC	0.05	0.16	0.30	.767	.817
	allSC - VI	0.17	0.22	0.77	.448	.566
	CC - VI	0.12	0.23	0.53	.601	.684
Face	allSC - CC	0.17	0.16	1.10	.277	.425
	allSC - VI	-0.06	0.22	-0.28	.778	.820
	CC - VI	-0.23	0.23	-1.00	.323	.470
Object	allSC - CC	-0.27	0.16	-1.71	.096	.173
	allSC - VI	0.10	0.22	0.46	.650	.715
	CC - VI	0.37	0.23	1.57	.126	.221
Scene	allSC - CC	-0.31	0.16	-1.97	.056	.107
	allSC - VI	0.12	0.22	0.54	.595	.683
	CC - VI	0.43	0.23	1.82	.077	.146

CoS-places

Table S28

Results of Pairwise Comparisons of Conditions Within the CoS-places_lh

contrast	estimate	SE	*t*(63)	p_{uncorr}	p_{corr}
Body - Face	0.38	0.07	5.65	**< .001**	**< .001**
Body - Object	-0.36	0.07	-5.34	**< .001**	**< .001**
Body - Scene	-1.03	0.07	-15.23	**< .001**	**< .001**
Face - Object	-0.74	0.07	-10.99	**< .001**	**< .001**
Face - Scene	-1.41	0.07	-20.88	**< .001**	**< .001**
Object - Scene	-0.67	0.07	-9.89	**< .001**	**< .001**

Table S29

Results of Pairwise Comparisons of Conditions Within the CoS-places_rh

contrast	estimate	SE	*t*(63)	p_{uncorr}	p_{corr}
Body - Face	0.41	0.06	6.97	**< .001**	**< .001**
Body - Object	-0.51	0.06	-8.74	**< .001**	**< .001**
Body - Scene	-1.16	0.06	-19.83	**< .001**	**< .001**
Face - Object	-0.92	0.06	-15.71	**< .001**	**< .001**
Face - Scene	-1.57	0.06	-26.80	**< .001**	**< .001**
Object - Scene	-0.65	0.06	-11.09	**< .001**	**< .001**

MTG-bodies

Table S30

Results of Pairwise Comparisons of Conditions Within the MTG-bodies_lh

contrast	Estimate	SE	*t*(63)	p_{uncorr}	p_{corr}
Body - Face	0.07	0.09	0.75	.455	.525
Body - Object	0.53	0.09	5.71	**< .001**	**< .001**
Body - Scene	0.97	0.09	10.57	**< .001**	**< .001**
Face - Object	0.46	0.09	4.96	**< .001**	**< .001**
Face - Scene	0.90	0.09	9.81	**< .001**	**< .001**
Object - Scene	0.45	0.09	4.85	**< .001**	**< .001**

Table S31

Results of Pairwise Comparisons of Conditions Within the MTG-bodies_rh

contrast	Estimate	SE	*t*(63)	p_{uncorr}	p_{corr}
Body - Face	-0.19	0.09	-2.03	**.047**	.076
Body - Object	0.29	0.09	3.11	**.003**	**.006**
Body - Scene	0.63	0.09	6.64	**< .001**	**< .001**
Face - Object	0.49	0.09	5.14	**< .001**	**< .001**
Face - Scene	0.82	0.09	8.66	**< .001**	**< .001**
Object - Scene	0.33	0.09	3.52	**.001**	**.002**

LOS-bodies

Table S32

Results of Pairwise Comparisons of Conditions Within the LOS-bodies_lh

contrast	Estimate	SE	*t*(63)	p_{uncorr}	p_{corr}
Body - Face	0.62	0.11	5.81	**< .001**	**< .001**
Body - Object	0.59	0.11	5.53	**< .001**	**< .001**
Body - Scene	0.60	0.11	5.63	**< .001**	**< .001**
Face - Object	-0.03	0.11	-0.28	.780	.807
Face - Scene	-0.02	0.11	-0.19	.851	.871
Object - Scene	0.01	0.11	0.09	.927	.937

Table S33

Results of Pairwise Comparisons of Conditions Within the LOS-bodies_rh

contrast	Estimate	SE	*t*(63)	p_{uncorr}	p_{corr}
Body - Face	0.36	0.11	3.38	**.001**	**.003**
Body - Object	0.42	0.11	3.96	**< .001**	**.001**
Body - Scene	0.62	0.11	5.85	**< .001**	**< .001**
Face - Object	0.06	0.11	0.58	.562	.620
Face - Scene	0.26	0.11	2.47	**.016**	**.030**
Object - Scene	0.20	0.11	1.89	.063	.100

ITG-bodies

Table S34

Results of Pairwise Comparisons of Conditions Within the ITG-bodies_lh

contrast	Estimate	SE	*t*(63)	p_{uncorr}	p_{corr}
Body - Face	0.47	0.10	4.88	**< .001**	**< .001**
Body - Object	0.64	0.10	6.70	**< .001**	**< .001**
Body - Scene	1.16	0.10	12.17	**< .001**	**< .001**
Face - Object	0.17	0.10	1.81	.075	.117
Face - Scene	0.69	0.10	7.28	**< .001**	**< .001**
Object - Scene	0.52	0.10	5.47	**< .001**	**< .001**

Table S35

Results of Pairwise Comparisons of Conditions Within the ITG-bodies_rh

contrast	Estimate	SE	*t*(63)	p_{uncorr}	p_{corr}
Body - Face	0.17	0.08	2.12	**.038**	.063
Body - Object	0.43	0.08	5.41	**< .001**	**< .001**
Body - Scene	0.95	0.08	11.93	**< .001**	**< .001**
Face - Object	0.26	0.08	3.28	**.002**	**.004**
Face - Scene	0.78	0.08	9.80	**< .001**	**< .001**
Object - Scene	0.52	0.08	6.52	**< .001**	**< .001**

pOTS-characters_lh

Table S36

Results of Pairwise Comparisons of Conditions Within the pOTS-characters_lh

contrast	Estimate	SE	*t*(63)	p_{uncorr}	p_{corr}
Body - Face	0.08	0.09	0.92	.363	.458
Body - Object	-0.18	0.09	-2.10	**.040**	.065
Body - Scene	0.37	0.09	4.27	**< .001**	**< .001**
Face - Object	-0.26	0.09	-3.02	**.004**	**.008**
Face - Scene	0.29	0.09	3.35	**.001**	**.003**
Object - Scene	0.55	0.09	6.37	**< .001**	**< .001**

IOS-characters_lh

Table S37

Results of Pairwise Comparisons of Conditions Within the IOS-characters_lh

contrast	Estimate	SE	*t*(63)	p_{uncorr}	p_{corr}
Body - Face	-0.22	0.07	-3.00	**.004**	**.008**
Body - Object	-0.26	0.07	-3.60	**.001**	**.002**
Body - Scene	0.06	0.07	0.88	.383	.472
Face - Object	-0.04	0.07	-0.60	.548	.614
Face - Scene	0.28	0.07	3.88	**< .001**	**.001**
Object - Scene	0.33	0.07	4.48	**< .001**	**< .001**

TOS-places_rh

Table S38

Results of Pairwise Comparisons of Conditions Within the TOS-places_rh

contrast	Estimate	SE	*t*(63)	p_{uncorr}	p_{corr}
Body - Face	0.30	0.07	4.48	**< .001**	**< .001**
Body - Object	-0.16	0.07	-2.43	**.018**	**.032**
Body - Scene	-0.39	0.07	-5.82	**< .001**	**< .001**
Face - Object	-0.46	0.07	-6.92	**< .001**	**< .001**
Face - Scene	-0.69	0.07	-10.31	**< .001**	**< .001**
Object - Scene	-0.23	0.07	-3.39	**.001**	**.003**

hMT

Table S39

Results of Pairwise Comparisons of Conditions Within the hMT_lh

contrast	Estimate	SE	*t*(63)	p_{uncorr}	p_{corr}
Body - Face	0.48	0.09	5.09	**< .001**	**< .001**
Body - Object	0.80	0.09	8.51	**< .001**	**< .001**
Body - Scene	1.20	0.09	12.69	**< .001**	**< .001**
Face - Object	0.32	0.09	3.42	**.001**	**.003**
Face - Scene	0.72	0.09	7.59	**< .001**	**< .001**
Object - Scene	0.39	0.09	4.18	**< .001**	**< .001**

Table S40

Results of Pairwise Comparisons of Conditions Within the hMT_rh

contrast	Estimate	SE	*t*(63)	p_{uncorr}	p_{corr}
Body - Face	0.22	0.07	2.95	**.004**	**.009**
Body - Object	0.77	0.07	10.34	**< .001**	**< .001**
Body - Scene	1.23	0.07	16.64	**< .001**	**< .001**
Face - Object	0.55	0.07	7.39	**< .001**	**< .001**
Face - Scene	1.01	0.07	13.69	**< .001**	**< .001**
Object - Scene	0.47	0.07	6.30	**< .001**	**< .001**

v1d

Table S41

Results of Pairwise Comparisons of Conditions Within the v1d_lh

contrast	Estimate	SE	*t*(63)	p_{uncorr}	p_{corr}
Body - Face	-0.05	0.06	-0.78	.437	.517
Body - Object	-0.13	0.06	-2.12	**.038**	.064
Body - Scene	-0.34	0.06	-5.63	**< .001**	**< .001**
Face - Object	-0.08	0.06	-1.33	.187	.258
Face - Scene	-0.29	0.06	-4.84	**< .001**	**< .001**
Object - Scene	-0.21	0.06	-3.51	**.001**	**.002**

Table S42

Results of Pairwise Comparisons of Conditions Within the v1d_rh

contrast	Estimate	SE	$t(63)$	p_{uncorr}	p_{corr}
Body - Face	0.07	0.07	1.01	.317	.415
Body - Object	-0.18	0.07	-2.47	**.016**	**.030**
Body - Scene	-0.51	0.07	-7.06	**< .001**	**< .001**
Face - Object	-0.25	0.07	-3.48	**.001**	**.002**
Face - Scene	-0.59	0.07	-8.07	**< .001**	**< .001**
Object - Scene	-0.33	0.07	-4.59	**< .001**	**< .001**

Table S43

Results of Pairwise Comparisons of Groups Within the v1d_rh

contrast	Estimate	SE	$t(21)$	p_{uncorr}	p_{corr}
allSC - CC	-0.27	0.14	-1.90	.163	.231
allSC - VI	0.37	0.20	1.80	.195	.267
CC - VI	0.64	0.22	2.96	**.020**	**.035**

v1v

Table S44

Results of Pairwise Comparisons of Conditions per Group Within the v1v_lh

group	contrast	Estimate	SE	*t*(63)	p_{uncorr}	p_{corr}
allSC	Body - Face	-0.19	0.07	-2.92	**.005**	**.010**
	Body - Object	-0.25	0.07	-3.74	**< .001**	**.001**
	Body - Scene	-0.79	0.07	-11.93	**< .001**	**< .001**
	Face - Object	-0.05	0.07	-0.81	.419	.502
	Face - Scene	-0.60	0.07	-9.01	**< .001**	**< .001**
	Object - Scene	-0.54	0.07	-8.19	**< .001**	**< .001**
CC	Body - Face	0.07	0.08	0.77	.443	.521
	Body - Object	-0.03	0.08	-0.38	.707	.746
	Body - Scene	-0.30	0.08	-3.54	**.001**	**.002**
	Face - Object	-0.10	0.08	-1.15	.255	.342
	Face - Scene	-0.36	0.08	-4.31	**< .001**	**< .001**
	Object - Scene	-0.27	0.08	-3.16	**.002**	**.005**
VI	Body - Face	-0.07	0.14	-0.49	.624	.671
	Body - Object	-0.08	0.14	-0.56	.578	.634
	Body - Scene	-0.49	0.14	-3.55	**.001**	**.002**
	Face - Object	-0.01	0.14	-0.07	.946	.953
	Face - Scene	-0.42	0.14	-3.06	**.003**	**.007**
	Object - Scene	-0.41	0.14	-2.99	**.004**	**.008**

Table S45

Results of Pairwise Comparisons of Groups per Condition Within the v1v_lh

condition	contrast	Estimate	SE	*t*(28)	p_{uncorr}	p_{corr}
Body	allSC - CC	-0.40	0.18	-2.24	**.033**	.057
	allSC - VI	0.18	0.25	0.72	.476	.544
	CC - VI	0.58	0.27	2.17	**.039**	.064
Face	allSC - CC	-0.14	0.18	-0.78	.444	.521
	allSC - VI	0.31	0.25	1.22	.232	.314
	CC - VI	0.45	0.27	1.67	.106	.158
Object	allSC - CC	-0.18	0.18	-1.02	.316	.415
	allSC - VI	0.35	0.25	1.40	.173	.243
	CC - VI	0.53	0.27	2.00	.055	.089
Scene	allSC - CC	0.10	0.18	0.54	.594	.646
	allSC - VI	0.48	0.25	1.91	.066	.104
	CC - VI	0.39	0.27	1.45	.158	.224

Table S46

Results of Pairwise Comparisons of Conditions Within the v1v_rh

contrast	Estimate	SE	*t*(63)	p_{uncorr}	p_{corr}
Body - Face	0.14	0.06	2.28	**.026**	**.045**
Body - Object	-0.04	0.06	-0.59	.558	.619
Body - Scene	-0.54	0.06	-8.61	**< .001**	**< .001**
Face - Object	-0.18	0.06	-2.87	**.006**	**.011**
Face - Scene	-0.69	0.06	-10.89	**< .001**	**< .001**
Object - Scene	-0.51	0.06	-8.02	**< .001**	**< .001**

v2d

Table S47

Results of Pairwise Comparisons of Conditions Within the v2d_lh

contrast	Estimate	SE	*t*(63)	p_{uncorr}	p_{corr}
Body - Face	0.15	0.06	2.31	**.024**	**.043**
Body - Object	0.04	0.06	0.60	.549	.614
Body - Scene	-0.11	0.06	-1.69	.095	.144
Face - Object	-0.11	0.06	-1.71	.092	.141
Face - Scene	-0.25	0.06	-4.01	**< .001**	**< .001**
Object - Scene	-0.14	0.06	-2.30	**.025**	**.044**

Table S48

Results of Pairwise Comparisons of Conditions Within the v2d_rh

contrast	Estimate	SE	*t*(63)	p_{uncorr}	p_{corr}
Body - Face	0.02	0.07	0.30	.767	.799
Body - Object	-0.22	0.07	-3.17	**.002**	**.005**
Body - Scene	-0.38	0.07	-5.63	**< .001**	**< .001**
Face - Object	-0.24	0.07	-3.47	**.001**	**.002**
Face - Scene	-0.41	0.07	-5.93	**< .001**	**< .001**
Object - Scene	-0.17	0.07	-2.46	**.017**	**.031**

v2v

Table S49

Results of Pairwise Comparisons of Conditions Within the v2v_lh

contrast	Estimate	SE	*t*(63)	p_{uncorr}	p_{corr}
Body - Face	-0.05	0.06	-0.87	.389	.477
Body - Object	-0.10	0.06	-1.62	.110	.163
Body - Scene	-0.46	0.06	-7.72	**< .001**	**< .001**
Face - Object	-0.04	0.06	-0.75	.454	.525
Face - Scene	-0.40	0.06	-6.85	**< .001**	**< .001**
Object - Scene	-0.36	0.06	-6.10	**< .001**	**< .001**

Table S50

Results of Pairwise Comparisons of Groups Within the v2v_lh

contrast	Estimate	SE	*t*(21)	p_{uncorr}	p_{corr}
allSC - CC	-0.30	0.21	-1.43	.342	.436
allSC - VI	0.59	0.30	1.97	.145	.209
CC - VI	0.89	0.31	2.81	**.027**	**.047**

Table S51

Results of Pairwise Comparisons of Conditions Within the v2v_rh

contrast	Estimate	SE	*t*(63)	p_{uncorr}	p_{corr}
Body - Face	0.05	0.06	0.89	.377	.471
Body - Object	-0.20	0.06	-3.41	**.001**	**.003**
Body - Scene	-0.66	0.06	-11.26	**< .001**	**< .001**
Face - Object	-0.25	0.06	-4.30	**< .001**	**< .001**
Face - Scene	-0.71	0.06	-12.15	**< .001**	**< .001**
Object - Scene	-0.46	0.06	-7.85	**< .001**	**< .001**

Table S52

Results of Pairwise Comparisons of Groups Within the v2v_rh

contrast	Estimate	SE	*t*(21)	p_{uncorr}	p_{corr}
allSC - CC	-0.27	0.18	-1.52	.301	.398
allSC - VI	0.54	0.26	2.12	.110	.163
CC - VI	0.82	0.27	3.01	**.017**	**.032**

v3d

Table S53

Results of Pairwise Comparisons of Conditions Within the v3d_lh

contrast	Estimate	SE	*t*(63)	p_{uncorr}	p_{corr}
Body - Face	0.26	0.06	4.27	**< .001**	**< .001**
Body - Object	-0.06	0.06	-0.97	.336	.430
Body - Scene	-0.14	0.06	-2.30	**.025**	**.044**
Face - Object	-0.32	0.06	-5.24	**< .001**	**< .001**
Face - Scene	-0.41	0.06	-6.57	**< .001**	**< .001**
Object - Scene	-0.08	0.06	-1.33	.187	.258

Table S54

Results of Pairwise Comparisons of Conditions Within the v3d_rh

contrast	Estimate	SE	*t*(63)	p_{uncorr}	p_{corr}
Body - Face	0.19	0.07	2.83	**.006**	**.012**
Body - Object	-0.12	0.07	-1.76	.083	.129
Body - Scene	-0.24	0.07	-3.61	**.001**	**.002**
Face - Object	-0.31	0.07	-4.59	**< .001**	**< .001**
Face - Scene	-0.43	0.07	-6.45	**< .001**	**< .001**
Object - Scene	-0.12	0.07	-1.85	.068	.107

v3v

Table S55

Results of Pairwise Comparisons of Conditions Within the v3v_lh

contrast	Estimate	SE	*t*(63)	p_{uncorr}	p_{corr}
Body - Face	0.05	0.06	0.85	.400	.488
Body - Object	-0.12	0.06	-2.02	**.048**	.077
Body - Scene	-0.39	0.06	-6.79	**< .001**	**< .001**
Face - Object	-0.16	0.06	-2.86	**.006**	**.011**
Face - Scene	-0.44	0.06	-7.64	**< .001**	**< .001**
Object - Scene	-0.27	0.06	-4.77	**< .001**	**< .001**

Table S56

Results of Pairwise Comparisons of Conditions Within the v3v_rh

contrast	Estimate	SE	*t*(63)	p_{uncorr}	p_{corr}
Body - Face	0.08	0.05	1.50	.138	.201
Body - Object	-0.29	0.05	-5.44	**< .001**	**< .001**
Body - Scene	-0.63	0.05	-11.67	**< .001**	**< .001**
Face - Object	-0.38	0.05	-6.94	**< .001**	**< .001**
Face - Scene	-0.71	0.05	-13.18	**< .001**	**< .001**
Object - Scene	-0.34	0.05	-6.23	**< .001**	**< .001**

Acknowledgements

Mein erster Impuls war, diese Danksagung denkbar einfach zu gestalten in Form eines einzelnen "Danke". Nicht, weil ich diesen Teil nicht ernst nehmen würde, sondern im Gegenteil, weil Worte nicht annähernd ausreichend scheinen (und ich wahrscheinlich die Hälfte an wichtigen Personen vergessen). Und dennoch, hier der Versuch:

Ich bedanke mich bei Brigitte Röder, dass Sie mir die Möglichkeit gegeben hat, zu so einem spannenden Thema zu promovieren. Außerdem möchte ich meinen Kommitteesmitgliedern Rainer Goebel, Barbara Hänel-Faulhaber, Patrick Bruns und Frank Schüttauf meinen Dank aussprechen.

Darüber hinaus möchte ich mich bei Maria Guerreiro, Cordula Hölig und Katarzyna Raczy-Illmer für ihre Betreuung, offenen Ohren, Taschentücher und aufmunternden Worte im Verlauf meiner Promotion bedanken. Doch nicht nur ihnen gilt mein Dank, sondern auch jedem einzelnen Mitglied der BPN, denn egal ob bei einem kurzen Schnack im Flur oder beim Kaffee in der Küche, diese Momente haben mich durchhalten lassen. Ich bedanke mich bei ILMA und insbesondere Laura Kuhne, Carolin Heitmann, Rashi Pant, Liesa Stange, Daniela Schönberger, Andreas Weiß und Alexander Kramer.

Wenn Familie Westphal-Linke-Schröder ein Familien-Clan bei Game of Thrones wäre, dann wäre unser Motto "Denn wir haben schon immer alles geschafft!". Aber nur durch euren Zuspruch, eure Unterstützung und Liebe war dies hier möglich. Von ganzem Herzen danke ich meinem Partner Simon Häring, der es geschafft hat Motivator und Ruhepol, Zuhörer und Therapeut, gedanklicher Sparringpartner, Grafikdesigner und Formatierungsexperte in sich zu vereinen und so letztendlich diese Dissertation möglich gemacht hat.

Danke!

Universität Hamburg
DER FORSCHUNG | DER LEHRE | DER BILDUNG

FAKULTÄT
FÜR PSYCHOLOGIE UND
BEWEGUNGSWISSENSCHAFT
Institut für Bewegungswissenschaft
Institut für Psychologie

Erklärung gemäß *(bitte Zutreffendes ankreuzen)*

☐ **§ 4 (1c) der Promotionsordnung des Instituts für Bewegungswissenschaft der Universität Hamburg vom 18.08.2010**

☒ **§ 5 (4d) der Promotionsordnung des Instituts für Psychologie der Universität Hamburg vom 20.08.2003**

Hiermit erkläre ich,

Madita, Linke (Vorname, Nachname),

dass ich mich an einer anderen Universität oder Fakultät noch keiner Doktorprüfung unterzogen oder mich um Zulassung zu einer Doktorprüfung bemüht habe.

Hamburg, d. 31.05.2023
Ort, Datum

M. Linke
Unterschrift

Universität Hamburg
DER FORSCHUNG | DER LEHRE | DER BILDUNG

FAKULTÄT
FÜR PSYCHOLOGIE UND
BEWEGUNGSWISSENSCHAFT
Institut für Bewegungswissenschaft
Institut für Psychologie

Eidesstattliche Erklärung nach *(bitte Zutreffendes ankreuzen)*

☐ **§ 7 (4) der Promotionsordnung des Instituts für Bewegungswissenschaft der Universität Hamburg vom 18.08.2010**

☒ **§ 9 (1c und 1d) der Promotionsordnung des Instituts für Psychologie der Universität Hamburg vom 20.08.2003**

Hiermit erkläre ich an Eides statt,

1. dass die von mir vorgelegte Dissertation nicht Gegenstand eines anderen Prüfungsverfahrens gewesen oder in einem solchen Verfahren als ungenügend beurteilt worden ist.
2. dass ich die von mir vorgelegte Dissertation selbst verfasst, keine anderen als die angegebenen Quellen und Hilfsmittel benutzt und keine kommerzielle Promotionsberatung in Anspruch genommen habe. Die wörtlich oder inhaltlich übernommenen Stellen habe ich als solche kenntlich gemacht.

Hamburg, d. 31.05.2023	M. Linke
Ort, Datum	Unterschrift